EFFECTS OF SILIBININ ON ETHANOL-MEDIATED HEPATOCELLULAR CARCINOMA PROGRESSION IN MALE AND FEMALE MICE

by

Elizabeth Brandon-Warner

A dissertation submitted to the faculty of
The University of North Carolina at Charlotte
in partial fulfillment of the requirements
for the degree of Doctor of Philosophy in
Biology

Charlotte

2011

Approved by:

_____
Iain H. McKillop

_____
Laura W. Schrum

_____
Mark G. Clemens

_____
Inna Sokolova

_____
Patrick Moyer

ABSTRACT

ELIZABETH BRANDON-WARNER. Effects of silibinin on ethanol-mediated hepatocellular carcinoma progression in male and female mice (Under the direction of DR. IAIN H. MCKILLOP)

Ethanol is a significant risk for the development of hepatic cirrhosis and progression to hepatocellular carcinoma (HCC). While females are more susceptible to the deleterious effects of ethanol, the incidence of cirrhosis and HCC is significantly higher in males than females. Previous reports identify a role for oxidative stress and inflammation in mediating the effects of ethanol on hepatocarcinogenesis, suggesting antioxidants may protect the liver from the deleterious effects of ethanol. Plant-derived antioxidants have been used for millennia to treat liver disease, yet rigorous scientific validation of efficacy is rare. Silibinin, a flavinoligand derived from Milk thistle (*Silybum marianum*), is one such compound indicated to possess potent antioxidant properties and historically cited as a hepatoprotectant.

In these studies we sought to determine the effects of ethanol on HCC promotion and progression using *in vitro* and *in vivo* rodent models. Using dedifferentiated rat hepatoma cells (H4IIE) that constitutively express alcohol-metabolizing enzymes, we demonstrated ethanol enhanced cellular oxidative stress, and proliferation. Pre-treatment of cells with silibinin significantly inhibited ethanol metabolism (*via* cytochrome P4502E1), oxidative stress, and proliferation. These data indicate silibinin may be an effective antioxidant with which to inhibit ethanol-dependent HCC progression.

We next employed an *in vivo* diethylnitrosamine (DEN) model of hepatocarcinogenesis in male and female mice (21-25 day old). Using this model foci

develop within ~20 weeks and HCC within ~40 weeks. Mice were fed dietary silibinin (0.5%, (*w/w*), 9 weeks) with or without chronic alcohol feeding (10/20% (*v/v*) in drinking water, alternate days, 8 weeks) to coincide with foci or HCC development. Using this approach, ethanol preferentially promoted foci formation in males *versus* females, effects exacerbated during HCC progression. Ethanol-dependent increases in tumor incidence and volume in males occurred concomitant with increased CYP2E1 expression and activity, depleted glutathione/increased oxidative stress, and hepatic injury. Conversely, ethanol did not alter tumor incidence or volume in females, and changes in oxidative stress were not evidenced. Analysis of cellular apoptosis demonstrated increased cell death in female mice maintained on ethanol that developed DEN-induced hepatic foci.

Inclusion of silibinin in the diet did not significantly reduce DEN-initiated foci formation or HCC progression in either males or females, with or without ethanol. Of note, measures of liver injury and oxidative stress were improved in animals fed silibinin during foci development, yet silibinin exacerbated the effects of ethanol during later-stage HCC progression. Finally, analysis of immune system signaling cascades demonstrated a net increase in cytokine expression and Th1/Th2 effectors in female, ethanol fed mice, effects inhibited by silibinin.

In conclusion these data demonstrate silibinin effectively inhibits ethanol-dependent HCC cell growth *in vitro*. However, while chronic ethanol feeding promoted foci formation and HCC progression in male mice *in vivo*, dietary silibinin did not reverse these effects. Conversely, ethanol failed to significantly affect tumor incidence or burden in females. This lack of ethanol-dependent hepatocarcinogenesis enhancement in females is due, at least in part, to altered immune and apoptotic responses.

ACKNOWLEDGEMENTS

I have learned many things during the course of my graduate work. The most important being that there are some great people in my life, without whom, I would not have succeeded. Earning a PhD is not an endeavor done in isolation. There were many times when it seemed that culinary school would have been a more prudent choice. Taking this risk, at this point in my life was often overwhelming; each milestone in the process was more anxiety producing than the last, with the risk of failure more terrifying. What began as a simple decision to return to school to finish my under-graduate degree evolved into a 10 year quest. Family and friends have graduated from college and gotten married. There have been births and deaths as life has punctuated the stages of my progress. I think my father would have liked to know that I persisted; he would have been proud of me.

I first must sincerely thank my mentor, Dr. Iain McKillop for giving me this opportunity. He has been a source of invaluable advice and assistance, with the willingness for judicious application of a cattle prod when warranted. There are current and former members of the General Surgery Laboratories at Carolinas Medical Center who deserve my thanks, Dr. David Foureau, Dr. Eugene Sokolov and Dr. Adrian Mattocks who were available with advice and assistance when needed. I am also grateful to my committee for their insights and guidance, Dr. Laura Schrum, Dr. Mark Clemens, Dr. Inna Sokolova and Dr. Patrick Moyer.

This process is one that benefits from friends, who can listen to the occasional rant, commiserate over a glass of wine, and offer their support and encouragement because they understand the process. I was fortunate to have that support from Dr.

Rebecca Powell and Dr. Ashley Lakner. My family has probably made as many sacrifices as I have during my pursuit of this goal. My children, Megan, Jacob and Adam, I am so proud of the people you are. The love and support you have given me has always meant so much, thank you. Finally, to my husband Bruce, who has patiently provided his love and support through all these years, even when he questioned the wisdom of this decision. I simply could not have done this without you.

TABLE OF CONTENTS

LIST OF FIGURES

LIST OF TABLES

LIST OF ABBREVIATIONS:

4-HNE	4-hydroxy-2-nonenal
8-OHdG	8-hydroxy-2-deoxyguanosine
ADH	Alcohol dehydrogenase
AFP	α-fetoprotein
AHF	Altered hepatic foci
ALD	Alcoholic liver disease
ALDH	Aldehyde dehydrogenase
ALT	Alanine aminotransferase
ANA	Anti-nuclear antibody
AP-1	Activator protein-1
AR	Androgen receptor
ATP	Adenosine triphosphate
BAC	Blood alcohol content
BCL-2	B-cell lymphoma-2
BCLC	Barcelona Clinic Liver Cancer
CCL	β-chemokine ligands
CCR	β-chemokine receptors
CIN	Chromosomal instability
CT	Computed tomography
CXCL	Chemokine (x-motif) ligand
CXCR	Chemokine (x-motif) receptor
CYP2E1	Cytochrome P450 enzyme 2E1

DNA	Deoxyribonucleic acid
EGF	Epidermal growth factor
EGR-1	Early growth response-1
ER	Estrogen receptor
ERK 1/2	Extracellular signal-related kinase 1 and 2
EtOH	Ethanol
FAEE	Fatty acid ethyl ester
GSH	Glutathione
GADD45β	Growth arrest DNA damage 45β
H_2O_2	Hydrogen peroxide
HBV	Hepatitis B Virus
HCC	Hepatocellular carcinoma
HCV	Hepatitis C Virus
HER	1-hydorxyethyl radical
HIF1α	Hypoxia inducible factor 1α
ICAM	Intercellular adhesion molecule
IGF	Insulin-like growth factor
IL-*X*	Interleukin –(1β, 6, 8, 12p70,10)
JNK	c-JUN NH2 terminal kinase
LPS	Lipopolysaccharide
MAPK	Mitogen activated protein kinase
MDA	Malondialdehyde
MDR	Multi-drug resistant

MEOS	Microsomal ethanol oxidizing system
MES	2-(N-morpholino) ethanesulphonic
MHC	Major histocompatability complex
MRI	Magnetic resonance imaging
mRNA	Messenger ribouncleic acid
NAD	Nicotinamide adenine dinuleotide
NADH	Reduced nicotinamide adenine dinucleotide
NADPH	Nicotinamide adenine dinucleotide phosphate
NAFLD	Non-alcoholic fatty liver disease
NFκB	Nuclear factor kappa B
$NO^{\bullet}$	Nitric oxide
$O_2^{\bullet -}$	Superoxide anion
$OH^{\bullet}$	Hydroxyl radical
$OONO^{-}$	Peroxynitrite anion
PBS	Phosphate buffered saline
PCNA	Proliferating cell nuclear antigen
PEI	Percutaneous ethanol injection
PGDFR	Platelet derived growth factor receptor
REDOX	Reduction - oxidation
RFA	Radiofrequency ablation
RIPA	Radioimmunoprecipitation assay
RNS	Reactive nitrogen species
ROS	Reactive oxygen species

SAMe	S-adenysyl-methionine
SMA	Smooth muscle α-actin
SOD	Superoxide dismutase
STAT	Signal transducer activator of transcription
TACE	Transarterial chemoembolization
TARE	Transarterial radioembolization
TGFβ	Transforming growth factor β
TNFα	Tumor necrosis factor α
VAP	Vascular adhesion protein
VCAM	Vascular cell adhesion molecule
VEGFR	Vascular endothelial growth factor receptor

CHAPTER 1: GENERAL INTRODUCTION

1.1. Hepatocellular Carcinoma:

1.1.1. Epidemiology and Risk Factors: The liver is a multi-cellular organ organized into several discrete, interactive cell types that can give rise to distinct types of hepatic tumors. Hepatocellular carcinoma (HCC) is a cancer arising from the transformation of hepatocytes, the parenchymal cells of the liver, and accounts for 85 to 90% of all primary liver tumors (McKillop, 2005; Okuda, 2000). HCC is the fifth most common malignancy diagnosed worldwide with an incidence of approximately 1 million new cases diagnosed annually (El-Serag, 2007; Ferlay, 2008; Gomaa, 2008; McKillop, 2006; Ogawa, 2009). Globally, ≈600,000 deaths are attributed to HCC, making it the third leading cause of cancer related mortality (El-Serag, 2007; McKillop, 2006; Ogawa, 2009).

The highest frequency of HCC occurs in Southeast Asia and sub-Saharan Africa which account for >80% of cases. Documented risks for HCC are largely preventable, environmental factors that include Hepatitis C (HCV) and B (HBV) viral infection, aflatoxin B exposure, non-alcoholic fatty liver disease (NAFLD) and chronic alcohol abuse (Altekruse, 2009; El-Serag, 2007; McKillop, 2006). Unlike other commonly diagnosed malignancies, HCC lacks familial markers and develops primarily in the context of persistent inflammation, injury and cirrhosis associated with exposure to underlying risk factors. Geographical variations in prevalence of these risk factors

parallels disease distribution related morbidity and mortality (Altekruse, 2009; El-Serag, 2007). Rates for HCC have been increasing in Western societies with men 3 to 5 times more likely to develop HCC than women (Davis, 2008; El-Serag, 2007; McKillop, 2005). In the United States age adjusted incidence of HCC has tripled in the three decades from 1975 to 2005 (Altekruse, 2009). The most common risk factor in the United States is HCV infection, followed by chronic alcohol abuse, metabolic syndrome and NAFLD associated with obesity and diabetes mellitus (El-Serag, 2007; McKillop, 2005).

Eighteen million Americans are estimated to abuse alcohol which remains a major risk associated with HCC in the United States (Christof et al., 2008; El-Serag, 2002). Disease pathology follows a predictable course, 100% of chronic ethanol abusers will develop steatosis. Despite the high incidence of fatty liver, only 10-30% of those individuals will progress to hepatitis, and only 8-20% of those will progress to cirrhosis. Finally, of those that progress to cirrhosis, only 15% eventually develop HCC (Vidali, 2007). Incidence of HCC increases progressively with age, as it is rarely diagnosed before age 40 except where HBV viral infection is endemic (El-Serag, 2002). The mean age distribution at diagnosis is between 50-70 years of age with women presenting with disease an average of 5 years later than men (El-Serag, 2007). Recent studies indicate a trend towards a younger age of acquisition in both males and females (El-Serag, 2002). Differences in disease development between males and females may be related to sex-specific differences in environmental exposure to carcinogens as males tend to drink more alcohol and have higher rates for cigarette smoking (Ferlay, 2008).

1.1.2. Diagnosis, Staging and Treatment: Hepatocellular carcinoma is complex and presents with a high degree of heterogenicity that is influenced by underlying

etiology. Currently, prognosis remains poor, due in part to long disease latency and lack of early diagnostic markers (Bosch, 2005; Ogawa, 2009; Thorgeirsson, 2002). HCC is a slow-growing malignancy that, when detected early, can be treated by surgical resection. However, the interval between initial onset of disease to clinically detectable HCC is typically measured in decades (Gomaa, 2008; Ogawa, 2009). Confirmation is often delayed until advanced stage, and is usually accompanied by advanced fibrosis and cirrhosis with impaired hepatic function (El-Serag, 2007; McKillop, 2006; McKillop, 2005). By the time patients present with symptoms of abdominal pain, weight loss and fatigue, the tumor is typically ≥10 cm in diameter and has usually metastasized (Domínguez-Malagón, 2001). This delay in diagnosis limits therapeutic options and contributes to an abysmal survival rate, which is estimated at only 7 to 8 months following diagnosis (El-Serag et al., 2008).

In clinical practice, individuals at high risk for developing HCC are screened by ultrasoundography and serum markers for α-fetoprotein (AFP) (Zhang et al., 2004). Use of AFP is not an accurate predictor of disease as 40% of patients with HCC do not produce AFP, and patients of African descent have normal AFP levels at 500 ng/mL (Ferenci et al.). On detection of liver lesions in patients with cirrhosis further testing utilizing contrast-enhanced x-ray computed tomography (CT) or magnetic resonance imaging (MRI) is conducted followed by percutaneous liver biopsy of lesions greater than 1 cm (Bruix and Sherman, 2005). Multiple staging systems have been developed, including the Barcelona Clinic Liver Cancer (BCLC) scale, which is the currently endorsed system for evaluating clinical HCC (Bruix and Sherman, 2005; El-Serag et al., 2008). Treatment options are commensurate with the grading scale. Surgical resection,

liver transplantation or local ablation techniques are viable in early HCC (Grade A); disruption of tumor arterial blood supply combined with delivery of either drugs or radioactive partials is recommended for patients at intermediate stage (Grade B); advanced stage (Grade C) is generally treated by chemotherapy agents, of which sorafenib is the only one currently recommended; terminal stage (Grade D) is restricted to palliative and supportive care (Bruix and Sherman, 2005).

Surgical resection is potentially curative; however the 5 year risk for cancer recurrence exceeds 70% (Duffy et al., 2008; El-Serag et al., 2008). Liver transplantation is considered an optimal treatment because it removes both the malignancy and diseased liver which may contain small undetected focal lesions that contribute to recurrence (Thomas and Zhu, 2005). The severity of liver dysfunction and features of comorbidity complicate surgical intervention. In these cases, tumors are treated by ablation techniques. One alternative, percutaneous ethanol injection (PEI) is administered in tumors less than 2 cm in diameter (Lencioni et al., 2003). Radiofrequency ablation (RFA) is currently used more frequently and affords a higher rate of complete tumor necrosis and may have an efficacy similar to that of surgical resection (Forner et al., 2009; Goldberg et al., 2000).

Hepatic tumors are highly vascular, receiving most of their blood supply from the hepatic artery, while in normal hepatic tissue, 80% of the blood flow is supplied by the hepatic portal vein (Llovet et al., 2008). One treatment option exploits this feature by disrupting the arterial blood supply to the tumor through transarterial chemoembolization (TACE). In this procedure a cocktail of chemotherapeutic agents and gel-foam particles is delivered into the hepatic artery supplying the tumor; it is recommended in patients

without metastasis (Forner et al., 2009; Nicolini et al., 2010). Alternately, transarterial radioembolization (TARE) is a similar method that utilizes radioactive resin or glass beads (Forner et al., 2009).

Few pharmacological or chemotherapeutic agents are available to treat HCC, in part due to increased resistance to conventional treatments (Thomas and Zhu, 2005). Additionally, as the liver is the primary site of xenobiotic metabolism, severe hepatic dysfunction results in poor tolerance to systemically delivered therapies. It has also been demonstrated that HCC is characterized by a multi-drug resistant (MDR) phenotype that results from over-expression of an energy-dependent efflux pump, encoded by the MDR1 gene (Lasagna et al., 2006). Currently, Sorafenib, an oral multi-kinase inhibitor that targets Raf kinase, vascular endothelial growth factor receptor (VEGFR) and platelet-derived growth factor receptor (PGDFR) signaling pathways is the only therapeutic offered for HCC (Zhu, 2008). However, treatment has been reported to provide only a marginal increase in survival from 7.9 months to 10.7 months (Llovet et al., 2008).

1.2. Hepatocarcinogenesis:

1.2.1. Etiology: Eighty-five percent of HCC occurs within a background of chronic liver disease, advanced fibrosis, and cirrhosis. This pathobiology suggests a role for oxidative stress with a pattern of recurrent hepatocyte injury and regeneration that may facilitate the accumulation of tumorigenic mutations (Farazi et al., 2003; Karin and Greten, 2005; Sasaki, 2006). Tumorigenesis is a multistage process that occurs with the accumulation of genetic and epigenetic mutations that allow cells to overcome multiple barriers to cancer development (He et al., 2008; Karin and Greten, 2005; Sasaki, 2006; Thorgeirsson, 2002). Tumorigenesis in HCC is influenced by factors produced in

surrounding liver tissue and liver cell types, although specific mechanisms are poorly understood and vary according to underlying risk factors (Farazi et al., 2003; Sasaki, 2006; Thorgeirsson, 2002).

Multiple carcinogenic pathways are altered in HCC; but, changes in hepatocyte growth factors, somatic mutations, protease and matrix metalloproteinase overexpression, and oncogene activation can all be identified early during hepatic inflammation and chronic hepatitis (McKillop, 2006; Thorgeirsson, 2002). These changes become more extensive during the progression of liver injury through fibrosis to cirrhosis and HCC (Thomas and Zhu, 2005). Cirrhosis is the single most common underlying risk for HCC and is associated with hepatic injury due to viral infection or chronic ethanol abuse. There is a common pattern of disease progression beginning with steatosis, necrosis and inflammation. Inflammation precipitates activation of hepatic stellate cells leading to increased collagen deposition, fibrosis and cirrhosis (McKillop, 2006; McKillop, 2005; Thorgeirsson, 2002). Hepatocarcinogenesis is considered a multi-hit model; beginning with initial exposure to a carcinogen which can initiate hepatocyte transformation followed by chronic hepatitis and inflammation that leads to fibrosis and cirrhosis (Thorgeirsson, 2002). Malignant cells pass through three stages, initiation, promotion and progression whereby transformed cells progress histologically from benign precursor lesions to malignant neoplasms (Domínguez-Malagón, 2001) (Figure 1.1: schematic illustration of initiation, promotion and progression). This multistage process has been described in a variety of organ systems (Dragan and Pitot, 1992).

1.2.2. Initiation of HCC: The first stage in hepatocarcinogenesis is marked by formation of abnormal individual cells with irreversible genetic changes. This occurs

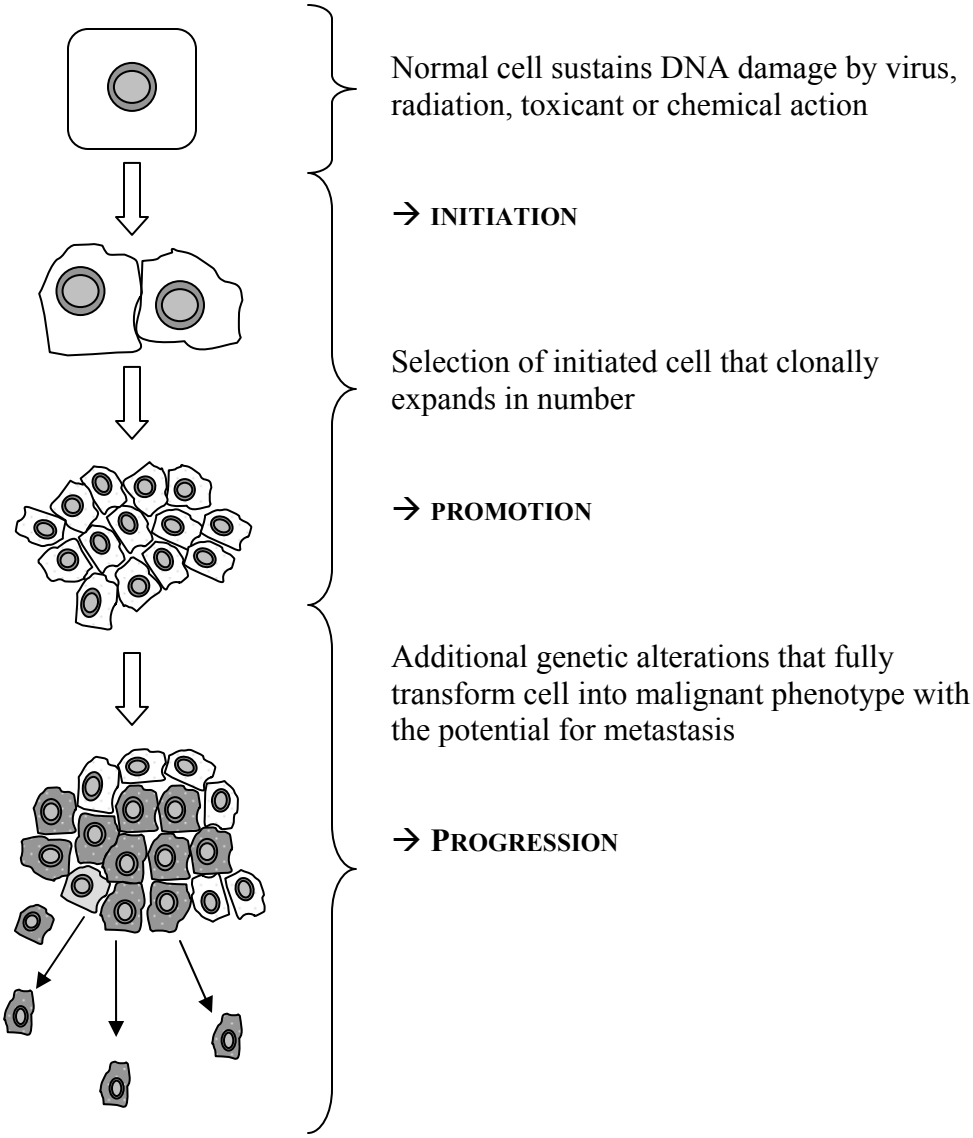

Figure 1.1: Multistage carcinogenesis can be divided into three distinct stages: In the first phase tumor initiation is characterized by mutational events affecting the DNA leading to activation of oncogenes and/or inactivation of tumor suppressor genes. Tumor promotion is characterized by the clonal expansion of selected initiated cells, and the final stage is malignant conversion which occurs through the accumulation of additional mutations that allow for increase in tumor growth and the acquisition of invasion and metastasis potential. Modified from (Lin and Karin, 2007)

through activation or disabling of cellular circuits that control cell division, survival, and senescence (Hanahan and Weinberg, 2000; Thorgeirsson, 2002). These cells are generated through somatic mutations in normal hepatocytes or by genotoxic actions of hepatocarcinogens. Many xenobiotic compounds ingested and metabolized by the liver can become activated by cytochrome P450 enzymes to pro-carcinogens that induce structural and regulatory genetic changes that generate these early mutations, thereby increasing the potential for hepatocarcinogenesis (Czekaj, 2004; Dragan and Pitot, 1992). Additionally, these hepatocarcinogens are often both mutagenic and cytotoxic and contribute to increased generation of intrahepatic reactive oxygen species (ROS) (Ogawa, 2009). DNA-damaging agents, such as ROS, increase the mutation rate within cells (Storz, 2005). ROS can induce direct effects on DNA, as well as modulate signaling cascades that contribute to tumor development (Storz, 2005). Early stages of initiation are associated with increased chromosomal instability (CIN) and genetic mutations, which can lead to a malignant phenotype (Barash et al., 2009; Domínguez-Malagón, 2001). Genetic mutations that activate genes capable of promoting cell proliferation or survival potential drive the initiation phase of carcinogenesis (Czekaj, 2004; He et al., 2008; Ogawa, 2009; Sasaki, 2006). However, initiation by itself is not sufficient for cancer to progress. Additional selective pressure on these cell populations can be derived from non-parenchymal cells within the lesion creating a favorable microenvironment for promotion and progression (Ogawa, 2009; Thorgeirsson, 2002). Selected initiated cells have the potential to expand clonally in the presence of promoting factors (Dragan and Pitot, 1992).

1.2.3. Promotion of HCC: Promotion occurs when the pool of initiated cells expand to form pre-neoplastic lesions. Promotion requires the expression of growth factors or cytokines that initiate a proliferative phenotype (He et al., 2008). This process occurs either through cellular, or extracellular, signals that lead to immortalized cells that are concomitantly resistant to growth inhibitory signals, apoptosis and anti-tumor immunity (He et al., 2008). During promotion selected initiated cells clonally expand into foci of altered hepatocytes (AHF) that are responsive to a promoting agent. This step is thought to be reversible and may require chronic exposure to the promoting agent for an extended period of time (Domínguez-Malagón, 2001). Key to the actions of the promoting agent during this stage is the potential reversibility of its actions on initiated cells on withdrawal (Dragan and Pitot, 1992). These cells are thought to be heterogeneous precursor cells that possess a variety of genetic alterations. One (or more) of these genetic changes likely conferring enhanced survival, and these cells have the potential for full malignant transformation (Dragan and Pitot, 1992).

1.2.4. Progression of HCC: During progression, subsets of AHF (1-5%) progress to a completely neoplastic phenotype (Domínguez-Malagón, 2001). This process is marked by accumulation of additional genetic mutations that permit these cells to overcome restrictions on proliferation, escape apoptosis, and obtain a motile phenotype. Unlike the stages of initiation and promotion, progression is an irreversible transition (Dragan and Pitot, 1992). Transformation into a malignant immortalized cell is associated with increases in expression of oncogenes and inhibition of tumor suppressors. Necessary changes in gene expression are not limited to transcriptional activation, but also translation and post-translational mechanisms (Domínguez-Malagón, 2001). Tumor

progression can be enhanced by the presence of superoxide anions ($O_2^{-\bullet}$), and hydrogen peroxide (H_2O_2), both of which have been reported to activate pathways that induce cell proliferation and promote survival during tumor progression (Sasaki, 2006; Storz, 2005). Oxidative stress and hypoxia within the tumor environment can also activate signal pathways that promote neovascularization, a critical step in tumor progression (Storz, 2005).

1.3. Role of ethanol/ethanol metabolism in hepatic injury:

1.3.1. Ethanol Metabolism in Hepatocytes: As with many xenobiotic compounds, the liver is the primary site of ethanol metabolism and absorption (Lieber, 2000; Nagy, 2004). There are three metabolic pathways for catabolism of ethanol. Two successive oxidation reactions are required to metabolize ethanol and produce acetate and water (Lieber, 2000; Nagy, 2004). Each pathway contributes differently to the elimination of ethanol and each is localized to different sub-cellular compartments. These pathways generate the same primary metabolite, but exert different metabolic consequences on hepatic function (Lieber, 2000; Nagy, 2004). The liver removes approximately 90% of ethanol in circulating blood following oral ingestion (Lundquist, 1962). The first metabolite in the oxidation of ethanol is acetaldehyde, a toxic and highly reactive intermediate that is a known carcinogen (Cunningham, 2003; Lieber, 2000; Lundquist, 1962; McKillop, 2005; Nagy, 2004; Poschl and Seitz, 2004; Seitz and Becker, 2007). Ethanol is first converted to acetaldehyde by removing two electrons which are transferred to nicotinamide adenine dinucleotide (NAD) to form reduced nicotinamide adenine dinucleotide (NADH) and acetaldehyde (Cunningham, 2003; Lieber, 2000). Acetaldehyde is, in turn, oxidized by aldehyde dehydrogenase (ALDH) to acetate and

water within the respiratory chain of the mitochondria (Cunningham, 2003; Lieber, 2000). Polymorphisms in the enzymes associated with these pathways can influence rate of absorption, distribution and elimination of ingested ethanol (Cunningham, 2003; Lieber, 2000; Nagy, 2004). The contribution of each pathway to the elimination of ethanol are regulated, in part, by the rate and amount of ethanol consumed as well as duration of exposure (Figure 1.2, Major pathways of ethanol metabolism).

Alcohol dehydrogenase (ADH), a zinc metalloenzyme is located in the cytosol and accounts for the majority of ethanol metabolism with moderate, short term exposure (Lieber, 2000; McKillop, 2005; Nagy, 2004). The microsomal ethanol oxidizing system (MEOS), located in the endoplasmic reticulum, utilizes an inducible mixed function oxidase; cytochrome P450 2E1 (CYP2E1), which is activated under conditions of excessive or chronic ethanol exposure (Lieber, 2000; McKillop, 2005). The third pathway mediated by catalase and located in the peroxisomes requires a mechanism for generating hydrogen peroxide (H_2O_2) (Lieber, 2000). It appears to act only in the presence of high concentrations of ethanol and has a limited role in ethanol metabolism (Alter, 2009; Lieber, 2000; Nagy, 2004).

1.3.1.1. Alcohol Dehydrogenase Pathway: Alcohol dehydrogenase (ADH) genes encode a family of enzymes that metabolize several substrates that enter the liver for biotransformation and elimination. Five different classes are encoded in seven genes (ADH1-ADH7) (Edenberg, 2007; Jelski, 2008b; Lieber, 2000; Lieber, 1997b). These enzymes function to metabolize hydroxysteroids, lipid peroxidation products, ethanol and retinol (Jelski, 2008b; Lieber, 2000). They are zinc-dependent homo- or heterodimeric isoforms, class I, II and IV are important for ethanol metabolism. Class I and II being

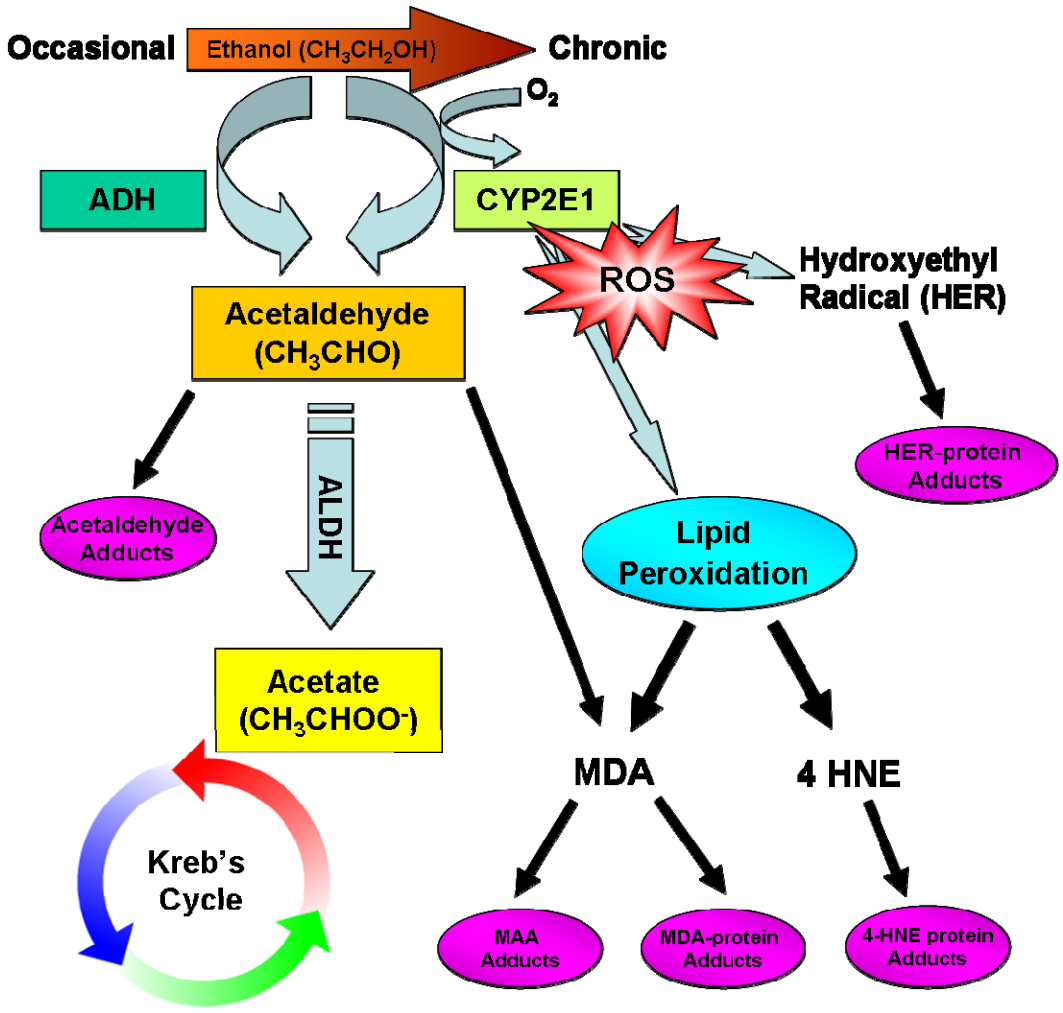

Figure 1.2: ADH and CYP2E1 pathways of ethanol metabolism: Under moderate occasional consumption, most EtOH is metabolized by ADH/ALDH to acetate and water. Chronic, long term consumption induces the microsomal ethanol oxidizing system (MEOS) pathway and cytochrome P450 2E1 (CYP2E1). This pathway generates reactive oxygen speices (ROS), partially reduced EtOH product – hydroxyethyl radical (HER) and lipid peroxidation by-products MDA and 4-HNE (modified from McKillop and Schrum 2006).

identified and characterized in the liver (Jelski, 2008b; Lieber, 2000). Several ADH isoenzymes are expressed in the gastric mucosa and account for first pass ethanol metabolism (Lieber, 2000). Chronic long term exposure reduces the expression of gastric ADH and impairs the efficacy of first pass metabolism (Lieber, 2000).

Three different polymorphisms of ADH2 have been identified; ADH2*1, ADH2*2 and ADH2*3 produce enzymes with varying rates of ethanol metabolism and production of acetaldehyde (Jelski, 2008b; Monzoni, 2001). Numerous studies have attempted to link these variations to both ethanol dependence and the severity of hepatic disease (Jelski, 2008b; Lieber, 2000; Nagy, 2004). Isoform ADH2*2, which may be more prevalent in individuals of Asian descent, is the most active isoenzyme. It produces acetaldehyde at a rapid rate that leads to untoward side effects, such as facial flushing, and tachycardia. This isoform has been linked to formation of hepatic lesions (Jelski, 2008b; Monzoni, 2001). Early hepatic effects initiated by ADH mediated metabolism relate to changes in REDOX status through alterations in hepatocyte NAD/NADH ratios.

1.3.1.2. Cytochrome P450 2E1 Pathway: Chronic long-term exposure to ethanol induces the microsomal CYP2E1 enzyme. It has been reported to increase 4-10 fold in livers of chronic ethanol users (Lieber, 2000; Lieber and Decarli, 1989). CYP2E1 is an enzyme from the cytochrome P450 superfamily of hemeproteins that serve as terminal oxidases during biotransformation of ingested and endogenous compounds. Oxygen is required for its catalytic function, as such small amounts of $O_2^{\cdot -}$ can be produced during decay of oxygenated p450 complexes. This enzyme is not limited to metabolic conversion of ethanol to acetate and water, but participates in the metabolism of many xenobiotics that produce reactive, often toxic metabolites and activate pro-carcinogens

(Cederbaum, 2006; Lieber, 2000; Lu, 2008). This activity is enhanced in alcoholics and has been reported to persist for weeks after cessation of ethanol consumption (Lieber, 2000). The induction of this enzyme is thought to contribute to enhanced ethanol tolerance that has been identified in alcoholics (Lieber, 2000; Lu, 2008). Metabolism mediated by CYP2E1 represents a major source of ROS during its catalytic cycle (Cederbaum, 2006; Lieber, 2000; Lu, 2008). In addition to acetaldehyde, this enzyme is poorly coupled and produces several species of oxy-radicals that can contribute to ethanol-mediated injury. This pathway is a source of partially reduced O_2 to $O_2^{\bullet-}$ with generation of H_2O_2 following dismutation of the superoxide anion. It also allows for incomplete oxidation of ethanol, resulting in the formation of 1-hydroxyethyl radical (HER) (Cederbaum, 2006; Koop, 1992; Lu, 2008). CYP2E1 mediated metabolism is a major source of oxidative stress resulting from the imbalance between ROS formation and clearance, combined with the repair of ROS mediated cell damage. Reactive oxygen species react with cell constituents, inactivating enzymes, denaturing proteins and damaging DNA. These processes promote depletion of cellular antioxidant GSH which can exacerbate free-radical toxicity and lipid peroxidation (Albano, 2006; Lieber, 2000).

A genetic polymorphism has been identified in the promoter region of the CYP2E1 gene (Cederbaum, 2006; Monzoni, 2001; Nagy, 2004). This polymorphism, identified as C2, is characterized by increased CYP2E1 gene expression. The contribution of the C2 variant on ethanol-induced liver injury and oxidative stress has not been determined (Cederbaum, 2006; Monzoni, 2001; Nagy, 2004). Most ethanol is metabolized by ADH, but chronic long-term or excessive consumption induces CYP2E1, amplifying its function during clearance of ethanol from the body (Caro, 2004;

Cederbaum, 2006). A major source of ROS in hepatocytes is from ethanol-inducible CYP2E1, and ethanol exposure increases CYP2E1 activity by 4-10 fold (Albano, 2008; Cederbaum, 2006; Lieber, 2000; Ronis, 1996). This increase in levels of CYP2E1 is primarily by a post-translational mechanism involving substrate binding and stabilization of the enzyme (Cederbaum, 2006). (Figure 2: Major pathways of ethanol metabolism).

1.3.1.3. Acetaldehyde Metabolism: Acetaldehyde dehydrogenase catalyzes the oxidation of 90% of all acetaldehyde produced from ethanol, converting it into acetate and water (Jelski, 2008a; Lieber, 2000). Hepatic clearance of acetaldehyde is primarily dependent on the action of ALDH I, a cytosolic enzyme, and ALDH II located in the mitochondrial matrix (Jelski, 2008a). Liver mitochondrial ALDH II accounts for the catabolism of more than 65% of acetaldehyde, while ALDH I removes approximately 20% of acetaldehyde generated during ethanol metabolism (Jelski, 2008a). As with ADH, there are polymorphisms in ALDH that influence the rate of acetaldehyde elimination (Jelski, 2008a). Two alleles have been identified for ALDH II; ALDH2*1 and ALDH2*2 (Vasiliou, 1999). It has been reported that individuals possessing the ALDH2*2 variant are deficient in ALDH activity (Jelski, 2008a; Vasiliou, 1999). This leads to rapid accumulation of acetaldehyde on consumption of ethanol that is accompanied by adverse side effects, facial flushing, increased heart rate, and headache (Jelski, 2008a).

1.3.1.4. Sex-mediated differences in ethanol metabolism: Individual variations are known to exist in the metabolic clearance of ethanol. In some cases these variations can be attributed to polymorphisms in the genes encoding transforming enzymes ADH, ALDH and CYP2E1 (Edenberg, 2007; Monzoni, 2001; Simon, 2002). Additionally, sex related differences have been reported to contribute to variations in the absorption,

distribution and elimination of ethanol (Chen, 1999; Crabb, 1995; Lieber, 2000; McKillop, 2005; Qulali and Crabb, 1992). On consumption, ethanol is rapidly absorbed into the bloodstream from the stomach and small intestine (Mumenthaler, 1999). This rate of absorption is influenced by the amount and concentration of ethanol ingested, the presence or absence of food in the digestive tract, and the rate of hepatic metabolism of ethanol entering the liver from the portal vein. Women demonstrate higher blood alcohol content (BAC) following ingestion of equal amounts of ethanol compared to men (Mumenthaler, 1999).These differences relate in part to body composition, women have a lower total water content and higher fat content compared to men which can influence the volume of distribution of ethanol (Mumenthaler, 1999). Women also demonstrate a lower rate of first pass metabolism. Although this remains controversial, some studies reporting that women have lower gastric ADH activity that accounts for a small fraction of first pass metabolism (Frezza et al., 1990; Lieber, 2000; Mumenthaler, 1999). Other factors including genetics, age, chronic ethanol ingestion, and gastric morphology, also influence expression and efficacy of gastric ADH during first pass metabolism (Julkunen, 1985; Yin, 1997). Additional evidence suggests that estrogen influences the expression of both ADH and CYP2E1 (Chen, 1999; Simon, 2002).

Women are reported to have an increased susceptibility to the toxic effects of ethanol and ethanol induced liver injury in response to chronic ethanol ingestion (Becker, 1996 ; Donato et al., 2002; Frezza et al., 1990; Lieber, 2000). This is likely due to a combination of factors that relate to metabolism, pharmacokinetics and estrogen-dependent immune response. Livers of females exposed to ethanol tend to have increased fat accumulation, high levels of plasma endotoxin, more infiltrating neutrophils and

increased oxidative stress and free-radical adducts (Thurman, 1998). Estrogens are reported to increase gut permeability and portal endotoxin levels which in turn amplifies Kupffer cell activity and increases expression of pro-inflammatory cytokines (Kono et al., 2000; Thurman, 1998).

Female rats exposed to ethanol demonstrated a two-fold increase in nuclear factor-κB (NFκB), a transcriptional factor that mediates immune response, and a 3-fold increase in inflammatory cytokine TNFα mRNA (Kono et al., 2000). Despite an increased susceptibility to ethanol induced liver injury identified in females, the long term sequela with progression to fibrosis, cirrhosis and HCC are more common in males (Becker, 1996 ; El-Serag, 2007; McKillop, 2005; Yu and Chen, 1993)

1.3.2. Ethanol and Hepatocarcinogenesis: Chronic ethanol abuse in humans is defined as ingestion of more than 50-70 grams per day for a prolonged period of time, and there is a strong correlation with heavy alcohol intake and hepatic disease (Cunningham, 2003; Lieber, 2000). Initial injury following chronic, prolonged exposure consists of steatosis (fatty liver). As consumption persists, injury advances to alcoholic hepatitis, fibrosis, cirrhosis, and can ultimately lead to HCC (Bosch, 2005; McKillop, 2006; Thorgeirsson, 2002). The mechanisms involved remain unclear, in part due to the impact of other complicating factors such as nutritional deficits, and variations in the types and frequency of beverages consumed, as well as exposure to other toxins (Lieber, 2001; McKillop, 2005). There is no consensus on the relationship between dose-effect and risk of HCC (Donato et al., 2002). HCC develops in people with cirrhosis caused by chronic excessive ethanol abuse. Ethanol by itself has not been identified as a carcinogen in animal studies, and a direct link between alcohol liver injury and HCC has not been

established, (Seitz et al., 1998; Seitz and Becker, 2007). Rather, it is the metabolism of alcohol and metabolites produced in the liver are thought to contribute to injury and hepatocarcinogenesis (Poschl and Seitz, 2004; Seitz and Becker, 2007). Many of the deleterious consequences of ethanol and ethanol metabolism on hepatic function relate to the specific metabolic and toxic disturbances that are inherent to each metabolic pathway. Actions of ethanol can be direct or indirect and can differ for men and women in part due to differences in metabolic clearance (Donato et al., 2002). In addition, there is synergy between ethanol consumption and other risk factors in the progression of liver disease to fibrosis, cirrhosis and HCC (Donato et al., 2002).

1.3.2.1. Altered REDOX Status and ROS: Effects of ethanol in the liver can be direct and indirect in nature, and their severity is dependent on many factors. Major metabolic changes resulting from ethanol metabolism produce a shift in hepatic REDOX status (Lieber, 2000; Nagy, 2004). Oxidation of ethanol produces acetaldehyde and H^+ which reduces NAD to NADH. Oxidations of acetaldehyde by ALDH in the second step of this process generate additional H^+ and lead to the accumulation of excess reducing equivalents which overwhelm the ability of hepatocytes to maintain REDOX homeostasis (Lieber, 2000; McKillop, 2006). This shift in cell REDOX status impairs carbohydrate and lipid metabolism and contributes to overall metabolic stress and morphological changes within hepatocytes (Lieber, 2001).

There are multiple mechanisms for production of free-radicals during ethanol metabolism (Albano, 2006; Bailey and Cunningham, 2002; Lieber, 2001; McKillop, 2006). Major sources of ethanol-induced ROS and reactive nitrogen species (RNS) occur at different sub-cellular levels during enzymatic reactions (Albano, 2006; Lieber, 2001).

The formation of ROS, such as $O_2^{\bullet-}$ and H_2O_2 represent important mediators of oxidative injury in many diseases (Albano, 2006). Superoxide is produced in several reactions, while it is not a potent oxidant *per se*, many other oxy-radicals are derived from it (Albano, 2006). Reduction of $O_2^{\bullet-}$ by superoxide dismutase (SOD) generates H_2O_2. When this reaction occurs in the presence of transition metals such as iron (Fe^{2+}/Fe^{3+}), which is often released from hepatocytes, hydroxyl radicals ($OH^{\bullet}$) can be generated in a Fenton reaction (Albano, 2006; Cunningham, 2003; Knect, 1993; Lieber, 2001). Superoxide can also react with nitric oxide $NO^{\bullet}$ to form peroxynitrite ($ONOO^-$). Either of these (hydroxyl or peroxynitrite) radicals can interact directly with ethanol to produce an α-hydroxy-ethyl radical (Knect, 1993). Most RNS are derived from $NO^{\bullet}$, but the extent to which this molecule is protective or damaging remains unclear. Hepatic nitric oxide signaling promotes cell survival and is anti-apoptotic in hepatocytes. It is also required for hepatic regeneration following liver injury (Fausto, 2000). Additionally, hepatic vasoconstriction associated with acute ethanol exposure and cirrhosis is associated with decreased synthesis of $NO^{\bullet}$ (Albano, 2008). Nitric oxide also inhibits lipid peroxidation by attacking lipid peroxyl radicals and terminating lipid peroxidation reactions (Rubbo, 2000).

1.3.2.2. Pathobiology of Aldehydes: The first metabolite produced in all metabolic pathways during hepatic ethanol metabolism is acetaldehyde (Jelski, 2008a; Lieber, 2000). Numerous *in vitro* and *in vivo* experiments have demonstrated that acetaldehyde has direct mutagenic and carcinogenic effects (Homann, 2001; Lieber, 2000; Muller and Sies, 1987; Seitz et al., 1998; Tuma and Casey, 2003). Induction of CYP2E1 is directly associated with the stimulation of lipid peroxidation and subsequent

production of 4-HNE and MDA. These are key components of oxidative stress in ethanol related hepatic injury (Albano, 2006; Cederbaum, 2006; Lieber, 2001).

Formation of malondialdehyde (MDA) and 4-hydroxynonanol (4-HNE) occurs through the activity of ROS produced during oxidation of ethanol and by acetaldehyde. Induction of CYP2E1 with ADH, and in conjunction with impairment of mitochondrial function, can overwhelm the capacity for ALDH mediated oxidation of acetaldehyde (Albano, 2006; Lieber, 2000). This can generate an imbalance in the level of acetaldehyde that favors lipid peroxidation, and the formation of acetaldehyde adducts with cell constituents (Albano, 2006; Tuma, 1996). Acetaldehyde readily interacts with cell membranes and is a potent inducer of lipid peroxidation forming additional toxic aldehydes, MDA and 4-HNE (Tuma and Casey, 2003) Acetaldehyde and other aldehydes produced in hepatocytes during metabolic processes are chemically reactive, capable of interaction with proteins and other biological molecules including DNA to form adducts (Lieber, 2000; Muller and Sies, 1987; Seitz et al., 1998; Tuma and Casey, 2003). The presence of ROS, and DNA-ethanol or aldehyde adducts are likely key events in DNA mutagenesis that lead to malignancies, and are associated with DNA damage in organs prone to inflammation induced carcinogenesis (Barash et al., 2009; Bartsch and Nair, 2004). Additionally, impaired DNA repair during acute inflammation and oxidative stress contribute to tumorigenesis. Acetaldehyde, MDA and 4-HNE also bind rapidly to cellular proteins inducing conformational changes and impairing function (Seitz et al., 1998). Unstable adducts formed in hepatocytes can be rapidly converted to other products, or to stable adducts which can remain in the cell for extended periods of time. Acetaldehyde preferentially reacts with the lysine residues in protein sequences, while 4-HNE interacts

primarily with lysine, cysteine and histadine (Tuma and Casey, 2003). In addition, there are multiple cross reactions between aldehydes and other byproducts of ethanol metabolism, including HER that can exacerbate adduct related damage. Acetaldehyde and MDA react with proteins in a synergistic manner generating hybrid adducts consisting of two molecules of MDA and one of acetaldehyde that also target lysine (Tuma and Casey, 2003). The formation of aldehyde adducts are considered key events in the development and progression of ethanol induced liver injury.

Ethanol exerts additional effects on lipids and fatty acids in hepatocytes. Excess ethanol in hepatocytes can condense with free fatty acids in a reaction catalyzed by fatty acid ethyl ester synthase to form fatty acid ethyl ester (FAEE) (Alter, 2009; Nagy, 2004). Concentrations of these FAEEs are highest in the heart, pancreas and liver; organs that are also sensitive to the toxic effects of ethanol (Alter, 2009; Nagy, 2004). They accumulate in the plasma, mitochondrial, and lysosomal membranes and can impair the function of cell membranes and organelles (Alter, 2009).

1.3.2.3. Altered Energy Metabolism: Chronic ethanol consumption alters hepatic mitochondrial structure, impairs function, and disrupts hepatic energy homeostasis by depletion of cellular ATP (Bailey et al., 1999). Concomitantly, oxidation of ethanol in hepatocytes increases the metabolic demand for oxygen (Cunningham, 2003). This can produce oxygen deficits (hypoxia) in liver tissue, primarily the centrilobular area and central vein (Cunningham, 2003; Lieber, 2001). This localized hypoxia impairs cellular energy production during nutrient catabolism thereby inhibiting synthesis of sufficient adenosine triphosphate (ATP) to carry out biochemical reactions (Cunningham, 2003). Oxidation reactions produce excess reducing equivalents (NADH) during the transfer of

electrons. These electrons are released from NADH and transferred to a series of molecules during oxidative phosphorylation in the respiratory chain of the mitochondria (Bailey and Cunningham, 2002). Physical changes in the mitochondrial membrane produce increased membrane permeability and inhibit efficient transfer of electrons. This results in the production of superoxide anion, a source of hepatic ROS and oxidative stress (Cunningham, 2003; Lieber, 2001). Chronic ethanol consumption alters the function and activity of all complexes, except complex II of the respiratory chain (Bailey and Cunningham, 2002). These changes are associated with decreased concentrations of two sub-units of the membrane-spanning portion of the ATP synthase complex and impedes ATP synthesis in mitochondria of ethanol-exposed hepatocytes. This results in a deficit of usable energy and may impair cell stress responses (Bailey and Cunningham, 2002). Additionally, presence of ROS in the hepatocytes directly damages mitochondrial proteins and DNA which accelerates mitochondrial aging and promotes cellular apoptotic pathways (Bailey and Cunningham, 2002).

1.3.2.4. Ethanol, Oxidative Stress and Inflammation: The major source of anti-oxidant defense in hepatocytes is Glutathione (GSH), a thiol compound synthesized primarily in the cytosol, then transported into the mitochondria and nucleus, where it functions as an antioxidant and the only source for mitochondrial metabolism of H_2O_2 (Alter, 2009). There is a 50-85% decrease in mitochondrial GSH associated with chronic ethanol exposure, but this deficit is due to impaired transport not reduced cytosolic synthesis (Albano, 2006; Fernandez-Checa, 1997). The potential for ROS production, combined with impaired transport of GSH, and associated with chronic ethanol consumption, results in a depletion of antioxidant defenses and precedes morphological

changes and impaired mitochondrial function (Albano, 2006; Bailey et al., 1999). Mitochondrial DNA (mtDNA) located in the mitochondrial matrix near the inner membrane is vulnerable to damage from ROS. It lacks protective histones and has incomplete repair mechanisms (Sasaki, 2006). This vulnerability to oxidative injury likely accounts for increases in mtDNA mutations which are found in tumor cells at a rate that is 2 to 3 times higher than those found in nuclear DNA (Sasaki, 2006). These mutations adversely affect the genes encoding proteins in the oxidative phosphorylation pathway. Mutations to mtDNA produce an increase in ROS and decrease in ATP production that may contribute to carcinogenesis.

Oxidative stress is thought to be a key mediator in the priming effect of ethanol on inflammatory responses (Lieber, 2001; Nagy, 2004). Hepatocytes, Kupffer and stellate cells all appear to be sensitized to inflammatory stimuli by chronic ethanol exposure (Lieber, 2001; Nagy, 2004). Development of steatohepatitis is due in part to the increased levels of LPS that enters the liver from the portal vein. LPS is a potent activator of inflammatory responses (Albano, 2006). Generation of ROS/RNS occurs partially through NADPH-oxidase activity in activated hepatic macrophages (Kupffer cells). This is a major contributor of pro-oxidants that promote inflammatory changes (Albano, 2006; Lieber, 2000; Lieber, 2001). Chronic ethanol exposure increases gut permeability allowing bacterial cell components to enter the liver (Albano, 2006; Lieber, 2001; Thurman, 1998). Kupffer cells are activated when increased LPS from gram-negative bacteria enters the portal vein from the gastrointestinal tract and interacts with the endotoxin receptor; CD14 (Enomoto, 2001; Thurman, 1998). These activated macrophages produce ROS and the inflammatory cytokine TNFα (Enomoto, 2001;

Thurman, 1998). Of note, females have been reported to have higher levels of gut-derived LPS in their blood following ethanol exposure than males; however, the expression of androgen receptor increases risk of infection (Ikejima et al., 1998; Kono et al., 2000). The response to gut-derived LPS in Kupffer cells is amplified with chronic ethanol exposure and makes hepatocytes more vulnerable to TNFα (Hoek, 2002), although other factors must also influence this process since tolerance develops with long term exposure (Jarvelainen, 1999). Hepatic accumulation of oxidants and acetaldehyde can stimulate stellate cells to produce type I collagen (Nieto, 2006). This response is initially mediated by acetaldehyde directly, but after long term ethanol/acetaldehyde exposure activation of cytokines TGFβ and TNFα contribute to the fibrogenic process (Nieto, 2006). This establishes a complex process of liver damage and repair associated with inflammation mediated by ROS, growth factors and cytokines produced by multiple cell types in the milieu of the liver (Albano, 2006; Nieto, 2006)

One of the earliest manifestations of alcohol induced liver injury is accumulation of fatty acids, micro- and macro-vesicular steatosis (Albano, 2006; Lieber, 2000; Nagy, 2004). In many patients this is followed by cell ballooning and necrotic cell death. Steatosis is thought to result from changes in the cell REDOX state and accumulation of NADH that shifts the balance from fatty acid oxidation to activity of fatty acid synthesis and fatty acid accumulation (Lieber, 2000; Nagy, 2004). Other metabolic disturbances may also contribute to the accumulation of triglycerides (fatty acids) in the liver, including increased mobilization of peripheral fat, enhanced hepatic uptake of circulating lipids, and enhanced lipid synthesis (Lieber, 2001). It is an important link between inflammation and inflammatory immune responses, and may increase hepatic sensitivity

to oxidative stress. Additionally, it may shift hepatic metabolic responses that contribute to ethanol induced liver injury and progression to HCC.

Reactive oxygen species in cells and tissues under pro-oxidant conditions are important triggers and modulators of cell signaling. ROS are also a source for chemical modifications of biological molecules that can interfere with normal function (Arteel, 2003). The cumulative effects of these changes result in a characteristic pattern of injury that begins with hepatic steatosis, apoptosis and necrosis of hepatocytes. This is accompanied by inflammation, formation of regenerative nodules, and activation of Kupffer cells and hepatic stellate cells that can contribute to HCC progression (Alter, 2009; Lieber, 2000). Prolonged exposure to ROS initiates nuclear DNA damage, alters epigenetic programs and modifies gene expression patterns (Sasaki, 2006). Oxidative stress causes specific DNA mutations that result in base mispairing through formation of 8-hydroxy deoxyquanosine (8-OHdG) (Sasaki, 2006). This can occur by direct ROS interaction with guanine at the C8 position on DNA, or guanine oxidation in the nucleotide pool during DNA replication (Sasaki, 2006). Formation of 8-OHdG in DNA produces G to T transversions. The primary pathway for repair of this transversion is through single-nucleotide repair (Sasaki, 2006). When 8-OHdG is incorporated into DNA from the nucleotide pool A:T to C:G transversions can occur. Both errors are widely associated with mutations in oncogenes and tumor suppressors (Sasaki, 2006). In addition, this DNA damage can affect DNA methylation. DNA methylation is important in regulating gene expression and protecting from DNA strand breaks under conditions of oxidative stress (James et al., 2003).

1.4. HCC promotion and progression:

1.4.1. Ethanol in HCC Promotion and Progression**:** The risk for developing HCC increases when daily ethanol consumption exceeds 80g/day for more than 10 years (Morgan, 2004). While cessation of ethanol consumption would seem an obvious intervention to prevent the progression of liver injury and cirrhosis to HCC, this has been demonstrated not to be the case. In fact, the odds ratio of developing HCC when compared to active drinkers was demonstrated to increase 5 fold if ethanol consumption stopped within 5 years, and 4 fold if it stopped in the past 6-10 years (Donato et al., 2002; Morgan, 2004). The odds ratio did not return to that of current drinkers until after a10 year abstinence from ethanol consumption. This raises intriguing questions as to the effects of ethanol and its inherent consequences on hepatic pathology and related oxidative stress on promotion and progression in initiated cells.

Oxidative stress is a critical factor in the pathogenesis of ethanol induced liver disease progressing to cirrhosis and the formation of early pre-neoplastic lesions (Sasaki, 2006). Additionally, oxidative stress has the potential to have dual, yet opposing roles that influence all three stages of carcinogenesis (Reuter et al., 2010). Production of ROS can have anti-tumor effects through induction of cellular senescence, genomic instability and subsequent induction of apoptosis. Alternately, continuous exposure to ROS can produce clones that have high tolerance for oxidative stress that allows them to acquire malignant qualities inducing a proliferative phenotype with high genomic instability and cellular motility that is resistant to apoptosis (Balkwill et al., 2005; Storz, 2005). Hepatic tumor progression is a multistage process that occurs in the setting of hepatic cirrhosis with scar formation and fibrous septae that encompass regenerative nodules of hepatocytes and dysplastic foci (McKillop, 2006; Okuda, 2002). Inflammation and

oxidative stress within this tumor environment places selective pressure on cells favored for growth and survival.

1.4.2. Oxidative Stress and Innate Immune Response: Oxidative stress occurs when there is an imbalance between the production of reactive metabolites, free radicals and ROS and the cellular mechanisms for eliminating them. This imbalance produces damage to cell structures and biomolecules as well as somatic mutations that can contribute to cancer (Reuter et al., 2010). On initiation of oxidative injury immune cells are recruited to the site through an acute phase response that activates the innate immune system; sustained activation leads to activation of adaptive immune(Albano, 2002). The immune system serves both as a major tumor suppressor during immune surveillance, as well as an initiator and tumor promoter. Recruitment of inflammatory cells with stimulation to produce ROS is an important aspect of tumor promotion (Albano, 2002; Reuter et al., 2010). Immune surveillance is a key defense mechanism against the development of cancer. Escape from immune surveillance by transformed cells increases the probability that it will become cancerous. The immune system has a key role in mediating hepatic inflammation, but ethanol exposure can impair immune function (Albano, 2002; Hoek, 2002; Osna, 2007). In addition, oxidative stress and ROS produced during ethanol metabolism contribute to abnormal gene expression, block cell-to-cell communication and modify signal cascades leading to unrestricted proliferation, inhibition or promotion of apoptosis (Reuter et al., 2010; Vidali, 2007). The consequences of this during cancer progression can vary depending on the cell type targeted. Ethanol mediated ROS can induce apoptosis in T-regulatory cells and hepatocytes, or alternately inhibit apoptosis in populations of hepatocytes (Ishihara et al.,

2010; Vidali, 2007). Additionally, H_2O_2 and superoxide anion have been reported to induce mitogenesis, which may selectively act on initiated cells and drive promotion (Devadas et al., 2002). Decreases in the population and function of multiple immune cell types are associated with poor prognosis in HCC and are influenced by chronic ethanol exposure (Jinushi et al., 2005; Mandrekar et al., 2004; Mantovani, 2008). For example, the lytic activity of natural killer (NK) cells is decreased by ethanol exposure (Morgan, 2004). In human ethanol-induced cirrhosis there is evidence of decreased numbers as well as impaired function of NK cells, impairment of dendritic cell maturation, and decreased expression of major histocompatability complex (MHC) (Bowen et al., 2004; Jinushi et al., 2005; Mandrekar et al., 2004; Morgan, 2004). These alterations impair immune cell response and function, as well as cytokine and chemokine responses within the tumor milieu and may abrogate immunosurveillance creating a permissive environment for HCC progression (Lin and Karin, 2007; Mantovani, 2008).

Multiple cell types are activated during ethanol-induced injury, and participate in the progression of hepatic disease to cirrhosis and HCC. Stellate cells become activated, following chronic ethanol exposure from a quiescent vitamin A (retinol) storing cell to a myo-fibroblastic-like collagen secreting cell phenotype that drives fibrotic changes in the liver (Lieber, 2001). Kupffer cells and lymphocytes enhance this response by secreting pro-fibrogenic mediators such as ROS, TNFα, IL-6, and TFG-β (Albano, 2006; Hoek, 2002; Thurman, 1998). Initial steps in ethanol induced inflammation occur when Kupffer cells increase production of TNFα, an important pro-inflammatory mediator (Nagy, 2004; Thurman, 1998). This cytokine can transduce signals that regulate cell activation and proliferation, cytotoxicity and apoptosis (Nagy, 2004; Vidali, 2007). In addition, pro-

inflammatory cytokines induce hepatocytes to express class II MHC, making them capable of directly presenting intracellular oxidized proteins to CD4+ lymphocytes (Osna, 2007; Vidali, 2007). Collagen deposition, fibrosis, and cirrhosis which are an integral part of alcoholic liver disease(ALD), as well as the major underlying risk for HCC are linked to cytokines secreted by CD4+T lymphocytes (Osna, 2007; Vidali, 2007). Activation of pro-inflammatory cascades in Kupffer cells stimulates secretion of other pro-inflammatory cytokines, chemokines and receptors; IL-1β, IL-6, IL-8, macrophage chemotactic protein-1 (MCP-1, also RANTES), CD14 receptor, ROS and NO through activation of transcription factor nuclear factor-κB (NFκB) (Thurman, 1998; Vidali, 2007; Wheeler, 2003). In addition, CXC and CC chemokines and receptors have been characterized in steatohepatits, fibrogenesis and cirrhosis; CXCL 1, 5 and 8 and CCL 2, 3, 4, and 5 and receptor CXCR3 (Haukeland et al., 2006). Of these, CCL2 is upregulated by both Kupffer and stellate cells in the portal tracts and fibrous septa of liver tissue and CXCR3 is an important receptor in regulating chronic liver inflammation (Haukeland et al., 2006). These chemokines, among other functions, can induce ROS production, attract neutrophils and promote their extravastation. This correlates with recruitment of CD8+ and CD4+ lymphocytes to areas of necrosis and intralobular inflammation that is associated with alcoholic hepatitis (Vidali, 2007). Under physiological conditions, Kupffer cells respond to low concentrations of endotoxin by producing TNFα, IL-10, and ROS that down regulate antigen presentation by dendritic and endothelial cells to suppress T-cell activation.

Cytokines and chemokines are crucial in initiating and sustaining the inflammatory response in steatohepatitis. Persistent inflammation results from the

accumulation of lymphocytes which become organized into a stable inflammatory infiltrate (Day, 2006). Lymphocytes and neutrophils can be recruited from the portal tract, sinusoids or hepatic veins by chemokines, such as intercellular adhesion molecule-1 (ICAM-1), vascular cell adhesion molecule-1 (VCAM-1) and vascular adhesion protein-1 (VAP-1) present in the endothelium (Chosay, 1997). Chronic ethanol exposure and alcoholic hepatitis are linked to an increase in the expression of these molecules in portal and hepatic endothelial tissue, due in part to TNFα (Adams, 1994; Hoek, 2002; Lieber, 2001). Additionally, cytokine expression can positively or negatively influence CYP2E1 expression (Wang et al., 2010; Z. Abdel-Razzak, 1993).

Increased titers of auto-reactive antibodies and antibodies that target acetaldehyde, MDA, 4-HNE adducts or HER have been identified in patients with ethanol-induced cirrhosis (Albano, 2002; Israel et al., 1988; Vidali, 2007). Additionally, liver specific antibodies, anti-nuclear (AN), smooth muscle-α-actin (SMA), as well as antibodies to ADH, and CYP2E1 have also been found in these patients (Stewart et al., 2004). The presence of these antibodies increases the ability to trigger antibody mediated cytotoxicity and correlates with both lymphocyte infiltration and frequency of hepatocyte apoptosis (Albano, 2002; Stewart et al., 2004). Clinical studies report elevated titers of antibodies towards lipid-peroxidation adducts, and oxidized phospholipids are more prevalent in chronic ethanol drinkers with fibrosis and cirrhosis than in patients with no liver injury or those with fatty liver only (Vidali, 2007). Presence of these antigens is associated with B-cell activation and leads to increased periportal infiltration of T-lymphocytes that express markers associated with activation, and memory phenotype that

also possess an increased capacity for secreting pro-inflammatory cytokines (Batey et al., 2002; Osna, 2007).

Metabolic and nutritional factors likely contribute to modulation of inflammatory and immune responses during ethanol induce injury. Obesity and diabetes have been identified as features of comorbidity in the development and progression of disease (Vidali, 2007). Adipose tissue secretes adipokines (leptin and adiponectin) that can modulate immune responses (Rogers et al., 2008; Tilg and Moschen, 2006). Adiponectin is reported to exert an anti-inflammatory action by depressing B-cell proliferation and T-cell activation. Conversely, leptin has demonstrated pro-inflammatory activity by favoring a Th1 cytokine profile and stimulating T-cell survival and proliferation (Tilg and Moschen, 2006). Chronic ethanol ingestion suppresses adiponectin which may potentiate a pro-inflammatory Th1 response (Rogers et al., 2008; Vidali, 2007). Disruption or exploitation of these processes by tumor cells may create a permissive environment for promotion and progression in HCC.

1.4.3. Cell and Molecular Signaling: Ethanol and ROS can directly activate signaling pathways that promote proliferation and survival, notably members of MAPK and NFκB family (Aroor and Shukla, 2004; Storz, 2005). Pro-inflammatory mediators activate AP-1, NFκB, STAT1 and STAT3 in myloid derived immune cells. However, in malignant or premalignant cells these transcription factors can mediate proliferation, survival and angiogenesis contributing to cancer progression (Yoshimura, 2006). Ethanol and oxidative stress are inducers of NFκB which up-regulates ≈100 genes on its activation to coordinate inflammatory and innate immune responses (Reuter et al., 2010). In addition to pro-inflammatory genes, many of these target genes induce proteins that

promote angiogenesis and inhibit apoptosis (Yoshimura, 2006). Pro-inflammatory cytokines also activate the MAPK cascade which leads to activation of cJune NH2-terminal kinase (JNK) and p38 or c-fos through IL-6 signaling. This induces AP-1 which has been demonstrated to have a role in cancer progression (Yoshimura, 2006). STAT1 and STAT3 are important links between inflammation and cancer as well as anti-tumor immunity. STAT3 is persistently phosphorylated in HCC and up regulates genes important for tumor progression, while STAT1 which induces growth inhibition and apoptosis, has comparatively low phosphorylation levels in HCC (Yoshimura, 2006). Oxidative stress and ethanol associated changes in energy metabolism can institute a state of hypoxia in hepatic tumors that leads to activation of genes involved in angiogenesis through HIF1α and VEGF. Neovascularization through this pathway has been reported to be a critical step in cancer progression (Behrend et al., 2003; Storz, 2005; Torimura et al., 1998). In addition to regulating growth and angiogenesis, ethanol and ROS can activate pathways that direct metastasis and motility. The cellular processes linked to this are associated with decreased cell adhesion and increased migratory potential that allows cancer cells to enter the vasculature and escape detachment-induced cell death (Storz, 2005).

1.4.4. Role of Sex Hormones in Promotion and Progression: Risk of developing HCC is 2 to 8 fold higher in males compared to females, suggesting a role for sex-hormones and sex-hormone signaling, in addition to variations in risk exposure (Eagon, 1996; Eagon, 1991; El-Serag, 2007; Lui et al., 2000). Sex hormone mediated differences in hepatic tumorigenesis may be due to differential response to toxic insults that disrupt normal sexually dimorphic gene expression (Rogers et al., 2007). Natural and synthetic

sex-hormone and steroid hormone signaling have been reported to promote ethanol-induced liver injury and HCC progression (Christopherson et al., 1975; Eagon, 2001; Guy and Auslander, 1973; Henderson et al., 1973). Several studies have reported that androgens and androgen receptor (AR) signaling directly influence HCC progression and may induce a proliferative state (Nakagama, 1991; Scoccia et al., 1991; Yu and Chen, 1993). Conversely, lower incidence of HCC in females has been linked to estrogen signaling and sex differences in modulation of immune responses, liver metabolic pathways and sex dependent differences in growth hormone and receptor expression during ethanol-induced liver injury (Becker, 1996 ; Bird, 2008; Eagon, 2001; Kovacs, 2002; Naugler, 2007). Over expression of epithelial growth factor receptor (EGFR) was identified in HCC, and is reportedly enhanced by AR signaling as levels were determined to be higher in males compared to females (Scoccia et al., 1991). Inflammatory immune responses appear to be reduced by estrogen receptor (ER) α and β activation, but steatosis and infection may be sustained by AR activity (Naugler, 2007). Nuclear receptors are implicated in signaling pathways that modulate all these cell responses and male sensitivity to disease progression may be based on imbalances in nuclear signaling or cross interaction between multiple receptors. Sexual dimorphisms in expression of NFκB, STAT3, STAT1 and AP-1 have been identified and are likely influenced by AR and ER signaling. With aging and menopause protective effects of estrogen are abated and risk for hepatocarcinogenesis increases (Shimizu et al., 2001).

1.5. Antioxidants:

1.5.1. Antioxidants in Ethanol-Induced Liver Injury: Ethanol and its metabolites influence multiple cell types within the liver parenchyma that contribute to the

progressive nature of liver injury (Hoek, 2002; Yoshimura, 2006). Reactive oxygen species are generated by several mechanisms during ethanol metabolism and drive many of the toxic and inflammatory processes. Ethanol and its metabolites initiate changes in energy metabolism, ROS, and inflammation (Albano, 2006; Cunningham, 2003; McKillop, 2006). These processes promote global disruptions in both innate and adaptive immune responses, cellular and molecular signaling, as well as modifications to epigenetic programming, expression that influences disease progression (Hoek, 2002; Osna, 2007). In addition, production of other toxic aldehydes interact with cell constitutes to impede cell function, alter gene transcription, and impair DNA replication and repair. Combined, this contributes to the pattern of disease progression mitigated by oxidative stress that leads to cirrhosis and produces genetic damage that may eventually result in HCC. The link between oxidative stress and cancer and many progressive diseases has been supported by epidemiological and experimental data. This connection is further supported by success of antioxidant therapies that prevent or inhibit cancer progression (Gonda et al., 2009).

Reactive oxygen species are generated under normal physiological conditions. They are formed by incomplete single-electron reduction of oxygen (Albano, 2006; Arteel, 2003; Medina and Moreno-Otero, 2005). They are generated during many enzymatic processes in numerous cell types. In excess they have a potentially deleterious effect especially when normal defense mechanisms, superoxide disumutase (SOD), catalase, glutathione peroxidase, GSH are overwhelmed leading to oxidative stress (Albano, 2006; Albano, 2008; Medina and Moreno-Otero, 2005). Chronic ethanol exposure contributes to a state of persistent oxidative stress that may facilitate all stages

of hepatocarcinogenesis (Medina and Moreno-Otero, 2005). Antioxidants may be an effective means of preventing these deleterious effects. Numerous *in vivo* and *in vitro* studies have demonstrated that antioxidants, iron chelators or GSH replenishing agents can be effective in preventing the damaging effects of ethanol, although these studies have not translated into an effective therapy (Arteel, 2003; Medina and Moreno-Otero, 2005). Additionally, the administration of antioxidants had been demonstrated to inhibit growth and progression of many cancers (Storz, 2005).

1.5.2. Silibinin: Silymarin is the extract of *Silybum marianum* (Milk Thistle) seeds, and is a mixture comprised of 70 - 80% flavinolignads and 20 - 30% undefined chemical fraction (Gazak, 2007; Lee, 2003). The major, and most biologically active component, is silibinin, which occurs as a 1:1 ratio of two diastereomers silybin A, and silybin B (Saller, 2001). Other flavinolignans are present in the silymarin complex, isosilybin A and B, silychristin, silydianin, (Figure 1.3: Flower and molecular structures) and taxifolin. The pharmacokinetics of silymarin are generally standardized as silibinin (Lee, 2003). There is considerable variability in the proportions of the various flavinoligands. This is influenced by the environmental conditions and location in which it is grown as well as the methods under which the extractions are prepared (Gazak, 2007; Saller, 2001). Silibinin is readily available as an over-the-counter herbal supplement. Its only prescribed medical use is to prevent uptake of *Amanita phalloides,* death cap mushroom toxin in hepatocytes, thereby protecting hepatic tissue (Carducci et al., 1996). Bioavailability of silibinin is relatively low and is dependent on many factors

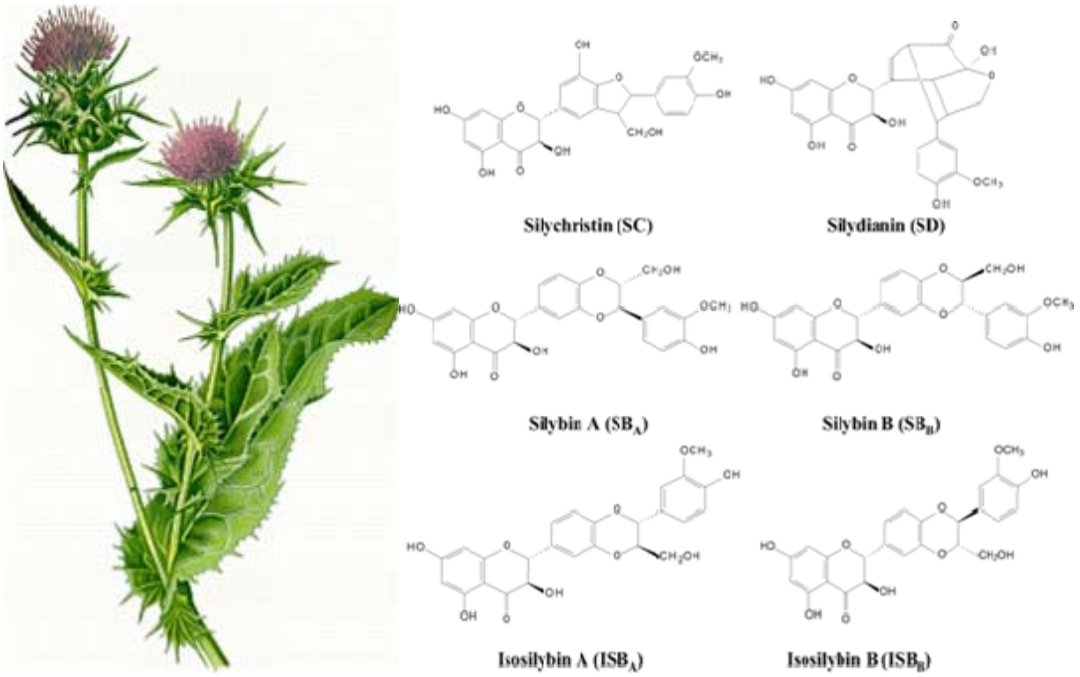

Figure 1.3: Drawing of *Silybum marianum* (Milk Thistle) and molecular structures of 6 major flavinoligands. Silymarin is derived from the seeds of the Milk Thistle plant. The extract contains a mixuture of flavinoligands consisting of, silychristin, silydianin, isosilybin A, isosilybin B, silybin A and silybin B. Silibinin is the most abundant and biological active compound in the mixture, and is comprised of a 1:1 ratio of diastereoisomers silybin A and silybin B (Wen et al., 2008)

including other components in the extract (such as fat, cholesterol, proteins), the concentration of the extract itself and variations in the individual flavinoligands (Saller, 2001). Peak concentrations in serum are reached between 2 and 9 hours after oral ingestion. A small fraction (3-8%) of silibinin is excreted in urine, 20-40% is stored in the bile as glucuronide and sulfate conjugates, and the remainder is excreted in feces unchanged (Saller, 2001). Silibinin has very few side effects, even at high dosages. This is due, inpart, to its low solubility which prevents development of toxic levels (Gazak, 2007). Side effects recorded during trials were limited to those associated with allergic reaction or gastrointestinal disturbance (Gazak, 2007).

1.5.2.1. History of silibinin: There is a long history for use of plants and plant derivitives as natural remedies by physicians, herbalists, and folk healers for treatment of diseases. Silymarin has been used for the treatment of liver and gallbladder pathologies, and as a hepatoprotectant against ingested poisons for thousands of years. It first appears in a written compendium as described by Theoprastus in the 4th century B.C (Gazak, 2007). Although largely forgotten during the Dark ages it has been mentioned in medical pharmacopeias for over 2000 years (Gazak, 2007). It is thought to function as an anti-oxidant, anti-lipid-peroxidant, anti-fibrotic, while producing anti-inflammatory, immuno-modulatory effects that promote liver regeneration. It has been used for treatment of viral and toxic hepatitis, fatty liver, cirrhosis, and ischemic injury (Saller, 2001). Currently, preparations of silibinin are used for treatment of cirrhosis, chronic hepatitis, and liver diseases associated with alcohol consumption or exposure to environmental toxins despite the fact that its efficacy in treating these diseases has not been firmly established (Gazak, 2007). Various studies report improvements in liver function as measured by

decreases in alanine-aminotranferase (ALT) levels, but there has been limited evaluation of other parameters or clinical measures (Gazak, 2007). Reports have cited both positive and negative effects in limited numbers of patients (Gazak, 2007; Saller, 2001). Additional reasons for the controversy, and lack of direct confirmation of its efficacy or mechanism of action may relate to inconsistencies in the formulations used, as well in the quality of scientific inquiries (Gazak, 2007). Additionally, the activity of silibinin on disease pathologies may be specific to the organ or cell type and bioavailability of the drug relative to dosage and time course of treatment (Saller, 2001).

1.5.2.2. Silibinin in ethanol-induced hepatic injury: Flavinoids possess antioxidant activity, which was thought to be the basis of their therapeutic effect. However, studies conducted on the free-radical scavenging properties of silibinin found that it was ineffective at scavenging superoxide anion and had no reaction with hydrogen peroxide, but reacted rapidly with hydoxy radicals (Mira et al., 1994; Saller, 2001). Silibinin is associated with increased SOD activity *in vitro* and *in vivo* as well as decreased lipid peroxidation and increased cellular GSH (Feher, 1988; Saller, 2001). Early emphasis on medical use of silibinin focused on efficacy to ameliorate high degrees of oxidative injury associated with free-radical damage in acute and chronic ethanol toxicity with and without cirrhosis (Saller, 2001). Measures of liver function as determined by ALT, and histology were improved, oxidative stress and lipid peroxidation were decreased and GSH levels were preserved (Stickel and Schuppan, 2007). In addition, patients were found to have decreased fibrotic response associated with decreased leukotriene formation in Kupffer cells. This prevented activation of stellate

cells and corresponded to a decrease in collagen type I expression (Stickel and Schuppan, 2007).

1.5.2.3. Silibinin in cancer: The majority of studies using silibinin have focused its antioxidant properties, but recent studies have identified new mechanisms of action that may have therapeutic uses in cancer treatment (Gazak, 2007). There are inconsistencies in the formulations used, which complicates assessment of efficacy. The scope of its potential application has spread beyond the liver to include the heart, brain, kidneys, skin and prostate (Gazak, 2007). These additional modes of activity, besides regulation of inflammation, include modulation of steroid hormone receptor activity and drug transporters, and chemoprotection (Cornelli, 2007; Gazak, 2007). Cellular mechanisms of its anticancer properties can be categorized as growth inhibitory, anti-angiogenic, anti-invasive, and pro-apoptotic (Bhatia et al., 1999; Chen et al., 2005; Lee et al., 2007; Momeny et al., 2008; Singh, 2004b; Tyagi, 2004; Zi, 2008). Many of these properties are activated in a very cell specific manner and are not always replicated in different cancer cell types (Cheung et al., 2010).

Silibinin exerts multiple effects on growth stimuli and growth factors. Growth inhibition associated with silibinin was identified in both LNCaP and DU134 (human prostate cancer cell line) mediated by increased expression of cell cycle inhibitors (Kip1/p27, Cip1/p21 and p53) (Chen et al., 2005; Cornelli, 2007; Varghese, 2005) . Alternate mechanisms of inhibition occurred through decreased activity of pathways activated by specific growth factors (EGF, IGF) (Cornelli, 2007; Zi, 2008). Mitogen activated protein kinase signaling (MAPK/ERK1/2) is a component of these pathways, and signaling was inhibited in prostate, cervical and bladder cancer. This occurred

through decreased phosphorylation, corresponding to decreases in cell proliferation (Cornelli, 2007; Momeny et al., 2008; Ramasamy and Agarwal, 2008; Singh, 2004a). Multiple intermediary steps are involved in growth-factor mediated pathways. Interruption of these intermediates has also been demonstrated to impede tumor growth (IRS-1, P13K/Akt) (Bhatia, 1999; Ramasamy and Agarwal, 2008; Singh, 2004a).

Silibinin has been reported to inhibit inflammatory responses and subsequently improve apoptotic responses within tumors, and decreases angiogenesis through suppression of NFκB (Saliou, 2001; Singh, 2004a). Inhibitory properties may in part be related to silibinin-mediated inhibition of mitogen activated protein kinase cascades, and JNK (Manna, 1999; Saliou, 2001). Transcription activation by NFκB is modulated by REDOX regulation and contributes to IL-6, IL-1, and TNFα expression. These cytokines, can in turn activate NFκB, which creates a positive feedback loop. Dampening of NFκB activity induces anti-cancer properties by decreasing TNFα inflammatory response, increasing apoptosis and impaired angiogenesis (Karin and Greten, 2005; Tyagi et al., 2009). This activity was modulated by silibinin, through decreased phosphoryaltion and degradation of inhibitory protein IκB (Hill et al., 1999; Saliou, 2001). Reported anti-cancer benefits of silymarin relate in part to inhibitory effects on growth and promotional effects on apoptosis. This occurs through multiple possible pathways, including p53 and facilitated release of cytochrome C with downstream activation of caspase 3 and 9 combined with a corresponding decrease in surviving protein (Manna, 1999; Singh and Agarwal, 2004).

Nuclear hormone receptors also play an integral role in activating transcription programs that can stimulate cancer growth. Silibinin, diasteriomer silybin B has been

reported to initiate partial activation of estrogen-receptors. This has implications for estrogen responsive tumors and those in which estrogen is deemed protective (Mueller, 2004). Both silymarin and silybin have demonstrated anti-androgenic activity in androgen-responsive prostate cancer cell line LNCaP (Singh, 2004a).

There has been a dramatic increase in published studies regarding the efficacy of silibinin as either an adjuvant therapy or directly to treat HCC over the past decade. Growth inhibitory effects were identified in HepG2 and HepG3 cell lines (Momeny et al., 2008; Varghese, 2005). Several pathways reported to be disrupted by silibinin are integral in the pathogenesis of HCC.

1.6. Hypothesis: Silibinin will inhibit ethanol-dependent hepatic tumor progression *in vitro* and *in vivo* by inhibiting hepatic oxidative stress associated with ethanol metabolism.

1.6.1. Specific aims:

1. Determine the effects of ethanol on cell proliferation and ethanol metabolism in the absence and presence of silibinin in a rat hepatoma cell line *in vitro*.
2. Identify mechanisms by which chronic ethanol intake alters HCC progression in male and female mice using a DEN model of hepatocarcinogenesis.
3. Define the effects and mechanisms whereby dietary silibinin alters ethanol-dependent changes in HCC progression in male and female mice using a DEN model of hepatocarcinogenesis.

CHAPTER 2: MATERIALS AND METHODS

2.1. *In vivo* Models of Hepatocellular Carcinoma

2.1.1 Animal Assurances: Male and female B6C3 $_{F1}$ mice, Jackson Laboratories (Bar Harbor, ME) were used for these studies. All animal Protocols were approved by Carolinas Medical Center Institutional Animal Care and Use Committee (IACUC). Animals were housed in the vivarium at Cannon Research Center, Carolinas Healthcare Systems, and approved by the Association for Assessment and Accreditation of Laboratory Animal Care (AAALAC).

2.1.2 Materials**:** Neonatal (21-25 day old) male and female B6C3 mice were purchased from Jackson Laboratories (Bar Harbor, ME), Diethylnitrosamine, olive oil, Heparin, 99% ethanol CH_3CH_2OH (200 proof), and silibinin (Batch # 128K1503, certified as a 1:1 ratio of silybin A and silybin B) were purchased from Sigma-Aldrich Chemical (St. Louis, Mo). Syringes (1 ml) with 23 gauge needles were purchased from VWR Scientific. Isoflurane was purchased from Abbott Labs (Abbott Park, IL). AIN-93M mouse chow and AIN-93M mouse chow with silibinin (0.5% *w/w*) was purchased from DYETS (Bethlehem, PA). Ear tags were purchased from National Band and Tag Co. (Newport, KY). Goldenrod animal lancet 5 mm purchased from MEDipoint, (Mineola, NY).

2.1.3. DEN Initiation: Mice were given access to food and water *ad libitum* and maintained on a 12-hour dark/light cycle in compliance with Research Animal Use and

Care Guide. Male and female B6C3 mice (21-25 days old) were received from Jackson Labs and allowed to acclimate to the vivarium at CMC for 48 hours. After 48 hours, mice were transported to a satellite treatment area where they were randomly divided into 24 or 48 week treatment groups, and further divided into individual male or female treatment groups designated as control (C), ethanol-drinking water only (E), silibinin diet only (S), diethylnitrosamine (DEN) initiated only (D), DEN plus ethanol drinking water (D+E), DEN plus silibinin diet (D+S), and DEN plus ethanol drinking water and silibinin diet (D+ES). Animals were then individually anesthetized by isoflurane inhalation in a bell jar. Anesthesia was confirmed by gauging response to pain stimulus. Animals were weighed and DEN, dissolved in olive oil to a final concentration of 0.1 mg/ml was administered at 1 milligram per kilogram (1 mg/kg) body weight by intraperitoneal injection using a 1 ml syringe with a 1", 23 gauge needle. Alternately, animals were given an ip injection of an equal volume of olive oil without DEN as determined by body weight. Following ip injection with DEN or vehicle animals were ear tagged and caged in individual groups and monitored for signs of distress for 4 hours prior to being transferred back to vivarium. Mice were monitored daily with weights measured and recorded once per week. Animals were allowed to recover for 15 or 39 weeks before any additional treatments were administered (Figure 2.1, Experimental timeline).

2.1.4. Silibinin diet and ethanol-drinking water regimes: Silibinin diet formulated from AIN93M mouse chow with or without 0.5% (*w/w*) Silibinin, DYETS (Bethlehem, PA) was introduced to male and female animals in Sil, D+S and DES groups commencing at 15 or 39 weeks. Animals were weighed everyday for one week and dietary intake was estimated and compared to pair-matched animals not receiving

silibinin diet. At 16 or 40 weeks animals were weaned onto ethanol drinking water regime. Initially, animal groups designated to receive ethanol drinking water (E, D+E and DES) were introduced to 5% (*v/v*) ethanol in drinking water for 3 days, on day 4 ethanol concentration was increased to 10% (*v/v*) for 2 days followed by an increase to 20% (*v/v*) at which time ethanol drinking water was alternated daily 10/20% (*v/v*) for the remainder of the experiment, with animals sacrificed at 24 or 48 weeks. On beginning either silibinin diet or ethanol drinking-water regime, alone or in combination, animal weights were measured and recorded twice each week.

2.1.5. Liver resection and tissue collection: At 24 or 48 weeks, animals were transported to satellite treatment area, and anesthetized by isoflurane inhalation. Once anesthetized, blood was collected following a sub-mandibular venipuncture into microcentrifuge tubes with Heparin (1000 Units/ml) followed by cervical dislocation. A midline incision was made with liver and spleen tissue excised. Livers were weighed, examined for visible lesions, and representative liver sections (4-6mm) taken from the left, right, median, and anterior lobes. Sections were either snap frozen in liquid nitrogen and stored prior to analysis (-80^{0}C), or fixed in 10% neutral buffered formalin (24 hours) prior to transfer to 70% (*v/v*) EtOH for histological processing/analysis.

Multiple lobes of the liver were dissected, with whole spleen and liver dissections placed in cryovials, flash frozen in liquid nitrogen, with additional sections placed in tissue cassette with optimal cryostat tissue (OCT) compound and rapidly frozen by submerging in a slurry of dry ice in -70^{o}C isopentane. Remaining liver tissue was placed in 10% neutral buffered formalin for histology.

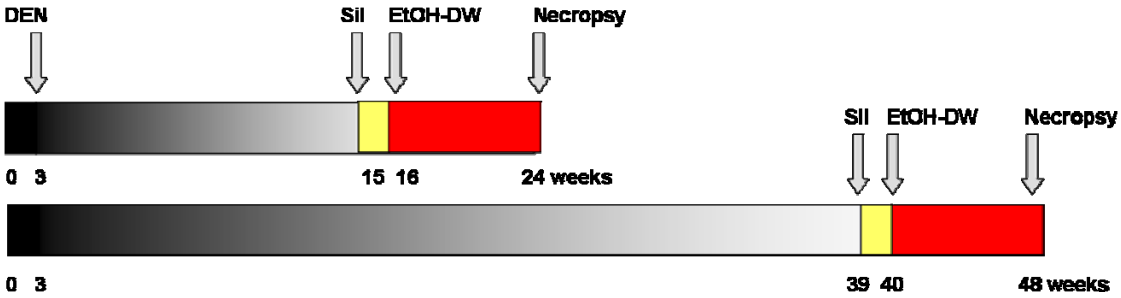

Figure 2.1: Experimental timeline. Infant mice (21-25) were give i.p. injections of vehicle (olive oil) or DEN (1 mg/kg). Silibinin diet was begun at 15 or 39 weeks continuing for 9 weeks, ethanol drinking-water was introduced at 16 or 40 weeks continuing for 8 weeks. Animals were sacrificed at 24 or 48 weeks.

2.2. Isolation of RNA:

2.2.1. Materials: RNeasy and Qia-shredder kits were purchased from Qiagen (Valencia, CA). Isopropyl alcohol, 100% ethanol, glycerol, sodium acetate, 100x Tris (hydroxymethyl) aminomethane (Tris)-Ethylenediaminetetraacetic acid (EDTA) solution ethidium bromide solution and diethyl pyrocarbonate (DEPC) were purchased from Sigma Aldrich (St. Louis, MO). Model 5402 and 5415 centrifuges and a model 5331 thermocycler were purchased from Eppendorf (Hauppauge, NY). CFX96 Touch Real-time polymerase chain reaction (PCR) detection system and SYBR Green Supermix master mix, agarose powder, gel boxes and DNA loading dye were purchased from BioRad (Hercules, CA). RQ1 DNase treatment, ImpromII reverse transcriptase with random primers for cDNA synthesis, GoTaq Green PCR master mix kits and 100 b.p. DNA ladder were purchased from Promega (Madison, WI). Primer pairs were purchased from IDT (Coralville, IA) (Table 2.1). 10x Tris-Boric Acid-EDTA (TBE) buffer was purchased from USB (Cleveland, OH). A digital camera, camera box and transilluminator, and photo acquisition software were purchased from Eastman-Kodak (Rochester, NY).

2.2.2. RNA Isolation from Animal Tissue: RNA was isolated from liver and spleen tissue from individual animals in each treatment group, as per the manufacturer's instructions using RNeasy® kits. Briefly, flash frozen tissue was homogenized in RTL buffer. This solution was then loaded into Qia-shredder® spin columns and the columns centrifuged at 16,000 *x g* for 1 minute at RT. One volume of 50% EtOH (*v/v)* in ultra-pure water was added to the flow through, pipetted and transferred to an RNeasy® column. Columns were centrifuged at 16,000 *x g* for 15 seconds at RT. Washed three

times (16,000 *x g*: 15 seconds, 15 seconds, 2 minutes at RT) with proprietary buffers as supplied in the kit. A final spin at 16,000 *x g*, 1 minute at RT was performed with 35-50 µl of DEPC water. Typical yields were between 250-500 ng/µl in 40 µl.

2.2.3. Reverse transcription PCR**:** Reverse transcription was performed, as per the manufacturer's instructions using the Promega ImProm II® RT system. Reaction mixtures were prepared in 0.5 mL PCR tube, and consisted of 0.5 µl of random hexamers (supplied as 0.5µg/ml in water), 1µg RNA template (equal amounts,1 µg from individual animals in each treatment group pooled), 1 µl RQ1 buffer and 1 µl RQ1 DNAse and nuclease-free water was added to adjust each reaction mixture to a final reaction volume/tube of 9 µl. Tubes were placed in an Eppendorf thermocycler and incubated at 37^{o}C for 30 minutes. After this incubation, the reaction was paused and 1µl RQ1 stop reagent was added, then reaction was incubated at 75^{o}C for 10 minutes followed by 25 ^{o}C for 30 seconds. At this time the reaction was paused, and a master mix, consisting of the following components (per reaction) was added: 2 µl nuclease-free water, 4 µl ImPromII-5x reaction buffer, 2 µl $MgCl_2$ (6 mM), 1 µl dNTP mix, 1 µl ImPromII Reverse Transcriptase. The total master mix volume per reaction was 10 µl, and this was aliquoted into PCR tubes and the following program completed in the thermocycler: 25 ^{o}C (5 minutes), 42 ^{o}C (30 minutes), 95 ^{o}C (5 minutes), after which the reaction was cooled to 4 ^{o}C. At this time, 300 µl 100% EtOH with 2 µl 3.0M sodium acetate (pH 5.2) was added to RT product and precipitated overnight at -70 ^{o}C, Following precipitation, cDNA was centrifuged at 4 ^{o}C, 14,000 *x g* for 10 minutes and 100% EtOH was aspirated, 300 µl 70% EtOH was added and sample vortexed followed by second centrifugation (4 ^{o}C, 14,000 *x g*, for 10 minutes). Following centrifugation 70% EtOH was aspirated and cDNA was

suspended in 35 µl nuclease-free water. cDNA was quantified yields, were typically between 100-350 ng/µl.

Measures of CYP2E1 mRNA expression performed using mouse or rat specific CYP2E1 primer pairs (Table 2.1). cDNA was diluted to 100 ng/µl and Promega GoTaq Green® master mix prepared with the following constituents (12.5 µl master mix, 1 µl forward primer (1.0 µM), 1 µl reverse primer (1.0 µM), 8 µl nuclease-free water). The total volume of master-mix per reaction was 23 µl. This was aliquoted into 0.2 mL PCR tubes and 2 µl cDNA (100 ng/µl) template was added and amplified using an initial denaturing of 95^{o}C for 2 minutes, followed by 30 cycles of 95 ^{o}C (45 seconds), 55 ^{o}C (45 seconds), 72 ^{o}C (45 seconds) and a final extension of 72 ^{o}C for 2 minutes. Final product was eluted on a 2% agarose gel containing 10µl/100 mL of ethidium bromide (EtBr), 8 µl 100 b.p DNA ladder was added to the first well and 10 µl of each reaction sample was added to subsequent wells. The gel was resolved at 90 mA until the dye front reached the end of gel, at which time, the gel was transferred to a transilluminator and digital images captured. Signal intensity was semi-quantified using NIH-ImageJ software and corrected to β-2 microgoblulin (β2M mouse) or β-actin (rat) (housekeeping gene) specific levels.

2.2.4. Quantitative reverse transcriptase PCR: qRT-PCR was performed as follows: cDNA was diluted to 25 ng/µl and a SYBR Green Supermix® master mix was prepared with the following constituents: 8.5 µl nuclease-free water, 1.0 µl forward primer (10 µM), 1 µl reverse primer (10 µM), 12.5 µl SYBR Green master mix for a total volume of 23 µl per reaction, 23 µl master mix was then aliquoted into 96 well plates and 2 µl cDNA (50 ng) template from individual samples was aliquoted into individual wells. Quantitative analysis of mRNA for mouse specific primer pairs for T-bet, GATA3,

Table 2.1: Primer pair sequences: Primer sequences against mouse (*Mus musculus*) specific CYP2E1, GATA3, SMAD3, T-bet and , β2M and rat (*Rattus norvegicus*) CYP2E1 and β-actin were selected using Primer3 software. All primer sequences were BLAST analyzed to assure specificity.

GENE	Direction	Sequence	Product
CYP2E1 *Mus musculus*	Forward	5' AGG CTG TCA AGG AGG TGC TA 3'	210 bp
	Reverse	5' GGA AGT GTG CCT CTC TTT GG 3'	
GATA3	Forward	5' GCA AAA AGG AGG GTT TAG GG 3'	190 bp
	Reverse	5' GTG GTC ACA CTC GGA TTC CT 3'	
SMAD3	Forward	5' GGG CCA ACA AGT CAA CAA GT 3'	232 bp
	Reverse	5' CTG GCT GGC TAA GGA GTG AC 3'	
T-bet	Forward	5' CCT GGA CCC AAC TGT CAA CT 3'	173 bp
	Reverse	5' AAC TGT GTT CCC GAG GTG TC 3'	
β2M	Forward	5' ATG GGA AGC CGA ACA TAC TG 3'	177 bp
	Reverse	5' CAG TCT CAG TGG GGG TGA AT 3'	
CYP2E1 *Rattus norvegicus*	Forward	5' CCT ACA TGG ATG CTG TGG TG 3'	171 bp
	Reverse	5' CTG GAA ACT CAT GGC TGT CA 3'	
B-actin	Forward	5' GAG CTA TGA GCT GCC TGA CG 3'	150 bp
	Reverse	5' GGA TGT CAA CGT CAC ACT TC 3'	

SMAD3 (Table 2.1) were analyzed on a CFX96 Touch® real time PCR detection system (BioRad) using an annealing temperature of 54^{o}C (Mantel et al., 2007; Yu et al., 2006). Samples were assayed in duplicate, and relative gene expression of each transcript was expressed as ΔcT and normalized to β-2 microgoblulin (housekeeping gene) from pair-matched controls (Livak, 2001).

2.3. Preparation of Tissue Lysates:

2.3.1. Materials: Hepes, sodium chloride (NaCl), magnesium chloride ($MgCl_2$), Triton X-100, β-glycerophostate, sodium dodecyl sulfate (SDS), sodium deoxycholate, ethylenediaminetetraacetic acid (EDTA), KH_2PO_4, K_2HPO_4,**2**-(*N*-morpholino)ethanesulfonic acid, Tris-HCl, dithiothreitol (DTT), sodium vanadate and Igepal CA-210 (nonident p40), and β-mercaptoethanol were all purchased from Sigma Aldrich (St. Louis, MO) complete protease inhibitor cocktail (PMSF, Leupeptin, Apotinin, Pepstatin) was purchased from Roche (Indianapolis, IN), Laemmli buffer was purchased from BioRad (Hercules, CA).

2.3.2. Lysates from Animal Tissue: Flash frozen Liver tissue (25 mg) was collected in the one of the buffer preparations (Table 2.2). Laemmli buffer (50 µl β-mercaptoethanol to every 950 µl Laemmli buffer was prepared for Western blots. Tissue was homogenized followed by 30 seconds of sonication, protein was quantified by BCA and equalized appropriate buffer.

2.4. Western Blot.

2.4.1. Materials: BCA Protein Assay Reagent Kit, CL-X Posure film and ECL detection reagents were purchased from Pierce Biotechnology (Rockford, IL). Tris-base, glycine, ammonium persulfate (APS), TEMED, Tween-20, NaCl, 12M hydrochloric acid

Table 2.2: Buffers used for preparation of tissue lysates: List of buffers used with chemical components required for each preparation.

Buffer	Constituents	Concentration
Radioimmunoprecipitation assay (RIPA) buffer	Tris-HCL	50 mM
	Nonident p40 (Igepal)	1% *(v/v)*
	Sodium deoxycholate	0.25% (*w/v*)
	Sodium chloride	150 mM
	EDTA	1 mM
Buffer prepared in ultra pure H_2O as a stock solution, protease inhibitors added to working solution.		
mitogen activated protein kinase (MAPK) lysis buffer	Hepes	25 mM
	NaCl	0.3 M
	$MgCl_2$	1.5 mM
	Triton X 100	1% (*v/v*)
	β-glycerophostate	20 mM
	Sodium Dodecyl sulfate (SDS)	0.1%
	Sodium deoxycholate	0.5% (*w/v*)
	EDTA	0.25 mM
Buffer prepared in ultra pure H_2O as a stock solution, protease inhibitors added to working solution		
2-(*N*-morpholino) ethanesulfonic acid (MES) buffer	Tris-HCL	50 mM
	2-(*N*-morpholino) ethanesulfonic acid	50 mM
	EDTA	0.5 mM
	Sodium Dodecyl sulfate (SDS)	0.1% (*w/v*)
Buffer prepared in ultra pure H_2O as a stock solution, protease inhibitors added to working solution		
0.1M Potassium phosphate buffer pH 6.8	K_2HPO_4	1 M
	KH_2PO_4	1 M
49.7 mL of 1M K_2HPO_4 with 50.3 mL of KH_2PO_4 diluted to 1L in ultra pure H_2O		
Protease Inhibitors:	Phenylmethylsuflonyl fluoride (PMSF)	1 mM
	Na_3VO_4	1 mM
	NaF	1 mM
Stock solutions prepared 0.1 mM/µl added to working solutions to final concentration as indicated with complete protease inhibitor tablets purchased from Roche		

(HCL), β-mercaptoethanol (BME), methanol and SDS were all purchased from Sigma-Aldrich (St. Louis, MO). Laemmli buffer, bis-Acrylamide (30%), mini-Protran electrophoresis system, min-Trans-Blot module and blotting grade non-fat dry milk (NFDM) were purchased from BioRad Laboratories (Hercules, CA). Nitrocellulose membrane was purchased from Amersham Biosciences (Piscataway, NJ). See Blue Plus II pre-stained protein molecular weight marker was purchased from Invitrogen Life Sciences (Carlsbad, CA). X-ray film was developed using a Konica SRX-101 Medical film developer (Mahwah, NJ). Densitometry was determined using ImageJ imaging software from the NIH (Rasband, 1997-2011). Molecular Devices SpectraMax 5e plate reader (Sunnyvale, CA). Electrophoresis running buffer (25 mM Tris, 0.2 M glycine and 3.5 mM SDS). Electrophoresis transfer buffer (25 mM Tris, 0.2 M glycine, 20% (*v/v)* methanol). Tween-TBS was prepared with TBS with 0.05% (*v/v)* Tween 20.

2.4.2. BCA Protein Assay: Protein concentrations were determined using a BCA protein assay kit, as per manufacturer's protocol. Protein standards (0-2000 µg/mL) were prepared using bovine serum albumin (BCA kit) diluted in RIPA buffer (prepared as describe in Section 2.2, Table 2-2). Standards and sample lysates were assayed in duplicate using a 96 well microplate. Working BA reagent was prepared by diluting reagent B with Reagent A mixture (1:50) for a 200 µl volume per analyte) and solution was added to each well containing standards and sample lysates. The plate was sealed and incubated at 37^{o}C for 30 minutes. Absorbance at 562 nM was measured on a SpectraMax 5e plate reader. The mean absorbance was corrected to zero standard absorbance and plotted *versus* protein concentration. The resulting standard curve was used to calculate the protein concentration of unknown samples. Protein concentrations

from individual samples were equalized by standard buffers and diluted to a final concentration of 2µg/µl, or alternately equal concentrations of protein from individual samples in each group were pooled and normalized to final concentration of 2µg/µl in prepared Laemmli (section 2.4.2) and boiled for 5 minutes.

2.4.3. Preparation of SDS-PAGE/ Western blot gels: SDS-PAGE gels were prepared using the mini-protean 3 electrophoresis system. The lower gel (resolving) contained 10-15% (*v/v*) 30% (*w/v*) bisacrylamide solution made with 1.5 M Tris buffer (1.5 M Tris, 15 mM SDS, pH 8.8), ultra-pure water, APS (0.75 mM) and TEMED (7mM). The upper gel (stacking) contained 13.5% (*v/v*) 30% (*w/v*) bisacrylamide solution , 32% (v/v) SDS PAGE lower buffer (0.5 M Tris, 14 mM SDS, pH 6.8), ultrapure water, APS (0.75mM) and TEMED (7 mM). Wells for protein loading were created in the upper gel using performed combs.

2.4.4. Methods immunoblot**:** Sample protein lysates were prepared in RIPA buffer, concentrations were equalized in Laemmli buffer and boiled for 5 minutes prior to loading (25-40 µg) on SDS-PAGE gel. See-blue marker plus II (10 µl) was loaded into the gel. Proteins were electrophoresed using the Mini-Protean 3 electrophoresis system and electrophoresis buffer. Proteins were transferred to nitrocellulose membranes in a Mini-Trans Blot module on ice using electrophoresis buffer. Membranes were blocked with blocking solution (5% NFDM *w/v* in TBS) for 1 hour at room temperature (RT) with rocking. Following blocking, membranes were washed 3 x 10 minutes each wash in TBS/Tween-20. Membranes were incubated overnight with primary antibody (1:1000 dilution) in blocking solution. After incubation with primary antibody, membranes were washed 3x 10 minutes each wash in TBS/Tween-20 followed by 2 hour incubation at RT

with appropriate peroxidase conjugated secondary antibody diluted 1:5000 or 1:1000 in blocking solution with rocking. Membranes underwent a final set of 3 – 10 minute washes and were incubated with ECL detection system and exposed to X-ray film before processing in Konica medical film developer. Films were scanned on an Epson scanner and digitally stored for analysis of optical integrated volume using ImageJ software.

2.4.5. Antibodies: Monoclonal anti-phosphorylated ERK 1/2 Thr202/Tyr204, Thr185/Try187 (AW39R) and polyclonal Anti-cytochrome P450 Enzyme 2E1 (CYP2E1) (AB1252) was purchased form Millipore (Temecula, CA), Anti-alcohol dehydrogenase (ADH) (SC-22750), -aldehyde dehydrogenase (ALDH 1/2)(SC-50385), Anti-Actin (SC1616), anti-extracellular regulated kinase (ERK1)(SC-93) were purchased from Santa Cruz Biotechnology (Santa Cruz, CA). Anti-rabbit biotinylated secondary antibody and anti-goat HRP conjugated secondary antibody were purchased from Santa Cruz Biotechnology (Santa Cruz, CA).

2.4.6. Densitometry and statistical analysis: All densitometry was performed using ImageJ (Rasband, 1997-2011). All statistics were calculated and charts created using Prism5, Graphpad (La Jolla, CA).

2.5. Histology, Immunohistochemistry, and TUNEL:

2.5.1. H&E and Picrosirius Red staining

2.5.1.1. Materials Histology: Superfrost plus slides 75 x 25 mm were purchased from Cardinal Health, (Dublin, OH), cover slips and permamount were purchased from Fisher Scientific (Waltham, MA). Modified Mayer's Hemotoxylin, Eosin and Picrosirius Red were purchased from American MasterTech Scientific (Lodi, CA). Xylene, hydrogen peroxide, and phosphate buffered saline were purchased from Sigma Aldrich, (St. Louis,

MO). Graded ethanol (70%, 95% and 100% (*v/v*)) were purchased from Pharmo Products (Brookfield, CT)

2.5.1.2. Methods H&E and Picrosirius Red: Tissue sections from multiple liver lobes were mounted on slides and stained with Hemotoxylin and Eosin (H&E) for morphology and Picrosirius red stained for collagen deposition. Hepatic tissue was collected at sacrifice and stored in 10% neutral buffered formalin (section 2.1.4) for at least 24 hours at RT. Liver tissue was sectioned and transferred to an appropriate tissue mold. Tissue in mold was dehydrated by a series of graded ethanol washes and processed into paraffin blocks by a series of xylene washes followed by paraffin embedding in an automated tissue processor machine. The resulting embedded blocks were cut to 4 μm sections and each section adhered to a positively charged glass slide. Mounted sections were heated to 60^{o}C for 20 minutes, and paraffin was removed and sections rehydrated in a series of xylene, graded ethanol and water washes at RT as follows: xylene (3 washes 3 minutes per wash), graded ethanol (2 washes 3 minutes/ 100% ethanol (*v/v*), 1 wash 3 minutes/70% (*v/v*) ethanol), slides were placed in distilled water (2 washes 2 minutes per wash or until clear). Rehydrated, deparaffinized sections were stained at RT in Meyer's modified Hematoxylin (4 minutes), rinsed under running water until clear and placed in a coplin jar with fresh dH_2O for final rinse prior to Eosin stain (45 seconds). Alternately, sections were stained in modified Meyer's hemtoxylin (5 minutes) for nuclear staining, Picrosirius red (1 hour) and followed by subsequent washing steps. After staining, sections were rinsed and dehydrated in a series of graded ethanol and xylene washes before coverslip mounting.

2.5.1.3. Scoring H&E and Picrosirius Red: Sections were imaged on an Olympus 1X70 microscope and digital images recorded at 100x magnification. A minimum of 10 fields per liver from multiple lobes were imaged. H&E stained slides were blind scored by three independent reviewers per modified criteria previously reported (Table 2.3) (French et al., 1993; Morgan et al., 2002). Picrosirius red staining for collagen was quantified using ImageJ software (Rasband, 1997-2011). Images were first converted to grayscale and scale was set to 200 μm as and scale bar on micrograph was measured to establish scale. Image was stacked into red, blue and green channels threshold was adjusted in green channel which demonstrated the best contrast, and set for use in all slides, % Sirius red staining as a measure of collagen was calculated.

2.5.2. Immunohistochemistry

2.5.2.1. Materials Immunohistochemistry: Superfrost plus slides 75 x 25 mm were purchased from Cardinal Health, (Dublin, OH), cover slips and permamount were purchased from Fisher Scientific (Waltham, MA). Proteinase K, phosphate buffered saline (PBS) and, hydrogen peroxide were purchased from Sigma Aldrich (St. Louis, MO), 10mM citrate buffer (pH 6.0), and methyl green stain were purchased from Poly Scientific (Bay Shore, NY), Modified Mayer's Hemotoxylin, was purchased from American MasterTech Scientific (Lodi, CA). Graded ethanol (95% and 100% (*v/v*)) were purchased from Pharmo Products (Brookfield, CT), ABC staining kit and goat or rabbit normal serum were purchased from Santa Cruz Biotechnology (Santa Cruz, CA). Steamer was purchased from Black & Decker (Towson, MD). Tissue processor model (ATP1) was purchased from Triangle biomedical Sciences (Durham, NC). Rodent

Table 2-3: Pathological scoring criteria: Scoring criteria employed in blind scoring of hisotology slides after H&E and Picro sirius red staining. Modified from standards as reported in (French et al., 1993; Morgan et al., 2002).

Pathological parameter	**Score**				
	0	**1**	**2**	**3**	**4**
Steatosis	Normal liver	Micro-vesicular fat, vesicles in <10% of hepatocytes	Micro/macro-vesicular fat vesicles, present in 10-30% of hepatocytes	Micro & macro-vesicular fat vesicles, present in >30% of hepatocytes	Macro-vesicular fat vesicles, present in multiple zones with bridging
Necrosis	Normal liver	Individual scattered necrotic cells	Scattered necrotic cell clusters <10 cells	Scattered necrotic cell clusters > 10 cells	Multiple necrotic cell clusters within field
inflammation	Normal liver	Scattered inflammatory cells	Scattered small cells inflammatory cells, hepatocyte damage in zones 1-3	Scattered small inflammatory cell collections, hepatocyte damage multiple zones	Large, multiple scattered small inflammatory cell collections extensive hepatocyte damage
Fibrosis	Normal liver	0-4%	5-9%	10-14%	>15%

Decloaker, rodent block, Tris-buffered saline (TBS), goat or rabbit polymer kit, denaturing solution Betazoid, Bajoran Purple and Vulcan fast Red DAB chromagen, were purchased from Biocare Medical (Concord, CA). A fluorescein *In situ* cell death terminal dUTP nick end label (TUNEL) detection kit was purchased from Roche (Indianapolis, IN). Olympus IX70 fluorescent microscope was used for imaging.

2.5.2.2. Methods GSTpi staining: Section (4 μm) from formalin fixed, paraffin embedded tissues were cut and mounted on Superfrost Plus slides. Sections were air dried overnight and baked in an oven at 60^{o}C for 20 minutes, after cooling they were deparaffinized and rehydrated (as described Section 2.6.1.2). After rehydration slides were placed in a staining dish containing 10 mM citrate buffer and staining dish was placed in a Black& Decker steamer (1 hour). Sections were cooled to RT and treated with 3% H_2O_2 to quench endogenous peroxidase activity for 3 minutes followed by 2x wash with dH_2O (1 minute). Sections were placed in a humidified chamber at RT and blocked with goat serum (30 minutes). Sections were incubated with anti-glutathione S-transferase placental isoform (GSTpi) (1:100 dilution). Detection was performed using an ABC kit counterstained with Mayer's hematoxylin for GSTpi. Sections were imaged at 100x magnification on Olympus IX70 microscope and digital images captured, minimum of 10 sections per liver. Area (mm^2) and multiplicity of altered hepatic foci (AHF) were determined by counting clusters (>2) of GSTpi positive cells (multiplicity) or alternately, measuring clusters (mm^2) using ImageJ software (Rasband, 1997-2011).

2.5.2.3. Methods PCNA staining: Sections (4 μm) from formalin fixed, paraffin embedded tissues were cut and mounted on Superfrost Plus slides. Sections were air dried overnight and baked in an oven at 60^{o}C for 20 minutes, after cooling they were

deparaffinized and rehydrated (as described Section 2.5.2.1). Sections were treated with 3% H_2O_2 to quench endogenous peroxidase activity and washed 2x with dH_2O (1 minute each). After rehydration slides were placed in a staining dish containing antigen retrieval solution (Rodent decloaker) and heated in a Black&Decker steamer (40 minutes). After cooling on a bench for 20 minute, slides were rinsed 2x in dH_2O. Slides were laid flat in a humid chamber and Rodent Block M was applied for 20 minutes followed by two rinses with Tris-PBS (TBS). Primary goat polyclonal Anti-PCNA antibody was applied and incubated at RT for 30 minutes followed by 2 rinses with TBS. Goat probe and goat polymer were applied for 10 minutes each with TBS rinses between applications. Betazoid, DAB chromagen was applied and allowed to develop for 1 minute followed by 2x rinses dH_2O. Sectons were counterstained with methyl green for nuclear visualization, rinsed and slides were mounted with coverslips. Sections were imaged at 200 x magnification on an Olympus IX70 microscope.

2.5.2.4. Methods *in situ* TUNEL assay: An *In situ* TUNEL assay was performed and sections counterstained with 4'-6-Diamidino-2-phenylindole (DAPI) for nuclear visualization. Sections (10 μm) from formalin fixed, paraffin embedded tissues were cut and mounted on Superfrost Plus slides. Sections were air dried overnight and baked in an oven at 60^{o}C for 20 minutes, after cooling they were deparaffinized and rehydrated (section 2.6.1.3) and stored in dH_2O. Sections were treated with 3% H_2O_2 to quench endogenous peroxidase activity an washed 2x with dH_2O followed by Proteinase K (20 μg/ml) in Tris-PBS buffer at 37^{o}C (30 minutes). Slides were laid flat in a humid chamber and covered with enzyme-probe solution, incubated at 37^{o}C (1 hour) after which a final

wash series 3x in PBS. Slides were mounted with DAPI coverslips. Sections were imaged at 200 x magnification on an Olympus IX70 microscope.

2.5.2.5. Scoring**:** A minimum of 5 sections per lobe, 2 lobes/liver were viewed and digital images captured. PCNA positive and negative cells were quantified using cell counting features of ImageJ software and established as % PCNA positive cells (Rasband, 1997-2011). Positive control for PCNA was mouse spleen. A minimum of 5 sections per lobe, 2 lobes/liver were viewed and digital images captured. Images were analyzed using ImageJ software. Image for *in situ* slides was first converted to grayscale and RBG stacked. Threshold was set in green channel and TUNEL positive cells were counted in a minimum of 5 sections per lobe, 2 lobes/liver. To confirm antibody specificity embryonic tissue was used as positive control and enzyme-free probe as negative.

2.6. BioPlex Cytokine Assay:

2.6.1. Materials: A custom BioPlex suspension array of 7 cytokines key to development or maintenance of specific T-effector responses or those implicated in liver injury and HCC (Th1 – Il-1b, IFNγ, IL-12p70, Th2 – IL-13, T-regulatory – IL-10 and cytokines implicated in liver injury – IL-6 and TNFα) was purchased from BioRad (Hercules, CA). Mouse serum diluent, standards, 96 well filtration plate, BioPlex wash buffer, pre-mixed beads coated with target antibodies were all supplied by the manufacturer.

2.6.2. Methods: To access and compare cytokine expression patterns in male and female mice at both early (24wk) and late (48wk) HCC development, a Bio-Plex custom murine cytokine array for simultaneous quantification of 7 cytokines involved in

inflammatory and effector T- cell responses (TNFα, IL-6, IFNγ, IL-12p70, IL-1b, IL-10, IL-13) was performed. Pooled serum from each treatment group was diluted 1:4 in proprietary serum sample diluents. Premixed standards were reconstituted in 0.5 ml of murine serum diluent, generating a stock concentration of 32,000 pg/ml for each cytokine and serially diluted to generate a standard curve. The assay was performed in a 96-well filtration plate supplied with the assay kit and pre-wetted with 100 µl Bio-Plex assay buffer. Premixed beads (50 µl) coated with target capture antibodies were transferred to each well of the filter plate (5000 beads per well per cytokine) and washed twice with Bio-Plex wash buffer. Premixed standards or diluted samples (50 µl in Bio-Plex assay buffer were added to each well containing washed beads. The plate was shaken (1100 rpm) for 30 sec, followed by 60 min room temperature incubation with continued shaking (300 rpm). Following incubation, premixed detection antibodies (25 µl, final concentration 2 µg/ml) were added to each well. Incubation was terminated after an additional 30 min with shaking (1100 rpm, 30 sec reduced to 300 rpm) at room temperature; beads were washed 3 times in Bio-plex wash buffer, buffer removed by vacuum filtration. Streptavidin-PE (50 µl) and shaking as previously for 10 min and washed 3 times with Bio-plex wash buffer, buffer removed by vacuum filtration. Beads were resuspended in 125 µl Bio-Plex assay buffer and shaken (1100 rpm) for 30 sec before being read on the Bio-Plex suspension array system and analyzed using Bio-Plex manager software.

2.7. Serum ALT/AST:

2.7.1. Materials**:** Serum alanine-aminotransferase (ALT) and serum aspartate-aminotransferase (AST) were measured using an ALT/GPT or AST/GOT 2-part reagent

(Thermoscientific, Pittsburg, PA) in a SpectraMax 5e plate reader, (Molecular Devices Sunnyvale, CA).

2.7.2. Methods: Mouse serum was collected and stored at -80^{o}C as described (section 2.1.4). Aliquots stored for measuring serum ALT/AST. Serum analysis was conducted as per the manufacturer's protocol. Briefly, ALT/AST infinity reagent was warmed to 37^{o}C, individual serum samples were diluted 1:10 (25 µl sample:250 µl infinity reagent). 250µl was loaded into 96 well plates and 25 µl of serum or dH_2O were added to wells in duplicate. Absorbance at 340 nm was read at 0, 1, 2 and 3 minutes and the average change (decrease) was calculated over time. Serum concentration of ALT/AST was calculated by the following formula:

$$U/L = ((\Delta Abs \times 0.275\ mL) \times 1000)/(0.025\ mL \times 6.3 \times 1)$$

Activity in U/L as determined by mean change in absorbance per minute x factor where the factor is calculated as total reaction volume in mL x 1000 divided by sample volume in mL x coefficient of NADH at 340 nm (6.3) x path length (1 cm). Absorbance was first corrected by subtracting absorbance of blank well (reagent + water). An internal standard from rat serum calculated to be between 11-14 U/L was run in parallel with each assay.

2.8. Blood Alcohol Content:

2.8.1. Materials BAC mouse serum: EnzyChrom ™ Ethanol assay kit BioAssay systems. SpectraMax 5e plate reader, Molecular Devices (Sunnyvale, CA). This is a colorimetric assay used to determine serum ethanol concentration. Assay is based on alcohol dehydrogenase activity catalyzed oxidation of ethanol in which NADH is coupled to formazan (MTT) chromagen. The intensity of the color product measured at 565 nm is proportional to ethanol concentration.

2.8.2. Methods BAC mouse serum**:** Mouse serum was collected and stored at -80^{o}C as described (section 2.1.4). Aliquots were stored for measuring serum BAC. Serum analysis was conducted as per the manufacturer's protocol. Standards were prepared from a 1% ethanol standard provided in assay kit (1 vol % ethanol = 170 mM or 785 mg/dL) 0-1% range. A working reagent was prepared as follows: for each reaction 80 µl Assay buffer, 1 µl enzyme mix, 2.5 µl NAD and 14 µl MTT was prepared a total volume of 90 µl per well working reagent was added to 96 well plates with 10 µl standard or sample in duplicate and blank wells consisting of working reagent with dH_2O. The plate was tapped gently to mix and incubated at RT for 30 minutes and100 µl of stop reagent was added to each well. The plate was placed in plate reader, and following a 15 second mixing stage, absorbance was read at 565 nm. Concentration of ethanol was calculated as

[EtOH] = Abs (sample) – Abs (Blank) divided by slope of standard curve.

2.9. TBARS for malondialdehyde:

2.9.1. Materials TBARS**:** A thiobarbituric acid reactive species (TBARS) assay kit was purchased from Cayman Chemical. This is a colormetric assay that measures thiobarbituric acid reactive substances to assess lipid peroxidation, malondialdehyde (MDA) levels in plasma, serum, urine or tissue homogenates. A SpectraMax 5e plate reader, (Molecular Devices;Sunnyvale, CA). 13 x 110 mm snap cap glass test tubes were purchased from VWR.

2.9.2. Methods TBARS from animal tissue: A TBARS assay was performed on lysates from liver tissue. Liver tissue from individual animals was weighed with lysates prepared from 25 mg of tissue in 100 µl of RIPA buffer as described (section 2.3.2, table 1) and sonicated (15 seconds) at 40 V over ice. Lysates were centrifuged at 1600 *x g* for

10 minutes at 4^{o}C, and supernatant collected for analysis. Assay was conducted as per the manufactuer's protocol. MDA standards (0-400 μM MDA) were prepared from MDA stock solution provided in assay kit and diluted in RIPA buffer. Test tubes 13 X 110 mm with snap caps were labeled and 100 μl of supernatant was added to each tube with 100 μl SDS solution and 4 mL prepared color reagent supplied with kit. Tubes were capped and placed upright in 1000 mL beaker submerged to the volume of the sample and regents in vigorously boiling water (1 hour). At termination tubes were immediately placed in ice bath to stop reaction and placed on ice (10 minutes). Tubes were centrifuged for 10 minutes at 1600 *x g*, 4^{o}C. An aliquot (150 μl) of each sample and standard were loaded into 96 well plates in duplicate, and absorbance was read at 540 nm. Average absorbance of each well was calculated and absorbance for standard (0 MDA) was subtracted. A linear curve was plotted based on Abs verses MDA concentration. Concentration of MDA was calculated as follows:

MDA μm = corrected absorbance – y intercept divided by slope.

2.10 Tissue Content Glutathione:

2.10.1. Materials GSH assay: Glutathione (GSH) assay kit Cayman Chemical. GSH serves as a nucleophilic co-substrate to glutathione transferases in the detoxification of xenobiotics. Metaphosphoric acid, triethanolamine were purchased from Sigma Aldrich (St. Louis, MO). This is a colormetric assay that measures total glutathione (GSH/GSSG) levels in tissue homogenates. SpectraMax 5e plate reader, Molecular Devices (Sunnyvale, CA).

2.10.2. Methods GSH assay: 50 mg of liver tissue was lysed and prepared in 1 mL of MES buffer as previously described (section 2.4.2). Lysates were centrifuged at

10,000 *x g* , 15 minutes at 4^{o}C, and supernatant removed. Supernatant was deproteinated as per manufacturer's protocol. MPA reagent, consisting of 5 g of metaphosphoric acid was dissolved in 50 mL water, TEAM reagent: consisting of 4 M solution of triethanolamine 531 µl in 459 µl of water. 500 µl of each sample was added to an equal volume of MPA reagent in 1.5 mL microcentrifuge tubes and vortexed, samples were then centrifuged at 2,000 *x g*, 2 minutes.

Supernatant was removed and placed in a 2 mL screw cap centrifuge tube with 50 µl of TEAM reagent. Solution was vortexed and used to determine total GSH. GSH standards were prepared in MES buffer 0-16 µM GSH. All reagents were allowed to equilibrate to room temperature prior to the start of the assay. An aliquot of 50 µl of samples and standards were loaded into 96 well plates in duplicate. Assay cocktails consisting of the following constituents: MES buffer (11.25 mL), reconstituted cofactor mixture, prepared as per manufacturer's protocol (0.45 mL), and reconsititued enzyme mixture (2.1 mL), water (2.3 mL) and reconstituted DTNB (0.45 mL)/per 96 well plate.150 µl of assay cocktail was added to each well containing standards and samples, plate was wrapped in foil and placed on an orbital shaker.. Absorbance at 405 nm was measured at 25 minutes. A linear curve was plotted based on Abs verses GSH concentration. Concentration of GSH was calculated as follows

GSH µm = corrected absorbance – y intercept divided by slope.

2.11. CYP2E1 Activity:

2.11.1. Materials hydroxylation of *p*-nitrophenol: Chemicals, *p*-nitrophenol, 4-nitrocatechol, 60% 1N perchloric acid, sodium hydroxide (NaOH), and β-Nicotinamide adenine dinucleotide phosphate hydrate ($NADP^{+}$) were purchased from Sigma Aldrich

(St. Louis, MO). Absorbance was read on a SpectraMax 5e plate reader (Molecular Devices (Sunnyvale, CA).

2.11.2. Methods hydroxylation of *p*-nitrophenol: CYP2E1 activity was determined based on the hydroxylation of *p*-nitrophenol to 4-nitrocatechol(Koop, 1986). A 0.5 mL reaction mixture was prepared as follows: protein from individual liver tissue lysates was equalized to provide 50µg total protein/reaction with (100 µmol *p*-nitrophenol and 1mmol NADP cofactor) added to each sample to a total reaction volume of 0.5 ml. Stock solutions of *p*-nitrophenol (1.0 mmol) in potassium phosphate buffer and NADP cofactor (10 mmol) prepared in 10 mmol NaOH solution. Reaction mixture was incubated for 10 minutes at 37^{o}C. The reaction was stopped by the addition of 300µl 60% (*v/v*) 1N perchloric acid. Samples were centrifuged at 10,000 *x g* for 5 minutes at RT. The supernatant was then removed, and 100µl of 10M NaOH was added. An aliquot of 250µl of samples and standards were loaded in duplicate into 96 well plates and read on a spectrophotometer at 540nm. Activity was then calculated as the amount of *p*-nitrophenol metabolized against a standard curve of known 4-nitrocatechol. Standards of 4-nitrocatechol (0-1 µmol) were prepared in potassium phosphate buffer from a 1 µmol stock solution and used to generate a standard curve to calculate the amount of *p*-nitrophenol hydroxylation/ µg total protein/minute from the following equation:

nmol/µg protein = corrected absorbance – y intercept divided by slope

CHAPTER 3: SILIBININ INHIBITS CYP2E1 MEDIATED ETHANOL METABOLISM AND ETHANOL MEDIATED PROLIFERATION IN H4IIE CELLS

3.1. Introduction:

Hepatocellular carcinoma is the most rapidly increasing type of cancer diagnosed in the United States, and represents a major health burden on a global scale (El-Serag, 2007). Chronic ethanol consumption has been identified as a major causative factor (carcinogen) for HCC development (McKillop, 2005; Seitz and Becker, 2007) and acts synergistically with other know HCC risk factors (Farazi and DePinho, 2006). Prognosis for HCC remains poor due to the cryptic nature of the disease and long latency between onset and diagnosis, combined with a lack of viable treatment options (McKillop, 2006; McKillop and Schrum, 2009). Increasing clinical and experimental evidence suggest that, following consumption, many of the detrimental hepatic effects of ethanol are attributed to hepatic ethanol metabolism (Albano, 2008; McKillop, 2005; Seitz and Becker, 2007).

Ethanol and ethanol metabolism exert direct and indirect effects on hepatic pathology. The majority of hepatic ethanol metabolism occurs in the hepatocytes, by way of two primary metabolic pathways (Lieber, 1997b; McKillop, 2005; Seitz and Becker, 2007). In the setting of moderate/acute consumption, the majority of ethanol is metabolized by alcohol dehydrogenase (ADH) to acetaldehyde, a highly reactive carcinogen that is in turn rapidly metabolized to acetate by acetaldehyde dehydrogenase (ALDH) (McKillop, 2005; Seitz and Becker, 2007). In the setting of chronic ethanol

consumption, hepatic cytochrome P4502E1 (CYP2E1) is induced (Lieber, 1997b; Lu, 2008; McKillop, 2005). Induction of CYP2E1 is associated with an imbalance in ALDH-acetaldehyde oxidation, which favors the accumulation of acetaldehyde. In addition to increased acetaldehyde, CYP2E1-dependent ethanol metabolism is poorly coupled and generates partially reduced oxygen and reactive oxygen species (ROS) leading to intrahepatic oxidative stress (Albano, 2006). These factors increase the likelihood of genetic damage and alterations in the integrity of signaling pathways that regulate and maintain cell function (Lu, 2008). Additionally, CYP2E1 induction has been identified as an important factor in the (predominately hepatic) activation of pro-carcinogens (Lu, 2008). Oxidative stress, lipid peroxidation and pro-carcinogen activation influence other hepatic and non-hepatic cell types that contribute toward progressive hepatic diseases (Lieber, 2000; McKillop, 2005).

The identification of ethanol metabolism and ROS generation/oxidative stress as major components in mediating the effects of ethanol in the liver has led to increased interest in the use of antioxidants to blunt the deleterious effects of ethanol on hepatic function (Arteel, 2003). S-adenosyl-L-methionine (SAMe) is a precursor in the synthesis of the primary endogenous hepatic antioxidant glutathione (GSH) (Garcia-Ruiz and Fernandez-Checa, 2006). Supplementation with SAMe has been reported to exert hepatoprotective effects in a wide range of animal models of hepatic disease (Karaa et al., 2008; Lu and Mato, 2008; Mato and Lu, 2007). However, the use of SAMe in clinical trials has been controversial and the results less conclusive (Ramhaldi, 2001). This has led to renewed interest in alternative therapies based on naturally occurring, plant-derived compounds including those such as silibinin, a biologically active flavinoligand derived

from the milk thistle plant (*S. marianum*) (Dhiman and Chawla, 2005; Ramasamy and Agarwal, 2008; Saller, 2007).

The aims of the current study were to determine the effects of silibinin on ethanol metabolism and enzyme expression in HCC cells, and whether ethanol and/or silibinin could act to alter the rate of HCC cell proliferation in vitro. In doing so we also sought to identify underlying mechanism(s) by which silibinin may act to slow the rate of HCC progression in the absence or presence of ethanol.

3.2 Materials:

3.2.1. Cell lines: H4IIE cells and human HepG2 (ATCC, Bethesda, MD), and HepG2 cells that had undergone mock transfection (C37-HepG2) or transfection to express constitutively active CYP2E1 (E47-HepG2) were used (C37- and E47- HepG2 cell lines were a kind gift from the laboratory of Dr A. Cederbaum, Mount Sinai School of Medicine, New York, NY).

3.2.2. General materials: Fetal bovine serum (FBS), TRIZOL ®, Minimum essential media (MEMα) cell culture medium (Gibco), fungizone, penicillin/streptomyacin (Pen/Strep), sodium bicarbonate (7.5% *w/v*), trypsin-ethylenediaminetetraacetic acid (EDTA; 0.25% (*w/v)*), G418, and Image-iT® LIVE Green-ROS detection assay kit were purchased from Invitrogen (Carlsbad, CA). 500mL filtering system with 0.22 μm pore filter, 50 mL filtering conicals with 0.22 μm pore filter, a "Mr. Frosty" Cryo 1^{o}C freezing container (Nalgene, Rochester, NY), sterile tissue culture flasks and 6 well plates were purchased from VWR (West Chester, PA). Trypan blue, Chloroform, isopropyl alcohol, dimethylsulphoxide (DMSO), ethanol, and silibinin were purchased from Sigma Aldrich (St. Louis, MO). A bright line hemocytometer was

purchased from Hausser Scientific (Horsham, PA). A Countess , Invitrogen (Carlsbad, CA). Antibodies against ADH, ALDH, and β-actin were purchased from Santa Cruz Biotechnology (Santa Cruz, CA). Antibodies specific against CYP2E1, and total/active (phosphorylated) extracellular signal regulated kinase 1/2 (ERK/pERK) were purchased from Millipore (Temecula, CA). The Lipid Peroxidation Assay kit was purchased from Calbiochem/EMD Biosciences (San Diego, CA).

3.3. Methods:

3.3.1. Culture Medium Preparation: Culture medium was prepared in a sterile, laminar flow hood. Medium constituents were combined in the filter (0.22 μm pore filter) container of a 500ml flask (MEMα, 10% (*v/v)* or 0.1% (*v/v)* FBS, fungizone, pen/strep) and vacuum filtered. Stock concentrations of filtered (0.22 μm pore filter) EtOH 1 mM/μl in PBS and a stock solution of silibinin (10 mmol) was prepared by dissolving silibinin in dimethyl sulfoxide (DMSO; 0.01% (*v/v)*). Freezing medium was prepared in a 50 mL filtering conical tube with 0.22 μm pore filter as follows: 55.5% FBS, 33.3% MEMα, 11.1% DMSO (*v/v*) and vacuum filtered. Cells placed in storage were detached using trypsin-EDTA, and following centrifugation, the cell pellet was suspended in freezing medium solution and aliquoted into cryo vials (1 mL/vial). Vials were placed in a "Mr. Frosty" cryo 1^{o}C freezing container and stored in a -80^{o}C overnight. Cryo vials were removed from the freezer container and placed in liquid nitrogen for long term storage.

3.3.2. Cell Culture Conditions and Treatments: Vials of frozen H4IIE or HepG2 cells, were removed from liquid nitrogen storage, and rapidly thawed in a 37^{o}C waterbath. The cell suspension was transferred to a 15 mL conical tube and centrifuged at 700 *x g* for 5 minutes at RT. Supernatant was aspirated and pelleted cells suspended in

10% FBS MEMα medium (*v/v*). The cell suspension was instilled into culture flasks with 10% FBS MEMα medium (*v/v*). Monolayer cell cultures were removed from culture flasks using trypsin-EDTA. Initially, medium was aspirated from culture vessel, monolayer was washed one time with PBS, and 5 mL trypsin-EDTA/ cm^2 of 0.25% trypsin-EDTA (*v/v*) was instilled into flasks and incubated at 37^{o}C for 5 minutes. Cell suspension was collected in a 15 mL conical tube and centrifuged at 700 *x g* for 5 minutes at room temperature. Supernatant was aspirated and cells suspended into fresh 10% FBS MEMα medium (*v/v*) and aliquoted into appropriate culture flasks or 6 well plates.

The rat H4IIE hepatoma cell line (ATCC, Bethesda, MD) was cultured in MEMα medium supplemented with FBS (10% *v/v*) to 75-80% confluence. At this point cells were made quiescent by replacing the culture medium with low serum MEMα (LSM; 0.1% (*v/v*) FBS) for 36 hours. For cells exposed to alcohol, an aliquot of culture medium was removed and 200-proof alcohol (diluted in PBS) was added such that the final culture medium concentration (0-75 mmol/L) was achieved. In experiments employing silibinin a stock solution (10mmol) was prepared by dissolving silibinin in dimethyl sulfoxide (DMSO) and cells were pre-treated (2 hours, 0-10μmol) prior to alcohol treatment (0-75mmol/L). Control experiments were performed in which vehicle alone (DMSO; 0.01% *v/v*) was added in place of silibinin. Culture conditions for HepG2-C37 and HepG2-C47 were identical to those for HepG2 with the exception that G418 was added to culture medium (4mg/mL).

3.3.3. Cell proliferation: Cell proliferation was initially assessed by performing sequential cell counts over a 96 hour period as previously described (Moran, 2006).

Briefly, cells were made quiescent in LSM for 24 hours then pre-treated with silibinin (10μmol) or vehicle (DMSO; 0.1% (*v/v*)) for 2 hours. At the end of this period the culture medium was removed and replaced with MEMα containing 1% (*v/v*) FBS alone or 1% (*v/v*) FBS, 10μM silibinin and/or 25mmol/L alcohol. Cells were then detached and counted at 24 hour intervals using a Countess™ cell counter (Invitrogen, Carlsbad, CA). Cell numbers were averaged for 5 independent experiments. In studies lasting >24 hours, culture medium was removed and replaced at 24 hour intervals with fresh medium containing alcohol and/or silibinin. To confirm cell count data were due to proliferation *per se*, a parallel series of experiments were performed using MTT reduction/proliferation assay. Briefly, cells were counted and plated at 10^5 cells/well onto 96-well plates. Cells were then either pre-treated with silibinin (10μmol) or vehicle (DMSO; 0.01% (*v/v*)) for 90 minutes followed by alcohol (25mmol/L), or treated with alcohol alone (25mmol/L). The MTT assay was then performed according to the manufacturer's instructions (Invitrogen, Carlsbad, CA).

3.3.4. mRNA analysis: Following H4IIE cell treatment total RNA was extracted using TRIZOL ®. Cells were removed by trypsin-EDTA and centrifuged at 700 *x g* for 5 minutes at room temperature. The cell pellet was suspended in 0.75 ml of TRIZOL reagent and pipetted several times. 150 μl of chloroform was added to TRIZOL and the mixture vortexed gently. The suspension was incubated at RT for 5 minutes, followed by centrifugation at 4^{o}C for 10 minutes at 12,000 *x g*. The aqueous phase was transferred to a clean microcentrifuge tube and 15 μl sodium acetate (pH 5.5) in 500 μl ice-cold (-20^{o}C) isopropyl alcohol was added. The mixture was vortexed and placed at -20^{o}C overnight. The suspension was removed from -20^{o}C and centrifuged at at 12,000 *x g* for 30 minutes,

4°C. Isopropyl alcohol was aspirated and the pellet rinsed in 750 µl ice-cold (-20°C) 75% ethanol (*v/v*), and the mixture vortexed. The suspension was centrifuged at 7,500 *x g*, for 5 minutes at 4°C, ethanol aspirated, and the pellet resuspended in 35 µl RNase free water.

To perform RT-PCR, 1µg of total RNA was reverse transcribed by Improm II™ (Promega) using random hexamers to generate complementary DNA (cDNA), cDNA was precipitated and resuspended in nuclease-free water to be used in PCR reactions (as described, Section 2.2.3). Briefly, 100ng of cDNA was used in each reaction with the CYP2E1 gene specific primers (Section 2, Table 1). PCR reactions consisted of 95°C for 2 minutes followed by 35 cycles of 95°C, 55°C and 72°C for 45 seconds each with a final elongation at 72°C for 2 minutes. Amplified products were resolved using a 1.5% (*w/v*) Agarose gel and stained with ethidium bromide before conversion to digital images. The level of each PCR product was then semi-quantitatively determined using Quantity One software.

3.3.5. Western Blot Analysis: Following treatment, cells were washed with PBS (4°C) and lysates prepared using RIPA buffer (ADH, ALDH and CYP2E1 analysis) or MAPK lysis buffer for ERK 1/2 (Kovach et al., 2001) (as described Section 2.3.2). In both instances lysates were aliquoted and stored at -80°C and protein levels equalized prior to analysis. Protein expression was determined by Western blot whereby cell lysates were resolved by 12.5% SDS-PAGE as previously reported (Kovach et al., 2001). Primary antibodies were diluted 1:1000 in 5% (*w/v*) nonfat dry milk dissolved in 0.05% (*v/v*) Tween-20/Tris-buffered saline (TBS). Signal intensity was determined using NIH-ImageJ and equal protein loading confirmed by stripping/re-probing membranes using a β-actin antibody.

3.3.6. Analysis of ethanol metabolism: Aliquots (100µl) of culture medium were sequentially removed (0-24 hours) and stored at -80^{o}C prior to analysis. Alcohol concentration was determined using an EnzyChrom™ ethanol assay according to manufacturer's protocol and described (section 2.8.2)(Brandon-Warner et al., 2010a). To assess ethanol loss due to evaporation, cell free culture flasks containing medium plus ethanol were assayed in parallel.

3.3.7. Analysis of lipid peroxidation, ROS/oxidative stress: Lipid peroxidation was determined using the Lipid Peroxidation Assay kit as per the manufacturer's instructions. Changes in cellular oxidative stress/ROS generation were determined using an Image-iT® LIVE Green Reactive Oxygen Species Assay in conjunction with Hoechst 33342 (for cell/nuclear localization) as per the manufacturer's instructions. Using this approach cells were either plated to single-well cover slips for microscopic analysis or into 96-well plates for quantitative analysis (at 485nm excitation-530nm emission). Untreated cells were assigned an arbitrary value of 1 and relative ROS production expressed as % carboxy-DCF fluorescence ± SEM.

3.3.8. Analysis of CYP2E1 activity: To assess whether the effects of silibinin on CYP2E1 responsiveness to alcohol treatment in HCC cells were due to direct or indirect mechanisms. To perform these studies human HepG2 cells and HepG2 cells that had undergone mock transfection (C37-HepG2) or transfection to express constitutively active CYP2E1 (E47-HepG2) were used. Cells were grown to 75-80% confluence and made quiescent in LSM prior to the addition of alcohol (25 mmol/L). 100µl aliquots of culture medium were sequentially removed (0-24 hours) and stored at -80^{o}C prior to analysis for alcohol concentration using the EnzyChrom™ ethanol assay. To determine

the contribution of CYP2E1 activity during these events we next measured the rate of hydroxylation of *p*-nitrophenol to 4-nitrocatechol in H4IIE and HepG2-E47 cells in the presence or absence of silibinin following alcohol treatment (Koop, 1986). Briefly, cells were grown to 70% confluence and treated with silibinin and/or alcohol as previously. 24 hours later cells were washed with PBS (4^{o}C), collected in KH_2PO_4 (pH 6.8, 4^{o}C), sonicated, and stored at -80^{o}C prior to analysis. Following total protein determination and correction (to100 μg/ml) hydroxylation of p-nitrophenol was performed (described section 2.12.2).

3.3.9. Statistical analysis: Data are expressed as mean ± SEM. Statistical analysis was performed using a Student t-test or one-way ANOVA with Tukey's or Dunnett's multiple comparison post tests (as appropriate) between control and treatment groups. $p<0.05$ was considered significant.

3.4. Results:

3.4.1. Ethanol metabolizing enzyme expression: Western blot analysis of ADH and ALDH expression in H4IIE cells demonstrated no significant difference in expression of either enzyme following alcohol treatment (0-75mM, 24 hours) in the absence or presence of silibinin (10μM) (Figure 3.1a, n=4 separate experiments). In contrast alcohol treatment caused a dose dependent increase in CYP2E1 expression, a significant increase being detected at 10mmol/L increasing to a maximum at 25mmol/L (Figure 3.1a, n=4 separate experiments, $p<0.05$ *versus* untreated). Of note, at higher doses of alcohol (50 and 75mM), CYP2E1 expression was lower than that observed at 25mM. To address the possibility of alcohol exerting a toxic effect at higher doses we performed a trypan blue exclusion assay. These studies demonstrated a significant

decrease in cells excluding trypan blue at alcohol concentrations of 50mmol/L (73.49 ± 2.23%) and 75mmol/L (66.05% ± 2.89%) compared to cells treated with 25mmol/L alcohol (93.10% ± 2.86). Pretreatment of cells with silibinin (10 μM, 2Hrs) followed by alcohol (10 or 25mmol/L) significantly inhibited alcohol-induced increases in CYP2E1 expression (Figure 3.1b, n=4 separate experiments, $p<0.05$).

In light of data demonstrating the effects of ethanol on CYP2E1 protein expression in the absence and presence of silibinin, we next sought to determine whether these changes were also manifest at the mRNA level. RT-PCR analysis using primers specific against rat CYP2E1 mRNA demonstrated significantly increased CYP2E1 mRNA expression following treatment of H4IIE cells with ethanol (25 mmol/L) as compared to untreated cells (Figure 3.2, n=4 separate experiments, $p<0.05$). Furthermore, pre-treatment of H4IIE cells with silibinin (10 μM, 2 h) abrogated ethanol-dependent increases in CYP2E1 mRNA expression (Figure 3.2, n=3 separate experiments). To determine the functional significance of the effects of silibinin on CYP2E1 expression and alcohol metabolism, we analyzed culture medium alcohol content in the absence or presence of silibinin pretreatment (10μM, 2Hrs). These data demonstrate significant alcohol metabolism in H4IIE cells over a 24 Hr time period (Figure 3.3a, n=4 separate experiments, samples analyzed in triplicate, $p<0.05$ *versus* alcohol in medium alone ([no cells]). Pre-treatment of cells with silibinin significantly inhibited the rate of alcohol metabolism in H4IIE cells such that at the end of the 24 Hr period 28.1±1.7% percent of the initial alcohol added remained in silibinin pre-treated cells verses 16.4±1.1% in cells treated with alcohol alone (Figure 3.3b, n=4 separate experiments, samples analyzed in triplicate, $p<0.01$).

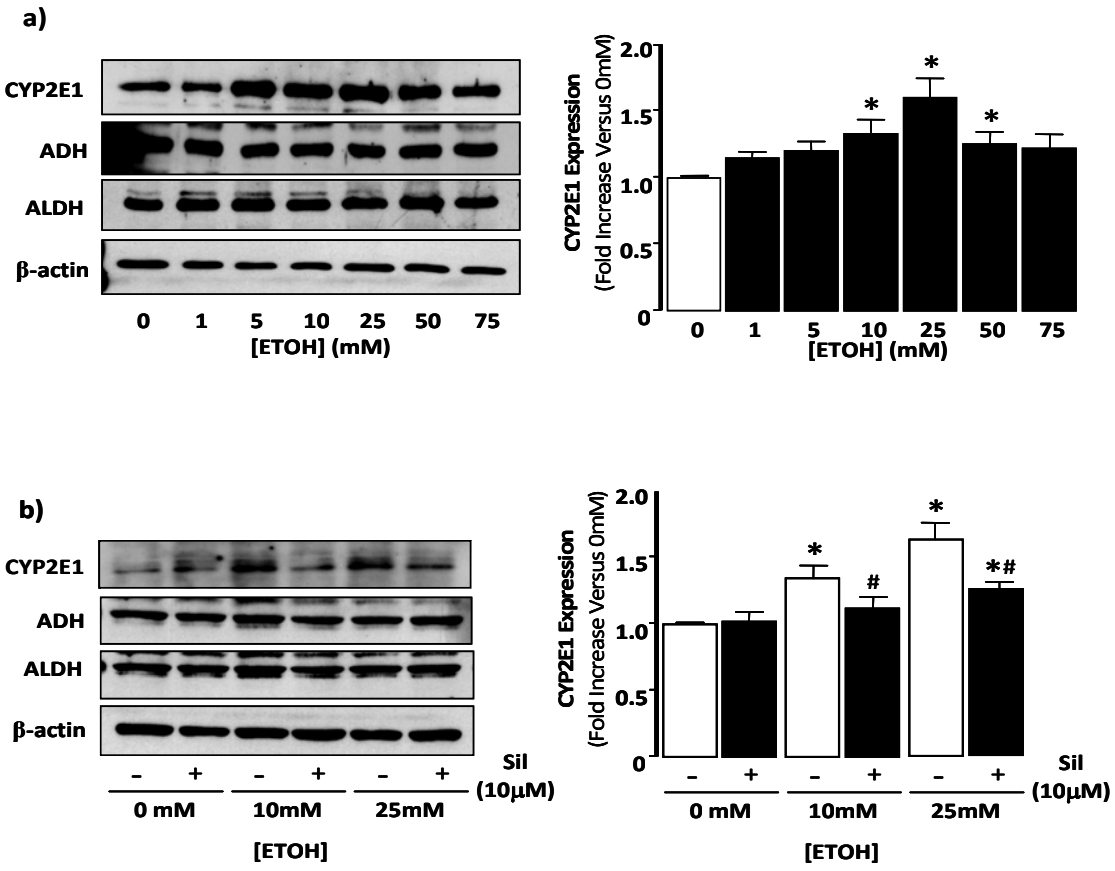

Figure 3.1: Ethanol stimulates cytochrome P4502E1 expression in H4IIE cells, an effect inhibited by silibinin pretreatment. a). Representative immunoblots demonstrating the effect of increasing doses of ethanol (EtOH) on the expression of cytochrome P4502E1 (CYP2E1), alcohol dehydrogenase (ADH), and acetaldehyde dehydrogenase (ALDH) in the H4IIE HCC cell line 24 hours after EtOH addition (0-75mM/L). Equal protein loading was confirmed using an antibody specific against β-actin. The effect of EtOH on CYP2E1 expression was then analyzed by optical integrated volume for repeat experiments and data expressed as fold change *versus* untreated (0mM/L EtOH, lower panel). n=4 separate experiments, *p<0.05*versus* untreated cells. **b)** Representative immunoblots demonstrating the effect of EtOH (10 and 25mM/L) on the expression of CYP2E1, ADH, ALDH in the H4IIE HCC cell line in the presence and absence of silibinin (10μM). Equal protein loading was confirmed using an antibody specific against β-actin. The effect of EtOH in the absence and presence of silibinin (10μM) on CYP2E1 expression was then analyzed by optical integrated volume for repeat experiments and data expressed as fold change *versus* untreated (0mM/L EtOH). n=4 separate experiments, *p<0.05 *versus* untreated cells, #p<0.05 EtOH + Sil *versus* EtOH alone.

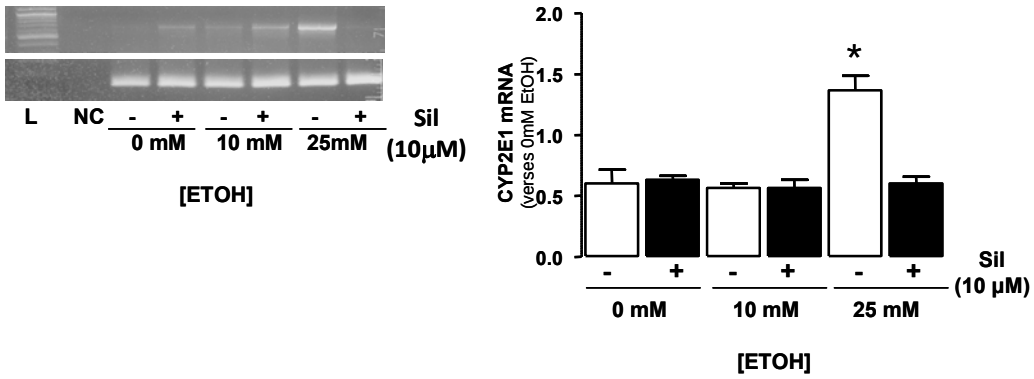

Figure 3.2: Ethanol stimulates CYP2E1 mRNA expression, an effect inhibited by silibinin pre-treatment: Representative RT-PCR analysis demonstrating the effect of EtOH (10 and 25 mmol/L) on the expression of CYP2E1 mRNA in the presences and absence of silibinin 10 μM. CYP2E1 mRNA expression was analyzed by optical integrated volume for repeat experiments and data expressed a fold change verses untreated (0 mmol/L EtOH). n= 3 separate experiments, *$p<0.05$ EtOH+Sil versus EtOH alone.

3.4.2. H4IIE Cell Proliferation: H4IIE cell proliferation was determined for cells cultured in 1% FBS (*v/v*) culture medium in the absence and presence of 25mmol/L alcohol with or without silibinin pretreatment (10μM, 2Hrs) over a 96 Hr period. In untreated cells total viable cell counts increased by a factor of 4.05 ± 0.31 fold compared to viable cell number at day 0 (Figure 3.4, n=5 independent experiments, $p<0.01$). No significant changes in the rate of proliferation were observed in H4IIE cells treated with silibinin or vehicle (DMSO, 01% (*v/v*)) only (Figure 3.4, n=5 independent experiments). In contrast, daily treatment with alcohol (25mmol/L) led to a significant increase in viable cell number as compared to 1% FBS (*v/v*) medium or 1% FBS (*v/v*) with silibinin (10μM) or vehicle (Figure 3.4, n=5 independent experiments, $p<0.05$ alcohol *versus* alcohol + Silibinin).

3.4.3. ERK 1/2 activity in H4IIE cells: The ERK-MAPK signaling pathway has been identified as a central pathway in mediating cell proliferation in H4IIE (and other) cells (McKillop et al., 1997; Roberts and Der, 2007). Western blot analysis of H4IIE cells treated with alcohol demonstrated active ERK1/2 (pERK 1/2) increased significantly 10 mins after addition (Figure 3.5 a and b, 4.46 ± 0.56 fold *versus* 3.22 ± 0.61 in untreated cells, n=5 separate experiments, $p<0.05$). Pretreatment of cells with silibinin (10μM) failed to significantly alter the magnitude or time course of ERK1/2 activity following treatment with alcohol as compared to alcohol alone (Figure 3.5 a and b, n=5 separate experiments)

3.4.4. Lipid peroxidation and ROS: Malondialdehyde (MDA) levels were significantly higher in cells exposed to 10 or 25mmol/L alcohol *versus* untreated cells (Figure 3.6a, n= 4 separate experiments, $p<0.05$). Pretreatment of cells with silibinin

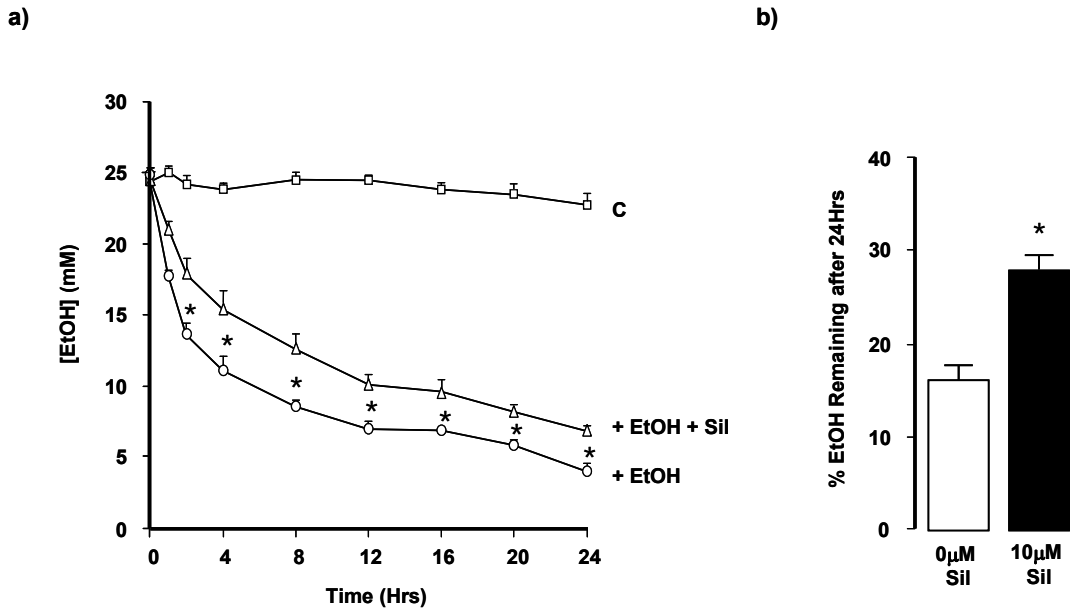

Figure 3.3: a) H4IIE cells metabolize ethanol, an effect inhibited by silibinin pretreatment. Ethanol (EtOH) content in cell culture medium was determined in the absence (○—○) or presence (△—△) of silibinin (Sil; 10μmol) over a 24 Hr period following the initial addition of 25mmol EtOH to H4IIE cell cultures. n=4 separate experiments analyzed in duplicate, *$p<0.05$ EtOH + Sil *versus* EtOH alone. To ensure changes in culture medium EtOH concentration were not due to evaporation, parallel experiments were performed in which EtOH containing (25mmol) culture medium was placed in cell culture flasks in the absence of H4IIE HCC cells (□—□). **b)** The percentage of EtOH remaining in culture medium following the addition of 25mmol/L EtOH to H4IIE cells in the absence or presence of silibinin. n=4 separate experiments, *$p<0.05$.

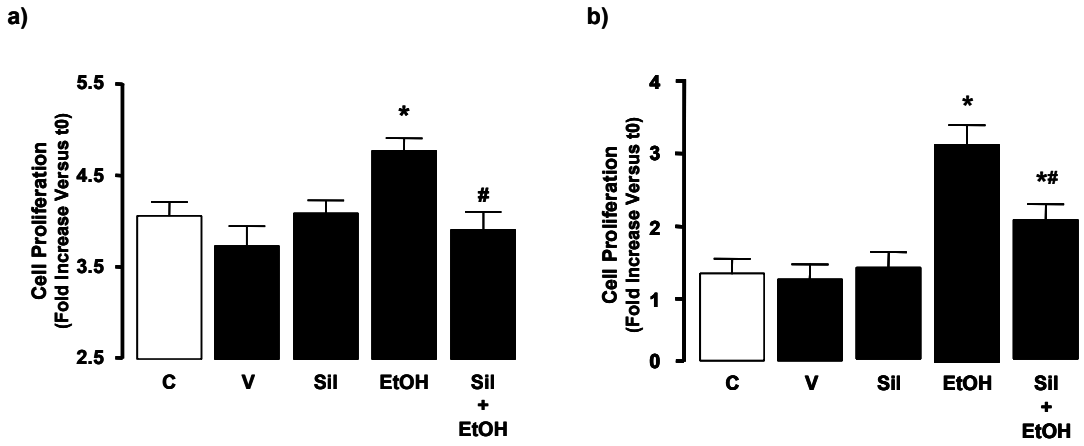

Figure 3.4: Silibinin inhibits ethanol-stimulated cell proliferation in H4IIE HCC cells. a) H4IIE HCC cells were cultured in medium containing 1% FBS in the presence or absence of silibinin (Sil; 10μmol) for 96 Hrs. Following cell counts the number of cells was calculated as a fold change *versus* the number of cells at day 0. n=5 separate experiments, *p<0.05 *versus* control (C; 1% FBS alone), $^{\#}$p<0.05 EtOH (25mmol/L) *versus* EtOH (25mmol/L) + Sil (10μmol). To ensure that DMSO (vehicle for dissolving Sil) did not affect proliferation parallel experiments were performed in which cells were treated with 1% FBS + 0.1% (*v/v*) DMSO (V). b) H4IIE HCC cells were cultured in medium in the presence or absence of silibinin pretreatment (Sil; 10μmol, 2 Hrs) prior to exposure to ethanol (EtOH, 0, 10 or 25 mmol/L) and an MTT proliferation assay performed. Data are expressed as fold change versus control (untreated; C). n=4 separate experiments analyzed in duplicate, *p<0.05 *versus* control (C), $^{\#}$p<0.05 EtOH (25mmol/L) + Sil (10μmol) *versus* EtOH (25mmol/L) only. To ensure that DMSO (vehicle for dissolving Sil) did not affect proliferation parallel experiments were performed in which cells were treated with 0.1% (*v/v*) DMSO (V).

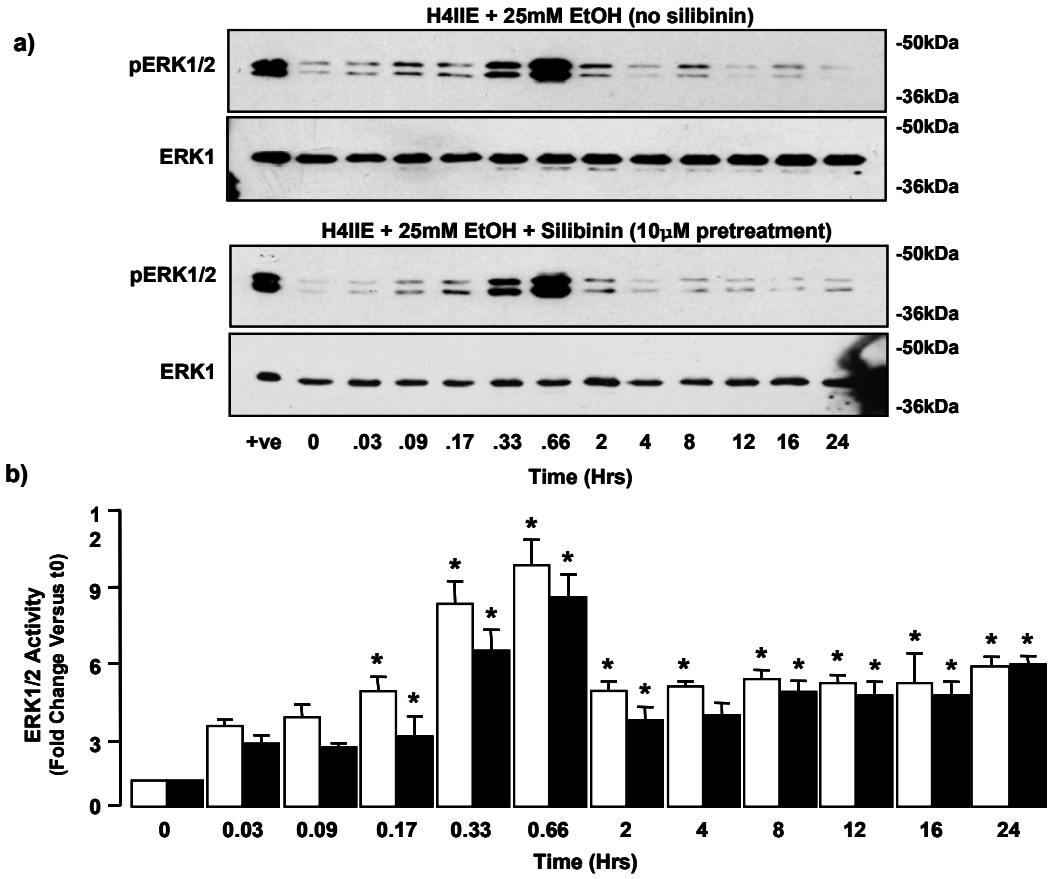

Figure 3.5: Silibinin does not affect ethanol-dependent ERK1/2 activation in H4IIE HCC cells. a) Representative immunoblots demonstrating the effect of ethanol (EtOH; 25mmol/L) on the activation (phosphorylation) of ERK1/2 in the absence (upper panel) or presence (lower panel) of silibinin (10μmol). **b)** Following analysis of pERK1/2 expression, membranes were stripped and probed for total ERK1 expression. The ratio of pERK1/2:ERK1 expression was then analyzed by optical integrated volume for repeat experiments and data expressed as fold change *versus* untreated. n=5 separate experiments, *$p<0.05$ *versus* untreated cells.

followed by alcohol (10 or 25mmol/Lt) significantly inhibited increases in MDA levels measured in cells treated with alcohol alone to levels not significantly different to untreated cells (Figure 3.6a, n=4 separate experiments, $P<0.05$ alcohol treated *versus* silibinin + alcohol). Silibinin alone did not significantly alter basal MDA levels in untreated cells (Figure 3.6a).

To further evaluate the effect of silibinin on alcohol-dependent increases in oxidative stress we next used the carboxy-H_2 DCFDA assay as a marker of intracellular peroxide levels. To perform quantitative analysis, experiments were performed using cells seeded to 96-well plates. These data confirmed that alcohol (25mmol/L) treatment led to a 3.55 ± 0.68 fold increase in fluorescence/ROS production compared to untreated cells (Figure 3.6b, n=4 separate experiments, $p<0.05$). Furthermore, pretreatment of cells with silibinin abolished the effects of alcohol on fluorescence/ROS production to levels not significantly different to untreated cells or, cells treated with silibinin alone. Treatment of cells with vehicle (DMSO, 0.1% (*v/v*) did not significantly alter fluorescence /ROS production compared to untreated cells (data not shown). Using a microscopic analysis approach, in parallel, relatively low fluorescence/ROS was detected in untreated cells and those treated with silibinin alone (Figure 3.6c). Conversely, a dramatic increase in fluorescence/ROS was observed following alcohol treatment (Figure 3.6c), an effect that was abrogated by pretreatment with silibinin (Figure 3.6c, n=4 separate experiments, $p<0.05$ silibinin+alcohol *versus* alcohol only).

3.4.5. Effect of silibinin on CYP2E1 activity and ethanol metabolism: To determine whether silibinin affects CYP2E1 induction, as compared to activity, we next employed the human HepG2 cell line in conjunction with HepG2 cells transfected to

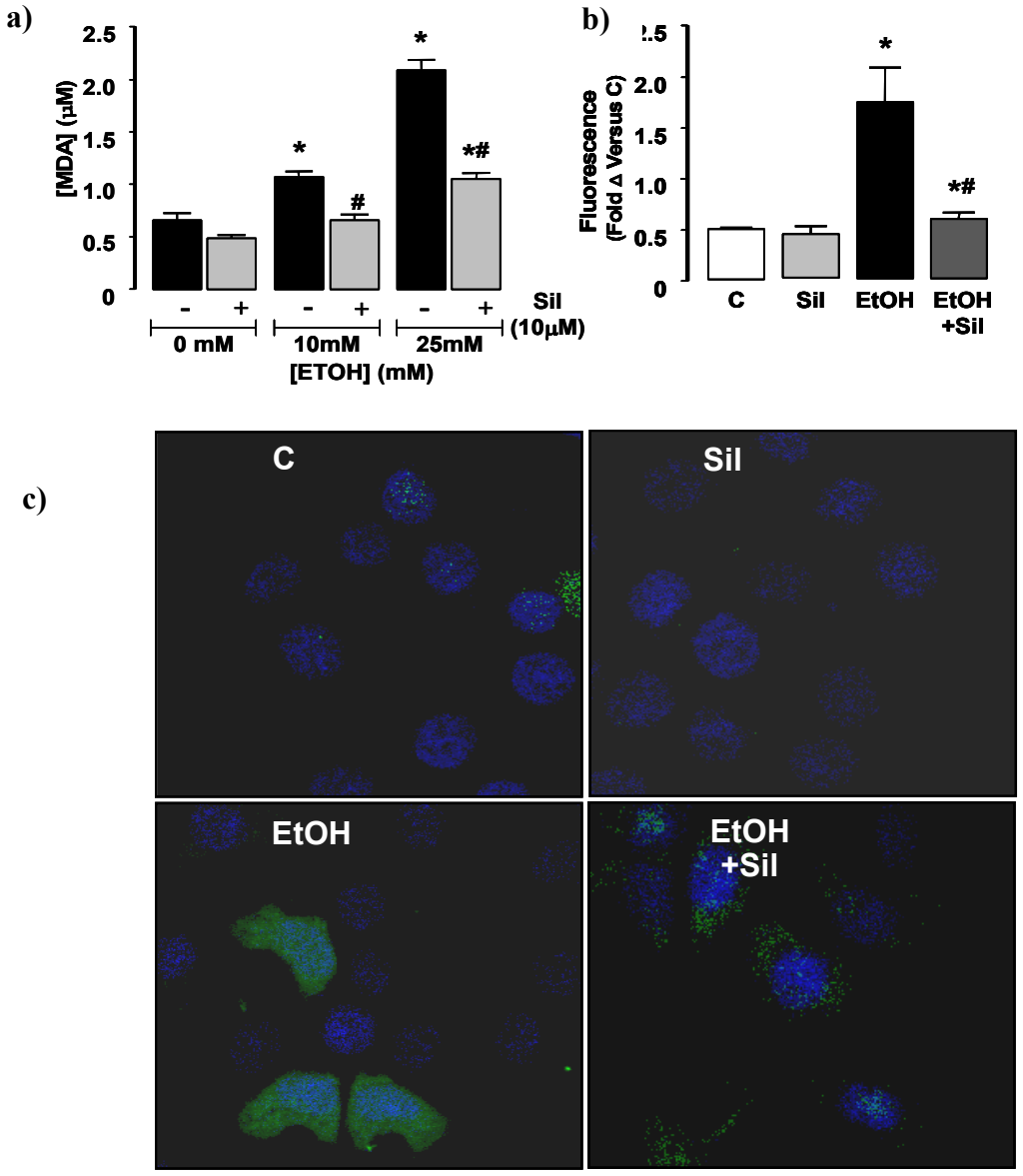

Figure 3.6: Silibinin inhibits ethanol-dependent oxidative stress in H4IIE HCC cells. a). Malondialdehyde (MDA) levels were determined in H4IIE HCC cells following treatment with ethanol (EtOH, 10 and 25mmol/L) in the absence (-) and presence (+) of silibinin (Sil; 10μmol). n=4 separate experiments,*$p<0.05$ EtOH *versus* no EtOH, #$p<0.05$ EtOH + Sil *versus* EtOH – Sil. **b)** Quantitative analysis of the carboxy-H_2 DCFDA assay was performed using a 96-well plate assay as described in the Methods. n=4 separate **c)** Representative immunofluorescent cytochemistry images of H4IIE HCC cells treated with EtOH (25mmol/L) in the absence or presence of silibinin (Sil; 10μmol) analyzed for ROS/peroxide generation using a carboxy-H_2 DCFDA assay in parallel studies. ROS/peroxide was detected as green fluorescence. Cells were counterstained with DAPI (blue) for nuclear localization. experiments analyzed in duplicate, *$p<0.05$ *versus* control (C; untreated), # $p<0.05$ EtOH treated (25mmol/L) *versus* EtOH (25mmol/L) + Sil (10μmol) treated.

express CYP2E1 (E47) or an empty vector control (C37). These data demonstrated significant alcohol metabolism by the HepG2 and C37 cell lines over a 24 Hr period, an effect that was not significantly different in the presence of silibinin (10μM) (Figure 3.7a and b). Conversely, while the rate of ethanol metabolism was significantly accelerated in the E47 (CYP2E1 expressing) HepG2 cell line, this effect was abrogated by pretreatment with silibinin to a level not significantly different to untransfected/C37 HepG2 cells (Figure 3.7c and d, $p<0.05$ alcohol metabolism in E47 *versus* HepG2 and C37 HepG2 cells).

3.5. Discussion and conclusions:

Ethanol has been identified as a causative agent in the development of several cancers including HCC (Baan et al., 2007; Seitz and Becker, 2007). The effects of ethanol on liver function and hepatic disease initiation and progression can be both direct and indirect in nature (Freeman et al., 2005; Seitz and Becker, 2007). However, considerable evidence suggests many of the intrahepatic effects of ethanol are due to metabolism in the hepatocyte and the associated increases in acetaldehyde production and oxidative stress (Seitz and Becker, 2007). The identification of oxidative stress as a major factor in the progression of liver disease towards cirrhosis and HCC has led to intense interest in the therapeutic

The current study utilized the rat H4IIE HCC cell line. Previous studies by our group show that this cell line expresses ADH and ALDH, is capable of metabolizing ethanol, and that this metabolism can be significantly inhibited using 4-methylpyrazole (Kovach et al., 2001). In the current study we demonstrate that exposure

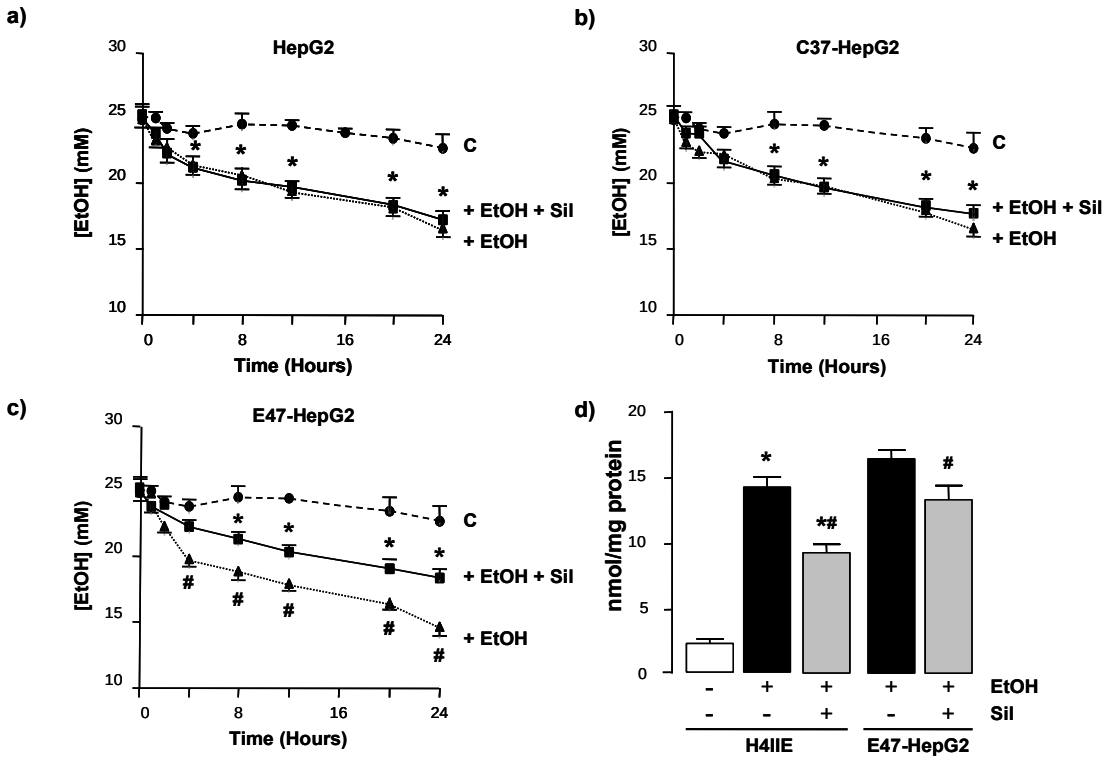

Figure 3.7: Silibinin inhibits ethanol metabolism in human HepG2 HCC cells transfected to express CYP2E1 and CYP2E1 activity in HCC cells. a) Human HepG2 HCC cells were treated with ethanol (EtOH; 25mmol/L) in the absence (▲—▲) or presence (■—■) of silibinin (Sil; 10μmol) for 24 Hrs and EtOH content in the culture medium determined. **b)** Human HepG2 HCC cells transfected with empty vector (C37-HepG2 cells) were treated with EtOH (25mmol/L) in the absence (▲—▲) or presence (■—■) of Sil (10μmol) for 24 Hrs and EtOH content in the culture medium determined. **c)** Human HepG2 HCC transfected to express CYP2E1 (E47-HepG2 cells) were treated with ethanol (EtOH; 25mmol/L) in the absence (▲—▲) or presence (■—■) of silibinin (Sil; 10μmol) for 24 Hrs and EtOH content in the culture medium determined. n=4 separate experiments analyzed in duplicate, *$p<0.05$ *versus* time 0, $^{\#}p<0.05$ cells treated with Sil (10μmol) and EtOH *versus* EtOH alone. **d)** Rat H4IIE and human E47-HepG2 cells were cultured in the presence and absence of ethanol (EtOH; 25mmol/L) and/or silibinin pretreatment (Sil; 10μmol) and CYP2E1 activity determined by measurement of *p*-nitrophenol hydroxylation to 4-nitrocatechol. n=4 separate experiments, *$p<0.05$ *versus* untreated H4IIE cells, $^{\#}p<0.05$ cells treated with Sil (10μmol) and EtOH *versus* EtOH alone.

to ethanol at doses similar to blood ethanol content observed in the setting of moderate ethanol use of antioxidants (Albano, 2008; Lu and Mato, 2008; Mato and Lu, 2007; Ramasamy and Agarwal, 2008).

consumption (10-25mmol/L), leads to a significant increase in CYP2E1 expression in the absence of changes in ADH or ALDH expression in vitro. Furthermore, CYP2E1 induction and the rate of ethanol metabolism are significantly inhibited by the pretreatment of cells with silibinin (10μmol). These data correspond to the inhibition of ethanol-dependent increases in cell proliferation in the H4IIE cell line *in vitro*. This evidence would suggest that, even in the setting of moderate ethanol consumption, HCC cells that express CYP2E1 may be subject to increased CYP2E1 induction and that these changes may significantly affect the rate of cell proliferation. Indeed, this may be of particular importance in considering the "two hit" model of hepatocarcinogenesis in which transformation and progression may be regulated by independent pathophysiological stimuli. However, it is important to highlight that the effects observed in vitro may not be similarly manifest in the in vivo setting in which the non-tumorigenic liver mass will, more than likely, play a more significant role in ethanol metabolism. Similarly, the concentrations and time of exposure to ethanol that the tumor mass is likely to experience in vivo will differ to that of a static in vitro culture employing HCC cell populations.

Previous studies demonstrate that silibinin inhibits human HCC cell proliferation in vitro (Lah et al., 2007; Momeny et al., 2008) and does so via inhibition of ERK-MAPK signaling in the (human) HepG2 cell line (Momeny et al., 2008). In contrast, we failed to detect a significant effect of silibinin on cell proliferation or ERK-MAPK activity profiles

in H4IIE cells treated with silibinin alone. However, studies by Momeny *et al*. (Momeny et al., 2008) and Lah *et al.* (Lah et al., 2007) demonstrated significant inhibitory effects of silibinin at doses of 50-75μmol and 120-240μmol respectively, whereas our studies employed silibinin at 10μmol final culture medium concentration. Indeed, both of these studies failed to observe significant effects of silibinin on proliferation and/or ERK-MAPK activity at this dose (Lah et al., 2007; Momeny et al., 2008). While our data raise the possibility that the dose of silibinin used in the current studies was too low to affect ERK-MAPK signaling and/or proliferation, we were cognizant of not using higher doses in vitro due to data regarding the bioavailability of silibinin following oral ingestion in animal models and humans in vivo (Kidd and Head, 2005; Wu et al., 2007). In addition to the potential effects of silibinin on an ERK-MAPK signaling cascade other signaling mechanisms have been identified whereby silibinin may act to inhibit net cell accumulation. Using the human HepG2 and Hep3B cell line Varghese *et al* report silybin treatment inhibits the expression of a range of cyclins and cyclin-dependent kinases and, in the case of the Hep3B line, inhibits regulators of proteins involved in transition between the G2-M phases (Meeran and Katiyar, 2008; Varghese, 2005). Conversely, silibinin has also been reported to exert pro-apoptotic effects (albeit at higher doses than those that inhibit ERK-MAPK signaling) in other cancer cells (Ramasamy and Agarwal, 2008; Singh and Agarwal, 2004), an effect that, in combination with inhibition of cell cycle progression, would result in decreased net cell accumulation (Ramasamy and Agarwal, 2008).

As with many complimentary/alternative medicines the efficacy and mechanisms of action whereby the active constituents of milk thistle exert their effects remain

controversial. Several recent reviews suggest that the clinical benefits of milk thistle for a range of hepatic (and other) disease states is difficult to assess due to a lack of high-quality, adequately conducted/reported clinical trials (Rambaldi et al., 2007; Saller, 2007). Similarly, increasing evidence indicates that, much like ethanol consumption, the systemic effects of silibinin following ingestion may play as important a role in influencing the hepatoprotective effects as the direct actions in the liver (Rambaldi et al., 2007; Varghese, 2005). The antioxidant/free radical scavenging capacity of milk thistle derivatives, including silibinin, appears to be directly related to the flavinoligand chemical structure(s) (Ramasamy and Agarwal, 2008). Currently no evidence has been presented to indicate silibinin acts to alter the rate of GSH synthesis although, the presence of silibinin has been demonstrated to reduce GSH depletion in isolated hepatocytes exposed to allyl alcohol (Miguez et al., 1994). Indeed, these data are supported by our findings that pre-treatment of cells with silibinin effectively decreases ROS/oxidative stress in H4IIE cells associated with ethanol metabolism. Specifically, data from our studies suggests that the ability to reduce oxidative stress is due to the ability to inhibit CYP2E1 induction/activity rather than affecting ADH-dependent ethanol metabolism. These data are consistent with ethanol metabolism studies that report the majority of hepatic oxidative stress associated with chronic ethanol consumption is due to CYP2E1 induction and the generation of ROS, including hydroxyethyl radicals (Albano, 2008; Lu, 2008). However, while our studies using E47-HepG2 cells (transfected to express constitutively active CYP2E1) raise the possibility that silibinin may interact directly with the CYP2E1 enzyme to inhibit activity, these data contradict previous

studies by Miguez et al that failed to provide evidence for the involvement of CYP2E1 as an underlying mechanism for the effects of silymarin (Miguez et al., 1994).

The effects of ethanol on hepatocyte integrity, and liver function as a whole, can be both direct and indirect in nature (Crabb and Liangpunsakul, 2007; McKillop, 2005; Seitz and Becker, 2007). Similarly, oral ingestion of silibinin can exert indirect and direct effects, the net result of which are hepatoprotective. For example, chronic ethanol consumption is documented to stimulate a hepatic immune responses due, at least in part, to changes in the balance of the bacterial flora of the GI-tract and increased permeability of the GI tract to LPS resulting in Kupffer cell activation (Bode and Bode, 2005). In this regard silibinin has been demonstrated to inhibit the transcription and DNA binding activity of NFκB, (Manna, 1999; Saliou, 2001) a key factor in regulating and coordinating the hepatic inflammatory response (Tacke et al., 2009). In addition to modulating the immune response silibinin, and other flavinoligands, have been reported to modulate steroid hormone receptor-dependent gene expression (Mueller, 2004; Seidlova-Wuttke et al., 2003). This may be of particular significance in alcoholic liver disease given the relationship between the liver and the regulation of sex hormone levels/activity and the effects of chronic ethanol consumption on hepatic sex hormone regulation and signaling (Kovacs, 2002; Ronis et al., 2007). Similarly, the progression of hepatic foci to HCC and subsequent tumor expansion is dependent on neoangiogenesis and, silibinin is reported to inhibit angiogenesis due to inhibition of vascular endothelial growth factor VEGF-dependent signaling (Singh et al., 2008).

In conclusion, data presented in this study demonstrate silibinin inhibits CYP2E1 induction/ethanol metabolism and cell proliferation in a rat HCC cell line in vitro and

does so at doses lower than those described in other (human) HCC cell lines. Our data suggest that the underlying mechanisms by which silibinin exerts these effects are due to decreased CYP2E1-dependent ROS generation, possibly via direct interaction with the CYP2E1 enzyme. While these data provide an insight into possible mechanisms whereby silibinin may slow the rate of HCC progression the wide spread systemic effects of both ethanol and silibinin are such that further studies are required to determine whether these mechanisms are equally important in vivo.

CHAPTER 4: CHRONIC ETHANOL FEEDING ACCELERATES HEPATOCELLULAR CARCINOMA PROGRESSION IN A SEX-DEPENDENT MANNER IN A MOUSE MODEL OF HEPATOCARCINOGENESIS

4.1. Introduction:

On a global scale hepatocellular carcinoma (HCC) is the most common primary liver cancer diagnosed, the fifth most common cancer diagnosed overall, and the third leading cause of cancer-related mortality (Altekruse, 2009; El-Serag, 2007). Unlike many other common cancers in which hereditary risk factors have been identified, similar patterns of incidence are not evidenced for HCC. Rather, incidence of HCC is directly linked to exposure to known risk factors, of which viral hepatitis B and C, aflatoxin, and chronic, heavy ethanol consumption are the most common (Altekruse, 2009). Despite the varied nature of these insults, exposure is most commonly linked to progressive liver disease toward hepatic cirrhosis, the most common precursor to HCC development (Yang and Roberts, 2010; Zaman et al., 1985). Similarly, while each factor alone represents a significant risk for progression to cirrhosis and HCC, these agents act synergistically to enhance the probability of eventual HCC.

The increasing prevalence of viral hepatitis infection represents a burgeoning health problem globally. In developed countries chronic ethanol intake, in the absence or presence of underlying viral hepatitis, remains an important risk factor for hepatic cirrhosis and progression to HCC (Yang and Roberts, 2010). Significant advances have been made in our understanding of how ethanol affects the liver. Following ingestion,

≈80% of ethanol is metabolized in the liver. Ethanol metabolism occurs (predominantly) in hepatocytes *via* three pathways; alcohol dehydrogenase (ADH), cytochrome P4502E1 (CYP2E1) and catalase (Crabb, 1995; McKillop and Schrum, 2009). In the setting of moderate and/or infrequent ethanol consumption, the majority of ethanol is oxidized by ADH to acetaldehyde that is, in turn, rapidly metabolized by acetaldehyde dehydrogenase (ALDH) to acetate (Crabb, 1995; McKillop and Schrum, 2009). Acetaldehyde represents a highly reactive compound capable of binding to cell constituents, including DNA, to form adducts. While direct DNA damage is a significant factor in ethanol toxicity, acetaldehyde also depletes glutathione (GSH), the main cellular antioxidant involved in detoxification (Albano et al., 1999; Lieber, 1997b). However, chronic, heavy ethanol ingestion leads to microsomal CYP2E1 induction (Crabb, 1995; McKillop and Schrum, 2009). CYP2E1-mediated metabolism induces direct cellular damage due to production of reactive oxygen species (ROS) /oxidative stress, as well as elevated acetaldehyde production and acetaldehyde-dependent cellular damage. Additionally, CYP2E1 induction has been reported to alter cell cycle progression, pro-carcinogen activation, and immune responses (Crabb, 1995; Ekstrom and Ingelman-Sundberg, 1989; McKillop and Schrum, 2009; Muller and Sies, 1987).

Ethanol metabolism profoundly affects hepatocyte integrity, as well as that of other hepatic cells. However, increasing evidence indicates that the effects of ethanol (metabolism) on hepatic cells are further augmented by other, systemic events. Prolonged ethanol intake causes a hepatic inflammatory response due to increased GI-permeability to LPS (Enomoto et al., 2001; Jirillo et al., 2002). Elevated intrahepatic LPS promotes pro-inflammatory cytokine release from Kupffer cells (KCs) and neutrophil/macrophage

infiltration, leading to increased cytokine release and apoptosis (Jirillo et al., 2002; Mathurin et al., 2000). Stimulation of stress-activated cytokine cascades also increases ROS formation which, given ethanol-related GSH depletion, further enhances stress responses, incidence of DNA damage, apoptosis, and compensatory regeneration (Jirillo et al., 2002; Mathurin et al., 2000). If the liver cannot compensate, necrosis occurs and a positive feedback loop of damage-regeneration is initiated.

Several studies in humans and animal models of HCC have identified sexual dimorphism during ALD development and progression. Differences in gene expression encoding for ethanol metabolizing enzymes influences predisposition to ethanol sensitivity, and ALD development/progression (Gramenzi et al., 2006). Differences in ADH activity exist between males and females, activity being lower in males than females, resulting in less acetaldehyde accumulation (Harada et al., 1998). Studies also report estrogens positively influence both ADH and CYP2E1, suggesting ethanol should be more rapidly metabolized in females *vs*. males (Harada et al., 1998). Yet this is not the case, and BACs following ethanol ingestion are not lower in females. Nonetheless, sex differences in ALD are well documented; women are more susceptible to the deleterious effects of ethanol than men, and are thus more likely to develop liver disease earlier (Muller, 2006). Several mechanisms have been proposed to explain this phenomena including different ADH activities in the stomach and liver, higher concentrations of toxic byproducts (from ethanol metabolism), and increases in estrogen (E2)-induced inflammation due to ethanol (Muller, 2006). Despite higher susceptibility of women to ethanol-induced liver damage, development of cirrhosis is more common in men than women (Zaman et al., 1985).

A considerable body of research has addressed the role of ethanol in ALD development and hepatocyte transformation. In comparison, relatively few studies have addressed potential mechanisms whereby ethanol may affect progression of hepatic tumorigenesis. In this study we sought to determine the effects of chronic ethanol intake on hepatocarcinogenesis in a well-described mouse model of HCC development generated *via* neonatal initiation with diethylnitrosamine (DEN). Additionally, we employed male and female mice for these studies in an attempt to identify potential sexual dimorphism in HCC progression in response to chronic ethanol feeding.

4.2. Materials & Methods:

4.2.1. Materials *In vivo* model of hepatocarcinogenesis: As listed in Section 2.1.2.

4.2.2. Methods *In vivo* model of hepatocarcinogenesis: B6C3 mice (21-25 days old) were randomized, weighed, and injected with a single dose of DEN (1mg/Kg body weight, (*i.p.*)) dissolved in sterile olive oil (DEN group; D) or vehicle (olive oil (*i.p.*)), control group; C) as described in Section 2.1.3. Animals receiving DEN or vehicle were randomized to receive control or ethanol feeding regimes for early (16-24-weeks) or late (40-48-weeks) hepato-carcinogenesis studies. Animals were allowed free access to AIN93M rodent chow until specialized diets were introduced.

4.2.3. Ethanol Drinking Water: Animals assigned to ethanol-feeding groups were weaned on to an ethanol-drinking water (EtOH-DW) regime as described in Section 2.1.4. For animals assigned to the early (16-24-weeks) hepatocarcinogenesis studies initiation of EtOH-DW began at 15 -weeks and ceased at 24-weeks. For animals assigned to the late (40-48-weeks) hepatocarcinogenesis studies initiation of EtOH -DW began at 39-weeks and ceased at 48-weeks. All animals were weighed twice weekly.

4.2.4. Necropsy: At 24 or 48-weeks (depending on pre-assigned groups) mice were weighed, anesthetized (isofluorane by inhalation), examined grossly and sacrificed as described in Section 2.1.5.

4.2.5. Histology: Multiple liver lobes (minimum of 2 lobes per animal) were sectioned (4-6μm) and stained with Mayer's hematoxylin and eosin (H & E) or Picrosirius red as described section 2.5.1.2. Representative sections (5 random fields/lobe) were examined microscopically (100x magnification) and blind-scored for steatosis (0-4), necrosis (0-4), inflammation (0-4), and/or fibrosis (0-4) using modified scoring scales reported by others (French et al., 1993; Morgan et al., 2002). Degree of fibrosis (mean % Picrosirius red staining) was performed using ImageJ software (NIH, Bethesda, MD). The four independent scores were combined to generate a total liver injury score (TLIS) as described Section 2.5.1.3.

4.2.6. Immunohistochemistry: For immunohistochemistry (IHC) sections (4-6μm) of fixed liver were immunostained following deparaffinization, rehydration and antigen retrieval. Sections were incubated with anti-glutathione S-transferase placental isoform (GSTpi; 1:100 dilution), as described in Section 2.5.2.1, or anti-proliferating cell nuclear antigen (PCNA; 1:1000 dilution), as described in Section 2.5.2.2. Five random fields/lobe (minimum of 2 lobes) were examined microscopically (200x magnification), photographed, and analyzed for number of foci and AHF area (mm^2), or number of PCNA positive nuclei (dark brown staining) using ImageJ software. To measure apoptosis, an in situ TUNEL assay was performed as per the manufacturer's instructions and sections counterstained with 4'-6-Diamidino-2-phenylindole (DAPI) for nuclear visualization, as described in section 2.5.2.3. To confirm antibody specificity mouse

spleen and embryonic tissue were used as positive controls (PCNA and TUNEL respectively). Negative control for TUNEL employed enzyme free probe.

4.2.7. PCR and quantitative RT-PCR: Total RNA was extracted from liver tissue, as described in Section 2.2.2. cDNA was synthesized from random hexamers, as described in Section 2.2.3 and used to perform PCR for CYP2E1 mRNA expression performed using mouse specific CYP2E1 primer pairs as listed in Table 1, Section 2.2 (Brandon-Warner et al., 2010b). Final product was semi-quantified using NIH-ImageJ software and corrected to β-2 microgoblulin (housekeeping gene) levels. qRT-PCR was performed using cDNA followed by SYBR Green Supermix using mouse specific primer pairs for T-bet, GATA3, or SMAD3, listed in Table 1, Section 2.2. Reactions were prefomed in an iCycler IQ™ real time PCR detection system (BioRad) as described section 2.2.4. Samples were assayed in duplicate, and relative gene expression of each transcript was expressed as Δ^{Ct} and normalized to pair-matched controls.

4.2.8. Western Blot Analysis**:** Liver tissue (≈100mg) was homogenized RIPA buffer, the resulting homogenate sonicated (4^0C), protein levels measured, and normalized using RIPA buffer as described in Section 2.3.2. Protein detection was performed by immunoblot using antibodies specific against ADH, ALDH, CYP2E1 or cyclin D1 as described in Section 2.4.3 (Brandon-Warner et al., 2010b). Signal intensity was determined using NIH-ImageJ software and equal protein loading confirmed by stripping/re-probing membranes with an anti-β-actin (housekeeping protein) antibody.

4.2.9. Liver Function and Oxidative Stress Status: Serum alanine-aminotransferase (ALT) was measured using an ALT/GPT 2-part reagent as described section 2.7.2. Hepatic lipid peroxidation was measured using a TBARS kit on liver tissue

homogenates, section 2.9.2. Hepatic GSH levels were determined by colorimetric analysis from liver tissue lysates collected in 2-(*N*-morpholino) ethanesulfonic acid (MES) buffer using a GHS assay kit, section 2.10.2.

4.2.10. Ethanol Assay: Aliquots (50µl) of serum were collected and stored at -80^{o}C prior to measurement of ethanol concentration, as described section 2.8.2 (Brandon-Warner et al., 2010b).

4.2.11. Cytochrome P4502E1 Activity: CYP2E1 activity was measured as the rate of oxidation of ρ-nitrophenol to 4-nitrocatechol in the presence of NADPH and O_2, as described 2.11.2 (Brandon-Warner et al., 2010b).

4.2.12. Serum Cytokine Levels: To evaluate and compare cytokine expression patterns a custom (7) Plex murine cytokine array purchased from BioRad, Hercules, CA) was performed as described in Section 2.6.2. Cytokines were selected to reflect changes in T-effector responses (Th1-IFNγ, IL1b, IL12p70 and Th2-IL13, T-reg-IL10) and inflammation-liver disease (TNFα and IL-6). Pooled serum (12.5µL) from each group was diluted 1:4 in proprietary serum sample diluents. Premixed standards were used to generate a standard curve. The assay was performed in a 96-well filtration plate supplied with the assay kit as per the manufacturer's instructions, before being read on the Bio-Plex suspension array system and analyzed using Bio-Plex manager software.

4.2.13. Statistical Analysis: Comparisons of tumor positive animals in each group were made by Fisher's exact test. Comparisons of tumor size (mm^2), multiplicity, ALT/AST, TBARS and GSH levels were made by either one-way ANOVA followed by Tukey's or Dunnet's post-hoc test, as appropriate or two-way ANOVA followed by Bonferonni correction.

4.3. Results:

4.3.1. Mortality, body-liver weight, and necropsy: Male and female mice tolerated the EtOH-DW regime well either without, or with prior DEN initiation. Male mice were significantly heavier than female counterparts at all time points (Table 4.1, and Figure 4.1). Overall no significant difference in body weight was measured within male or female groups maintained on control (C) *versus* EtOH-DW regimes (E), nor between these groups and pair matched animals initiated with DEN alone (D), or DEN concomitant with EtOH-DW (D+E) (Table 4.1, and Figure 4.1). Of note, male mice in the D and D+E group (48 -weeks) exhibited significantly lower body weight compared to pair-matched male C or E groups at the end of the 48-week experimental period (Figure 4.1A and Table 4.1). No mortality occurred in any of the experimental groups in the 24-week group. Within the 48-week group, 1 male DEN and 1 female DEN+EtOH animal died prior to time course completion (47-weeks and 13-weeks respectively).

At necropsy, livers were resected, photographed, and weights recorded. Upon gross examination no visible lesions were observed in any of the groups at 24-weeks (Table 4.1). By 48-weeks visible lesions were observed in both male and female mice initiated with DEN, a significantly greater number being visible in males (87.5% *versus* 44.4%, male *versus* female, $p<0.05$, Figure 4.2, Table 4.1). In male mice (48-weeks) the effect of DEN was exacerbated by chronic ethanol feeding (93.7% (D+E) *versus* 87.5% (D)), whereas fewer visible lesions were observed in DEN-initiated females maintained on the EtOH-DW regime than DEN-initiated alone (35.7% (D+E) versus 44.4% (D); Figure 4.2 and Table 4.1). Calculation of liver-body weight ratios (L:BW) demonstrated no significant difference between male and female mice in pair-matched groups.

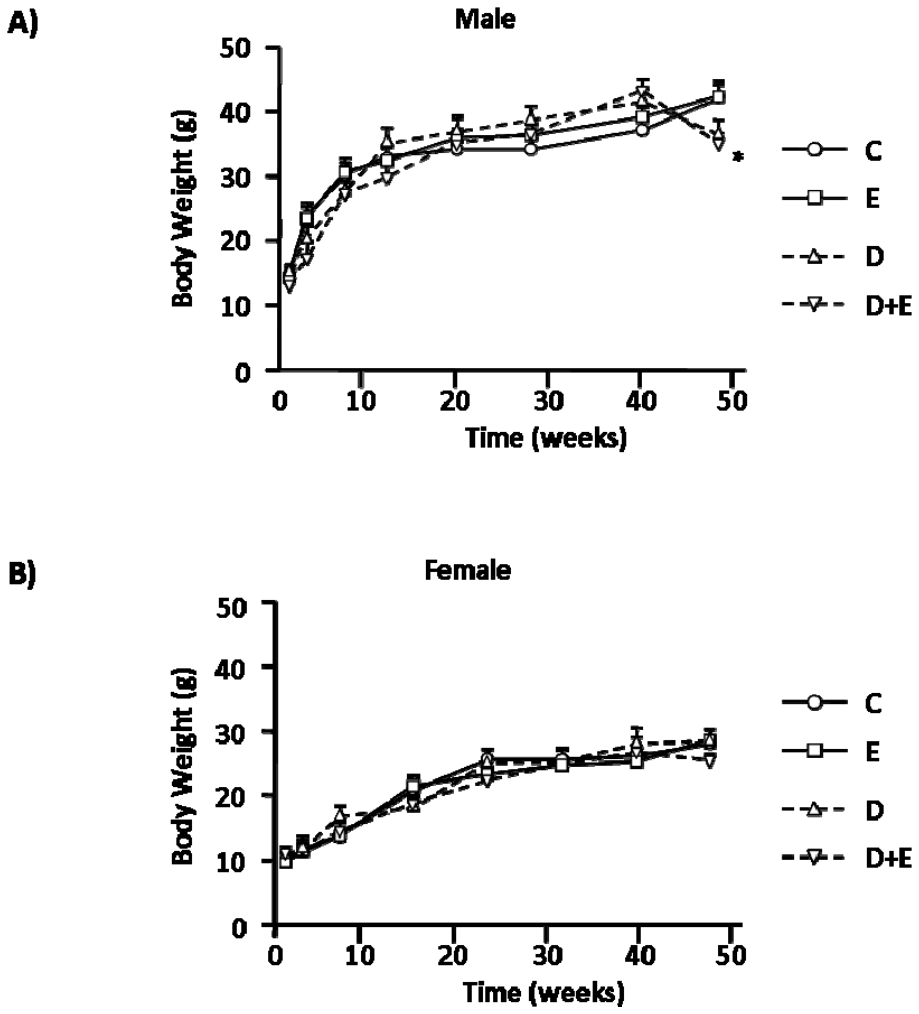

Figure 4.1: Ethanol alone or with DEN did not alter growth of male or female mice. Growth curves for both male and female mice in experimental groups, EtOH-DW (E), DEN-initiation (D) or DEN+EtOH-DW (D+E) were not significantly different from same sex control (C) animals, with the exception that D and D+E male mice demonstrated a significant decrease in body weight at 48 weeks *versus* male C and E treatment groups.

Table 4.1: Animal/liver weights and liver-body weight ratios at necropsy *p<0.05 *versus* all other treatment groups within male or female groups assayed at matching time points (24 or 48 weeks). #p<0.05 *versus* C or E within male or female groups.

Group		n		Liver (g)	Liver:BW ratio	Visible Lesions
MALE (24 Wks)	Control (C)	9	35.6±0.5	1.81±0.05	0.050±0.001	0
	EtOH (E)	9	35.1±0.7	2.14±0.09	0.056±0.002	0
	DEN (D)	9	36.9±2.4	2.10±0.17	0.057±0.002	0
	DEN+EtOH (D+E)	14	34.8±0.7	2.08±0.12	0.059±0.002	0
FEMALE (24 Wks)	Control (C)	10	25.7±0.4	1.30±0.03	0.051±0.001	0
	EtOH (E)	10	27.5±0.4	1.48±0.03	0.054±0.015	0
	DEN (D)	9	27.9±0.6	1.64±0.09*	0.059±0.003	0
	DEN+EtOH (D+E)	14	25.4±0.4	1.35±0.03	0.053±0.006	0
Group		**n**	**Weight (g)**	**Liver (g)**	**Liver:BW ratio**	**Visible Lesions**
MALE (48 Wks)	Control (C)	9	41.2±1.0	1.93±0.05	0.047±0.001	0
	EtOH (E)	9	42.1±0.8	2.19±0.06	0.054±0.001	0
	DEN (D)	8	36.3±2.3#	2.59±0.35#	0.070±0.007#	87.5% (7/8)
	DEN+EtOH (D+E)	14	34.7±0.7#	4.44±0.16*	0.129±0.006*	93.7% (13/14)
FEMALE (48 Wks)	Control (C)	10	27.9±0.6	1.37±0.05	0.049±0.001	0
	EtOH (E)	10	28.6±0.5	1.41±0.04	0.049±0.001	0
	DEN (D)	9	28.2±0.8	1.78±0.14*	0.063±0.005*	44.5% (4/9)
	DEN+EtOH (D+E)	14	25.7±1.1*	1.31±0.07	0.050±0.001	35.7% (5/14)

However, by 48-weeks, male D and D+E mice exhibited a significantly higher L:BW ratio as compared to C and E groups, and D+E *versus* DEN-initiated alone ($p<0.01$, Table 4.1). Conversely only DEN-initiated female mice in the 48-week groups, demonstrated significantly higher L:BW ratios. In comparing these data, differences in liver weight and L:BW ratios were attributed to increased size/number of tumors in the male (D and DE groups) and the female (D group) compared to control and ethanol only groups (Figure 4.2, Table 4.1).

4.3.2. Liver pathology and tumor burden: Total liver injury scores (TLIS) were generated following blind scoring for total fat, necrosis, inflammatory cell infiltration, and collagen deposition (Figure 4.3A; male and 4.3B; female 48-week images shown). Using this approach, increased injury was identified in male EtOH, DEN and DEN+EtOH mice in all lobes at both 24 and 48-weeks (Figure 4.3C). Conversely, pair-matched female mice were observed to exhibit more localized liver injury that was typically identified in only one or two lobes. Moderate, though significant, liver injury was measured in both male and female mice maintained on EtOH alone (E) compared to controls (C) at both 24 and 48-week time points (Figure 4.3C). Additional analysis demonstrated DEN-initiation alone (D) significantly increased the TLIS in both male and female mice at 24 and 48-week time points compared to C and E groups (Figure 4.3C, $p<0.05$). Within the 24-week group, maintenance on the EtOH-DW regime led to significantly greater TLIS in male mice compared to female (Figure 4.3C, $p<0.05$). This effect was further magnified in the 48- week study groups in which EtOH-DW significantly increased TLIS in male mice *versus* pair-matched female animals and male DEN-only initiated animals (Figure 4.3C, $p<0.01$). Finally, when comparing 24 to 48-

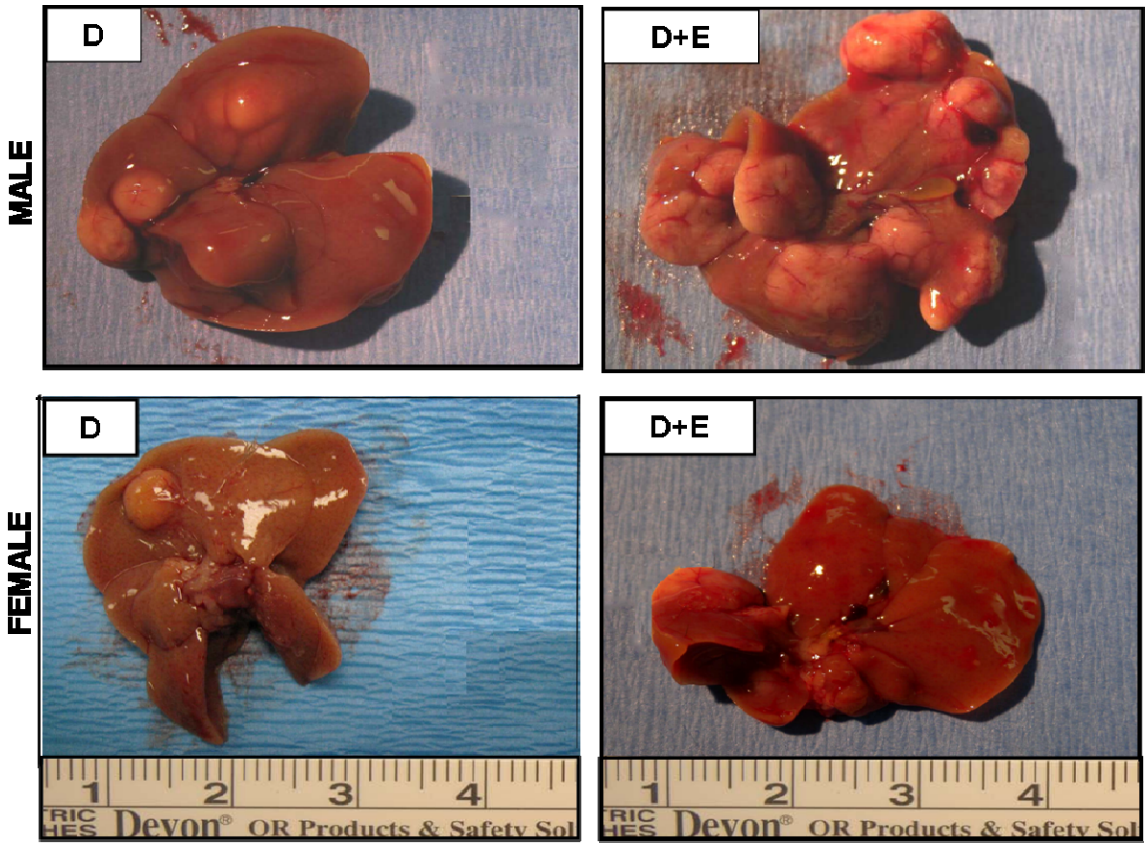

Figure 4.2: Ethanol feeding enhances DEN-induced hepatocarcinogenesis in male mice. Representative images of livers resected from male and female mice (48 weeks) initiated with DEN (D) or DEN with ethanol feeding (D+E)

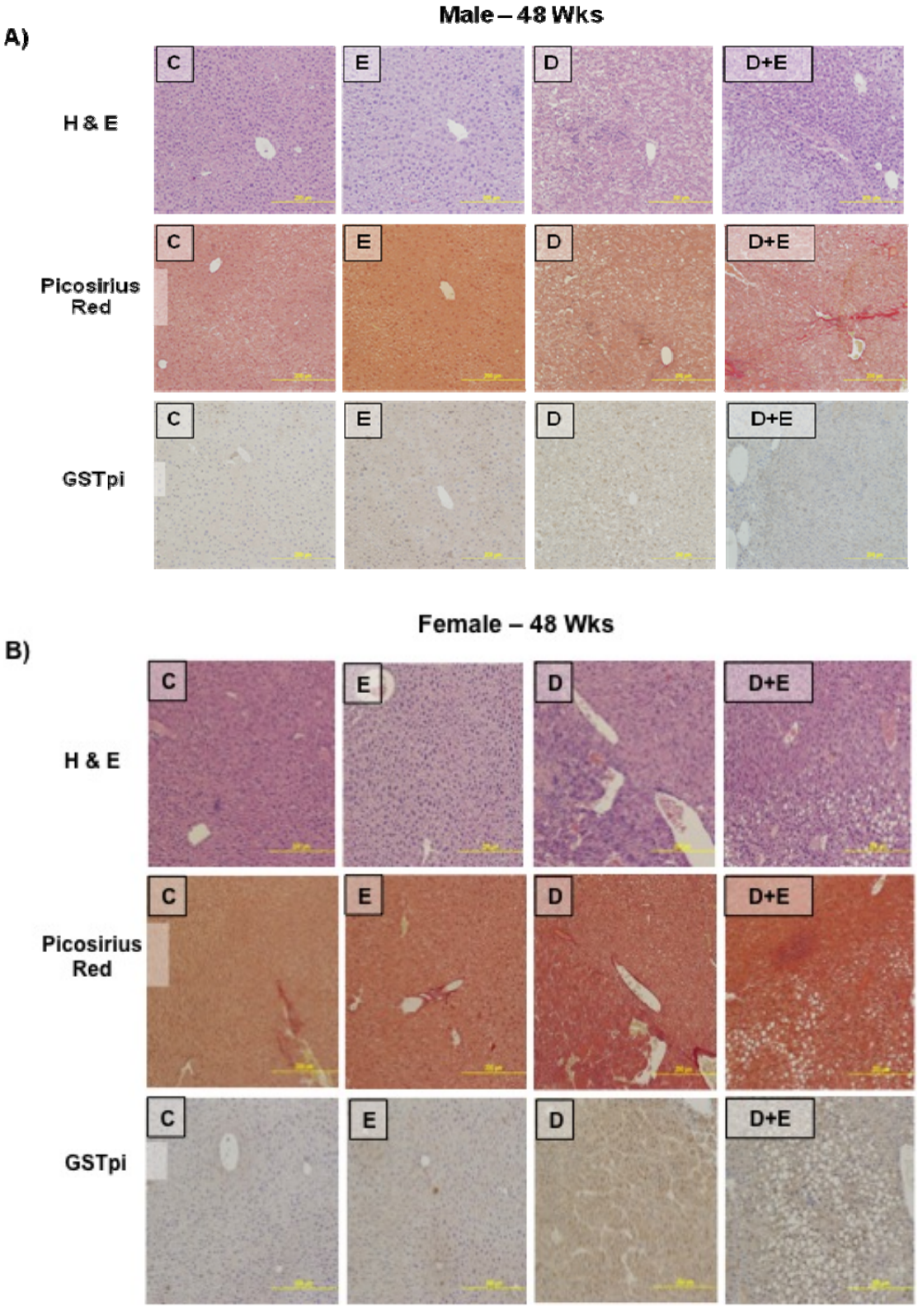
A)
Male – 48 Wks
H & E
Picosirius Red
GSTpi
C
E
D
D+E
B)
Female – 48 Wks
H & E
Picosirius Red
GSTpi
C
E
D
D+E

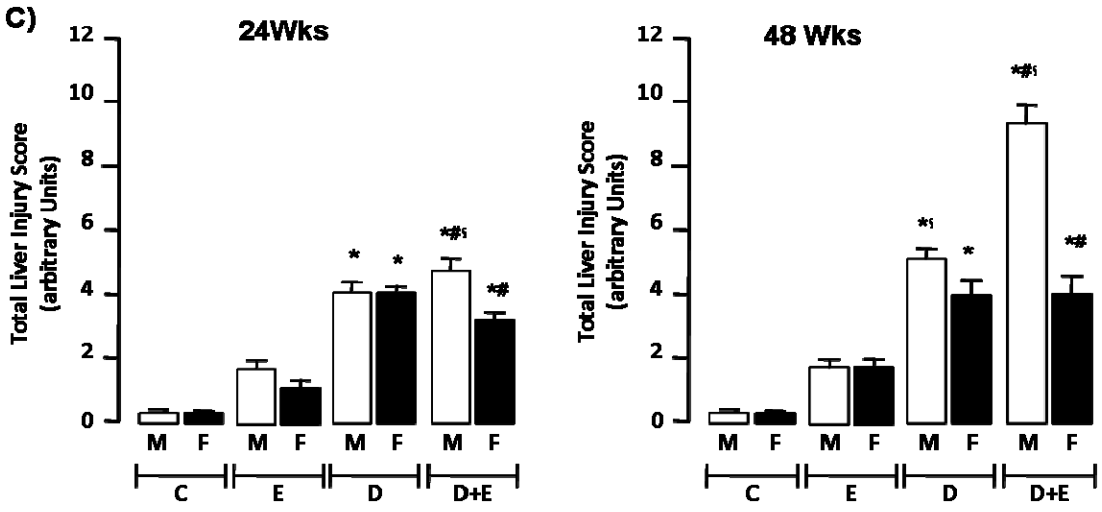

Figure 4.3: Ethanol feeding promotes hepatic injury in a DEN model of hepatocarcinogenesis in male mice A) Representative images (x100 magnification) of sections from control (C) male mice (48 weeks) and pair-matched male mice maintained on ethanol feeding (E), initiated with DEN (D), or initiated with DEN and ethanol fed (D+E). Sections were stained with H&E, Picrosirius Red or an antibody against Glutathione S-transferase placental isoform (GSTpi). **B)** Cumulative total liver injury score (TLIS) was blind scored from representative sections (2 lobes/mouse, 5 fields/lobe) from each experimental group (male and female, 24- and 48-weeks; C, E, D, D+E). *$p<0.05$ versus respective male or female controls (C), #$p<0.05$ D+E (male or female) *versus* D mice, §$p<0.05$ male *versus* female within same treatment group/time points. Minimum n = 8 independent mice/group.

week groups, no significant difference in TLIS was measured between pair-matched groups in female mice (Figure 4.3C). Conversely, the effects of D or D+E had significantly greater impact on TLIS in male mice at 48 -weeks compared to 24 -weeks (Figure 4.3C, $p<0.05$).

Analysis of individual components of the TLIS revealed that the primary mode of hepatic injury was lipid accumulation in DEN-initiated groups at both 24 and 48 -weeks, and lipid scoring was further increased by EtOH exposure, this effect being more pronounced in male compared to female mice (Table 4.2).

4.3.3. Immunohistochemistry (IHC): was initially performed using an antibody against GSTpi to identify altered hepatic foci (AHF). Using this approach AHF was significantly greater in female D *versus* male groups at 24-weeks ($p<0.05$) (Figure 4.4A). Conversely, by 48-weeks, number of AHF/field was significantly greater in male D+E mice *versus* female counterparts (Figure 4.4B, $p<0.005$). Area of AHF were next calculated and expressed as mean foci area (MFA; mm^2). These data demonstrated significantly greater MFA in D and D+E groups compared to E and C in males and females at 24 and 48 -weeks (Figure 4.4A and B, $p<0.05$). In analyzing male *versus* female DEN-initiated animals, greater MFA were measured in males compared to females in D+E mice (24 weeks) and in D and D+E mice groups (48 weeks) (Figure 4.4B, $p<0.05$).

4.3.4. Proliferation: To assess mitogenesis a second series of IHC was performed using an antibody specific against proliferating cell nuclear antigen (PCNA;Figure 4.5A). Quantification of these results demonstrated significantly increased PCNA staining in

Table 4.2: Mean pathological scores following blind scoring for steatosis, necrosis, inflammation and fibrosis in control male and female mice (C), and mice maintained on ethanol (E) DEN-initiated (D) or DEN-initiated followed by ethanol (D+E). Data were collected at 24 and 48 weeks and totaled to generate a total liver injury score

Pathological parameter	**MALE (24 Weeks) Group (n)**				**FEMALE (24 Weeks) Group (n)**			
	C (9)	E (9)	D (9)	D+E (14)	C (10)	E (10)	D (9)	D+E (14)
Steatosis	0±0	0.69±0.10	1.84±0.26	1.93±0.13	0±0	0.39±0.05	1.37±0.08	1.35±0.14
Necrosis	0±0	0.25±0.05	0.97±0.12	1.14±0.12	0±0	0.14±0.02	0.51±0.10	0.45±0.05
Inflammation	0.04±0.02	0.14±0.05	0.80±0.18	1.01±0.13	0.03±0.02	0.2±0.04	0.96±0.12	0.73±0.08
Fibrosis (% sirius red)	0.18±0.04	0.46±0.20	0.57±0.15	0.68±0.13	0.20±0.06	0.37±0.06	0.78±0.07	0.68±0.07
TLIS	**.22±0.04**	**1.54±0.15**	**4.18±0.51**	**4.75±0.32**	**0.23±0.07**	**1.10±0.11**	**3.61±0.18**	**3.21±0.23**
	MALE (48 Weeks) Group (n)				**FEMALE (48 Weeks) Group (n)**			
	C (9)	E (9)	D (8)	D+E (14)	C (10)	E (10)	D (9)	D+E (14)
Steatosis	0.01±0.01	0.93±0.17	1.76±0.27	3.00±0.13	0.01±0.01	0.40±0.13	1.10±0.21	1.24±0.30
Necrosis	0.03±0.03	0.31±0.08	0.93±0.06	2.19±0.16	0±0	0.14±0.05	0.60±0.08	0.84±0.10
Inflammation	0.10±0.04	0.16±0.05	0.64±0.13	1.61±0.31	0.13±0.04	0.40±0.14	0.89±0.10	1.63±0.31
Fibrosis (% sirius red)	0.20±0.01	0.35±0.03	1.83±0.08	2.31±0.11	0.16±0.08	0.44±0.12	1.37±0.07	1.51±0.13
TLIS	**0.34±0.05**	**1.75±0.25**	**5.16±0.29**	**9.11±0.54**	**0.30±0.12**	**1.39±0.19**	**3.96±0.44**	**5.13±0.53**

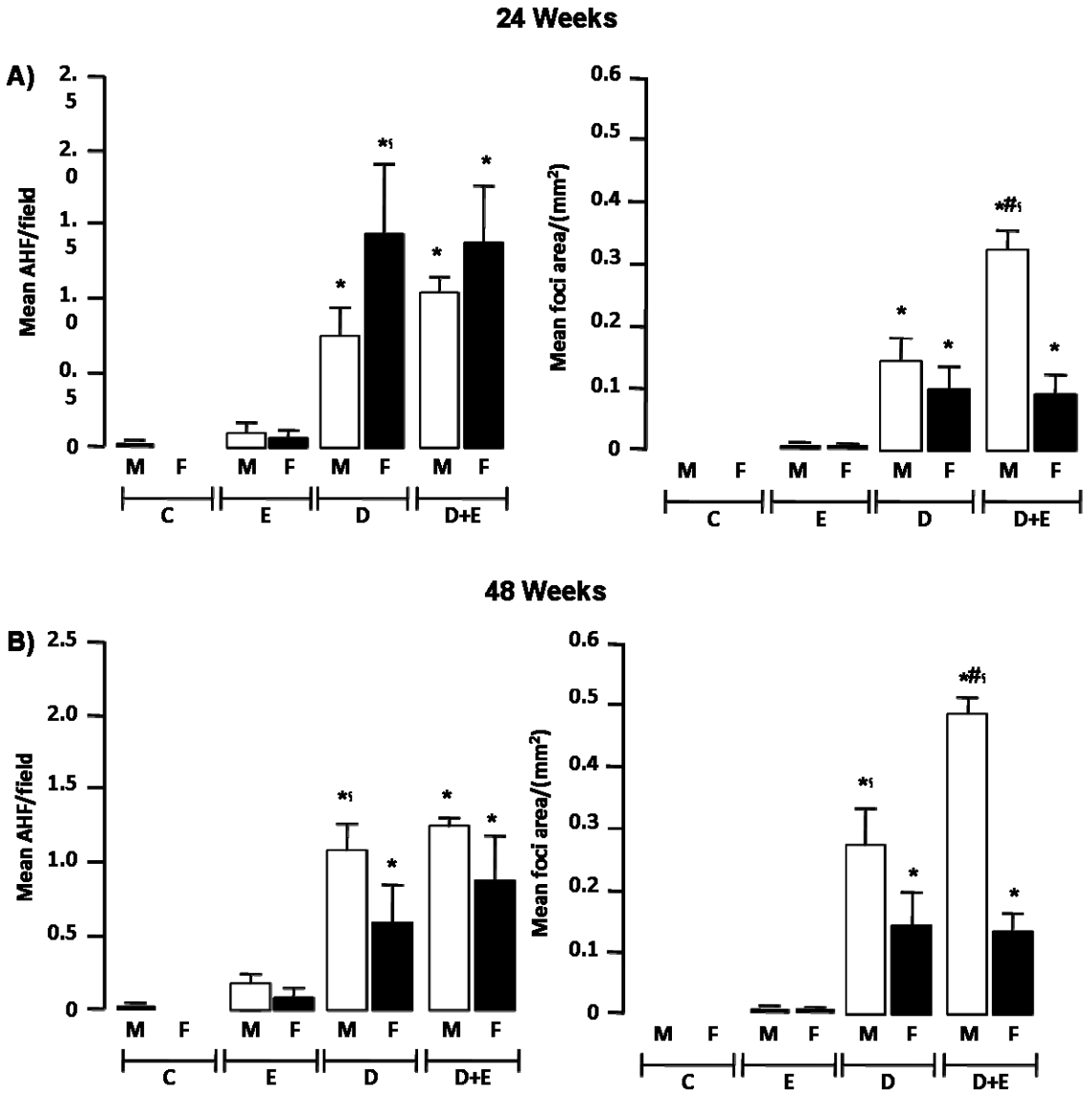

Figure 4.4: Ethanol feeding promotes hepatic tumor incidence and size preferentially in male mice A) Mean number of altered hepatic foci (AHF)/field and mean foci area (MFA) were calculated from glutathione S-transferase placental isoform (GSTpi) positive cells in microscopic fields (x200 magnification, 2 lobes/mouse, 5 fields/lobe) from control (C) male and female mice, and mice undergoing ethanol feeding (E), DEN-initiation (D) or DEN initiation followed by 8 weeks of ethanol feeding (D+E). *p<0.05 versus respective male or female E, #p<0.05 D+E versus respective male or female D mice, §p<0.05 male versus female within same treatment group/time points. Minimum n = 8 independent mice/group. **B)** Mean AHF and mean area occupied by foci were calculated from GSTpi+ cells from microscopic fields (x200 magnification, 2 lobes/mouse, 5 fields/lobe) from control (C) male and female mice, and mice undergoing E, D, or D+E. *p<0.05 versus respective male or female E, #p<0.05 D+E versus respective male or female D mice, §p<0.05 male versus female within same treatment group/time points. Minimum n = 8 independent mice/group.

male and female mice initiated with DEN (D) or DEN+EtOH (D+E) compared to control (C), or EtOH-only (E) groups at 24 and 48-weeks (Figure 4.5B, $p<0.05$). Furthermore, significantly increased PCNA staining was measured in male D+E mice *versus* D in both 24 and 48-week groups (Figure 4.5B, $p<0.05$). Finally, PCNA staining in D and D+E was significantly higher in male and female mice from 48-week groups compared to the 24-week groups (Figure 4.5B, $p<0.05$). Since increased PCNA staining is also associated with DNA repair (Essers, 2005), we performed immunoblot analysis of cyclin D1 in hepatic tissue lysates. These data showed significantly increased cyclin D1 expression in D+E male and female mice compared to other groups (Figure 4.5B, $p<0.05$). Furthermore, higher cyclin D1 expression was apparent in male D+E mice at 48-weeks compared to pair-matched female counterparts (Figure 4.5C, $p<0.05$).

4.3.5. Apoptosis: An *in situ* TUNEL assay was performed and TUNEL positive nuclei/field (T+) calculated. These data demonstrated a significant increase in T+ nuclei in male D+E *versus* D only at both 24 and 48-weeks (Figure 4.6, $p<0.05$). Of interest, the number of T+ nuclei was significantly greater in female D+E mice at 24 -weeks compared to all other groups (Figure 4.6), and in female D-only mice compared to male counterparts in the 48-week group (Figure 4.6B, $p<0.05$).

4.3.6. Blood-alcohol content (BAC), Liver Function and REDOX Status: As anticipated, blood alcohol content (BAC) was elevated in animals maintained on the EtOH-DW regime, a range of 10.4 ± 1.0 to 14.3 ± 1.2mmol/L being detected (Table 4.3). No significant differences were measured between male and female DEN-initiated animals maintained on ethanol (D+E) compared to ethanol alone (E), and no significant differences were measured between respective groups at 24 *versus* 48-weeks (Table 4.3).

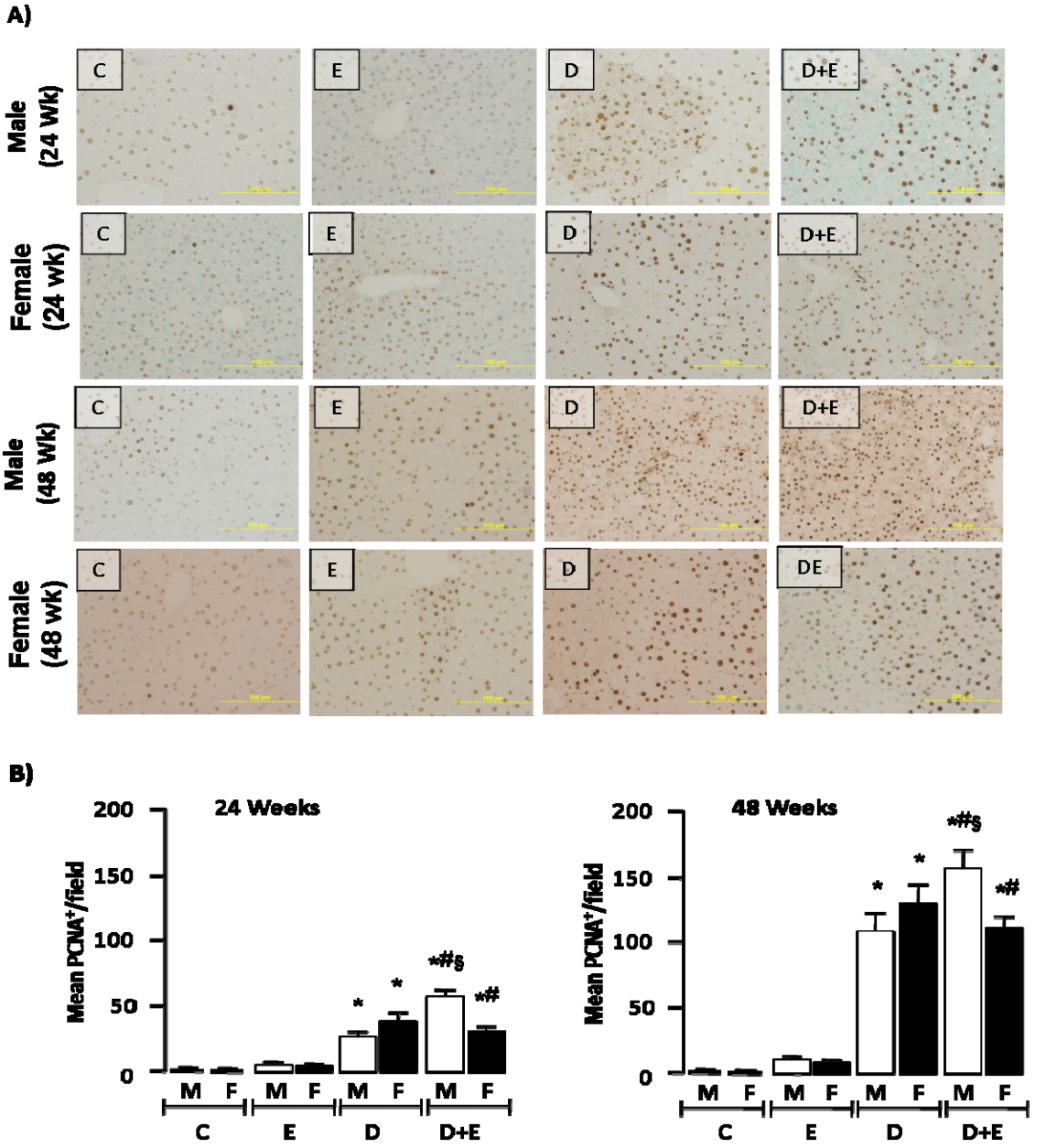

Figure 4.5: Ethanol feeding promotes hepatic tumorigenesis preferentially in male mice A) Representative proliferating cell nuclear antigen (PCNA) immunohistochmistry of hepatic sections (x200 magnification) from control (C) mice, or mice maintained on ethanol (E), DEN-initiation (D), or DEN and ethanol (D+E) at 24 or 48 weeks. **B)** Number of PCNA positive cells per microscopic field (x200 magnification) were measured in representative sections (2 lobes/mouse, 5 fields/lobe) from individual male and female mice on different treatment regimes (24 and 48 weeks) and mean values (± SEM) were calculated. *p<0.05 versus respective male or female E, #p<0.05 D+E versus respective male or female D mice, §p<0.05 male versus female within same treatment group/time points. Minimum n = 8 independent mice/group.

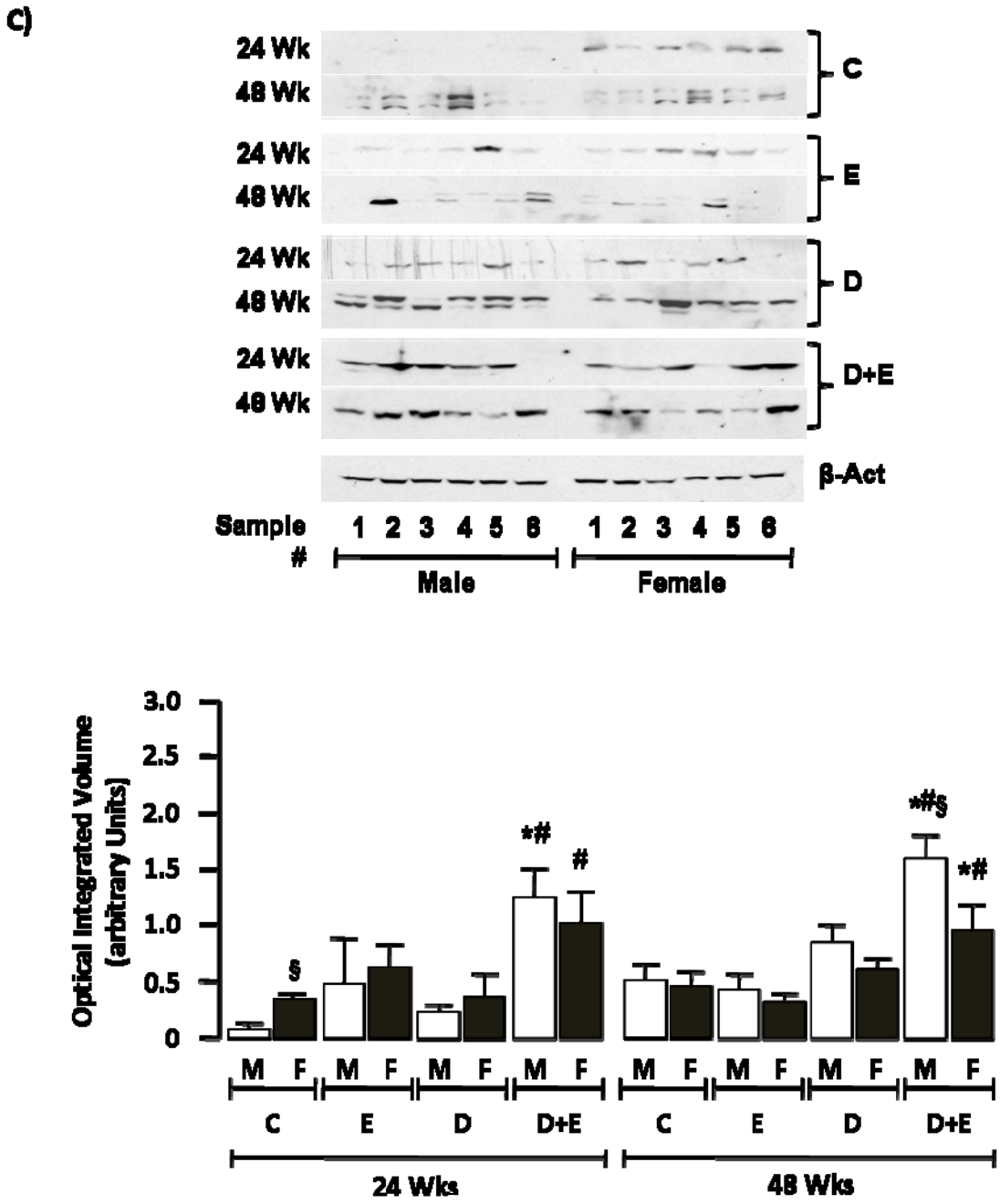

Figure 4.5: Ethanol feeding promotes hepatic tumorigenesis preferentially in male mice C) Representative immunoblots of cyclin D1 expression in hepatic tissue lysates from male and female mice on different treatment regimes at 24 and 48 weeks. Optical integrated volume was calculated, corrected for sample loading (stripping-re-probing membranes with anti-β-actin (β-Act)) and expressed as mean values (arbitrary units) ± SEM (lower panel). *$p<0.05$ versus respective male or female E, #$p<0.05$ D+E versus respective male or female D mice, §$p<0.05$ male versus female within same treatment group/time points. Minimum n = 6 independent samples per group.

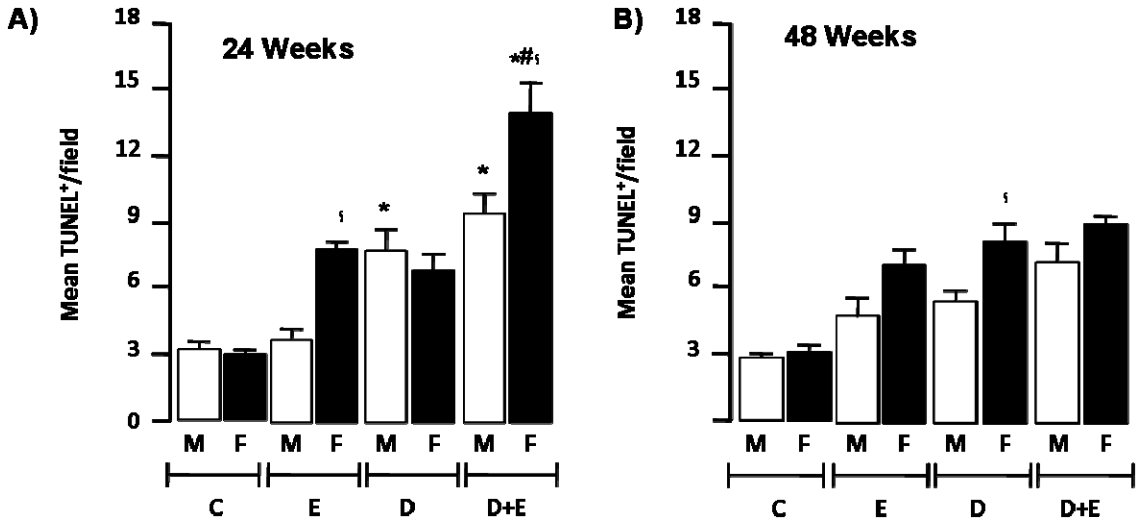

Figure 4.6: Ethanol feeding promotes cell death in hepatic tumorigenesis preferentially in female mice A) Fluorescein *In situ* cell death detection assay was performed on representative sections of control male and female mice (C) and mice maintained on ethanol (E), DEN-initiated (D), or DEN-initiated followed by ethanol feeding (D+E) at **A)** 24 and **B)** 48 weeks. Number of TUNEL positive cells per microscopic field (x200 magnification) were measured in representative sections (minimum of 2 lobes/mouse, 5 fields/lobe) and mean values (± SEM) calculated. *$p<0.05$ versus respective male or female E, #$p<0.05$ D+E versus respective male or female D mice, §$p<0.05$ male versus female within same treatment group/time points. Minimum n = 8 independent mice/group.

As an indicator of liver injury/function serum alanine transferase (ALT) levelsNo significant differences were measured between male and female DEN-initiated animals maintained on ethanol (D+E) compared to ethanol alone (E), and no significant differences were measured between respective groups at 24 *versus* 48-weeks (Table 4.3).

As an indicator of liver injury/function serum alanine transferase (ALT) levels were measured. Within the 24-week groups ALT levels were significantly elevated in all three treatment groups (E, D and E+D) compared to control, although these levels remained within the normal range expected for ALT levels in mice (11-70U/L) (Yan and Stanley, 2001). Of note, ALT levels in both male and female mice initiated with DEN and maintained on EtOH-DW (D+E) were significantly higher than either D, or E alone at 24-weeks (Table 4.3, $p<0.05$). In the 48-week groups ALT was again significantly greater in E, D and D+E groups compared to control (Table 4.3, $p<0.05$). Furthermore, in male mice, D+E and D alone caused significant increases in ALT levels compared to E alone at 24- and 48-weeks, while in female animals this effect was only evident in the 48-week mice (Table 4.3, $p<0.05$). In both instances, ALT levels were significantly higher than in corresponding groups at 24-weeks (Table 4.3, $p<0.05$).

To measure hepatic REDOX status tissue lipid peroxidation (maliondialdehyde; MDA) and glutathione levels were measured. These data demonstrated significantly increased MDA levels in E, D and D+E groups at both 24 and 48-weeks compared to control (Table 4.3, $p<0.05$). Within the 24-week treatment groups no significant difference was measured between MDA levels between the different treatment regimes, or between male and female mice. Conversely, in the 48-week groups, MDA levels were significantly higher in the D+E groups compared to all other groups, and MDA levels

were significantly higher in male D+E animals compared to females (Table 4.3, $p<0.05$). Analysis of GSH levels revealed and inverse correlation to MDA data; all three treatment groups (E, D and D+E) exhibited significantly less GSH compared to controls, the most significant differences being measured in the D+E groups at both 24 and 48 -weeks. Additionally, the most pronounced effect on GSH depletion was measured in the male D+E group at 48-weeks (Table 4.3, $p<0.05$).

4.3.7. Ethanol metabolizing enzyme expression and activity**:** Expression of ADH, ALDH and CYP2E1 were measured by immunnoblot using liver tissue lysates. These data demonstrated no significant differences in ADH or ALDH expression within the groups analyzed at 24 or 48-week time points (Figure 4.7A). Conversely, analysis of CYP2E1 protein demonstrated increased CYP2E1 expression in E and D+E *versus* C and D mice at 24 weeks. In contrast CYP2E1 expression was only significantly increased in E and D+E *versus* C and D counterparts (Figure 4.7B). Additionally, there was no significant difference in CYP2E1 expression between DEN-initiated animals (D) compared to C, nor between male and female mice within the C and D groups at either 24 or 48 weeks time points (Figure 4.7B). To further understand these differences, CYP2E1 mRNA expression was measured by RT-PCR. Using this approach no differences in CYP2E1 mRNA were detected in male or female animals in any of the groups at either 24- or 48-weeks (Figure 4.7D). To determine whether biochemical differences in CYP2E1 activity existed *p*-nitrophenol hydroxylation was measured. This approach demonstrated *p*-nitrophenol hydroxylation was significantly higher in E male and female mice compared to C and D at 24 and 48-weeks (Figure 4.7E, $p<0.05$). Furthermore, CYP2E1 activity was significantly higher in D+E *versus* E mice at 24- and 48-weeks

Table 4.3: Blood Alcohol Content (BAC), alanine aminotransferase (ALT), malondialdehyde, (MDA), and glutathione (GSH) levels at necropsy. *p<0.05 *versus* respective male or female E mice #p<0.05 D+E mice *versus* respective male or female D mice, and §p<0.5 male *versus* female within treatment groups

Group		**n**	BAC mg/dL	ALT IU	MDA nmol/mg	GSH µmol/mg
MALE (24 Wks)	Control (C)	9	1.3±0.1*	11.3±0.9*	1.64±0.16*	5.74±0.16*
	EtOH (E)	9	14.3±1.2	29.1±3.9	7.70±0.75	4.58±0.24
	DEN (D)	9	1.2±0.1*	45.5±4.4*	6.87±0.67§	4.02±0.04§
	DEN+EtOH (D+E)	14	13.3±1.1#	60.7±7.2*#	8.81±0.49*#	2.98±0.11*#§
FEMALE (24 Wks)	Control (C)	10	1.3±0.1*	11.2±1.1*	2.10±0.27*	6.06±0.15*
	EtOH (E)	10	10.4±1.0	35.3±3.2	8.12±0.72	5.15±0.13
	DEN (D)	9	1.3±0.1*	37.3±4.0	5.43±0.83*	4.99±0.08
	DEN+EtOH (D+E)	14	12.2±1.0#	57.0±5.2*#	8.51±0.61#	3.87±0.18*#
Group		**n**	BAC mg/dL	ALT IU	MDA nmol/mg	GSH µmol/mg
MALE (48 Wks)	Control (C)	9	1.5±0.1*	14.7±0. 9*	2.77±0.09*	5.86±0.14*
	EtOH (E)	9	11.5±0.9	53.5±7.5	6.85±0.92§	4.34±0.36
	DEN (D)	8	3.0±0.6*	116.1±16.1*§	8.16±0.53*	4.09±0.14§
	DEN+EtOH (D+E)	14	14.2±0.8#	131.3±17.3 *#§	14.35±0.76*#§	2.43±0.11*#§
FEMALE (48 Wks)	Control (C)	10	1.3±0.2*	15.3±2.2*	2.19±0.31*	5.97±0.14*
	EtOH (E)	10	12.5±0.9	45.2±6.8	5.26±0.79	4.91±0.08
	DEN (D)	9	2.5±0.2*	124.6±19.6*	7.79±0.81*	4.90±0.08
	DEN+EtOH (D+E)	14	13.1±0.8#	107.0±13.9*#	11.52±1.14*#	3.06±0.15*#

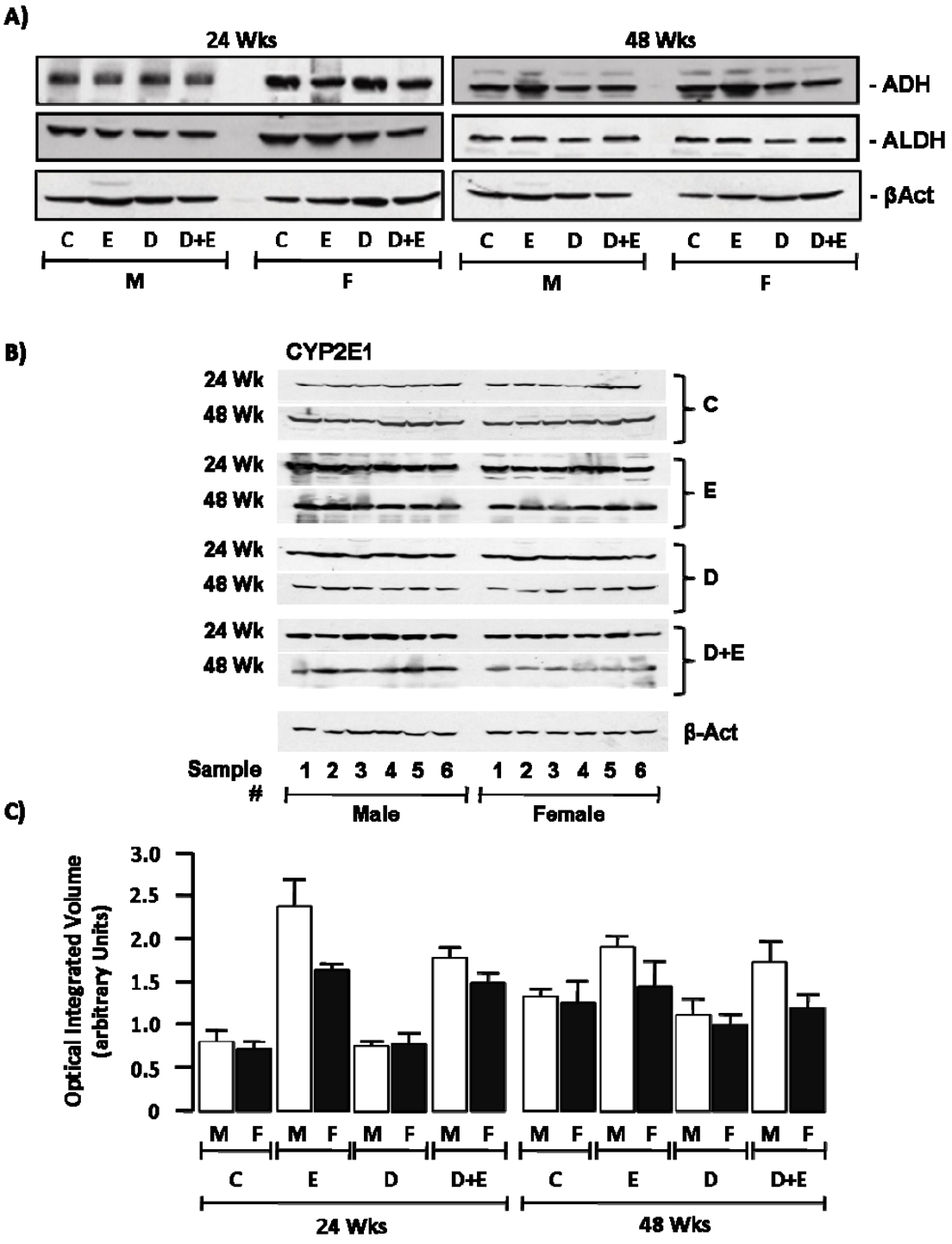
A)
24 Wks
48 Wks
- ADH
- ALDH
- βAct
C E D D+E C E D D+E C E D D+E C E D D+E
M
F
M
F
B)
CYP2E1
24 Wk
48 Wk
C
E
D
D+E
β-Act
Sample #
1 2 3 4 5 6 1 2 3 4 5 6
Male
Female
C)
Optical Integrated Volume (arbitrary Units)
3.0
2.5
2.0
1.5
1.0
0.5
0
M F M F M F M F M F M F M F M F
C E D D+E C E D D+E
24 Wks
48 Wks

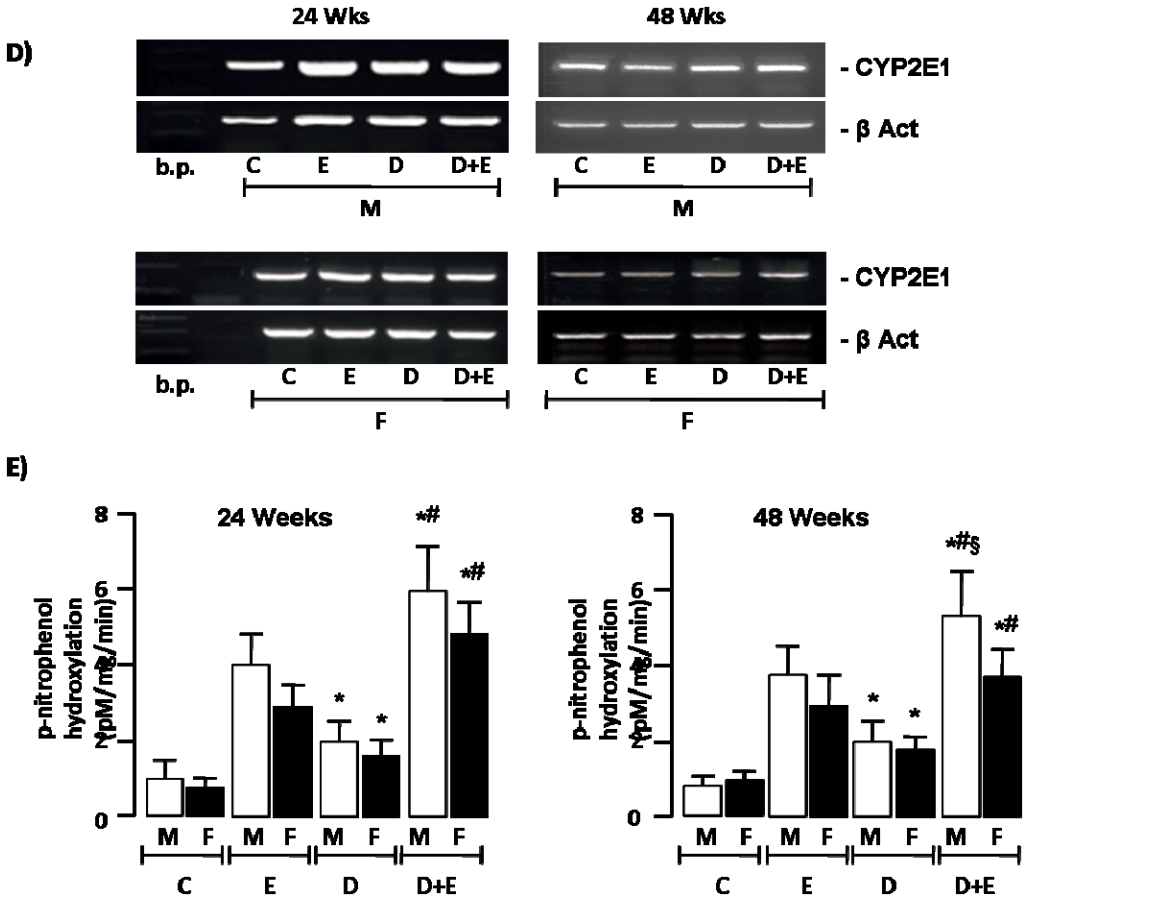

Figure 4.7. Ethanol induces cytochrome P4502E1 expression and activity preferentially in male mice. A) Representative immunoblots for ADH and ALDH expression in pooled hepatic tissue lysates from male and female control (C) and pair-matched animals maintained on ethanol (E), DEN-initiated (D), or DEN-initiated followed by ethanol feeding (D+E) at 24 and 48 weeks **B)** Immunoblots of cytochrome P4502E1 (CYP2E1) expression in hepatic tissue lysates from male and female mice from each experimental group. C) Optical integrated volume was calculated, corrected for sample loading (stripping-re-probing membranes with anti-β-actin (β-Act)) and expressed as mean values (arbitrary units) ± SEM. *p<0.05 versus respective male or female E, #p<0.05 D+E versus respective male or female D mice, §p<0.05 male versus female within same treatment group/time points. Minimum n = 6 independent samples per group. **D)** RT-PCR analysis of CYP2E1 mRNA expression from pooled total mRNA samples from male and female mice on the different treatment regimes indicated at 24 and 48 weeks. **E)** p-nitrophenol hydroxylation was measured as a marker of CYP2E1 activity in hepatic lystaes from male and female mice on different treatment regimes at 24 and 48 weeks. *p<0.05 versus respective male or female E, #p<0.05 D+E versus respective male or female D mice, §p<0.05 male versus female within same treatment group/time points.

(male and female), and by 48-weeks CYP2E1 activity was significantly higher in male *versus* female D+E mice (Figure 4.7E, $p<0.05$).

4.3.8. Immunological status: To identify changes in hepatic immune responses, we performed qRT-PCR analysis of hepatic T-bet, GATA3, and SMAD3 mRNA expression (Levings et al., 2002). These data demonstrated significantly increased T-bet and GATA3 mRNA expression in female experimental groups (E, D, and D+E) compared to control (Figure 4.8A, $p<0.05$, in all groups *versus* C) and compared to male counterparts, with the exception of GATA3 mRNA expression in DEN-only initiated animals (Figure 4.8A). Furthermore, T-bet and GATA3 mRNA expression were significantly decreased in male E and D+E mice *versus* control and DEN-only male counterparts (Figure 4.8A, $p<0.05$). Concomitant with decreased T-bet/GATA3 mRNA expression, male mice demonstrated significantly increased SMAD3 mRNA expression in all experimental groups (E, D, and D+E) compared to control (Figure 4.8A, $p<0.05$, all groups *versus* C). Hepatic SMAD3 mRNA expression was in turn significantly increased in D and D+E male mice compared to E-only counterparts (Figure 4.8A, $p<0.05$). Conversely, SMAD3 mRNA was significantly decreased in female mice treatment groups as compared to male counterparts and female controls (Figure 4.8A, $p<0.05$).

In an attempt to further understand changes in hepatic markers of immune status a custom mouse bioplex assay for 7 immunological cytokines (IL-6, TNFα, IL-10, IL-13, IL12p70, IL1b, and IFNγ) was performed in serum pooled from C, E, D, and D+E, 48-week animals. IL-6 was not detectable in serum from any of the experimental groups (Figure 4.8B). In male animals, chronic ethanol feeding (E) did not alter cytokine levels as compared to control (C). However, serum levels of the 6 detectable cytokines

increased by 1.6-2.8 fold in DEN-initiated (D) males compared to pair-matched C and E mice. Conversely, levels of all 6 cytokines decreased in D+E mice to levels equal or lower than those measured in C and E mice (Figure 4.8B). Analysis of serum from female mice demonstrated E alone led to a 1.65 fold increase in IL-13 as compared to C, no notable differences being measured for the other detectable cytokines between E and C (Figure 4-8B). Unlike their male counterparts DEN-initiation (D) did not lead to any notable changes in detectable cytokine levels as compared to C (Figure 4.8B). However, female D+E mice demonstrated a substantial decreased IL-10, IL-13, IL-1b, and IFNγ as compared to C, E and D-only mice. Of particular note, IL-10 was ≈5.0 fold lower in female D+E mice compared to C, E or D mice, as well as pair-matched males, without any notable change in IL-12p70 or TNFα (D+E *versus* C, E and D, Figure 4.8B).

4.4. Discussion and Conclusions:

Chronic ethanol abuse, in the absence or presence of other factors, is a significant risk factor for developing HCC (Yang and Roberts, 2010). Considerable evidence points to many of the deleterious effects of ethanol arising from metabolic byproducts and ROS produced during ethanol metabolism. Similarly, epidemiological evidence points to sexual dimorphism for HCC development. To date though, relatively few studies have addressed the effects of ethanol on promotion of hepatocarcinogenesis, and the potential role that the gender plays in these disparities.

Epidemiological data report chronic, heavy ethanol consumption is a significant risk factor for the development of hepatic cirrhosis, the leading precursor to HCC development. However, experimental approaches to better understand these mechanisms report disparate results depending on the model employed. Using HCC cells *in vitro,*

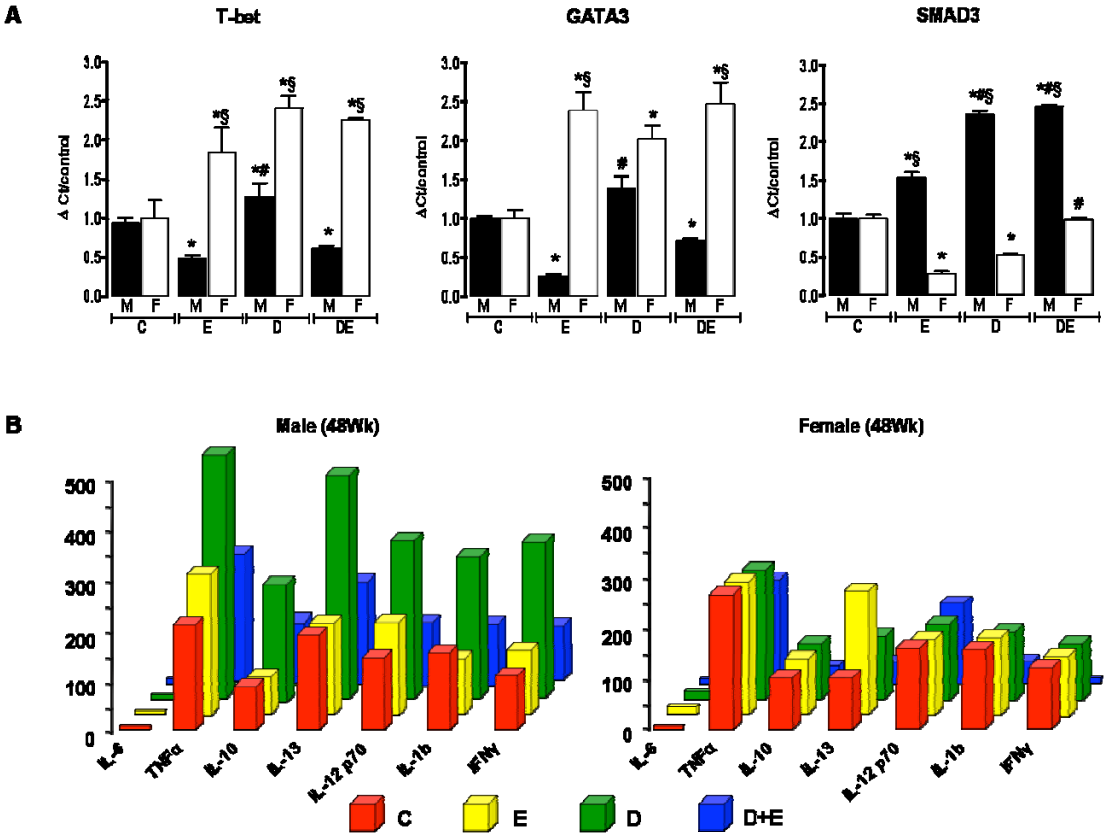

Figure 4.8. Ethanol feeding differentially affects immune responses in male versus female mice in the setting of hepatocarcinogenesis. A. Quantitative real time PCR (qRT-PCR) analysis of T-bet, GATA3, and SMAD3 mRNA expression in total hepatic mRNA isolated from C, E, D, and D+E mice at 48 week time points. *$p<0.05$ versus C, #$p<0.05$ versus respective male or female E mice, §$p<0.05$ male versus female within same treatment group/time points. **B.** custom BioPlex assay was used to determine cytokine expression in pooled serum samples from control male (left) and female (right) mice (C), and pair matched animals maintained on ethanol (E), DEN-initiated (D), or DEN-initiated followed by ethanol feeding (D+E) at 48 weeks. Minimum n = 8 independent samples per group.

ethanol is reported to either increase (Brandon-Warner et al., 2010b) or inhibit (Castañeda and Kinne, 2000) and Kinne, 2000) proliferation depending on the cell line employed. Studies aimed at evaluating the promotional effects of ethanol on hepatocarcinogenesis *in vivo* report similarly diverse results, whereby no effect, co-carcinogenesis, or promotional effects occur (Mandl, 1989; Schwarz, 1983; Takada, 1986). However, these studies were limited to male animals such that the role of gender has not previously been examined. Additionally, these models commonly utilize nutritional deficits (low methionine diet) or partial hepatectomy as a means to promote hepatocyte proliferation concomitant with ethanol feeding (Mandl, 1989; Schwarz, 1983; Takada, 1986). In doing so, it is possible that differences in timing, duration of ethanol exposure (relative to DEN initiation), and/or the effects of partial hepatectomy/altered nutritional may significantly affect outcome.

In this study DEN was administered to neonatal mice and dysplastic foci were allowed to develop prior to ethanol administration in the absence of nutritional deficits or partial hepatectomy. Following administration DEN, like ethanol, induces hepatic CYP2E1 resulting in hepatocyte transformation. As the animal/liver develops so, DEN-induced hepatic DNA damage is magnified (Goldsworthy, 2002; Kang, 2007). As the animal matures hepatic tumors form that exhibit a high proliferative index, a subtype genetically similar to that of human HCC, and correspondingly poor prognostic outcomes (Fausto and Campbell, 2010). To ensure that the effects of DEN did not interfere with effects of chronic ethanol feeding on CYP2E1 induction, DEN-initiation was performed in neonatal mice (21-24 days old) 13 or 37 weeks prior to commencing ethanol feeding. In this way ethanol feeding was timed to coincide with hepatic foci (16 weeks) or HCC

(40 week) formation (following neonatal DEN injection) (Fausto and Campbell, 2010; Goldfarb et al., 1983; Goldsworthy, 2002; Kang, 2007).

In this study, rate of HCC for males to females was ≈2:1 in DEN-only mice and 2.6:1 in DEN+EtOH mice at 48-weeks. Additionally increased incidence and size of tumors was measured in DEN-initiated male mice maintained on EtOH-DW (E+D) compared to DEN-initiation alone (D). In contrast, female mice maintenance on the EtOH-DW regime exhibited a decrease in both tumor size and burden. Of note, PCNA was higher in DEN-only female mice, while there was no apparent difference in cyclin D1 expression (compared to pair-matched males) in this group. This disparity may indicate changes in PCNA expression in female mice occurs, in part, due to activation of DNA repair mechanisms. That is, chemical carcinogens induce DNA damage that can, in turn, activate endogenous repair pathways, PCNA having been reported to accumulate at sites of DNA damage as a requirement for DNA repair (Essers, 2005). Given the importance of oxyradicals and changes in cellular REDOX balance during ethanol metabolism (Albano et al., 1999; Hoek, 2002), the differences in DNA repair mechanisms between male and female mice may thus be of significance in hepatic tumorigenesis in the setting of chronic ethanol feeding in a model pre-disposed to hepatic tumor formation. No differences in PCNA were detected between male and female E-only mice, but female D+E mice had significantly lower PCNA staining compared to pair-matched males with significant increases in TUNEL positive cells. This may indicate that females eliminate cells with ethanol-induced DNA-damage, and that these differences in apoptosis are more efficient during early hepatocarcinogenesis than late,

although apoptosis (as indicated by TUNEL+ cells) remains higher in females than males in E and D+E groups, even at 48 wks.

In addition to differences in timing of DEN administration and/or nutritional or surgical promotion, our model employed an ethanol-drinking water (EtOH-DW) feeding regime. Several models of chronic ethanol feeding have been described, including the Lieber DeCarli (LDC) liquid diet, the Tsukamoto-French intra-gastric model, daily gavage, and exposure to ethanol vapor (Tabakoff and Hoffman, 2000). Each of these models has advantages and potential limitations depending on study design and duration. The choice of the EtOH-DW model for our studies was based on practical and experimental considerations. While the LDC and intra-gastric approaches are most commonly reported for studying alcoholic liver disease (Nanji and French, 2003; Tabakoff and Hoffman, 2000), the number of animals in our study group, the use of calorically pair-matched control animals, and the feeding period (8-weeks) made this approach unfeasible. Rather preliminary data from pilot studies, and data generated from our experimental series, demonstrated no significant differences in body weight in animals maintained on EtOH-DW compared to pair-matched DW-only animals, with BACs of ≈10-14mmol/L.

Measures of morbidity (ALT, pathology scores: steatosis, necro-inflammatory changes) corresponded to tumor burden and incidence in male and females and was affected by ethanol. Serum ALT, was elevated in animals maintained on EtOH-DW, without or in addition to DEN-initiation, at both 24 and 48-weeks. Additionally, ALT levels were several fold higher in late (48-week) stage models while only modest increases over normal levels (11-70U/L) were identified at early time points (24-week).

To directly compare degrees of hepatic injury, we presented our data as total liver injury score (TLIS). Using this approach, data demonstrate TLIS are (generally) commensurate with ALT data. However, it is of interest to note that both male and female D and D+E mice had significantly elevated ALT values (compared to C or E counterparts), yet TLIS were significantly lower in female D+E mice *versus* male D+E mice. The most likely explanation for this disparity is the difference in tumor burden between the two groups; in females, HCC formation was most commonly restricted to 1 or 2 lobes, whereas in males tumors formed throughout all hepatic lobes. As such histological examination using 2 randomly assigned lobes (5 fields/lobe scored) is more likely to encounter/score non-tumor tissue in females compared to males resulting in a lower TLIS. Additionally, when considering the individual components used to compile TLIS, lipid deposition is observed as the most pronounced individual factor influencing TLIS at both early and late time points. Of further note, in the 24-week animals lipid scoring (male and female) was comprised primarily of microvessicular lipid droplets indicative of active lipid loading. However, by the 48-week time point lipid deposition was primarily large globules indicative of steady state steatosis. Additionally, male mice had high levels of foamy degeneration of cells with large areas of necrosis, effects exacerbated by ethanol exposure in DEN-initiated animals. Overall, scores for individual criteria were generally lower in female mice, the only exception being the presence of more infiltrating immune cells in female DEN-initiated mice at 24 and 48-weeks compared to pair matched males.

The differences we detected in hepatic injury are most likely to be related to changes in cell REDOX state due to ethanol metabolism, generation of ROS, and changes in cellular GSH. Induction of CYP2E1 accentuates the imbalance in acetaldehyde/ALDH

and contributes to the generation of ROS with subsequent depletion of GSH and oxidative injury. Male and female mice maintained on the EtOH-DW regime had consistently higher levels of MDA compared to control or DEN-initiated only mice at 24-weeks. Conversely, GSH levels were decreased in both male and female animals. However, female mice exhibited consistently higher GSH levels than males in both 24 and 48-week groups. These data suggest that, despite the increased potential for injury in females, greater GSH levels may protect against hepatic ROS/oxidative injury.

Hepatic inflammatory responses to ethanol, and their influence on the tumor microenvironment have been identified as important factors during hepatocarcinogenesis (Kakumu et al., 2000; Mandrekar and Szabo, 2009). mRNA analysis of transcription factors for Th1 (T-bet) and Th2 (GATA3) T-effector responses demonstrated that females maintained higher expression of both T-bet and GATA3 compared to pair-matched males in E, D and D+E groups. Furthermore, ETOH-DW alone or EtOH-DW in DEN-initiated male mice acted to suppress T-bet and GAT3 expression below that of c levels. Thee events also occurred in the presence of increased SMAD3 mRNA expression in male experimental mice compared to their female counterparts. Collectively, these data suggest females maintain a more robust inflammation response, a property reflected by lower tumor incidence and burden as compared to male counterparts. Indeed, as indicated by TUNEL analysis, increased apoptosis was detected in female E and D+E groups compared to male counterparts (24 weeks), an event that may be indicative of more efficient immunosurveillance and or clearance of transformed cells in females; factors that will directly contribute to subsequent decreases in hepatic tumor size and burden in females at later time point (48 weeks). Of further note, we also detected increased

SMAD3 mRNA in E, D and D+E male mice, a factor that may indicated increased activation of a T-regulatory response through TGFβ signaling and immunosuppression in male *versus* female mice.

Cytokine profiles within the tumor milieu can have critical effects on tumor promotion and progression. Data presented herein demonstrated that DEN-initiation led to increased expression of all measured cytokines in male mice compared to control. In contrast, no such increase in serum cytokines were measured in DEN-initiated female mice, an effect that is likely attributable to the increased incidence and tumor burden in male DEN mice compared to female. Ethanol alone did not noticeably alter cytokine expression in male mice, yet serum IL-13 was increased by a factor of 1.65 in female E-only mice compared to control and did correlate to increased GATA3 identified in this group. Serum cytokine levels were not completely reflective of hepatic gene expression, but indicate systemic immune responses. As such, they can be influenced by many factors outside the liver, including sex-hormone levels, blood LPS, and overall oxidative stress. It was also noted that male D+E mice exhibited an increased ratio of IL10/low IL12p70 expression relative to C that was not detected in female mice. This is significant as high IL-10/low IL-12p70 has been reported to influence alternative activation of macrophages which can in-turn impair dendritic cell (DC) maturation Endogenous IL-12 p70 is important for host response to tumors, and is reported to inhibit tumoriogenesis (Lin and Karin, 2007) by promoting the maturation of dendritic cell (DC) maturation (Corinti et al., 2001). This is associated with conversion of macrophages from an inflammatory (M1) phenotype, to a tumor associated (M2) phenotype that promotes

tumor progression. It is noteworthy, that suppression of dendritic cell function has been reported in human cases of HCC

Multiple factors influence cytokine expression, and this is particularly true in the setting of chronic ethanol consumption. For example, a significant component of hepatic immune responses are attributed to oxidative stress arising from ethanol metabolism (Crabb, 1995; Hoek, 2002). Additionally, there are indirect effects of ethanol on intestinal permeability, as well as composition of the gut flora that are equally important in defining Kupffer cell (KC) activation and intrahepatic immune signaling (Enomoto et al., 2001; Mandrekar and Szabo, 2009). As such, changes in serum cytokine levels we report may not accurately reflect specific immune responses within the milieu of tumor *per se*, or for that matter the environment around the tumor. Similarly, this type of cytokine panel does not allow us to address the potential role of the multiple cell types likely to be contributing to change in systemic cytokine levels (e.g. KCs, stellate cells, endothelial cells, monocytes and/or T/B-cell populations). However, gender differences are reported in cytokine signaling as well as recruitment of neutrophils and macrophages to the site of injury (Bird, 2008; Naugler, 2007). The potential to differentially effect DC activation, immunosuppression and modulation of T-regulatory cells described herein thus raises intriguing questions regarding the potential role of cytokines/immune responses in mediating inherent differences in male and female responses during EtOH-dependent changes in tumor promotion (Butura, 2009; Hoek, 2002; Lin and Karin, 2007).

While differences in immune system responsiveness are likely to be important mediators of the gender specific effects of ethanol on tumor promotion, other factors must also be considered. Most notable amongst these are the likely effects of ethanol on

sex hormone signaling. While our study did not measure androgen or estrogen levels, or signaling pathways regulated by these sex hormones, a considerable body of data indicates ethanol plays a significant role in regulating the synthesis and action of sex hormones in the liver and other organs. Gender specific differences have been identified in IL-6 expression, and transcriptional activation through NFkB, p38, AP-1 and STAT3 that may influence HCC progression and immune response (Karin, 2009). Additionally, small molecule mediators such as adeponectin have been demonstrated to possess hepatoprotective and anti-tumor qualities and exhibit sex-dependent differences in expression (Shen et al., 2010; You and Rogers, 2009).

Indeed, it seems increasingly likely that future studies of the dynamic between sex hormone synthesis, metabolism and signaling, and the intra and extra-hepatic immune system responses will prove central to fully understanding the dramatic gender differences that occur during hepatic tumorigenesis in the setting of chronic ethanol intake. These data demonstrate ethanol promotes hepatocarcinogenesis in a mouse model primed to develop HCC, but this activity is more pronounced in males than females. Additionally, this is accompanied by increases in MDA and measures of oxidative stress combined with depletion of cellular GSH in males compared to their female counterparts.

These data demonstrate that ethanol promotes HCC progression in male mice, and that male mice exposed to ethanol after DEN initiation have inherently higher levels of oxidative stress with depletion of antioxidant defenses (GSH) when compared to female counterparts. Theses changes in REDOX status are associated with increased tumor size and burden. This suggests that antioxidant therapy may be beneficial in ameliorating these effects and preventing ethanol mediated promotion of HCC. Our *in vitro* studies

using a rat hepatoma cells (H4IIE) demonstrated that pre-treatment of ethanol exposed cells with silibinin deceased the rate of cell proliferation and improved measures of oxidative stress. These data supported a mechanism of direct interaction between silibinin and CYP2E1 that altered ethanol metabolism thereby decreasing the associated toxic effects while inhibiting proliferation. Further studies remain to determine if silibinin would confer any protective effects in this mouse model of HCC and if these effects occur differently in male and female mice. Additionally, we can determine if anti-cancer properties attributed to silibinin could reduce the rate of tumor promotion or progression in the absence of ethanol exposure.

CHAPTER 5: DIETARY SILIBININ POTENIATES THE PROMOTIONAL EFFECTS OF ETHANOL ON HEPATOCARCINOGENESIS IN AN INVIVO MOUSE MODEL

5.1. Introduction:

Hepatocellular carcinoma (HCC) is a significant global health burden. In the United States (US) rates for HCC have doubled over the last three decades (Altekruse, 2009). HCC most commonly occurs in the context of chronic inflammation leading to fibrosis and cirrhosis (McKillop, 2005). In the US nearly 18 million people abuse ethanol, making this a major risk for development of hepatic cirrhosis, the leading risk for subsequent HCC development (Altekruse, 2009; El-Serag, 2002; McKillop, 2005). The mechanisms by which chronic ethanol consumption leads to cirrhosis and HCC remain poorly defined. Ethanol is not considered a hepatic carcinogen *per se*; rather injury is thought to be related to its metabolism in hepatocytes. Additionally, ethanol works synergistically with other risk factors to further increase incidence and severity of disease onset (El-Serag, 2007; McKillop and Schrum, 2009).

Within the liver, hepatocytes account for the majority of ethanol metabolism to acetaldehyde via ADH and/or CYP2E1 dependent pathways (Lieber, 2000; McKillop, 2005). Acetaldehyde is in turn oxidized by acetaldehyde dehydrogenase (ALDH) to acetate, which enters the Kreb's cycle. With infrequent, moderate consumption, the ADH/ALDH pathway accounts for most ethanol oxidation. However, in the setting of chronic, long term, ethanol exposure induction of CYP2E1 occurs and acetaldehyde

production is increased (Lieber, 1997b; McKillop, 2005). Acetaldehyde is a toxic, volatile intermediate that can rapidly bind to DNA, proteins and lipid membranes (Muller, 1987). These interactions produce DNA and protein adducts, or lipid peroxidation, which leads to additional toxic aldehyde products (e.g. malondialdehyde (MDA) and 4-hydroxynonenol (HNE)). In addition, CYP2E1 enzyme is also poorly coupled to oxygen leading to partially reduced ethanol; hydroxylethyl radical (HER), and reactive oxygen species (ROS) that combine to further exacerbate the genotoxic and cytotoxic effects of ethanol metabolites (Albano, 2006; Wu and Cederbaum, 2003). Cumulative effects of these events can be the generation of genetic changes that drive malignant transformation. Additionally, ethanol/ethanol metabolism influences cell signaling pathways, affecting proliferation, DNA repair, and apoptosis (Albano, 2006). In doing so, ethanol may act as a promoting agent on select transformed cells allowing for clonal expansion.

The underlying effects of ethanol are largely determined by the generation of toxic intermediates, such as ROS that lead to increased oxidative stress. Hepatic GSH serves as the major endogenous antioxidant involved in detoxification (Lu, 1998). Cell GSH levels can be depleted by chronic oxidative stress which generates an imbalance in ratio of GSH to its disulfide-oxidized form (GSSG). Structural changes in mitochondria occurring as a result of oxidative stress and ethanol exposure mediate effects on membrane permeability that impair GSH transport (Cunningham and Bailey, 2001). Oxidative stress is a key mediator of hepatic inflammation which can be critical in the promotion and progression of HCC (Albano, 2008; Lieber, 2001).This has led to numerous studies on the efficacy of utilizing antioxidant therapies to ameliorate oxidative

injury occurring from increased generation of oxygen radicals and loss of cellular REDOX homeostasis associated with chronic ethanol abuse.

Antioxidants have been reported to reduce ethanol mediated double strand DNA breaks, and inhibit formation of lipid peroxidation byproducts (Bartsch, 2005; Navasumrit, 2000). *Silybum marianum* (Milk Thistle) has been used as an hepatoprotectant for (at least) several millennia. It is derived from plant seeds as silymarin, a mixture of flavinoligands consisting of silybin A, silybin B, isosilybin A and B, silychristin and silydianin (Saller, 2007). Of these, the most abundant and biologically active the diasteroisomers silybin A and B with exist in a 1:1 ratio, and collectively identified as silibinin (Lee, 2003; Saller, 2007). Silibinin is a potent scavenger of hydroxy radicals and is reported to stimulate increased synthesis of superoxide dismutase (SOD) (Mira et al., 1994; Pradeep et al., 2007). Additionally, other properties may act to inhibit cancer growth or progression. Ramakrishnan, et al. report that silymarin inhibits proliferation in HepG2 cells in a dose dependent manner, with a corresponding increase in apoptotic cells (Ramakrishnan et al., 2009). Protective effects of silibinin have also been reported in several *in vivo* studies of liver injury in which protection from oxidative injury, stellate cell activation and T-cell mediated liver injury is evidenced by oral silibinin (Pradeep et al., 2007; Schumann et al., 2003; Trappoliere et al., 2009).

Data from previous chapters demonstrate ethanol promotes hepatic carcinogenesis in a DEN mouse model, effects restricted to males. In this case a single dose of DEN (1 mg/kg, i.p.) was administered to infant B6C3 mice (21-28 days) followed by chronic ethanol feeding at points predicted for foci (16 weeks), or HCC (40 weeks) development (Goldfarb et al., 1983; Vesselinovitch and Mihailovich, 1983). Of specific note, these

events were associated with sex-dependent differences in GSH-GSSG status between the sexes, while previous in vitro studies demonstrated silibinin inhibited the promotional effects of ethanol on HCC cell proliferation.

In light of these data, the aims of the final set of studies for my dissertation were to determine the effects of dietary silibinin, in the absence and presence of chronic ethanol feeding on promotion and progression in a mouse model primed to develop HCC. As in previous studies, silibinin administration was timed to coincide with the kinetics of DEN initiated tumorigenesis (Goldfarb et al., 1983; Vesselinovitch and Mihailovich, 1983).

5.2. Materials and Methods:

5.2.1. Materials: Materials for the *in vivo* model of haptocarcinogensis as previously described (Section 2.1.2). Materials for immunohistochemistry studies were as described previously (Section 2.5.2.1). Additionally, anti-F4/80 and anti-CD3 antibodies were purchased from Abcam (Cambridge, MA). Rabbit HRP, DAB chromagen, Rat AP polymer kit, and Vulcan Fast Red were purchased from Biocare (Concord, CA). Antigen retrieval 1 mM EDTA was purchased from GibcoBRL (San Francisco, CA). Proteinase K was purchased from Qiagen (Valencia, CA). Materials for immunohisotchemistry Enzyme- Immuno-Assay (EIA) for detection of 8-OHdG was purchased from Cayman Chemical (Ann Arbor, MI). A DNA isolation kit and Monococcal nuclease were purchased from Zymo Research (Irvine, CA). Glycerol, Alkaline phospatase 2000 U/mL, $MgCl_2$, $CaCl_2$, EDTA, NaCl and Tris-HCL were purchased from Sigma Aldrich (St. Lousi, MO).

5.2.2. Methods *In vivo* model of hepatocarcinogenesis: B6C3 mice (21-28 days

old) were randomized, weighed, and injected with a single dose of DEN (1mg/kg body weight, (*i.p.*)) dissolved in sterile olive oil (DEN group; D) or vehicle (olive oil (*i.p.*)), control group; C) as described in Section 2.1.3. Animals receiving DEN or vehicle were randomized to receive control (AIN93-M) diet or diet supplemented with silibinin (AIN93-M+0.5% (*w/w*) silibinin). DEN-initiated animals designated to receive silibinin diet were further divided into groups designated to receive water or EtOH-DW regimes for early (16-24-weeks) or late (40-48-weeks) hepatocarcinogenesis studies. Prior to experimental treatments, animals were allowed free access to AIN93M rodent chow.

5.2.3. Silibinin diet: Animals assigned to groups receiving silibinin diet (AIN93M mouse chow + 0.5% silibinin (*w/w*) (silibinin diet alone (Sil)), DEN initiated + silibinin diet (D+Sil), or DEN-initiated + EtOH-DW + silibinin diet (D+E+Sil)) were introduced to diet at 15 weeks for early (24 week) or 39 weeks for late (48 week) hepatocarcinogenesis studies and maintained on diets for 9 weeks prior to necropsy (Section 2.1.4). All animals were weighed twice weekly and an n assessment of food intake was conducted during the second and sixth weeks in those studies. Six animals from male and female C, Sil, D+Sil, and D+E+Sil groups were randomly selected and cages isolated. Regular AIN93M mouse chow and AIN93M+Sil (0.5% *w/w*) mouse chow was weighed and placed into feeding chutes on cages. Cages were checked and remaining food weighed daily for 5 days. Mean rate of consumption was calculated based on the amount of food consumed divided by number of animals.

5.2.4. Necropsy: At 24 or 48 weeks (depending on pre-assigned groups) mice were weighed, anesthetized (isofluorane by inhalation), examined grossly and sacrificed as described (Section 2.1.5).

5.2.5. Histology: Multiple liver lobes (minimum of 2 lobes per animal) were sectioned (4-6μm) and stained with Mayer's hematoxylin and eosin (H & E) or Picrosirius red as described (Section 2.5.1.2). Representative sections (5 random fields/lobe) were examined microscopically (100x magnification) and blind-scored for steatosis (0-4), necrosis (0-4), inflammation (0-4), and/or fibrosis (0-4) using modified scoring scales reported by others (French et al., 1993; Morgan et al., 2002). Degree of fibrosis (mean % Picrosirius red staining) was performed using ImageJ software (NIH, Bethesda, MD). Four independent scores were combined to generate a total liver injury score (TLIS) as described previously (Section 2.5.1.3).

5.2.6. Immunohistochemistry (IHC): Staining for anti-glutathione S-transferase placental isoform (GSTpi, 1:100 dilution), and proliferating cell nuclear antigen (PCNA1:1000 dilution) were conducted as previously described (Sections 2.5.2.1 and 2.5.2.2).

Additional sections were stained with an antibody specific for 8-hydroxy deoxyquanosine (8-OHdG) as an indicator of oxidative DNA damage. Sections (4-6μm) of fixed liver were immunostained following deparaffinization, rehydration and antigen retrieval. Sections were examined microscopically (200x magnification), photographed and number of 8-OHdG positive nuclei (dark brown staining), positive and negative nuclei were counted using cell counter features of NIH ImageJ software, and stated as a percent positive.

To assess immune cell infiltration sections (4-6 μm) were dual stained for immune cell markers macrophage (F4/80, 1:250 dilution) and T-cells (CD3, 1:250 dilution) positive cells. Sections (4-6 μm) were immunostained following antigen

retrevial in 1mM EDTA. Immune cells were identified as positive stained macrophage (F4/80, DAB chromagen, dark brown staining) or T-cells (CD3, Vulcan fast-red chromagen) as number of positively stained cells/field, using cell counting feature of ImageJ as previously described. A total of 5 fields per section, 2 sections per liver were examined.

5.2.7. Reverse trancriptase PCR and quantitative RT-PCR: Total RNA was extracted from liver tissue, as described (Section 2.2.2), and cDNA was synthesized from random hexamers (Section 2.2.3) and used to perform PCR for CYP2E1 mRNA expression using mouse specific CYP2E1 primer pairs (Table 1, Section 2.2 (Brandon-Warner et al., 2010b)). Final product was semi-quantified using NIH-ImageJ software and corrected to β-2 microgoblulin (housekeeping gene) levels. qRT-PCR was performed with cDNA followed by SYBR Green Supermix using mouse specific primer pairs for T-bet, GATA3, or SMAD3, listed in Table 1 (Section 2.2). Reactions were preformed in an iCycler IQ™ real time PCR detection system (BioRad) as described section 2.2.4. Samples were assayed in duplicate, and relative gene expression of each transcript was expressed as Δ^{Ct} and normalized to pair-matched controls (Baker et al., 2010; Livak, 2001).

5.2.8. Western Blot Analysis: Liver tissue (≈100mg) was homogenized in RIPA buffer, the resulting homogenate sonicated ($4^{o}C$), protein levels measured, and normalized using RIPA buffer. Protein detection was performed by immunoblot using antibodies specific against ADH, ALDH, CYP2E1 or cyclin D1 (Section 2.4.3) (Brandon-Warner et al., 2010b). Signal intensity was determined using NIH-ImageJ

software and equal protein loading confirmed by stripping/re-probing membranes with an anti-β-actin (housekeeping protein) antibody.

5.2.9. Liver function and REDOX status: Serum alanine-aminotransferase (ALT) was measured using an ALT/GPT 2-part reagent (Section 2.7.2). Hepatic lipid peroxidation was measured in liver tissue homogenates based on thiobarbituric acid reactive species (TBARS). Hepatic GSH levels were determined by colorimetric analysis from liver tissue lysates collected in 2-(*N*-morpholino) ethanesulfonic acid (MES) buffer using a GHS assay kit.

5.2.10. Ethanol assay: Aliquots (50µl) of serum were collected and stored at -80^{o}C prior to measurement of ethanol concentration, as previously described section 2.8.2 (Brandon-Warner et al., 2010b).

5.2.11. Cytochrome P4502E1 activity: CYP2E1 activity was measured as the rate of oxidation of ρ-nitrophenol to 4-nitrocatechol in the presence of NADPH and O_2 (Section 2.11.2) (Brandon-Warner et al., 2010b).

5.2.12. Measurements of serum cytokine levels: To evaluate and compare cytokine expression patterns a custom (7) Plex murine cytokine array (BioRad, Hercules, CA) was preformed.

5.2.13. Silibinin levels: Determination of silibinin levels in serum and liver tissue were conducted at the David H. Murdock Research Institute (DHMRI) by mass spectrometry (LC-MS). Serum (pooled samples from each treatment group) and individual liver tissue samples (n=5) from each treatment group were collected as described Section 2.1.5. Liver tissue was prepared and homogenized in KCl (0.15 mol/L) or Tris HCl (pH 7.4) buffer. Tissue homogenates were centrifuged and supernatants

collected for analysis. Total silibinin from both conjugated and un-conjugated fractions in serum and liver were initially digested with β-glucuronidase and sulphatase at 37^{o}C for 1.5 hours. After digestion, 3 volumes of internal standard (naringenin 10 µl/mL in acetonitrile) was added and mixtures centrifuged at 3,500 rpm for 20 minutes at RT. A UPLC-tandem MS system was used for silibinin quantification following chromatographic separation of 5 µl aliquot of each sample supernatant on an Acquity UPLC analytical column.

5.2.14. Statistical analysis**:** Comparisons of tumor positive animals in each group were made by Fisher's exact test. Comparisons of pathological scoring, foci size and number, mRNA or protein expression, ALT, GSH, TBARS and silibinin were made by one-way ANOVA followed by Dunnet's or Tukey's post-hoc test, as appropriate or two-way ANOVA followed by Bonferonni correction.

5.3. Results:

5.3.1. Mortality, liver-body weight, necropsy**:** No significant differences were measured in body weight of male and female mice in C or Sil groups during the course of the study (Figure 5.1). Male mice were significantly heavier than female counterparts at all time points (Figure 5.1, Table 5.1). Male mice maintained on EtOH-DW where significantly heavier than C at 24 weeks (Figure 5.1, Table 5.1, *$p<0.05$). Male D, D+E, and D+E+Sil demonstrated significant weight gain beginning at 24 weeks when compared to control, but after 44 weeks weight declined rapidly, and by necropsy they were significantly smaller than pair-matched C (Figure 5.1, Table 5.1, *$p<0.05$). No significant increase in liver weights were measured in male mice compared to control at 24 weeks; however, liver:body weight (L:BW) ratio was significant in D+E mice

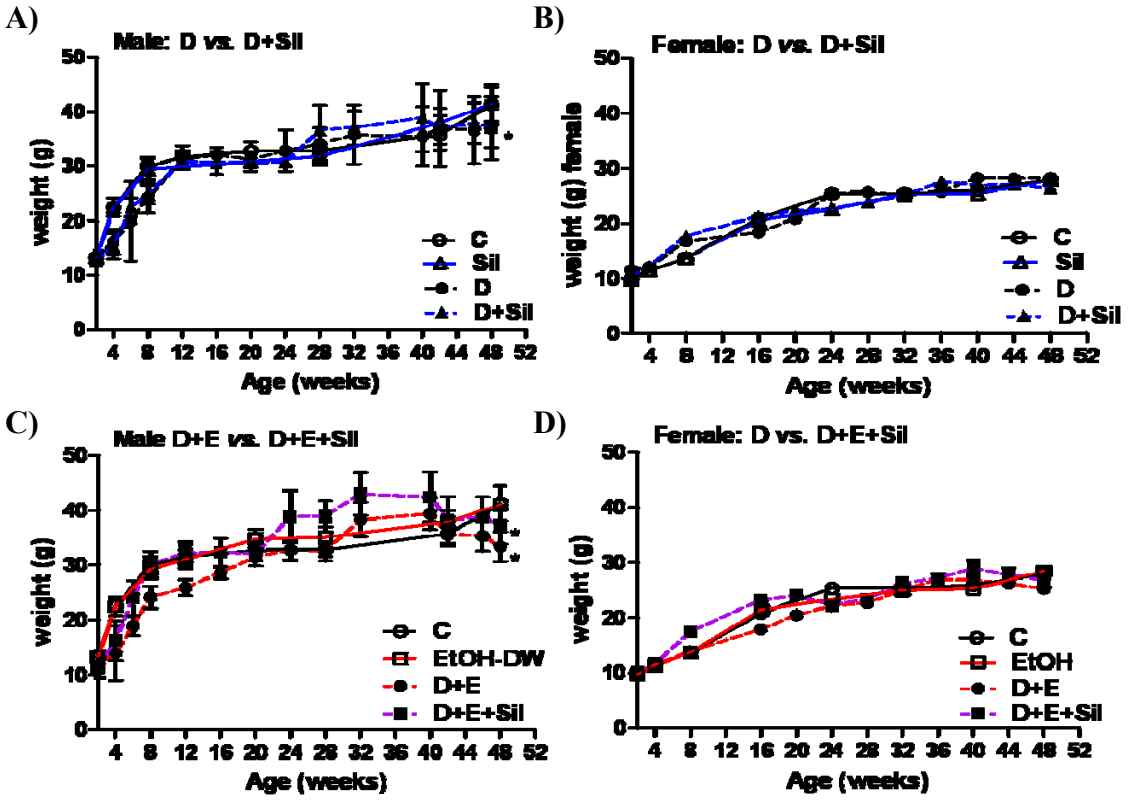

Figure 1: Silibinin diet alone or with concomitant EtOH-DW in DEN-initiated mice had limited effects on growth rates in male and female mice. Growth curves for both **A)** male and **B)** female mice in experimental groups, Silibinin diet (Sil), DEN-initiated only (D), DEN initiated + silibinin diet (9 weeks) (D+Sil) were not significantly different from same-sex control (C). Male D and D+Sil mice had significantly decreased body weight at 48 weeks compared to pair-matched C or Sil mice. **C)** male and **D)** female mice in experimental groups EtOH-DW (8 weeks) EtOH, DEN initiated + EtOH-DW (8 weeks) D+E, and DEN+EtOH-DW +Silibinin diet (D+E+Sil).

compared to control (Table 5.1). In 24 week female mice, liver weight and L:BW ratio were significantly increased in female DEN mice compared to C (Table 5.1, *p<0.05). Conversely, D+Sil group had significantly reduced liver weight compared to pair-matched C and DEN-only animals, this corresponded to significantly reduced L:BW ratio compared to D (Table 5.1, #p<0.5 *versus* DEN). No differences in growth, liver weight, L:BW were identified in D+E or D+E+Sil female mice. In 48 week male mice liver weight and L:BW ratios in all DEN initiated groups were significantly increased compared to C (Table 5.1, *p<0.05). No differences were identified in D *versus* D+Sil or D+E *versus* D+E+Sil male groups. Conversely, in female mice only the DEN-initiated group had significantly increased liver weight and L:BW ratio compared to C (Table 5.1, *p<0.05). However, D+Sil females had significantly lower liver weight and L:BW ratio compared to D-only (Table 5.1, #p<0.05). These changes in liver weight and L:BW ratio, corresponded to tumor burden identified in male and female mice (Figure 5.2).

Upon gross examination no visible lesions were identified in C or Sil male or female mice. Visible lesions were identified in male and female DEN initiated mice. There was no significant difference in the number of animals presenting with lesions at 24 or 48 weeks (Table 5.1). No significant differences in the number of animals identified with visible lesions were detected in either male or female D *versus* D+Sil groups at 24 or 48 weeks. Silibinin feeding concomitant with EtOH-DW did not significantly alter the number of male or female animals presenting with visible lesions at 24 or 48 weeks (Table 5.1).

Male and female animals tolerated the silibinin diet well without, or with prior DEN initiation and in combination with EtOH-DW. Measures of dietary intake

Table 5.1: Liver/Animal weights and Liver:Body weight ratios at necropsy. *p<0.05 *versus* C, or #p<0.05 *versus* DEN-only within male or female groups assayed at the matching timepoints (24 or 48 weeks).

	Group	n	Visible lesions	Liver wt (g)	Body wt (g)	L:BW ratio
Male 24 wk	C	9	0	1.81± 0.05	35.6 ± 0.5	0.050 ± 0.001
	Sil	9	0	1.67± 0.02	33.6 ± 0.8	0.050 ± 0.001
	EtOH	9	0	2.14 ±0.09	42.1 ± 0.8 *	0.056 ± 0.002
	D	9	67% (6/9)	2.10 ± 0.17	36.9 ± 2.4	0.057 ± 0.002
	D+S	8	88% (7/8)	1.96 ± 0.14	37.7 ± 1.9	0.052 ± 0.002
	D+E	14	93% (13/14)	2.08 ± 0.12	34.7 ± 0.7	0.059 ± 0.002 *
	D+E+Sil	14	93% (13/14)	2.01 ± 0.14	34.8 ± 0.7	0.057 ± 0.004
Female 24 wk	C	10	0	1.30 ± 0.03	25.7 ± 0.4	0.051 ± 0.001
	Sil	9	0	1.32 ± 0.04	23.9 ± 0.5	0.055 ± 0.001
	E	10	0	1.48 ± 0.03	27.5 ± 0.4	0.054 ± 0.015
	D	9	55% (5/9)	1.64 ± 0.09 *	27.9 ± 0.6	0.059 ± 0.003 *
	D+S	9	44% (4/9)	1.14 ± 0.07 #	24.1 ± 0.4	0.047 ± 0.001 #
	D+E	14	50% (7/14)	1.35 ± 0.03	25.4 ± 0.4	0.053 ± 0.006
	D+E+Sil	14	64% (9/14)	1.31 ± 0.06	26.7 ± 1.1	0.049 ± 0.001

	Group	n	Visible lesions	Liver wt (g)	Body wt (g)	L:BW ratio
Male 48 wk	C	9	0	1.93 ±0.05	41.2 ± 1.0	0.047 ± 0.002
	Sil	9	0	2.00 ± 0.07	41.4 ± 1.2	0.047 ± 0.001
	EtOH	9	0	2.19 ± 0.06	42.1 ± 0.8	0.054 ± 0.001
	D	8	75% (6/8)	2.59 ± 0.35 *	36.3 ± 2.3 *	0.070 ± 0.007 *
	D+S	9	89% (8/9)	2.64 ± 0.21*	37.1 ± 1.3	0.071 ± 0.005 *
	D+E	14	100% (14/14)	4.44 ± 0.16 *	34.7 ± 0.7 *	0.129 ±0.006 *
	D+E+Sil	14	93% (13/14)	3.96 ± 0.18 *	36.5 ± 0.9 *	0.107 ± 0.007 *
Female 48 wk	C	9	0	1.37 ± 0.05	27.9 ± 0.6	0.049 ± 0.001
	Sil	9	0	1.44 ± 0.05	28.7 ± 0.7	0.050 ± 0.001
	EtOH	9	0	1.41 ± 0.04	28.6 ± 0.5	0.049 ± 0.001
	D	9	44% (4/9)	1.78 ± 0.14 *	28.2 ± 0.8	0.063 ± 0.005 *
	D+S	8	50% (4/8)	1.32 ± 0.11 #	26.4 ± 0.5	0.050 ± 0.004 #
	D+E	14	42% (6/14)	1.31 ± 0.07	25.7 ± 1.1	0.050 ± 0.001
	D+E+Sil	14	64% (9/14)	1.33 ± 0.11	25.9 ± 1.6	0.049 ± 0.003

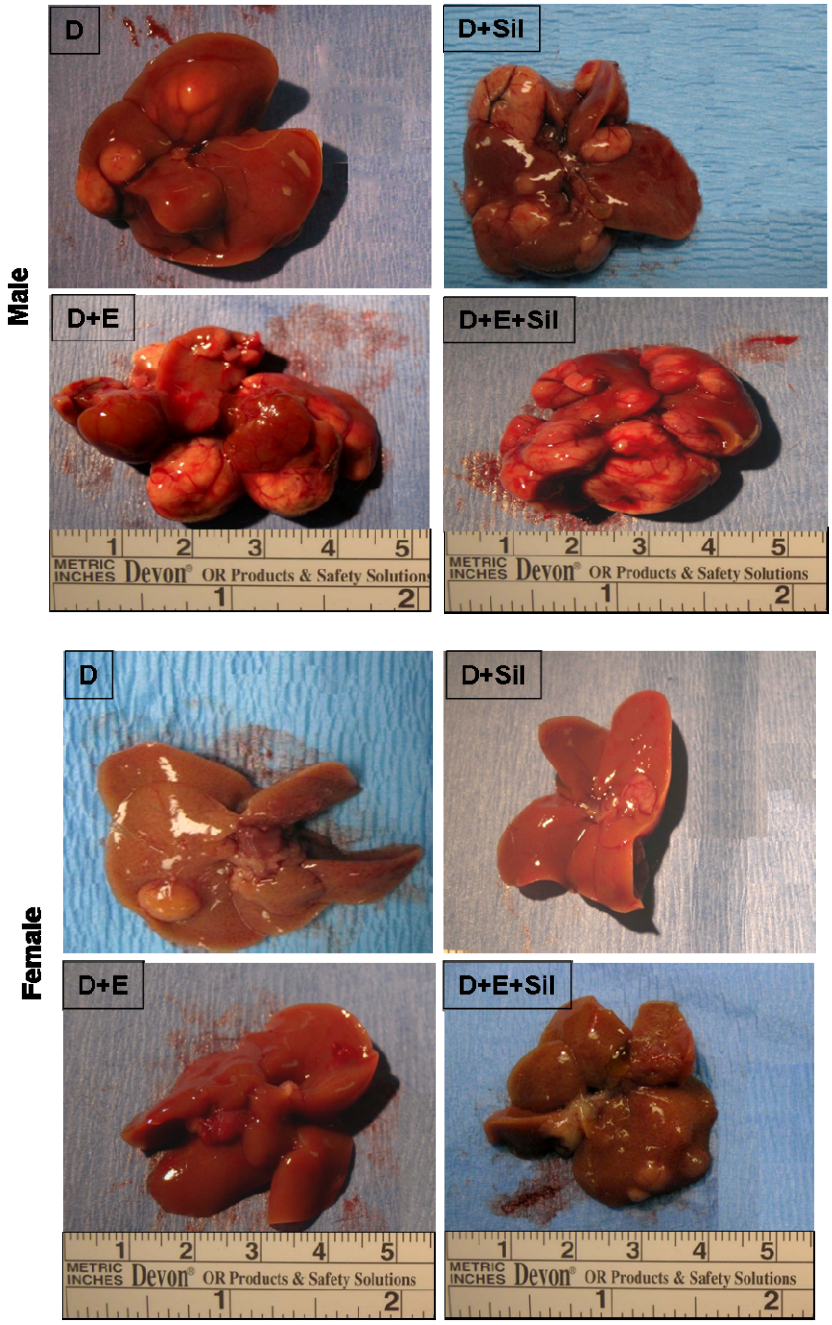

Figure 5.2: Silibinin feeding provided minimal or no protection in male and female DEN initiated mice, but exacerbated hepatocarcinogenesis when combined with EtOH-DW regime. Representative images of livers resected from male and female mice (48 weeks) initiated with DEN (D) and DEN initiated mice maintained on silibinin diet (D+Sil), DEN initiated mice +EtOH-DW (D+E), and DEN initiated mice + EtOH-DW + Silibinin diet (D+E+Sil).

demonstrated no significant differences in consumption of AIN93M mouse chow plus silibinin (0.5% *w/w)*, without (Sil) or with prior DEN initiation (D+Sil), and with DEN+EtOH-DW and silibinin diet (D+E+Sil), or AIN93M mouse chow only (C) without or with prior DEN initiation (D) in male or female mice. Male mice consumed 3.52±.011g of food/mouse/day in animals maintained on silibinin diet *versus* to 3.64±0.12g of food/mouse/day in control. Females consumed 3.12±0.12g of food/mouse/day in animals maintained on silibinin diet *versus* 3.04±0.08g of food/mouse/day in control. Of note, 1 male (D+Sil) mouse in the 24 wk group and 1 female (D+Sil) mouse in the 48 wk group died three weeks post DEN initiation.

5.3.2. Hepatic tissue and serum silibinin levels: Measures of silibinin in liver tissue were decreased in DEN-initiated female mice at 24 and 48 weeks, but appeared to have little effect on serum levels (Figure 5.3A). Measures of silibinin in liver tissue were decreased in D+Sil male mice at 24 weeks, this decrease was not identified in male D+EtOH+Sil mice (Figure 5.3A). At 48 weeks silibinin levels were significantly increased in all male DEN-initiated mice compared to those measured at 24 weeks, and this was enhanced by concomitant EtOH-DW. Increased serum levels detected in 48 week male D+E+Sil animals corresponded to increased tissue levels (Figure 5.3B).

5.3.3. Liver pathology: Total liver injury scores (TLIS) were generated following blind scoring of H&E and Picrosirius red stained slides for total fat, necrosis, inflammatory cell infiltration and collagen deposition (*Figure A.1-A.12, appendix A*, representative images). Using this approach as a means of directly comparing groups, signficant increases in measures of hepatic injury were identified in all DEN initiated male and female groups (Figure 5.4A, *$p<0.05$) compared to C, Sil, or EtOH only

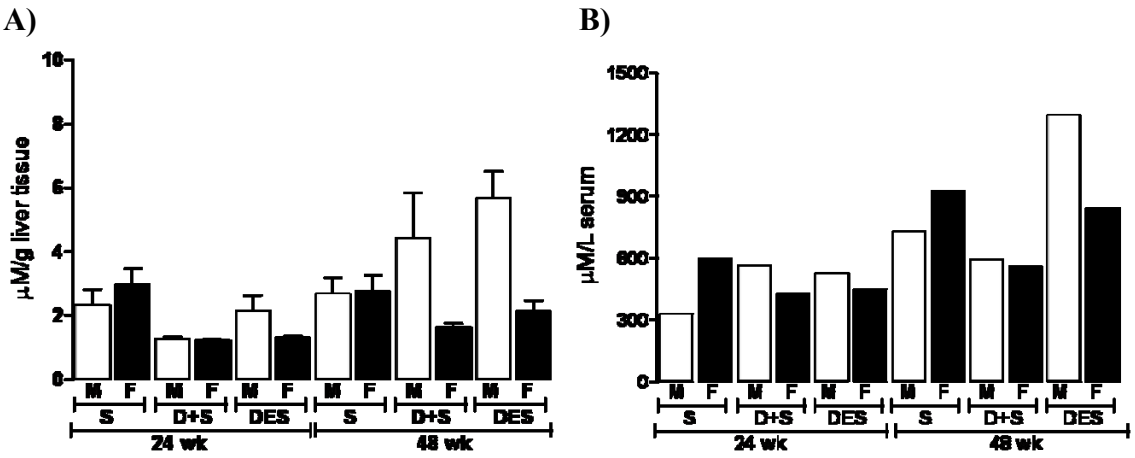

Figure 5.3: Tissue and serum silibinin levels were increased in 48 week DEN-initiated mice and was further increased by concomitant EtOH-DW. A) Silibinin levels in liver tissue following 9 weeks of silibinin supplemented AIN93M (0.5% *w/w*) mouse chow. No significant differences were measured between male and female mice without (Sil) or with prior DEN initiation (D+S) at 24 weeks, or with EtOH-DW regime (DES). Male mice measured increased tissue silibinin levels at 48 weeks. **B)** Silibinin levels in pooled serum measured in male and female mice with or without prior DEN initiation. Increased serum levels were identified in both male and female mice at 48 weeks when compared to same sex groups at 24 weeks.

animals at 24 and 48 weeks. It is of note, male and female mice maintained on silibinin diet only had similar TLIS as those maintained on EtOH-DW alone. Males had increased TLIS in all DEN-initiated groups compared to females. Silibinin diet in D+Sil mice did not decrease TLIS compared to D-only in males or females; in fact, in 48 male mice TLIS was significantly increased compared to pair-matched DEN-only animals. Silibinin given with EtOH-DW (D+E+Sil) had no impact on liver injury at 24 or 48 weeks in either male or female mice when compared to D+E animals.

Further examination of individual components of liver injury indicated that increased lipid deposition was associated with silibinin diet without or with prior DEN initiation in male and female mice. Increased total fat identified in D+Sil and D+E+Sil male mice at 48 weeks demonstrated a corresponding increase in foamy degeneration and necrosis with infiltration of inflammatory cells (*Table A.1; appendix A*). Scores for female mice indicated increased lipid deposition in D+Sil and D+E+Sil groups, however measures of necrosis were decreased and inflammation increased in these groups when compared to D or D+E respectively at 24 weeks.

5.3.4. Immunohistochemistry and tumor burden: Immunohistochemistry (IHC) was initially performed using an antibody specific against GSTpi to identify multiplicity and area of altered hepatic foci (AHF). Using this approach, AHF were measured and counted as an indicator of tumor burden. Measures of tumor area were significant in male and female DEN-initiated experimental groups compared to respective male and female C, EtOH, or Sil only animals at 24 and 48 weeks (Figure 5.5A(24 week), 5.5B (48 week), *$p<0.05$). Male mice measured significantly increased area of AHF versus pair-matched female mice in all DEN-initiated experimental groups. At both 24 and 48 weeks silibinin

A)

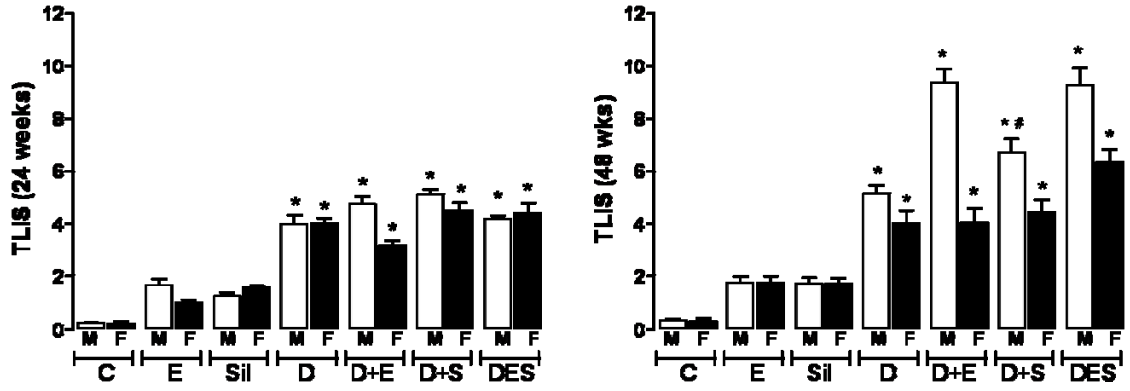

Figure 5.4: Silibinin feeding had no effect on TLIS in male or female mice. A) Cumulative total liver injury score (TLIS) was blind scored from representative sections (total fat, inflammatory cell infiltration, necrosis and collagen – male and female 24 and 48 weeks; C, Sil, E, D, D+E, D+Sil, D+). *$p<0.05$ *versus* respective male or female controls (C), EtOH-DW (E), or silibinin diet (Sil) only; #$p<0.05$ *versus* respective pair-matched DEN-only (D). Minimum of n=8 independent mice/group.

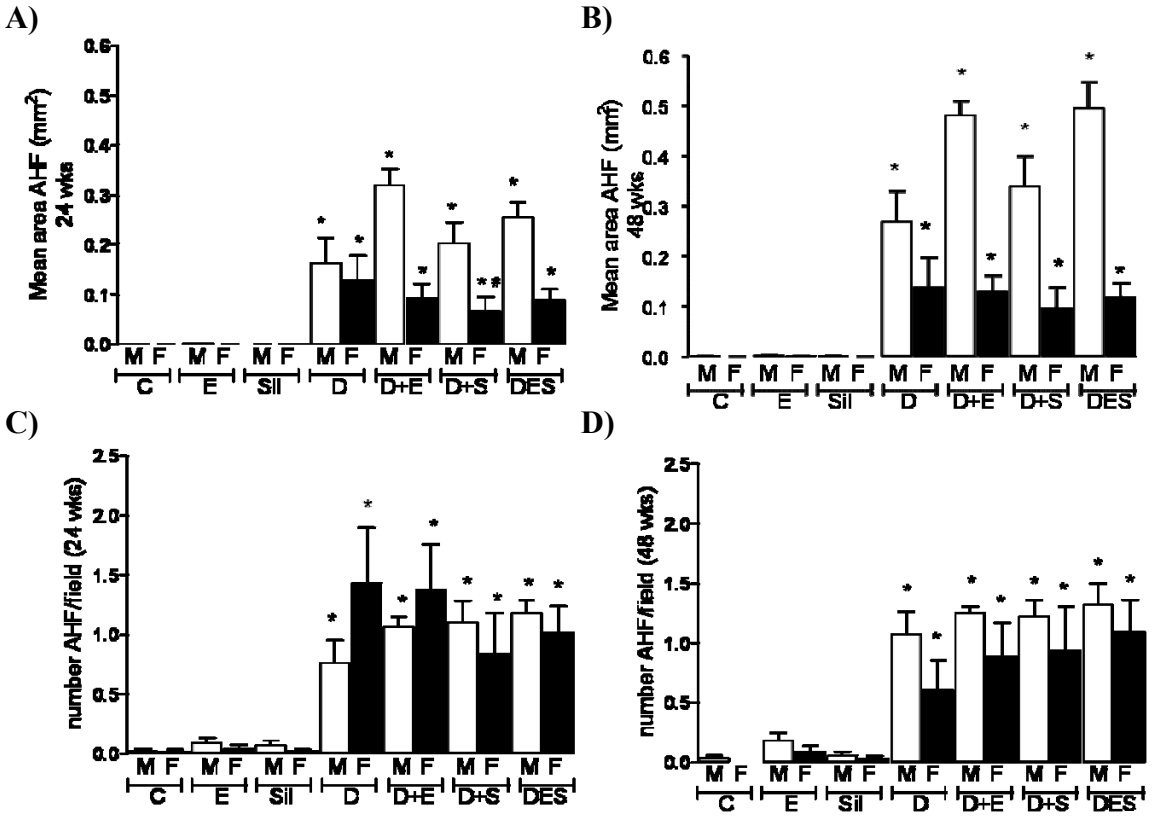

Figure 5.5: Silibinin feeding decreased tumor size and burden preferentially in female mice during early hepatocarcinogenesis. A) Measures of mean area (mm^2) and multiplicity, mean number of altered hepatic foci/field (AHF) were calculated from glutathione S-transferase - placental isoform (GSTpi) positive cells (clusters of 2 or more cells) in a microscopic field (x200 magnification), 2 lobes/mouse 5 fields/lobe) from male and female, 24 and 48 weeks, control (C), 9 weeks silibinin diet (0.05% *w/w*) (Sil), DEN-initiated (D), and DEN+silibinin diet (D+SIL). *$p<0.05$ *versus* respective male or female C, #$p<0.05$, D+SIL *versus* respective male or female DEN (D) **B)** Multiplicity of AHF as calculated by count of GSTpi positive cells (200x magnification, 2 lobes/mouse, 5 lobes/field). *$p<0.05$ *versus* respective male or female C, #$p<0.05$, D+SIL *versus* respective male or female DEN (D). Minimum n=8 independent mice/group

feeding in D+Sil male mice did not significantly reduce tumor area *versus* D-only. Additionally, no differences in multiplicity were detected. Silibinin diet in combination with EtOH-DW regime (D+E+Sil) did not significantly reduce area of AHF *versus* D+E male mice. Conversely, female mice demonstrated a significant decrease in measured tumor area in D+Sil mice versus female DEN-only mice at 24 weeks (Figure 5.5A, #$p<0.05$). However, this effect was not evidenced in female mice at 48 weeks, although area measures of AHF in female D+Sil mice were smaller than DEN-only counterparts. Additionally, silibinin diet in combination with EtOH-DW regime did not significantly reduce area of AHF in female mice at 24 or 48 weeks.

Multiplicity of AHF were increased in male and female mice at 24 and 48 weeks in all DEN-initiated experimental groups compared to pair-matched C, E, or Sil only mice (Figure 5.5C (24 week), 5.5 D (48 week), *$p<0.05$). Numbers of AHF were not significantly altered in D+Sil *versus* D or D+E+Sil *versus* D+E groups in either male or female pair-matched animals.

5.3.5. Proliferation: In order to assess mitogenesis, in light of increases in area measured in AHF, a series of IHC was performed using an antibody specific against proliferating cell nuclear antigen (PCNA; Figure 5.6A (24 weeks), 6C (48 weeks)). Quantification of these results demonstrated significantly increased PCNA staining in both male and female mice in all DEN-initiated experimental groups *versus* same-sex control animals at matching time points (Figure 5.6B-24, and D-48 weeks ,*$p<0.05$). Additionally, these data demonstrate that expression was not altered in D+Sil *versus* D, or D+E+Sil *versus* D+E male mice. Conversely, PCNA staining was reduced in female D+Sil *versus* D mice at 24 weeks and this was decrease was significant at 48 weeks

(Figure 5.6B, #p<0.05).

Since PCNA localizes to sites of DNA damage, and is associated with activation of DNA repair pathways (Essers, 2005), we next performed immunoblot analysis of cyclin D1 in hepatic tissue lysates. These data demonstrate that cyclin D1 expression is increased in all male DEN-initiated experimental groups when compared to C at 24 and 48 weeks (Figure 5.7A and B, *p<0.05). Additionally, in 24 week male mice cyclin D1 expression is significantly increased in D+Sil male mice *versus* D-only animals (Figure 5.7A, #p<0.05). However, no significant differences were identified in D *versus* D+Sil or D+E *versus* D+E+Sil in male or female groups at 48 weeks.

5.3.6. Apoptosis: To identify differences in apoptosis, an *in situ* TUNEL assay was performed and TUNEL positive nuclei/field (T+) calculated. These data demonstrated significantly increased T+ nuclei in female mice maintained on EtOH-DW regime (E) or silibinin diet (Sil) without, or with prior DEN initiation (D+E, D+Sil, and D+E+Sil) at 24 and 48 weeks versus control (Figure 5.8A and B, *p<0.05), and this was significant compared to pair matched male mice (Figure 5.8A and B, §p<0.05). Furthermore, significantly increased T+ nuclei were identified in female D+Sil mice *versus* D only (Figure 5.8A, #p<0.05).

5.3.7. Liver injury and REDOX status: Serum alanine transferase (ALT) levels were measured as an indicator of liver injury/function. In the 24 week groups ALT levels were elevated in male and female DEN-initiated mice compared control (Table 5.2, *p<0.05 *versus* C). Silibinin feeding reduced serum ALT in DEN-initiated male and female in the absence or presence of concomitant EtOH-DW, this was significant in male D+Sil mice *versus* D (Table 5.2, #p<0.05 *versus* D). Within 48 week groups ALT levels

A)

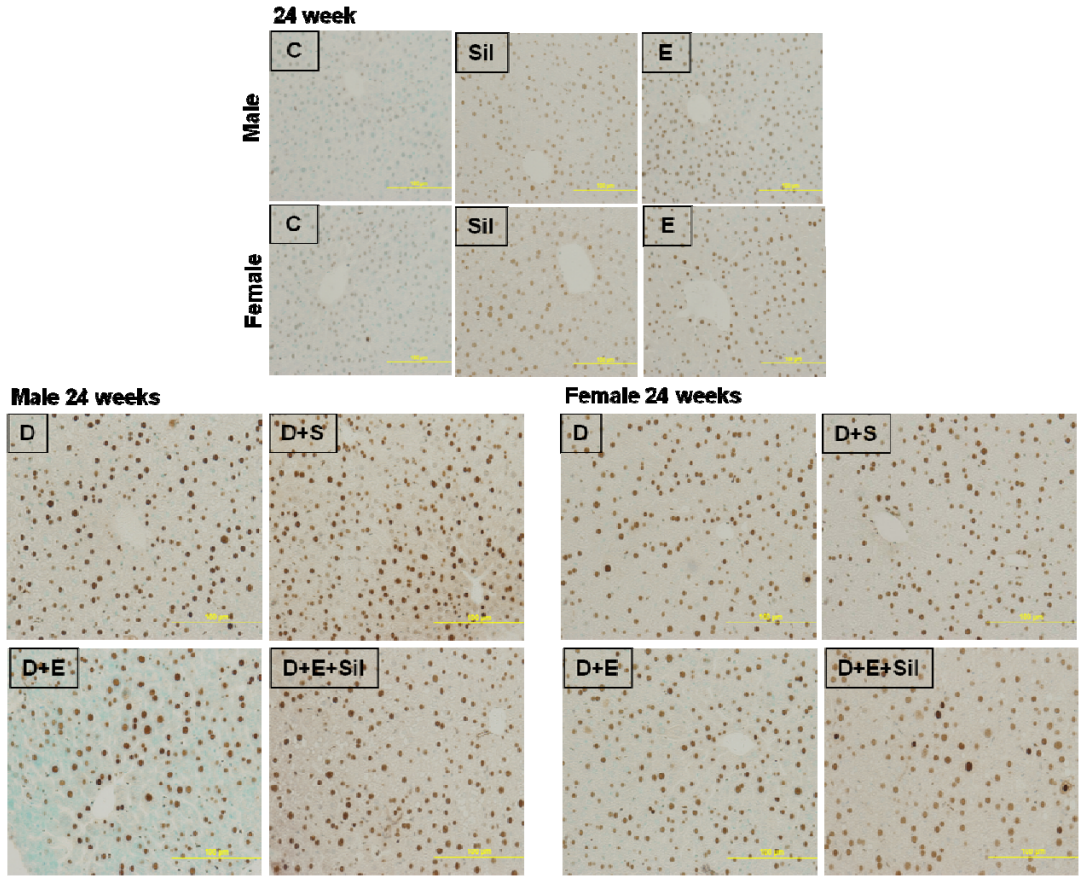
24 week
Male
Female
C
Sil
E
Male 24 weeks
Female 24 weeks
D
D+S
D+E
D+E+Sil

B)

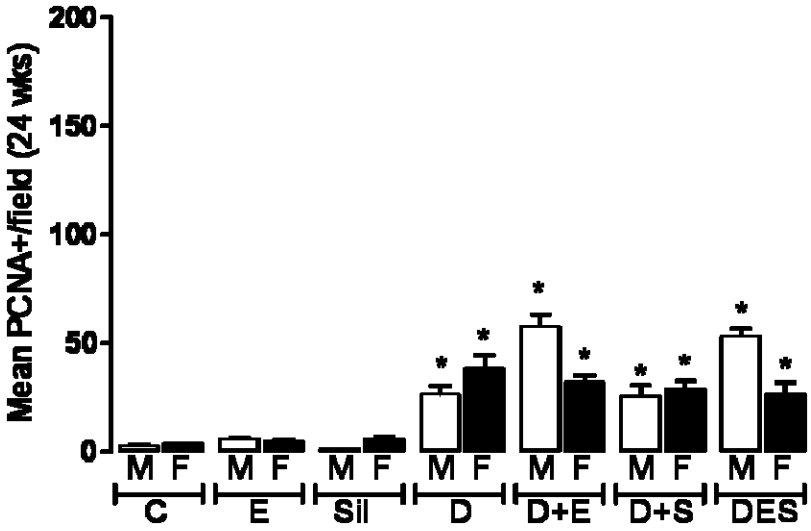
Mean PCNA+/field (24 wks)
200
150
100
50
0
M F
C
E
Sil
D
D+E
D+S
DES

Figure 6 continued.

C)

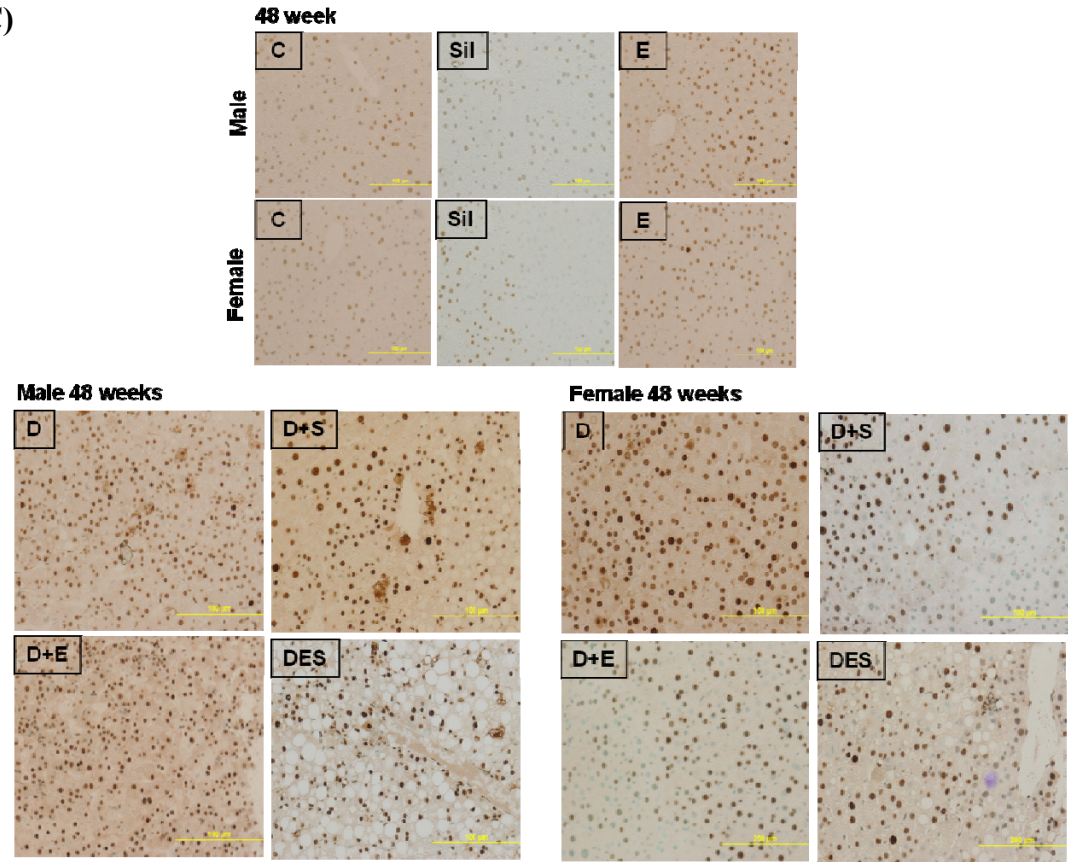

D)

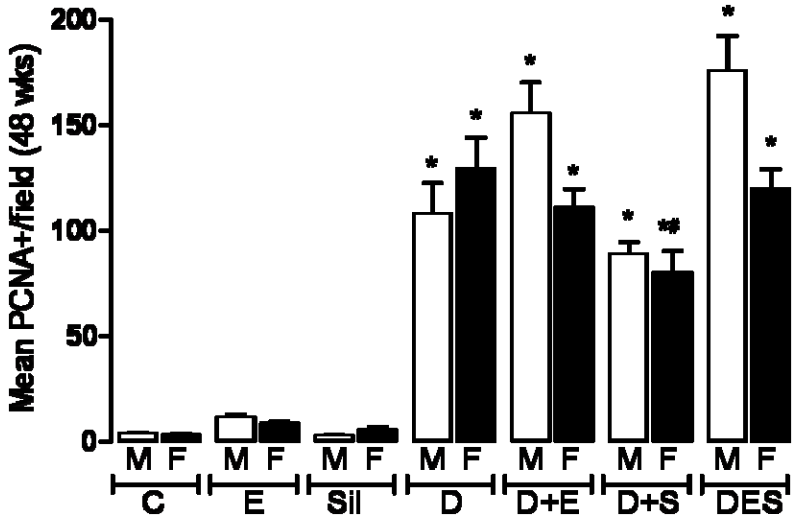

Figure 5.6: Silibinin feeding was associated with decreased PCNA expression in female mice during early and late hepatocarcinogenesis. A) 24 week and **C)** 48 week representative proliferating cell nuclear antigen (PCNA) immunohistochemistry of hepatic sections (x200 magnification) from 24 week control male and female (C) mice, or mice maintained on EtOH-DW (E), Silibinin diet (Sil), initiated with DEN (D), DEN+EtOH (D+E), DEN+Silibinin diet (D+SIL), and DEN+EtOH-DW+Silibinin diet, (D+E+Sil or DES) **B)** 24 week and **D)** 48 week; number of PCNA positive cells per microscopic field (x200 magnification) measured in representative sections (2 lobes/mouse, 5 fields/lobe) from individual male and female mice from each experimental group with mean values ± SEM calculated. *$p<0.05$ *versus* respective C or Sil only animals, #$p<0.05$ *versus* respective male or female pair-matched DEN-initiated mice. Minimum n=8 independent mice/group.

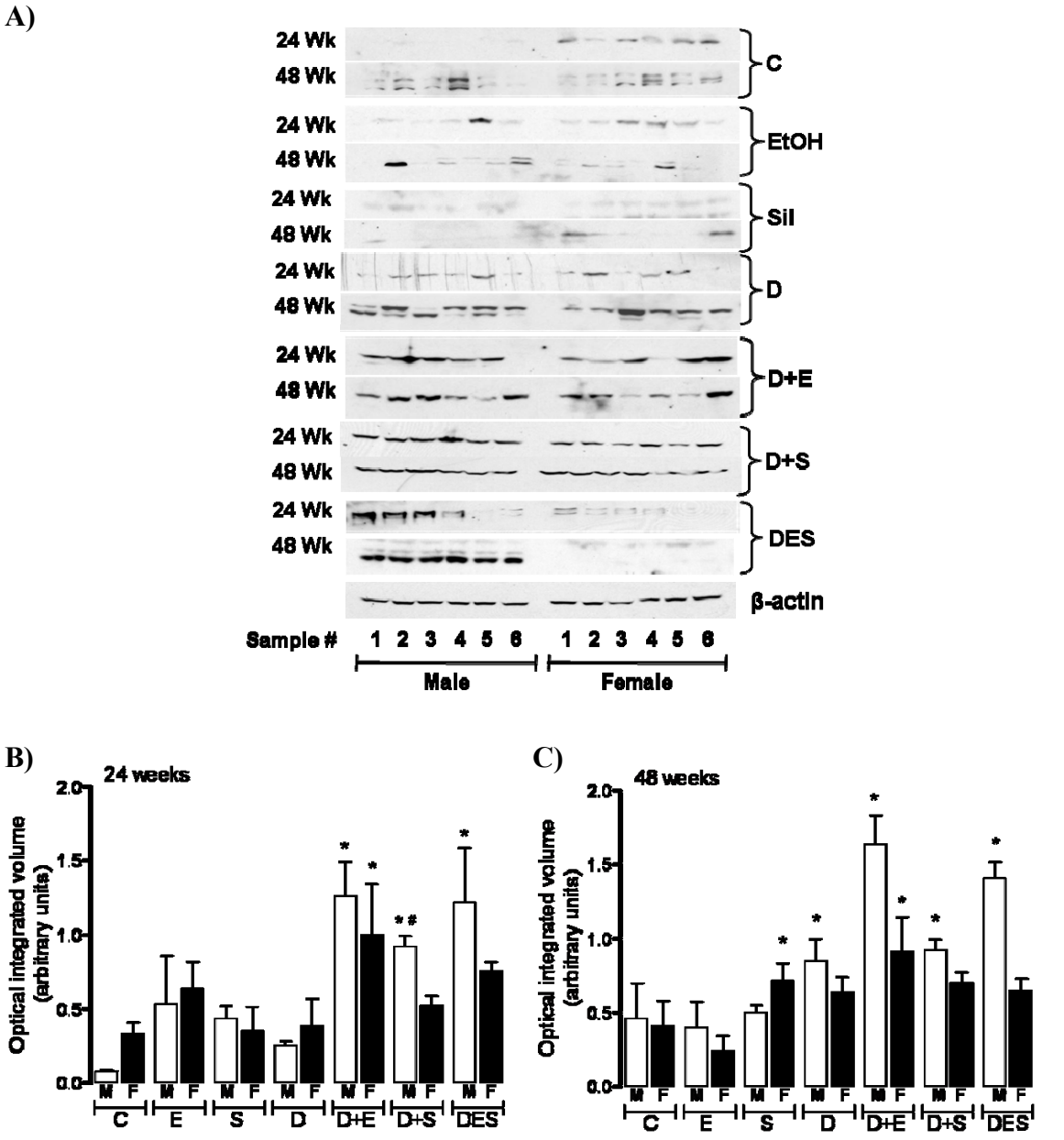

Figure 5.7: Silibinin feeding was associated with increased cyclin D1 expression in male DEN-initiated mice during early hepatocarcinogenesis. A) Representative immunoblots of cyclin D1 expression in hepatic tissue lysates from male and female mice in each experimental group at 24 and 48 weeks. **B)** 24 week and **C)** 48 week animals optical integrated volume calculated, corrected for sample loading (stripping-re-probing membranes with anti-β-actin (β-act), and expressed as mean value (arbitrary units) ± SEM. $p<0.05$ *versus* respective C, or Sil only animals, #$p<0.05$ *versus* respective male or female pair-matched DEN-initiated mice. Minimum n=6 independent samples per group.

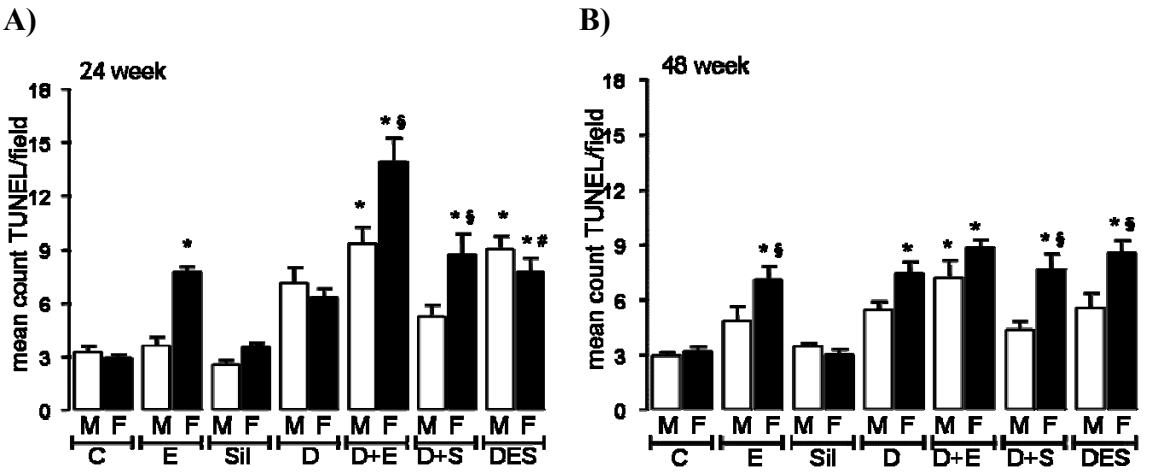

Figure 5.8: Silibinin feeding was associated with increased apoptotic cell death during early and late hepatocarcinogenesis in female DEN-initiated mice. Fluorescein *In situ* cell death detection assay was performed on representative sections from male and female Control (C), EtOH-EW (E), Silibinin diet regime (Sil), DEN initiated (D), DEN+EtOH-DW (D+E), and DEN initiated + silibinin diet (D+S) or DEN+EtOH-DW+Silibinin diet (DES) experimental groups at **A)** 24 weeks and **B)** 48 weeks; number of TUNEL positive cells per microscopic field (x400 magnification) were measured in representative sections (minimum of 2 lobes/mouse, 5 field/lobe) and mean values ± SEM calculated. *$p<0.05$ *versus* respective male or female C or Sil, #$p<0.05$ versus pair-matched male or female DEN+EtOH, §$p<0.05$ male *versus* female in pair-matched experimental group.

were significantly elevated in male and female DEN-initiated experimental groups *versus* same-sex controls (Table 5.2, *p<0.05 *versus* C). Silibinin feeding did not significantly alter serum ALT in male DEN-initiated mice in the absence or presence of concomitant EtOH-DW; however ALT was significantly reduced in D+Sil female mice versus D (Table 5.2, #p<0.05 *versus* D).

To further evaluate hepatic REDOX status, tissue thiobarbituric acid reactive species (TBARS) were measured as an indicator of (malondialdehyde; MDA) lipid peroxidation. These data demonstrated significantly increased MDA in experimental groups compared to C in male and female mice at 24 and 48 weeks (Table 5.2, *p<0.05 *versus* C). Silibinin feeding significantly decreased MDA in male DEN-initiated mice presence of concomitant EtOH-DW, and in female D+Sil *versus* D-alone and in D+E+Sil *versus* D+E (Table 5.2, #p<0.05 *versus* D or D+E). Additionally, female mice measured significantly lower MDA levels in experimental groups (Sil, D, D+Sil, and D+E+Sil) compared to pair-matched male mice. Within the 48 week groups, male and female animals measured increased MDA in E-only and all DEN-initiated treatment groups compared to C (Table 5.2, *p<0.05). In male mice silibinin feeding did not significantly reduce MDA levels in DEN-initiated mice in the absence or presence of EtOH-DW. Conversely, silibinin feeding in DEN-initiated female mice measured significantly decreased MDA in D+Sil versus D-only and D+E+Sil versus D+E mice (Table 5.2, #p<0.05 *versus* D or D+E). Measures of MDA were increased in male *versus* pair-matched female mice.

On analysis of GSH levels a similar pattern was observed at 24 weeks, GSH was significantly reduced in DEN-initiated experimental male and female mice (Table 5.2,

*p<0.05 *versus* C). Male GSH levels were decreased compared to pair-matched female mice. GSH in D+Sil female mice was significantly increased *versus* DEN-only female mice (Table 5.2, #p<0.05 *versus* D). In 48 week male and female groups GSH was significantly decreased in E, and all DEN-experimental groups compared to C (Table 5.2, *p<0.05). Female mice maintained increased GSH levels compared to pair-matched male mice. GSH levels in 48 week DEN-initiated male and female mice were not significantly altered by silibinin feeding in the absence or presence of EtOH-DW.

To further assess oxidative DNA damage measures of hepatic anti-8-hydroxy-deoxyguanosine (8-OHdG) were assessed by IHC on liver sections using an anti-8-OHdG specific antibody and a parallel assay by mouse-specific Enzyme Immuonassay (EIA) of purified, nuclease treated DNA were performed. IHC data demonstrated that increased 8-OHdG staining was identified in DEN-initiated male and female mice at 24 and 48 weeks. In addition, 8-OHdG positive staining was identified in male Sil only mice (Figure 5.9A). Analysis of EIA data demonstrated similar results, male and female mice had significantly increased 8-OHdG in DEN-initiated groups *versus* control at 24 and 48 weeks (Figure 5.9B, *p<0.05). Levels in male DEN-initiated treatment groups were significantly increased versus pair-matched females in 48 week groups (Figure 5.9B, §p<0.05 male *versus* female). Silibinin feeding did not significantly reduce 8-OHdG in D+Sil *versus* D-only male or female animals, but was associated with a significant decrease in female D+E+Sil mice *versus* pair matched D+E mice at 24 weeks (Figure 5.9B, #p<0.05 *versus* D+E). No decreases in 8-OHdG were measured in silibinin fed male or female mice at 48 weeks.

5.3.8. Blood alcohol content (BAC), ADH, ALDH, and CYP2E1 expression:

Table 2: Measure of liver injury/function and REDOX status. Alanine aminotransferase (ALT), malondialdehyde (MDA) and glutathione (GSH) levels at necropsy. *p<0.05 *versus* respective pair-matched C or Sil, #p<0.05 *versu*s respective pair-matched DEN only, and §p<0.05 male *versus* female in pair-matched experimental group.

	Group	n	ALT (IU)	MDA (nmol/mg)	GSH (µmol/mg)
Male 24 wk	C	9	11.3 ± 0.9	1.64 ± 0.16	5.74 ± 0.16
	E	9	29.1 ± 3.9	7.70 ± 0.75 *	4.58 ± 0.24
	Sil	9	14.8 ± 1.0	5.85 ± 0.69 *	5.72 ± 0.15
	D	9	45.5 ± 4.4 *	6.87 ± 0.67 *	4.02 ± 0.04
	D+Sil	8	19.2 ± 3.0 #	5.78 ± 0.46 *	4.20 ± 0.31
	D+E	14	60.7± 7.2 *	8.81 ± 0.48 *	2.98 ± 0.11 *
	D+E+Sil	14	42.9±2.7	6.54±0.53 * #	2.92±0.15 *
Female 24 wk	C	10	11.2 ± 1.1	2.10 ± 0.27	6.06 ± 0.15
	E	10	35.3 ± 3.2 *	8.12 ± 0.72 *	5.15 ± 0.13
	Sil	9	13.1 ± 0.9	4.21 ± 0.27 *	5.53 ± 0.27
	D	9	37.3 ± 4.0 *	5.43 ± 0.83 *	4.99 ± 0.08 *
	D+Sil	9	26.8 ± 6.7	4.36 ± 0.22 * #	5.60 ± 0.19
	D+E	14	57.0 ± 5.2 *	8.51± 0.61 *	3.87 ± 0.18 *
	D+E+Sil	14	41.4±4.9 *	5.09±0.38 * #	5.04±0.11 #

	Group	n	ALT (IU)	MDA (nmol/mg)	GSH (µmol/mg)
Male 48 wk	C	9	14.7 ± 0.9	2.77 ± 0.09	5.86 ±0.14
	E	9	53.5±7.5 *	6.85±0.92 *	4.34±0.36
	Sil	9	23.8 ± 2.5	1.97 ± 0.23	5.98 ± 0.08
	D	8	116.1 ± 16.1 *	8.16 ± 0.53 *	4.09 ± .014 *
	D+Sil	9	124.6 ± 15.2 *	7.61 ± 0.52 *	3.64 ± 0.24 *
	D+E	14	131.3±17.3 *	14.35±0.76 *	2.43±0.11 *
	D+E+Sil	14	159.4±17.5 *	13.40±0.69 *	2.35±0.16 *
Female 48 wk	C	9	15.3 ± 2.2	2.19 ± 0.31	5.97 ± 0.14
	E	9	45.2±6.8 *	5.26±0.79 *	4.91±0.08
	Sil	9	25.1 ± 2.4	2.56 ± 0.38	6.03 ± 0.10
	D	9	124.6 ± 19.6 *	7.79 ± 0.81 *	4.90 ± 0.08
	D+Sil	8	85.8 ± 17.0 * #	4.98 ± 0.54 * #	4.65 ± 0.17 *
	D+E	14	107.0±13.9 *	11.52±1.14 *	3.06±0.15 *
	D+E+Sil	14	97.8±14.6 *	7.62±0.18 * #	3.11±0.17 *

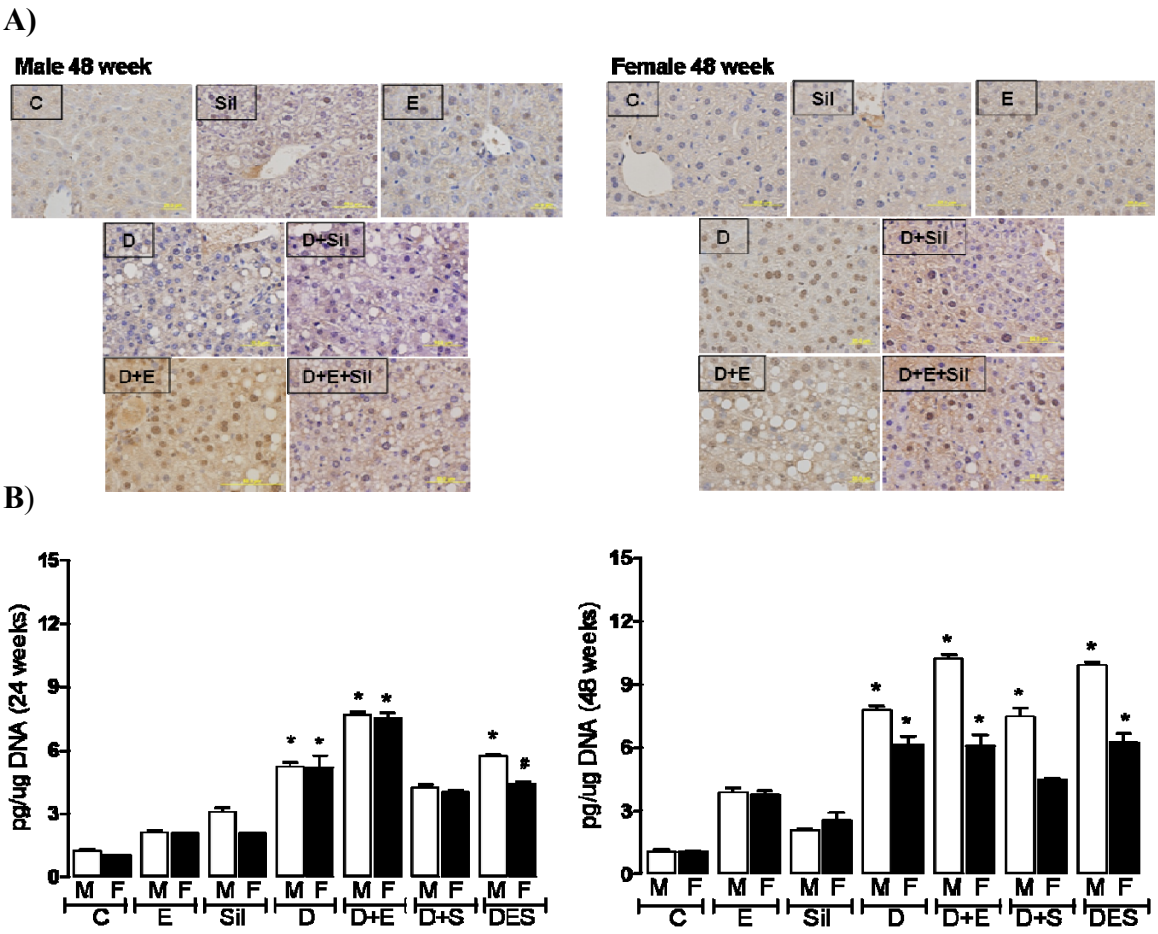

Figure 9: Silibinin feeding was associated with decreased formation of 8-OHdG during early and late hepatocarcinogenesis in female mice. A) Representative 8-hydroxy-deoxyguanasine (8-OHdG) IHC of hepatic sections (200x magnification) from control (C) mice, mice maintained on silibinin diet (Sil), Den-initiated mice (D), DEN initiated mice on silibinin diet (D+S) experimental groups (48 week time point shown). IHC analysis was conducted by counting positively stained nuclei/field as a percent of total cells at 400x magnification, a minimum of 5 fields/lobe and 2 lobes per animal were examined. **B)** Parallel measures of 8-OHdG nucleoside concentrations per 1μg/DNA isolated from hepatic tissue, samples were assayed in duplicate by enzyme immunoassay (EIA) (24 week-left panel, 48 week –right panel). *$p<0.05$ *versus* respective male or female C, #$p<0.05$ versus pair-matched male or female DEN+EtOH-DW, §$p<0.05$ male *versus* female in pair-matched experimental group. Mimum n=6 independent mice/group.

Animals maintained on EtOH-DW regime, without or with prior DEN-initiation and with concomitant silibinin diet had elevated BAC versus pair-matched C. Serum BAC ranges measured between 13.3±1.1 to 14.3±1.2 in male and from 10.4±1.1 to 11.4±1.2 in female E, D+E, and D+E+Sil mice at 24 weeks and ranges measured between 11.4±0.5 to 14.2±0.8 in male and 10.9±0.6 to 13.1±0.8 in female E, D+E, and D+E+Sil mice at 48 weeks. No significant differences were measured between male and female non- and DEN-initiated mice on EtOH-DW and in DEN-initiated mice in the absence or presence of silibinin diet. No significant differences were measured in male *versus* female mice in pair-matched groups at the same time points.

Expression of ADH, ALDH and CYP2E1 were determined by immunoblots using pooled liver tissue lysates. These data demonstrated no significant differences in ADH or ALDH expression within any experimental groups analyzed at 24 and 48-week time points (Figure 10A). However, analysis of CYP2E1 protein demonstrated increased CYP2E1 expression in male and female mice maintained on EtOH-DW regimes without (E) and with prior DEN initiation (D+E), and with silibinin diet D+E+Sil at 24 and 48 weeks (Figure 10A). To further understand changes in CYP2E1, immunoblots of lysates from individual animals (Minimum n=6) were analyzed for CYP2E1 expression. These data demonstrated significantly increased CYP2E1 in DEN-initiated male and female mice maintained on EtOH-DW regime at 24 and 48 weeks (Figure 10B, *$p<0.05$ versus C). In addition, expression in male D+E and D+E+Sil was significantly increased compared to pair-matched female mice. Silibinin feeding with concomitant EtOH-DW did not significantly alter CYP2E1 expression in DEN-initiated males or female mice at 24 or 48 weeks.

To further understand differences observed in CYP2E1 expression, we measured mRNA by RT-PCR. Using this approach we found lower mRNA levels in male and female Sil and D+S mice, but no differences were observed in any other groups at either 24 or 48 weeks (Figure 10C).

To determine if biochemical differences in CYP2E1 activity existed, hydroxylation of *p*-nitrophenol was measured. This approach demonstrated that *p*-nitrophenol hydroxylation was significantly higher in ethanol fed male and female mice at 24 and 48 weeks *versus* respective C mice (Figure 5.10D, *$p<0.05$). Males demonstrated higher CYP2E1 activity than pair-matched female mice. Silibinin feeding with concomitant EtOH-DW had no effect on hydroxylation of *p*-nitrophenol in either male or female DEN-initiated mice at 24 or 48 weeks.

5.3.9. Immunological profile: To evaluate how underlying immune response and cytokine levels may influence changes in pathology associated with HCC progression, we performed qRT-PCR analysis of hepatic T-bet, GATA3, and SMAD3 mRNA expression in an effort to determine dominant T-effector responses that may be present. These data were then analyzed by comparing C, Sil, DEN-initiated mice and D+Sil mice and alternately, C, EtOH, D+E and D+E+Sil experimental groups. These data demonstrate significant increases in expression of T-bet (Th1- effector Transcription factor) in female D and D+Sil mice (Figure 5.11A, *$p<0.05$ *versus* pair-matched control or Sil), and this was significant compared to pair-matched male animals (Figure 5.11 A, §$p<0.05$ male *versus* female). Conversely, males demonstrated increased SMAD3 expression in D and D+Sil groups, and this was significant in D+Sil males (Figure 5.11A, *$p<0.05$ *versus* C or Sil) Differences in SMAD3 expression in male D and D+S mice was significant

A)

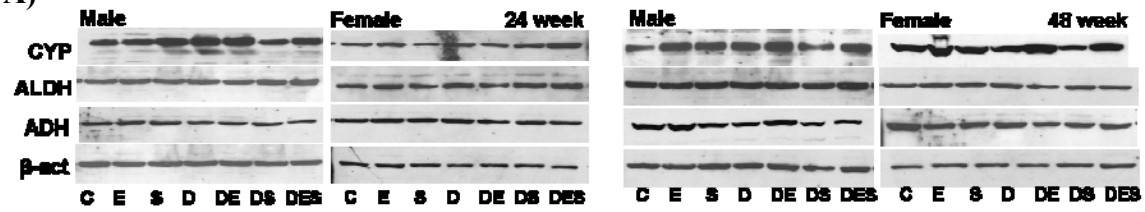
Male
Female
24 week
Male
Female
48 week
CYP
ALDH
ADH
β-act
C E S D DE DS DES
C E S D DE DS DES
C E S D DE DS DES
C E S D DE DS DES

B)

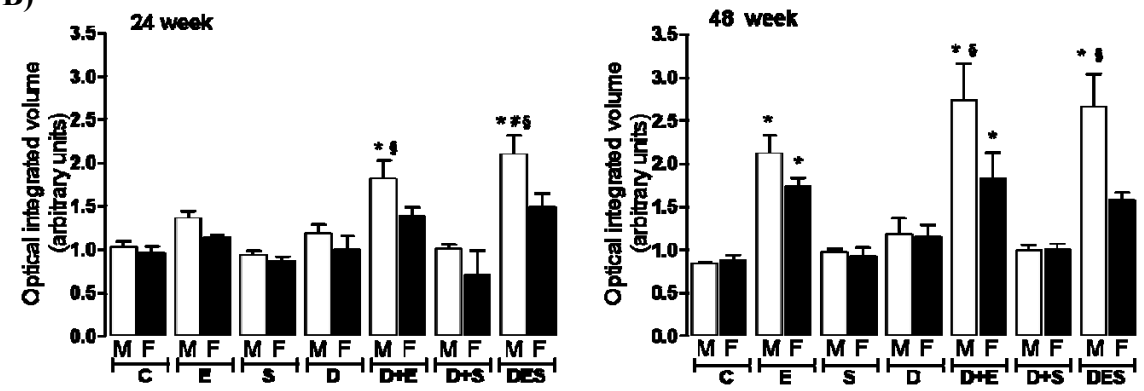
24 week
48 week
Optical integrated volume (arbitrary units)
3.5
3.0
2.5
2.0
1.5
1.0
0.5
0.0
M F
C
E
S
D
D+E
D+S
DES

C)

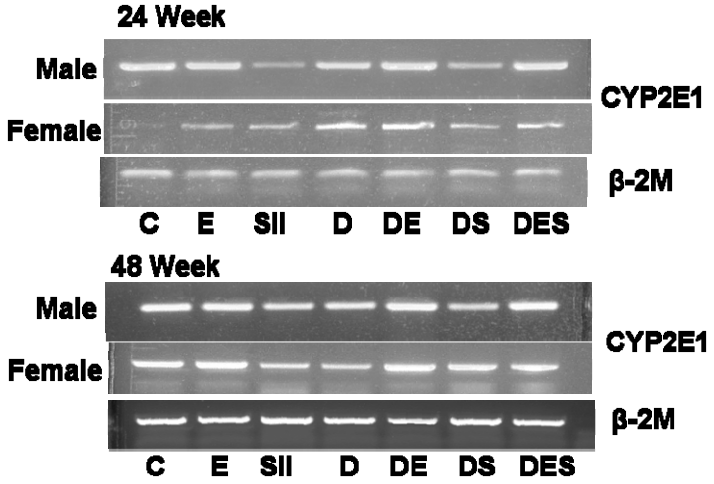
24 Week
Male
Female
CYP2E1
β-2M
C E SII D DE DS DES
48 Week
Male
Female
CYP2E1
β-2M
C E SII D DE DS DES

Figure 10 continued.

D)

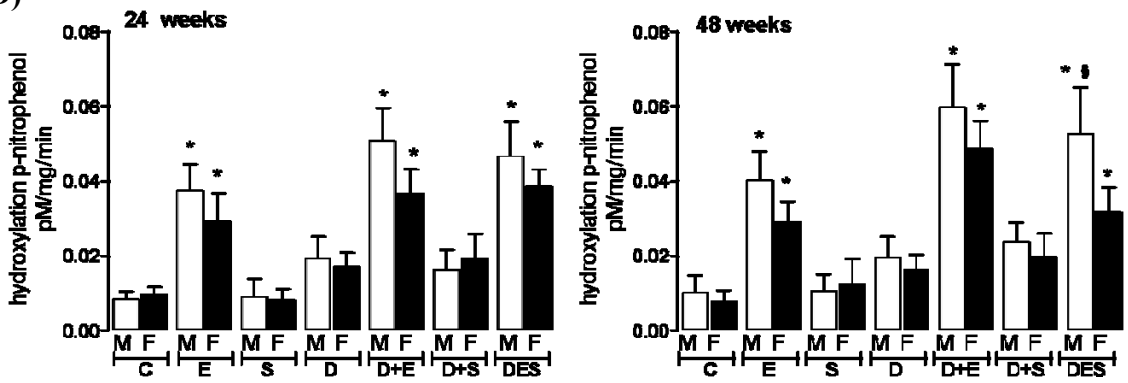

Figure 5.10: Ethanol induced cytochrome P450 2E1 expression and activity that was not abrogated by concomitant silibinin feeding. A) Representative immunoblots for ADH, ALDH and CYP2E1 expression in pooled hepatic tissue lysates from male and female control (C), and pair-matched EtOH-DW (E), Silibinin diet (S), DEN-initiated (D), DEN+EtOH-DW (D+E), DEN+Silibinin diet (D+S), and DEN+EtOH-DW+Silibinin diet D+E+Sil (DES). **B)** Optical integrated volume was calculated, corrected for sample loading (stripping-re-probing membranes with anti-β-actin (β-act)) and expressed as mean value (arbitrary units)±SEM for immunoblots of CYP2E1 from lysates of minimum n=6 individual animals/group, normalized to β-act, *p<0.05 *versus* control, #p<0.05 *versus* pair-matched DEN+EtOH-DW (D+E), and §p<0.05 male *versus* female at matching time points. **C)** Representative RT-PCR gels of CYP2E1 mRNA expression from pooled total mRNA from hepatic tissue in male and female mice on different experimental treatment regimes at 24 and 48 weeks **D)** *p*-nitrophenol hydroxylation was measured as a marker of CYP2E1 activity in hepatic lysates from male and female mice on different experimental treatment regimes at 24 and 48 weeks. *p<0.05 *versus* control, #p<0.05 *versus* pair-matched EtOH-DW, and §p<0.05 male *versus* female at matching time points.

compared to pair-matched female mice (Figure 5.11A, §p<0.05 male *versus* female in pair-matched experimental groups). Male and female D+Sil mice had significantly reduced GATA3 (Th-2-effector transcription factor), compared to DEN-only animals (Figure 5.11A, #p<0.05 versus male or female D).

Analysis of mRNA expression of T-bet, GATA3, and SMAD3 demonstrated similar differences between male and female mice on EtOH-DW regime in the presence or absence of silibinin diet. Female mice measured increased T-bet in E and D+E+Sil groups compared to C (Figure 5.11C, *p<0.05 *versus* same-sex C), this was Significant in D+E+Sil female mice compared to pair-matched male mice (Figure 5.11C, §p<0.05). A significant increase in T-bet mRNA was measured in male D+E+Sil mice compared to pair-matched C (Figure 5.11C, *p<0.05), and this was significant versus DEN-only male mice (Figure 5.11C, #p<0.05). Female mice also demonstrated significantly increased GATA3 in EtOH fed groups (E and D+E) *versus* pair-matched C (Figure 5.11C, *p<0.05), this was significant versus male counterparts (Figure 11C, §p<0.05). GATA3 expression was significantly reduced in ethanol feeding in male mice compared to C (Figure 5.11C, *p<0.05). However in D+E+Sil female mice GATA3 was significantly reduced compared to female D+E animals (Figure 5.11C, #p<0.05). GATA3 expression was unchanged in male D+E and D+E+Sil groups. Male mice demonstrated increased SMAD3 mRNA in all EtOH- fed groups, this was significant in D+E mice (Figure 5.11C, *p<0.05 *versus* C), and was *versus* pair-matched female mice (Figure 5.11C, §p<0.05).

To analyze cytokine profiles, a custom mouse bioplex assay for 7 immunological cytokines (IL-6, TNFα, IL-10, IL-13, IL12p70, IL-1b, and IFNγ) was performed in serum

pooled from C, Sil, D, and D+Sil in 48 week animals. IL-6 was not detected in any experimental groups (Figure 5.11B and 5.11C). Silibinin did not alter cytokine levels in either male or female groups when compared to C (Figure 5.11B). Cytokine levels were increased in male DEN-initiated experimental groups compared to pair-matched female groups. Further, no change was identified in female DEN-only mice compared to C. Conversely, male mice demonstrated increased levels of all analyzed cytokines in D and D+Sil mice compared to C and Sil groups (Figure 5.11B). In analyzing cytokine expression in ethanol fed groups, IL-6 was not detected in either male or female groups (Figure 5.11D). Cytokines were increased in male D+E+Sil compared to all other groups. Variations in specific cytokines were detected. Increased TNFα was identified in all male and female EtOH groups (E, D+E, and D+E+Sil) when compared to C (Figure 5.11D). Females E and D+E+Sil animals had increased IL13, which was also elevated in D+E+Sil male mice, despite the low mRNA expression of GATA3.

5.4. Discussion and Conclusions:

Hepatic cirrhosis is the primary underlying risk factor for subsequent development of HCC (El-Serag, 2007; McKillop, 2006; Vidali, 2007). Underlying mechanisms of hepatic injury leading to cirrhosis and HCC begin with chronic inflammation, dysregulation of lipid metabolism, and increased oxidative stress that arises from documented risk factors; Hepatitis C or B viral infection, aflatoxin, chronic ethanol abuse, and/or non-alcoholic fatty liver disease (El-Serag, 2007; McKillop, 2006). Chronic ethanol abuse is a major risk factor for hepatocarcinogenesis in the United States, but the deleterious effects of ethanol are primarily due to metabolic intermediates and ROS produced during metabolism (McKillop, 2005; Seitz and Becker, 2007). The

A)

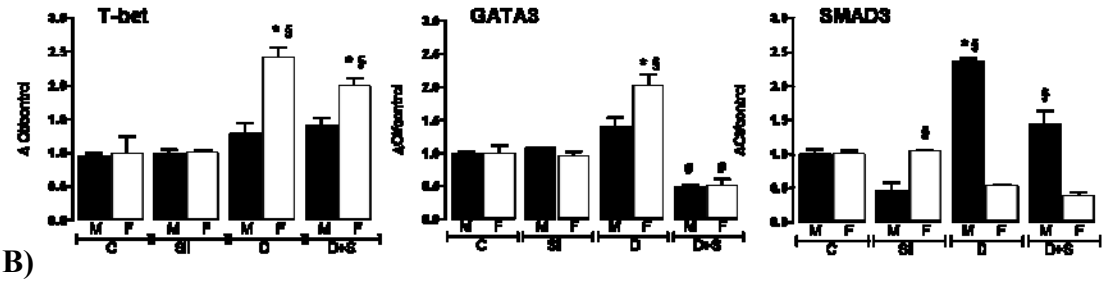

B)

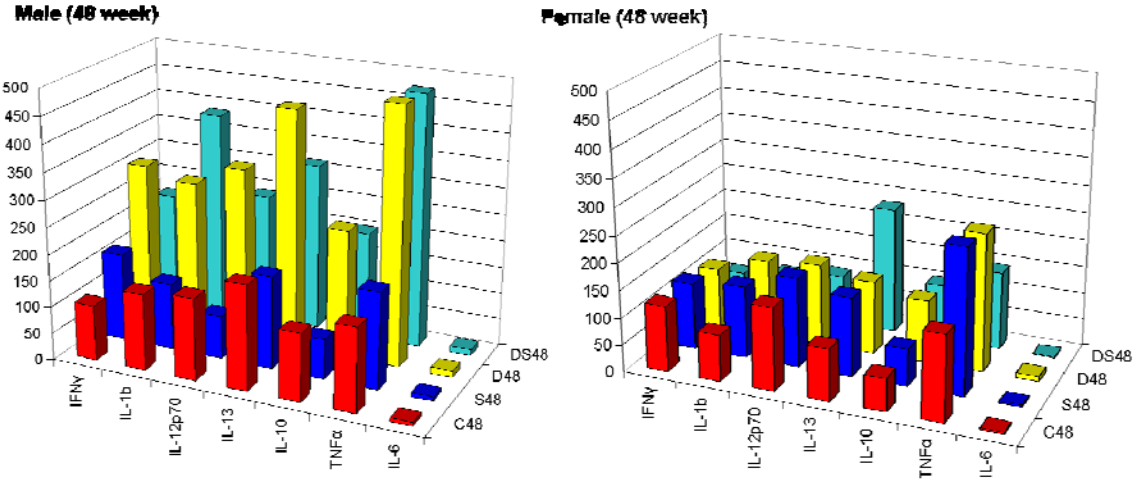

Figure 5.11 A and B: Silibinin feeding produced limited effects on immune response in male or female mice in the setting of hepatocarcinogenesis. A) Quantitative Real-time PCR analysis of T-bet, GATA3, and SMAD3 mRNA expression in total hepatic mRNA isolated from male and female control (C) mice, mice maintained on silibinin diet (Sil), Den-initiated mice (D), DEN initiated mice on silibinin diet (D+S) experimental groups at 48 week time points *p<0.05, *versus* same-sex control or Sil, #p<0.05 D versus D+S in male or female and §p<0.05 male *versus* female in pair-matched experimental group. Minimum n=6 independent mice/group **B)** Custom 7 cytokine Bioplex assay was used to determine cytokine expression in pooled serum samples from C, Sil, D, and D+S male (left) and female (right) mice. Minimum n=8 independent samples/group.

C)

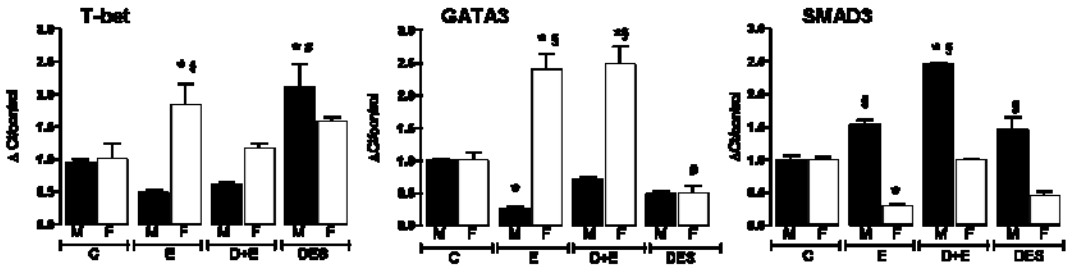

D)

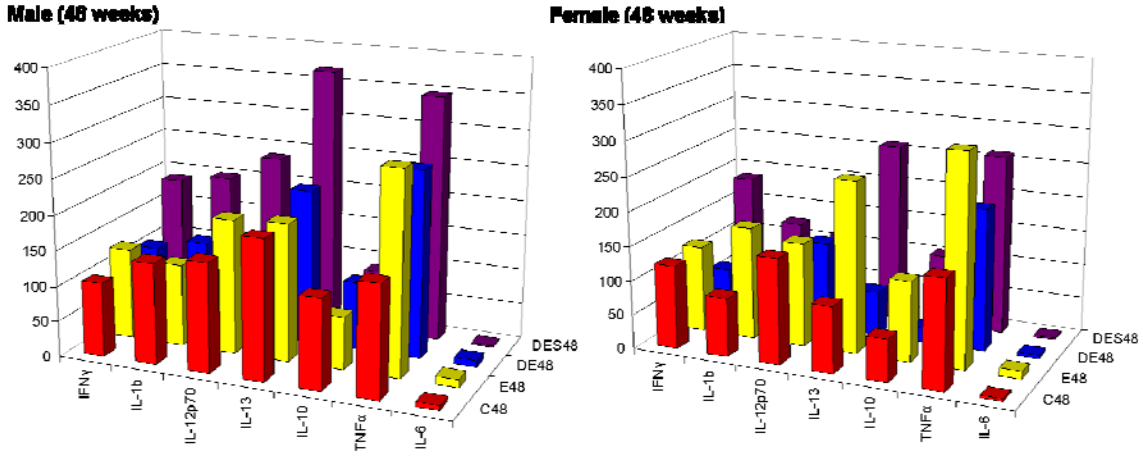

Figure 5.11 C and D: Cytokine levels were increased in DEN-initiated male mice maintained on silibinin feeding and concomitant EtOH-DW. C) Quantitative Real-time PCR analysis of T-bet, GATA3, and SMAD3 mRNA expression in total hepatic mRNA isolated from male and female from control (C), EtOH-DW (E), DEN+EtOH-DW (D+E), DEN+EtOH+Silibinin diet (DES) at 48 weeks *p<0.05 *versus* respective male or female C or Sil, #p<0.05 DE *versus* DES in pair-matched male or female experimental groups, §p<0.05 male *versus* female in pair-matched experimental group. Minimum n=6 independent mice/group **D)** Custom 7 cytokine Bioplex assay was used to determine cytokine expression in pooled serum samples from C, E, D+E and DES, male (left) female (right). Minimum n=8 independent samples/group.

link between oxidative stress mediated inflammation and promotion/progression has been established in many types of cancer (Karin and Greten, 2005; Lin and Karin, 2007; Reuter et al., 2010). Oxidative stress/ROS in the milieu of the tumor microenvironment can provide favorable conditions for promotion and progression during carcinogenesis (Balkwill et al., 2005; Dhanalakshmi et al., 2004). The mechanisms for these interactions have not been completely elucidated, but this relationship has been confirmed by the inhibitory effects achieved through the use of antioxidant and anti-inflammatory agents (Arteel, 2003; Reuter et al., 2010). In addition, individual variations based on sex, metabolic and nutritional differences, and modulation of immune responses may be critical factors in susceptibility to development and progression of cirrhosis to HCC.

The relationship between oxidative stress and hepatocarcinogenesis has stimulated increased interest in the use of natural plant derived flavinoids as therapeutics to reduce oxidative stress/inflammation and potentially restrict HCC promotion and progression. Milk thistle (*Silybum marianum*) has demonstrated anti-oxidant and anti-inflammatory activity, and has been used as a hepatoprotectant for thousands of years (Gazak, 2007; Saller, 2007). The extract derived from the seeds is composed of several flavinoligands, of which the major bioactive constituent is silibinin. Silibinin is comprised of a 1:1 ratio of diastereoisomers silybin A and silybin B (Saller, 2007). Silibinin is a potent antioxidant; however, studies of the effects of silibinin in prostate, breast, and lung cancers have demonstrated that it possesses additional properties that influence proliferation, apoptosis, angiogenesis, and immune modulation that interfere with cancer progression (Chen et al., 2005; Cheung et al., 2010; Lee et al., 2007; Singh, 2004b).

Epidemiological data indicates that males are three times more likely to develop HCC than females (El-Serag, 2007). Our previous studies reported that male mice were more susceptible to the promotional effects of ethanol than their female counterparts. These effects could occur through direct actions of ethanol on cell signaling pathways and immune function, or through increased oxidative stress and toxic metabolites generated, thereby creating a favorable environment for promotion and progression of HCC. Increased tumor mass and burden in DEN-initiated male mice maintained on EtOH-DW was accompanied by CYP2E1 induction, increased measures of oxidative stress and diminished GSH. Conversely, female mice demonstrated reduced tumor size and burden and maintained higher levels of GSH with decreased measures of hepatic injury and higher rates of apoptosis. In females, this was associated with decreased CYP2E1 induction and activity. These data suggest that the promotional effects may be due to the oxidative stress generated by CYP2E1 mediated ethanol metabolism and accumulation of acetaldehyde, and byproducts of lipid peroxidation. Additionally, increased intestinal epithelial permeability associated with ethanol consumption elevates bacterial endotoxin (LPS) in the liver activating Kupffer cells to release TNFα, and ROS that can synergize with CYP2E1 to increase liver injury (Ferenci et al., 1989).

The goal of this study was to determine if silibinin could reduce oxidative stress and inflammatory responses to prevent tumor promotion and progression during early (16-24 week) and late (40-48 weeks) DEN-initiated carcinogenesis alone; and additionally, if silibinin could blunt the promotional effects of EtOH when administered in combination with chronic EtOH-DW regime. HCC was induced by administration of a single ip injection of DEN (1 mg/kg) to neonatal mice (21-28 days old). Experimental

treatment regimes were established to coincide with kinetics of DEN-initiated hepatocarcinogenesis and formation of early dysplastic foci (16 weeks) and late when HCC can be anticipated (44 weeks) (Fausto, 2010; Goldfarb et al., 1983). CYP2E1 is induced in conjunction with hepatic transformation, but subsides during growth and development of DEN-initiated infant mice. Hepatic DNA damage is amplified and populations of transformed cells expand as initiated mice grow and develop (Goldsworthy and Fransson-Steen, 2002; Kang, 2007). The neoplasia formed in this model display a phenotype similar to that of human HCC with a high proliferative index with poor prognostic outcome. To ensure the effects of DEN-initiation on CYP2E1 had abated, dysplastic foci were allowed to develop for 15 or 39 weeks prior to commencing silibinin (0.05% *w/w,* 9 week) feeding without or with EtOH-DW (10/20% *v/v,* 8 week) regime.

Silibinin is reported to have low toxicity, even at high doses (Yang et al., 2011). Previous studies have demonstrated that dietary feeding in rodent models provided a viable means for silibinin administration, and was well tolerated (Singh and Agarwal, 2004; Zhao and Agarwal, 1999). Clearance of silibinin occurs through its conjugation to glucuronide and sulphate compounds followed by excretion in bile (Jacobs et al., 2002). Previous studies report that mice tolerated chronic EtOH exposure (8 weeks) via drinking water, and had measured BAC at levels comparable to moderate consumption in humans (Ishihara et al., 2010; Seitz, 2006). Dietary silibinin feeding paired well with EtOH-DW regime, and was practical and effective given the timing and duration of each experimental treatment.

In this study male mice developed HCC at a rate ≈2:1 compared to female mice in DEN-initiated groups with silibinin feeding (0.05% *w/w*), (D+Sil). The rate in D+E+Sil decreased to ≈1.4:1. Silibinin feeding in DEN-initiated mice, in the absence or presence of EtOH-DW was associated with decreased ALT, MDA and 8-OHdG in all animals, while females maintained higher GSH levels. These improvements in measures of hepatic injury did not result in significant histological improvement or decreases in collagen deposition when compared to DEN or DEN+EtOH mice. Females demonstrated less hepatic injury compared to pair-matched male mice, likely owing to decreased tumor burden identified in those animals. Additionally, hepatic lesions identified in females were restricted to one or two lobes, whereas male mice had extensive tumor burden affecting all lobes, this was exacerbated by EtOH-DW and further by combined EtOH-DW and silibinin diet.

Tissue and serum levels of silibinin demonstrated that male mice had increased accumulation of silibinin in hepatic tissue during late HCC. This was most likely due to impaired hepatic function and decreased drug clearance with progressive liver injury and tumor burden. Silibinin clearance was impaired by concomitant EtOH-DW when compared to dietary silibinin alone in male DEN-initiated animals. Additionally, there was a corresponding increase in serum silibinin levels in D+E+Sil male mice. These effects were not evidenced in female mice, where silibinin levels were consistent at both time points. Clearance of silibinin was reflective of hepatic function and increased percentage of non-tumor liver present in females at both time points. Silibinin has been reported to interfere with glucuronosyltransferase activity through direct inhibition of cytochrome P450 3A4 and 2C9 (Sridar et al., 2004). This inhibition combined with

decreased liver function may have contributed to increased silibinin concentrations. Silibinin has been reported to have low toxicity even at high dosages, however changes in cellular effects have been reported to be dependent on tissue/serum concentration (Cheung et al., 2010; Schwarz et al., 1983).

Silibinin feeding was associated with a 48.4% decrease in tumor size in female D+Sil mice during early (24 week) hepatocarcinogenesis and 30.4% decrease during late (48 week) HCC. Decreases in tumor size and burden were associated with improvements in measures of hepatic injury. Anti-oxidant functions of silibinin likely contribute to decreased ALT, MDA, and oxidative DNA damage identified these animals. In addition to improvements in the measures of hepatic injury, female D+Sil had decreased liver mass and L:BW ratios. However, tumor size and burden were not decreased by silibinin feeding in DEN-initiated male mice. Measures of ALT decreased 1.2 fold in male D+Sil animals during early hepatocarcinogenesis, but this was without significant decreases in MDA, 8-OHdG or preservation of GSH levels. Similar improvements were not identified during late hepatocarcinogenesis in male mice. Antioxidant functions of silibinin likely explain modest improvements in hepatic injury and oxidative stress, but these effects were not sufficient to inhibit increases in tumor size and number. Additionally, silibinin feeding did not reduce TLIS in male or female D+Sil versus DEN-initiated animals. On histological examination male mice had higher measures of hepatic injury commensurate with increased tumor burden. Examination of individual components of liver injury demonstrated that lipid deposition, necrosis and inflammatory cell infiltration were increased in male D+Sil animals compared to DEN-initiated animals at 24 and 48 weeks. Increased lipid deposition and inflammatory cell infiltration were increased in female

mice. In 48 week male and female mice, increased Sirius red staining was also identified, indicative of fibrosis and collagen deposition.

Tumor incidence was associated with increases in proliferating cell nuclear antigen (PCNA) expression in all DEN-initiated male and female experimental groups, with higher levels identified in males compared to females. This corresponded to increased tumor size and burden in these animals. However, cyclin D1 was significantly higher in male D+Sil mice, indicating that PCNA expression was related to proliferation in males. However, in female mice PCNA may be due to increased activation of DNA repair mechanisms, as PCNA accumulates at sites of DNA damage (Essers, 2005). Expression of PCNA in female mice may indicate a prolonged cell cycle with activation of DNA repair pathways. In non-melanoma skin cancer silibinin was reported to increase S-phase arrest, allowing for DNA repair with concurrent up-regulation of mismatched-base repair enzymes in response to UVB induced damage (Dhanalakshmi et al., 2004). Additionally, during early HCC, numbers of TUNEL positive cells were higher in female D+Sil animals. These data suggest that female mice have improved clearance of altered cells that may inhibit HCC promotion during early hepatocarcinogenesis. However, cyclin D1 levels in D+Sil female mice were comparable to those in DEN-initiated females during late HCC indicating that PCNA expression is likely due to proliferation during late HCC development. This suggests that inhibitory effects on HCC promotion identified during early HCC were dampened in late hepatocarcinogenesis. Male D+Sil mice demonstrated decreased TUNEL positive cells in D+Sil mice compared to DEN initiated mice during both early and late HCC. Loss of responsiveness to apoptotic signals in damaged cells is a hallmark of cancer progression (Hanahan and Weinberg,

2000). Necrotic cell death is an inflammatory process, unlike apoptosis. On histological examination male D+Sil demonstrated increased steatosis and ballooning necrosis of hepatocytes, an effect that was more pronounced during late HCC.

The balance of inflammatory and anti-inflammatory cytokines during hepatitis can enhance or inhibit tumor promotion. Additionally, multiple cell types within the liver parenchyma contribute to inflammatory immune function. An assessment of immune cytokines demonstrated increased expression of all cytokines in DEN males, and these levels were increased further in D+Sil males. Conversely, in females TNFα, was elevated in DEN initiated mice, but decreased in D+Sil animals. Serum cytokine levels can be influenced by many factors and are reflective of systemic pathology and may not be indicative of specific immune responses within the liver, and tumor stroma. Additionally, assessing serum cytokine levels at a single time point at sacrifice does not adequately reflect the dynamic nature of immune response. However, despite decreases in inflammatory cytokines identified in females, there was increased T-bet mRNA. The presence of substances released by necrotic hepatocytes is an important inducer of NFκB in liver macrophages, Kupffer cells (KC) (Scaffidi et al., 2002). Activation of Kupffer cells is associated with increases in pro-inflammatory cytokines including TNFα, IL-6, which can activate other cell types in the liver (Maeda et al., 2005). Loss of hepatocytes as a result of increased necrotic cell death, as identified in male D and D+Sil mice may drive compensatory proliferation with increased expression of hepatic growth factors that contribute to promotion. Serum cytokine levels in D+Sil males were higher when compared to DEN-initiated animals. Despite increased expression of pro-inflammatory cytokines systemically, higher levels of SMAD3 mRNA were detected in liver tissue

from D+Sil animals. SMAD3 is a key mediator of TGFβ signaling during growth, differentiation, and apoptosis (Baldi et al., 1996; Imoto et al., 2005). Modulation of TGFβ can be critical during cancer development. In addition, androgen and estrogen are co-regulators of SMAD3 induced transcription activation (Matsuda et al., 2001). Crosstalk between SMAD3 and estrogen/androgen signaling pathways appear to direct specific and differential actions in context of wound healing, estrogens accelerate healing associated with markedly reduction in inflammatory response and androgens inhibit repair and enhance leukocyte recruitment (Imoto et al., 2005). Signals mediated by TGFβ have roles in determining cell fate and growth control, as well as activation of fibrotic responses fundamental to liver disease, and are implicated in processes that mediate malignant progression (Ferenci et al.). Silibinin has been reported to inhibit nuclear factor κ B (NFκB) activation in hepatocytes during DEN-initiated hepatocarcinogenesis (Porta et al., 2009; Sakurai et al., 2006). Silibinin is reported to block nuclear translocation of NFκB, thereby blocking acute phase TNFα expression (Gharagozloo et al., 2010). Decreased TNFα expression identified in D+Sil females suggests that inhibiton of NFκB results in decreased expression of pro-inflammatory cytokines, TNFα, IL-1b, and IL-6 (Kono et al., 2000; Mandrekar and Szabo, 2009).

Ethanol is a major source of hepatic oxidative stress, and chronic ethanol feeding leads to induction of CYP2E1. Ethanol resulted in an increase in CYP2E1 expression without, or with prior DEN initiation, and this occurred preferentially in male *versus* female mice. In addition, the promotional effects of ethanol on HCC corresponded to increased CYP2E1 expression and activity, oxidative stress, MDA and decreased GSH. In vitro studies on H4IIE rat hepatoma cells had suggested that silibinin could directly

interacted with CYP2E1 to inhibit ethanol metabolism (Brandon-Warner et al., 2010a). Silibinin has been reported to inhibit activity of other cytochrome P450 enzymes, reducing the associated oxidative stress that accompanies P450 mediated metabolism (Sridar et al., 2004). However, in this model EtOH-DW induced CYP2E1 expression without any changes in ADH or ALDH, but silibinin feeding had no effect on CYP2E1 expression in D+E+Sil mice when compared to D+E mice in male or female animals. Interestingly, there was a decrease in mRNA message in male and female silibinin only and in D+S mice, but no changes in protein expression or activity were detected in silibinin fed groups without or with EtOH-DW. Ethanol metabolism mediated by CYP2E1 is a significant source of ROS and can facilitate the accumulation of acetaldehyde and contribute to lipid peroxidation and oxidative injury (Albano, 2006; Lieber, 1997a; McKillop, 2005; Wu and Cederbaum, 2003). In the context of initiatated cells, these factors can contribute to promotion and progression.

Promotional effects of ethanol previously identified in male D+E mice were not altered by concomitant silibinin feeding (D+E+Sil). Tumor area was reduced in these animals by ≈2.2% in early HCC, but was increased by ≈3.1% during late hepatocarcinogenesis, with increases in multiplicity at both time points. Measures of tumor area in female D+E+Sil mice were reduced by 30.4% in early, but only 8.5% during late stage when compare to D+E, however incidence was increased at both time points. Since both silibinin and ethanol treatments were postponed until HCC was expected to develop, it is likely that the accumulation of mutations had already progressed toward a malignant phenotype in 48 week animal groups. The combination of

EtOH-DW with silibinin at this point may have facilitated other changes in immune response, energy availability, or oxidative stress that served to enhance HCC progression.

Lesions identified in female mice were generally restricted to one or two lobes, the higher percent of non-tumor liver likely resulted in improved liver function, and when combined with anti-oxidant properties of silibinin was sufficient to decrease REDOX stress. Measures of hepatic function (ALT) were improved over pair-matched D+E mice during early stage (24 week) hepatocarcinogenesis in males and females, but only in females during late stage (48 week) HCC. This improvement in females was accompanied by significant reductions in MDA, and modest preservation of cell GSH. Conversely, in male mice tumor burden was extensive, livers were grossly enlarged with significantly increased L:BW ratios. Increased tumor burden, with decreased hepatic function was reflected in higher ALT, MDA, 8-OHdG, and depleted GSH identified in D+E+Sil animals. Despite improvements in measures of hepatic function and oxidative stress, the highest liver injury scores were identified in male and female D+E+Sil mice at both 24 and 48 weeks. Increased tumor burden was associated with increased measures of PCNA in male and female D+E and D+E+Sil animals indentified in late (48 week) HCC. This increase in PCNA corresponded to increases in cyclin D1 expression in male animals. Conversely, female mice had higher numbers of TUNEL positive cells during late HCC compared to male mice in both D+E and D+E+Sil groups. This may indicate that females continue to eliminate damaged cells more effectively than their male counterparts.

Ethanol metabolism is a major source of oxidative stress, but it also enhances intestinal permeability allowing for the translocation of bacterial endotoxin (LPS) into the

liver. Bacterial endotoxin is a major stimulator of pro-inflammatory signals (Ferenci et al., 1989; Mandrekar and Szabo, 2009). Females have been reported to sustain higher degrees of liver injury more rapidly in response to ethanol consumption, in part due to increased LPS and KC activation (Kono et al., 2000). Activation of KC occurs through LPS interaction with the CD14 receptor, leading to increased ROS, and production of pro-inflammatory cytokines. Pro-inflammatory mediators are increased in D+E+Sil male mice, but pathology and tumor burden were also increased, suggesting that increased inflammatory cytokines may be contributing to tumor progression. Ethanol can induce tolerance and sensitization of Kupffer cells by altering NFκB (Enomoto, 2001; Yamashina et al., 2005). Silibinin has been reported to increase lymphocyte proliferation, IFNγ, IL-4 and IL-10 secretion by inhibiting activation of NFκB in hepatocytes and Kupffer cells (Sakurai et al., 2006; Schwarz et al., 1983).

Tumor cells produce factors that can enhance their survival, direct alternate programming of macrophages within the tumor stroma (Mantovani et al., 2002; Porta et al., 2009). Liver macrophages are strategically located in the liver sinusoids where they are continually exposed to pathogen associated molecules. Conflicting signals mediated through ethanol, LPS or silibinin may alter the programming of KC from an M1 phenotype with high production of nitric oxide and ROS effective in killing intracellular micro-organisms and tumor cells to an M2 phenotype that is more adept at scavenging debris, repair, tissue remodeling, and promotion of angiogenesis (Porta et al., 2009). Alternate programming of tumor associated macrophages is more permissive for tumor survival and may be part of inflammatory circuits that promote tumor progression. Male and female D+E+Sil mice demonstrated increased IL1B, IFNγ, TNFα and IL-13 levels,

cytokines which may contribute to polarization of macrophages to a tumor permissive (M2) phenotype. Presence of Th2 cytokines with IL-10 are reported to direct this alternate activation (Mantovani et al., 2002). It is noteworthy that this cytokine profile is present in experimental groups with increased tumor burden. It seems likely that modulation of NFκB by ethanol and silibinin contribute to these effects. Further work remains to examine the role of NFκB activity or inhibition on HCC promotion and progression, and how these factors may be influenced by ethanol or silibinin. In light of the difference identified between male and female mice, it will be necessary to examine how sex-hormone signaling may also mitigate these processes.

These data demonstrated that silibinin was protective against oxidative injury and improved GSH levels in both D+Sil and D+E+Sil animals. Tumor size and burden were significantly reduced in D+Sil female mice, these protective effects were limited to early hepatocarcinogenesis and the effects were dampened in late HCC. Silibinin diet with concomitant ethanol feeding did not reduce tumor burden in male or female mice and silibinin may potentiate tumor promotion induced by ethanol. The effects of silibinin on promotion and progression in the absence or presence of ethanol raise questions about the safety of supplements, alone and in combination with other pharmacological agents. Many patients self medicate with natural herbal supplements, with the perception that even if they provide no benefit, they will do no harm, and most fail to share this information with their physicians. These data suggest there is a time-line for which supplements may provide some benefit in reducing measures of hepatic injury and that their effects can be mitigated by other interactions.

CHAPTER 6: GENERAL DISCUSSION

Hepatocellular carcinoma (HCC) is a global health burden, and accounts for nearly ≈6% of all human cancers worldwide (Bosch et al., 2005). This cancer develops in the absence of specific familial or genetic markers, but instead from documented and largely preventable risk factors. These risks include Hepatitis B and C viral infection, aflatoxin B mycotoxin, non-alcoholic fatty liver disease, and chronic ethanol abuse (El-Serag, 2007; McKillop, 2006; McKillop and Schrum, 2005). Most HCC occurs in Asia and sub-Saharan Africa. Incidence rates for many types of cancers have declined, but between 1975 and 2005, HCC rates in the United States have doubled (Altekruse, 2009). Epidemiological data report males to have an incidence of HCC that is 3-5 times higher than that of women (El-Serag, 2007). Additionally, women present with a later onset of disease (El-Serag, 2007). Hepatitis C infection remains the principal risk factor associated with HCC. However, chronic ethanol abuse is a significant factor for HCC development in the United States, and it synergizes with other risk factors (El-Serag, 2002). Regardless of underlying etiology, hepatocarcinogenesis is driven by inflammatory processes resulting from increased lipid deposition, hepatitis, leading to fibrosis and cirrhosis. Eighty to ninety percent of all HCC develops within the background of hepatic cirrhosis (Bartsch, 2005; El-Serag, 2007; McKillop, 2006; McKillop and Schrum, 2005). Clinical outcomes are dismal due to the lack of viable treatment options, an effect exacerbated by long disease latency. The time from onset to

clinical symptoms and diagnosis can be measured in decades (Okuda, 2000). Complicating diagnosis is the lack of biological markers. Currently, AFP and abdominal ultrasound are the initial tools used (Ferenci et al., 2010). Use of AFP as a diagnostic indicator has limitations as 40% of patients with HCC do not produce AFP, and many patients of African descent have normal AFP levels at 500 ng/mL (Ferenci et al., 2010).

Development of HCC is a multistage process beginning with genetic mutations in isolated cells. Over time selected cells clonally expand, accumulating additional genetic damage and mutations until they have overcome the barriers of growth inhibition, and apoptosis to become immortal, with a high proliferative index. These malignant cells have the ability to induce neo-vascularization and have increased invasion potential (Hanahan and Weinberg, 2000). Given the cryptic nature of the disease, diagnosis is often not made until late stage when treatment strategies are limited. Staging is currently determined based on the Barcelona Clinic Liver Cancer (BCLC) guidelines. Treatment options are dependent on the stage designation at the time of diagnosis. Early stage cancer can be treated by tumor resection; intermediates stages are treated by ablation techniques designed to destroy tumor tissue or its blood supply; as staging progresses treatment is restricted to palliative care (Bruix and Sherman, 2005). Additionally, the only currently approved chemotherapy agent is Sorafenib, but this has only been demonstrated to improve life expectancy by a few months (Thomas and Zhu, 2005).

Chronic ethanol abuse is a major cause of liver disease progressing to cirrhosis and eventual development of HCC, as liver hepatocytes are the primary site of ethanol metabolism (El-Serag, 2007; McKillop, 2005). Ethanol is not considered a hepatocarcinogen *per se*, but contributes to HCC through toxic metabolites, lipid

peroxidation and ROS generated during metabolism (Seitz, 2006). Oxidative stress is an important mechanism in this process. With occasional moderate ethanol consumption, it is rapidly metabolized in two successive oxidation reactions. The initial oxidation of ethanol is mediated by alcohol dehydrogenase (ALD) which produces acetaldehyde which is subsequently oxidized by acetaldehyde dehydrogenase (AHLD) to acetate and water. Data suggest that the carcinogenic effects are mediated by acetaldehyde, rather than ethanol (Poschl and Seitz, 2004; Seitz, 2006). Acetaldehyde is toxic, and has been demonstrated to be mutagenic and carcinogenic. It interacts with cell constituents causing lipid peroxidation, forms adducts with protein and DNA (Seitz, 2006; Seitz and Becker, 2007). Adducts formed with DNA interfere with synthesis and repair pathways. Additionally, adducts increase chromosomal instability and become more sensitive to sister chromatid exchanges (Seitz, 2006; Seitz and Becker, 2007). Lipid peroxidation produces additional toxic aldehydes, malondialdehyde (MDA) and 4-hydroxynonanol (HNE) that also promote DNA damage (Bartsch, 2005). Protein interactions and aggregates formed with acetaldehyde interfere with normal structure and function. As these processes persist there is depletion of intracellular antioxidant defenses, primarily glutathione (GSH) (Seitz, 2006). Multiple isoforms of ADH and ALDH enzymes have been identified that can influence the rate of acetaldehyde formation and its subsequent oxidation, their contribution to HCC development has not been established (Lieber, 2001). With chronic excessive ethanol consumption, microsomal cytochrome P450 2E1 (CYP2E1), a mixed function mono-oxidase is induced (Lieber, 1997a). Ethanol metabolism mediated by CYP2E1 also produces acetaldehyde as its first metabolite. Induction of CYP2E1 with ADH may result in an imbalance of acetaldehyde relative to

available ALDH that favors accumulation. This can increase hepatic metabolic stress and oxidative injury. Metabolism mediated by CYP2E1 is associated with increased oxidative injury and generation of reactive oxygen species (ROS), $O_2^{\cdot -}$ and H_2O_2 in hepatocytes (Albano, 2002; Lieber, 1997a). This enzyme is poorly coupled and results in incomplete ethanol oxidation and formation of hydroxyl-ethyl radical (HER) (Lieber, 2001). Generation of ROS is partially due to enhanced leakage of electrons from the mitochondrial respiratory chain and increased REDOX imbalance (Bailey and Cunningham, 2002; Lieber, 2001).

A secondary source of hepatic oxidative injury occurs due to increased gut permeability and translocation of bacterial endotoxin (LPS) from the intestinal tract to the liver from the hepatic portal vein (Albano, 2006; Lieber, 2001; Thurman, 1998). Bacterial endotoxin entering the liver activates hepatic macrophages, Kupffer cells by interacting with the CD14 receptor (Enomoto, 2001; Nagy, 2004; Thurman, 1998). These activated Kupffer cells produce pro-inflammatory cytokine TNFα and ROS (Thurman, 1998). This response is reported to be increased in females who have demonstrated higher levels of gut-derived LPS in their blood following ethanol exposure than males, and as a result females are thought to be more susceptible to ethanol induced hepatic injury (Enomoto, 2001; Ikejima et al., 1998; Kono et al., 2000). Additionally, ROS produced by CYP2E1 during ethanol metabolism exacerbate Kupffer cell responsiveness to LPS and hepatocytes are more vulnerable to the effects of TNFα (Hoek, 2002). Kupffer cells are the main effector cell for innate immune response within the liver and many responses associated with progressive injury, including lipid accumulation, inflammation, increased oxidant generation and necrosis during chronic ethanol exposure are mediated by Kupffer

cells (Hines and Wheeler, 2004). However, ethanol can have opposing effects on Kupffer cell activation, inducing both tolerance and sensitization (Yamashina et al., 2005). Impairment of immune response during hepatic injury is linked to modulation of cytokine production by Kupffer cells (Mandrekar et al., 2009). Classically LPS binds to the CD14 TLR/4 complex followed by activation of interleukin 1 receptor-associated kinase (IRAK-1), IKK complex and MAPK followed by the dissociation of IκBα and nuclear translocation of NFκB consisting of the p50 and Rel A subunits (Mandrekar et al., 2009). This leads to transcriptional activation of proinflammatory cytokines, TNFα, Il-1b, and I-6. Alternately, increased IL-1R associated kinase –monocyte (IRAK-M) is a negative regulator of LPS induced signaling and leads to impaired NFκB DNA binding and decreased TNFα producing an anti-inflammatory response (Enomoto et al., 1998; Liu et al., 2008; Mandrekar et al., 2009). Silibinin may directly interfere with these disparate processes generating tolerance or sensitization that impedes or promotes HCC progression or potentiates the effects of ethanol.

Persistent oxidative stress and inflammatory responses coupled with hepatic accumulation of acetaldehyde, ROS and activation of Kupffer cells stimulate hepatic stellate cells to produce type I collagen. This process is initially mediated by acetaldehyde directly, but with chronic ethanol exposure TGFβ and TNFα contribute to the fibrogenic process (Hoek, 2002; Nieto, 2006). The progressive nature of liver injury beginning with steatosis, and hepatitis leading to fibrosis and cirrhosis, occurs through chronic oxidative stress and inflammation. Antioxidants have been proposed as a means of ameliorating oxidative stress and preventing the chronic inflammatory processes that

drive fibrosis and cirrhosis especially during chronic ethanol use and thereby preventing progression to HCC.

Silibinin is a flavinoligand derived from the seeds of Milk thistle (*Silybum marianum*). Historically, it has been used as a hepatoprotectant for several millennia. Silibinin is the major and most biologically active component contained in the silymarin mixture (Gazak, 2007; Saller, 2007). Clinical trials in Europe demonstrated silibinin administered to patients with cirrhosis improved long term prognosis, however these studies have not been confirmed (Ferenci et al., 1989; Stickel and Schuppan, 2007). Silibinin is a potent antioxidant; however it may also reduce oxidative stress by means of inhibitory actions on cytochrome P450 3A4 and 2C9 activity through competitive interaction (Sridar et al., 2004).

Initial *in vitro* studies examined the effects of ethanol, in absence of, or with silibinin pre-treatment, on CYP2E1 metabolism, oxidative stress and proliferation in a rat hepatoma cell line; H4IIE. These studies demonstrated that ethanol increased proliferation in cultured H4IIE cells. Additionally, there were dose dependent increases (0-75 mM/L) in CYP2E1 expression associated with chronic ethanol exposure (24 hours). Peak expression was measured at 25 mM/L ethanol exposure. Based on this, additional experiments were conducted at ethanol concentrations of 25 mM/L. Previous studies reported therapeutic serum and tissue concentrations at 8.8-10 μM/L (Singh, 2004b). H4IIE cells exposed to 25 mM/L ethanol following silibinin pretreatment at 10 μM/L demonstrated decreased expression of CYP2E1 protein. We also identified an increase in CYP2E1 mRNA with ethanol exposure that was abrogated by silibinin pre-treatment. Further examination of ethanol metabolism in these cells demonstrated a ≈10% decrease

in metabolism associated with silibinin pre-treatment. To examine proliferation we conducted direct counts of H4IIE cells every 24 hours for 96 hours, these data demonstrated that ethanol promoted proliferation over silibinin or vehicle (DMSO) treated cells alone, and that pre-treatment inhibited this effect to rates comparable to that of control. Because ERK1/2 phosphorylation are associated with proliferation, we performed immunoblots for ERK1/2 and active (phosphorylated ERK1/2)(McKillop, 1999). Previous studies had suggested that silibinin may interfere with ERK activity by inhibiting phosphorylation (Momeny et al., 2008). We identified no changes in ERK activity between ethanol without or after silibinin pre-treatment. Assessment of oxidative stress demonstrated that ethanol resulted in increased thiobarbituric acid reactive species (TBARS) as a measure of malondialdehyde (MDA). This increase in TBARS was abrogated by silibinin pre-treatment. Additionally, we used fluorescent microscopy to evaluate celluar oxidative stress. Metabolism mediated by CYP2E1 is a source of both $O_2^{\cdot -}$ and H_2O_2 formation, as such we used carboxy-H_2 DCFDA a probe to detect intracellular ROS. On exposure to cellular peroxides carboxy-H_2 DCFDA is cleaved by cellular esterases and becomes sequestered in the cytoplasm. In this way we were able to demonstrate that ethanol alone produced increased cellular peroxides that were ameliorated by silibinin pre-treatment. Finally, we utilized a human HCC cell line HepG2, that was stably transfected to constitutively express CYP2E1(E47-HepG2), and cells stably transfected with empty vector (C37-HepG2) to demonstrate that silibinin pre-treatment inhibited ethanol metabolism and this inhibition was accompanied by a decrease in hydroxylation of p-nitrophenol as an measure of CYP2E1 activity.

These studies demonstrated that ethanol promotes HCC proliferation, and this effect is abrogated by silibinin pre-treatment. Furthermore, silibinin appeared to inhibit CYP2E1 protein expression and activity which reduced cellular oxidative stress and inhibited lipid peroxidation and this effect, may be from direct interactions with silibinin and CYP2E1 protein.

The promotional effects of ethanol have been controversial. Numerous studies have been conducted in an attempted to determine if ethanol can promote HCC progression. This is particularly important give the long disease latency and absence of symptoms, which makes it likely that chronic ethanol abuse could contribute to the clonal expansion of transformed cells that drives promotion and progression in HCC. Ethanol has the potential to influence tumorigenesis in multiple ways, facilitation of cellular uptake of carcinogens in hepatocytes, modification of metabolic pathways, stimulation of DNA synthesis with concurrent reduction in repair capacity, and modulation of immune responses (Seitz, 2006; Seitz and Becker, 2007). Additionally, the link between chronic inflammatory processes in fibrotic disease states as mediators of promotion in progression in cancer have been well documented (Vidali, 2007; Yang et al., 2011). Previous studies have utilized a well characterized mouse model of chemical carcinogenesis (diethylnitrosamine – (DEN)), whereby DEN is administered in a single ip dose to neonatal mice (14-21 days) and tumors develop over a predictable time course (Fausto, 2010; Goldfarb et al., 1983; Goldsworthy and Fransson-Steen, 2002; Vesselinovitch and Mihailovich, 1983). In most experimental studies administration of ethanol was usually accomplished by isocaloric Lieber-DeCarli liquid diet in which 36% of calories are derived from ethanol, or dextrose in pair-matched controls (Lieber and

Decarli, 1989). Alternately, a gastric infusion model has been employed (Tsukamoto et al., 1985). These studies also incorporated partial hepatectomy (removal of 70% of liver tissue), or nutritionally restricted diets (low methionine), to induce liver regeneration or impair metabolic function and exacerbate the effects of DEN initiation. These studies have produced conflicting results demonstration no effect (Mandl, 1989; Schwarz et al., 1983), co-carcinogenic effects (Seitz et al., 1998), and promotional effects (Takada, 1986). The variations in these studies complicate interpretation of their results. Additionally, these experiments were conducted on limited number of animals, and females were not included.

Given the sexual dimorphism that has been identified in HCC incidence, we sought to include males and females. These studies utilized a DEN mouse model; infant B6CH3 mice were given a single ip injection of DEN (1 mg/kg body weight). Animals were allowed to recover for 15 or 39 weeks to allow CYP2E1 induction by DEN to abate before any further treatment regimes were initiated. Male and female animals were randomly assigned to treatment groups for early (24 weeks) when altered hepatic foci are expected to form, or late (48 weeks) when HCC is expected to be present (Goldfarb et al., 1983; Goldsworthy and Fransson-Steen, 2002). These groups were further randomly divided to receive DEN, DEN plus silibinin diet (0.05% *w/w* for 9 weeks), DEN plus ethanol drinking water feeding (10/20% *v/v* alternating daily for 8 weeks), or DEN plus silibinin diet (9 weeks) and ethanol drinking water (8 weeks). Ethanol drinking water at doses of 5 to 20% is thought to mimic that of moderate human consumption. This method allows for intermittent and lower doses than liquid diets or intragastric infusion and results in blood level variations over time. Non-initiated male and female groups

were also established to receive no supplementation, ethanol drinking water alone (8 weeks), or silibinin diet alone (9 weeks). At the end of treatment regimes, mice were euthanized with liver and serum harvested.

These data demonstrated that ethanol promoted HCC progression during early and late hepatocarcinogenesis, but this effect was restricted to male mice. Tumors were initiated in both male and female mice, but males demonstrated an incidence 2.6 fold higher than female mice. This parallels human HCC whereby females generally have an incidence 3 times lower than males (El-Serag, 2007; McKillop, 2005). Progression of HCC was accompanied by increased CYP2E1 expression and activity with subsequent increases in measures of oxidative injury. Conversely, female DEN initiated mice exposed to ethanol presented with smaller tumors than pair-matched DEN initiated mice. Female DEN+ethanol mice also demonstrated decreased CYP2E1 expression and activity compared to pair-matched males. Additionally, measures of oxidative injury were not as severe and females maintained higher glutathione levels. These differences corresponded to increased tissue pathology in male compared to female animals. With steatosis as the dominate measure of injury. In males this resulted in ballooning degradation of hepatocytes with increased necrosis. Of note, females measured higher rates of apoptosis and determined by TUNEL positive staining. The differences identified in necrotic cell death, which is an inflammatory process versus apoptosis which is non-inflammatory likely contribute to differences in tissue pathology. Carcinogenesis is mitigated by alterations in growth inhibitory signals, evasion of apoptosis, immortalization, neo-vascularization and increased invasion potential (Hanahan and Weinberg, 2000). A link between inflammation and cancer may be dependent on NFκB, a critical regulator of

innate immune responses in the liver (Karin and Greten, 2005; Maeda et al., 2005). Chemical carcinogenesis was exacerbated by loss by inhibition of NFκB activation through IKKβ in hepatocytes. This corresponded to enhanced ROS production and lead to sustained JNK activation. However, similar inhibition of NFκB in liver macrophages (Kupffer cells) significantly reduced hepatocarcinogenesis (Maeda et al., 2005). Hepatocyte death in this model occurred by necrosis and led to compensatory liver regeneration. This suggests that differences in NFκB regulation in males and females may trigger responses that can promote or inhibit HCC progression.

In examining markers of proliferation we identified that both male and female mice had increased PCNA, but in males this increase corresponded to increased cyclin D1, indicating that PCNA was due to replication. However, female mice had decreased cyclin D1 indicating that PCNA expression may be due to DNA repair mechanisms. Proliferating cell nuclear antigen accumulates at sites of double-strand (ds) DNA breaks, the decrease in D1 relative to PCNA suggests that females may have induced repair pathways while males responded to hepatomitogens to induce proliferation. The effects of ethanol and its metabolites can produce oxidative DNA damage, ds DNA breaks and adducts. Proliferation in the context of DNA damage can lead to transverion mutations and increased chromosomal instability.

Clinical data indicates the women are more susceptible to ethanol induced liver injury and that gut-derived endotoxin and Kupffer cell activation likely plays a pivotal role in this difference (Kono et al., 2000). This is dependent on activation of NFκB through CD14 receptor. Females demonstrate early activation of Kupffer cells with increased CD14 expression and increased TNFα in response to NFκB activation (Kono et

al., 2000). This suggests that estrogen may modulate these responses. However, our model indicates that females are less susceptible to liver injury and promotional effects with chronic ethanol ingestion. Early acute phase response is increased, but long-term exposure to ROS, oxidative stress and KC activation does not result in increased tumor burden in females. Female mice in this study had decreased tumor burden, and decreased measures of liver injury compared to pair-matched male mice, and this was accompanied by increased apoptosis. Transcriptional activation by NFκB is an important mediator of inflammatory responses (Kono et al., 2000). Female mice maintained on ethanol in the absence of DEN initiation had higher TNFα levels. Most cytokines were decreased in ethanol fed DEN-initiated female mice, including TNFα, IL-1b, IFNγ, and IL-10. Cytokine levels were based on serum measures and reflective of systemic response. These data did not correspond to increased liver mRNA expression of transcription factors that initiate T-effector programming T-bet (Th1), and GATA3 (Th2). In female mice these transcription factors were increased indicating that females may mount a more robust immune response and maintain immunosurveillance in conjunction with DNA repair and apoptotic cell death. However, male mice demonstrated increased SMAD3 a mediator of TGFβ signaling programs. Male mice also had increased IL-10 an immune suppressive cytokine important in T-regulatory cell differentiation. This suggests that males may activate an immunosuppressive program in the context of increased necrosis and compensatory proliferation as suggested by increased measures of cyclin D1.

Alternate modulation of NKκB influences multiple cell types within the liver milieu. Progression of hepatocellular carcinoma is influenced by growth factors, cytokines, chemokines and small signaling molecules produced by multiple cell types

within the tumor stroma. These effects in the microenviroment are thought to be key mediators of progression (Balkwill et al., 2005; Yang et al., 2011). Ethanol induces NKκB activation in KC through increased LPS, but this response is not sustained with long-term ethanol use. Tolearance or alternate macrophage activation can be triggered by changes in the microenvironment that direct different functional programs, similar to T-cell differentiation into Th1 or Th2 effector cells (Porta et al., 2009). In this case, classic or M1 macrophage activation induces IFNγ, IL-12 and IL-23 production with high NO and reactive oxygen intermediates. The M1 macrophage phenotype produces pro-inflammatory cytokines and is a potent effector for killing intracellular micro-organisms and tumor cells. Conversely, differential programming produces an M2 phenotype that is characterized by decreased pro-inflammatory cytokines and is more effective at scavenging debris, promoting angiogenesis and remodeling of extra-cellular matrix (ECM). These are important events during tumor promotion (Porta et al., 2009). Cytokines associated with a Th2 effector response (IL-4, IL-13, IL-10), as well as other small molecule mediators may enable this shift. This shift is associated with cytoplasmic accumulation of the p50 subunit of NKκB may play a role in the polarization of tumor associated macrophages (Liu et al., 2008; Mantovani et al., 2002; Porta et al., 2009).

There are multiple sources for generation of ROS during chronic long term ethanol use. Pathological processes mediated by cellular immune response are also a major source of oxidative stress. Previous studies had demonstrated that silibinin may directly interact with CYP2E1 inhibiting its activity. This would directly reduce oxidative stress that is associated with CYP2E1 metabolism and slow the rate of acetaldehyde formation (Brandon-Warner et al., 2010a). Silibinin is a potent anti-oxidant, but in

addition it has been demonstrated to inhibit cell cycle progression, decrease angiogenic signaling, and inhibit metastasis in cell and animal models of cancer (Chen et al., 2005; Cheung et al., 2010; Singh, 2004b). We next sought to determine if the promotional affects identified in male animals exposed to ethanol could be abrogated by concomitant treatment with silibinin. We also wanted to determine if silibinin could reduce promotion and progression in DEN initiated mice in the absence of promoting agent ethanol.

In this mouse model of chemically induced hepatocarcinogenesis, silibinin alone was effective at reducing tumor size and burden in DEN initiated female mice during early formation of altered hepatic foci, however no protective effects were identified in male mice in pair-matched group. This benefit was absent during late stage. Tumor incidence for males was ≈2:1 compared to females in DEN+silibinin diet groups. Silibinin feeding with DEN initiation improved measures of oxidative stress and liver injury in both males and females. Markers of proliferation correlated to increased tumor burden. Measures of TUNEL positive cells in DEN mice on silibinin diet demonstrated reduced levels of apoptosis and increased necrotic cell death. This pathology was similar to that identified in ethanol alone, however most measures of injury and oxidative stress were improved. Additionally, silibinin diet in non-DEN initiated animals demonstrated increased lipid deposition in both males and females. This disparity supports altered NKκB activation in males that favors increased necrosis with compensatory hepatic regeneration that may lead to sustained JNK activation. While females had reduced growth response and increased apoptosis and activation of DNA repair programs. Examination of immune response demonstrated that silibinin feeding did not reduce cytokine expression compared to DEN initiation only. Increased IL-1b, TNFα, IL-13 and

IL-10 were measured in male mice in both DEN and DEN with silibinin diet groups. Conversely, females had reduced cytokine expression in DEN group on silibinin diet relative to DEN alone, with the exception of IL-13. Measures of mRNA for transcription factors T-bet and GATA3 in liver were also elevated in female compared to male groups, while SMAD3 was again increased in males. Females may maintain more robust immune responses, while males may promote development of T-regulatory cells. The infiltration of T-regulatory cells is a predictor of poor prognositic outcome (Chew et al., 2010).

Tumor incidence in female DEN-initiated mice maintained on both silibinin and ethanol was ≈1.4:1 and 2.6:1 in DEN-initiated animals without EtOH-DW compared to males. This suggests that ethanol combined with silibinin may increased tumorogeneicity in females. Measures of tissue pathology (steatosis, necrosis, inflammatory cell infiltration, collagen deposition) and oxidative stress (ALT, MDA and GSH) were improved in both males and females during early (24 week) hepatocarcinogenesis, but these affects were largely abrogated during late stage. This is likely due to the extent of the pathology and development of an increasingly malignant phenotype in both males and females. Increased tumor burden was associated with increased PCNA and decreased apoptosis in male mice. Additionally, as with ethanol alone, males had increased histological scoring for necrotic cell death. Silibinin had no effect on CYP2E1 expression or activity in silibinin diet groups or ethanol drinking water with silibinin. Males consistently demonstrated increased CYP2E1 expression and activity compared to females. This may enhance ROS and oxidative injury in these groups relative to females exceeding the antioxidant capability of silibinin. Immune responses continued to follow previously established trends at the systemic level of serum cytokines and in expression

of T-bet, GATA3, and SMAD3 mRNA with the exception that males have elevated T-bet mRNA in DEN groups on both ethanol and silibinin feeding regime. This did correlate to increased Th1 cytokines IL-1b, TNFα, IFNγ identified in this group, and in pair-matched females. However IL-13 was increased 2.4 fold in males and 1.6 fold in females in thse same experimental groups compared to control. These data suggest that similar mechanisms in ethanol mediated promotion are being affected with silibinin feeding alone and with concomitant ethanol exposure. Increased IL-1b, TNFα and IL-13 in males may indicate that macrophage phenotype is polarized from anti-tumor to one that is tumor permissive. However, improvements in measures of oxidative stress and the potential for accumulation of genetic mutations is decreased, resulting in no net improvement.

Clinical studies have demonstrated that an immune response with a Th1 signature in HCC is less likely to promote metastasis, while increased T-regulatory cells are associated with increased invasion potential and tumor growth (Chew et al., 2010). Our studies demonstrate that ethanol promotes HCC, preferentially in males; while silibinin is preferentially protective in female mice during early hepatocarcinogenesis. These responses may be influenced through activation of stress-mediated transcription factors. Immune function is directed, in part, by NKκB, yet that programming can be inhibited through different actions of both ethanol and silibinin. Suppression of NFκB has been reported to support sustained activation of c-Jun N terminal kinase (JNK) activity with subsequent activation of activating protein-1 (AP-1)(Baker et al., 2010). This is a REDOX sensitive transcription factor that can serve to promote or inhibit cancer progression (Jeong et al., 2005; Mandrekar et al., 2004; Sakurai et al., 2006). Increased

expression of hepatic growth factors and compensatory proliferation are associated with JNK and AP-1 (Sakurai et al., 2006; Schwarz et al., 1983). Transcriptional programming by AP-1 generates products that can suppress negative growth regulators (p53, $p21^{cip1/waf}$, and p16) and increases cyclin D1 expression through interactions with two distinct promoter regions (Shaulian and Karin, 2001). This shift in metabolically stressed or transformed cells could drive progression of HCC. Silibinin and ethanol have both been reported to interact with NKκB and can direct both programming pathways. It is possible that the silibinin potentiates the effects of ethanol on NKκB activation/suppression; but how this is mediated in other cell types and how it is affected by sex-hormone signaling remains unknown. The combination of ethanol and silibinin in DEN-initiated mice increases hepatocarcinogenesis in males and females, eliminating any protective effects achieved through silibinin alone in DEN-initiated female mice.

In vitro studies reported that ethanol promoted growth of H4IIE cells. Promotional effects of ethanol on H4IIE cells were abrogated by silibinin pre-treatment with concomitant decreases in CYP2E1 expression and activity. This suggested that silibinin could interact directly with CYP2E1 impairing its function and preventing the associated ROS/oxidative stress. However, in a DEN-initiated mouse model of hepatocarcinogenesis promotional effects of ethanol were restricted to male mice and occurred in early and late hepatocarcinogenesis. Female DEN-initiated mice maintained on EtOH-DW had reduced injury and tumor burden when compared to male mice and DEN-initiated females. Additionally, these data demonstrate that silibinin feeding improved measures of hepatic injury (ALT, MDA, and GSH) during early HCC, but did not improve histological characteristics of liver injury. However, silibinin feeding did

reduce tumor size by nearly 50% in female DEN-initiated mice, but this effect was restricted to early hepatocarcinogenesis. Silibinin feeding in combination with EtOH-DW potentiated the promotional effects of ethanol and increased tumorigenesis in both male and female DEN-initiated mice. This effect was exacerbated during late hepatocarcinogenesis as transformed hepatocytes acquired a more malignant phenotype. Millions of Americans are estimated to abuse ethanol, given the cryptic nature of HCC, ethanol may contribute to disease progression and formation of primary liver tumors with poor prognostic outcomes. The delay between initiation to onset of symptoms and confirmation of HCC establishes a protracted period whereby the effects of lifestyle choices, including diet and ethanol consumption, and comorbidity can enhance the potential for promotion and progression in HCC. In this context ethanol may enhance progression in HCC. Further work remains to understand the underlying mechanisms behind the sexual-dimorphism in both the response to EtOH-DW and silibinin, and how these effects may vary during chronic and acute, or binge ethanol consumption.

REFERENCES.

Adams D, Burra, P., Hubscher, SG., Elias, E., Newman, W., (1994) Endothelial activation and circulating vascular adhesion molecules in alcoholic liver disease. Hepatology 19:588-94.

Albano E (2002) Free radical mechanisms in immune reactions associated with alcoholic liver disease. Free Radical Biology and Medicine 32:110-114.

Albano E (2006) Alcohol, oxidative stress and free radical damage. Proc of Nutritional Soc 65:278-90.

Albano E (2008) Oxidative mechanisms in the pathogenesis of alcoholic liver disease. Molec Asp of Med 29:9-16.

Albano E, French SW, Ingelman-Sundberg M (1999) Hydroxyethyl radicals in ethanol hepatotoxicity. Front Biosci 4:D533-40.

Altekruse S, McGlynn, KA., Reichman, ME. (2009) Hepatocellular carcinoma incidence, mortality, and survival trends in the United States from 1975 to 2005. J Clinic Oncology 27(9):1485-1491.

Alter H, Boyer, JL., Cohen, DE., Fausto, N., Shafritz, DA., Wolkoff, AW. (2009) The Liver Biology and Pathobiology. 5th ed. Wiley-Blackwell, West Sussex, UK.

Aroor A, Shukla S (2004) MAP kinase signaling in diverse effects of ethanol. Life Sciences 74(19):2339-2364.

Arteel GE (2003) Oxidants and antioxidants in alcohol-induced liver disease. Gastroenterology 124(3):778-790.

Baan R, Straif K, Grosse Y, Secretan B, El Ghissassi F, Bouvard V, Altieri A, Cogliano V (2007) Carcinogenicity of alcoholic beverages. Lancet Oncol 8(4):292-3.

Bailey S, Cunningham C (2002) Contribution of mitochondria to oxidative stress associated with alcoholic liver disease. Free Radical Biology and Medicine 32(1):11-16.

Bailey S, Pietsch C, Cunningham C (1999) Ethanol stimulates the production of reactive oxygen species at mitochondrial complexes I and III. Free Radical Biology and Medicine 27(7-8):891-900.

Baker SS, Baker RD, Liu W, Nowak NJ, Zhu L (2010) Role of Alcohol Metabolism in Non-Alcoholic Steatohepatitis. PLoS ONE 5(3):e9570.

Baldi L, Brown K, Franzoso G, Siebenlist U (1996) Critical role for lysines 21 and 22 in signal-induced, ubiquitin-mediated proteolysis of I kappa B-alpha. J Biol Chem 271(1):376-9.

Balkwill F, Charles KA, Mantovani A (2005) Smoldering and polarized inflammation in the initiation and promotion of malignant disease. Cancer Cell 7(3):211-7.

Barash H, R. Gross E, Edrei Y, Ella E, Israel A, Cohen I, Corchia N, Ben-Moshe T, Pappo O, Pikarsky E, Goldenberg D, Shiloh Y, Galun E, Abramovitch R (2009) Accelerated carcinogenesis following liver regeneration is associated with chronic inflammation-induced double-strand DNA breaks. Proceedings of the National Academy of Sciences 107(5):2207-2212.

Bartsch H, Nair J (2004) Oxidative stress and lipid peroxidation-derived DNA-lesions in inflammation driven carcinogenesis. Cancer Detect Prev 28(6):385-91.

Bartsch H, Nair, J. (2005) Accumulation of lipid peroxidation-derived DNA lesions: Potential lead markers for chemoprevention of inflammation-driven malignancies. Mutation Research 591:34-44.

Batey R, Cao Q, Gould B (2002) Lymphocyte-mediated liver injury in alcohol-related hepatitis. Alcohol (Fayetteville, NY) 27(1):37-41.

Becker U, Deis, A., Sorensen, TI. (1996) Prediction of risk of liver disease by alcohol intake, sex and age, a prospective population study. Hepatology 23:1025-9.

Behrend L, Henderson G, Zwacka RM (2003) Reactive oxygen species in oncogenic transformation. Biochem Soc Trans 31(Pt 6):1441-4.

Bhatia N, Zhao J, Wolf DM, Agarwal R (1999) Inhibition of human carcinoma cell growth and DNA synthesis by silibinin, an active constituent of milk thistle: comparison with silymarin. Cancer Lett 147(1-2):77-84.

Bird M, Karavitis, J., Kovacs, EJ. (2008) Sex differences and estrogen modulation of the cellular immune response after injury. Cell Immuno 252:57-67.

Bode C, Bode JC (2005) Activation of the innate immune system and alcoholic liver disease: effects of ethanol per se or enhanced intestinal translocation of bacterial toxins induced by ethanol? Alcohol Clin Exp Res 29(11 Suppl):166S-71S.

Bosch F, Ribe J., Cleries R., Diaz M. (2005) Epidemiology of hepatocellular carcinoma. Clin Liver Dis 9:191-211.

Bowen DG, Zen M, Holz L, Davis T, McCaughan GW, Bertolino P (2004) The site of primary T cell activation is a determinant of the balance between intrahepatic tolerance and immunity. J Clin Invest 114(5):701-12.

Brandon-Warner E, Sugg JA, Schrum LW, McKillop IH (2010a) Silibinin inhibits ethanol metabolism and ethanol-dependent cell proliferation in an in vitro model of hepatocellular carcinoma. Cancer letters 291(1):120-129.

Bruix J, Sherman M (2005) Management of hepatocellular carcinoma. Hepatology 42(5):1208-36.

Butura A, Nilsson, K., Morgan,K., Morgan, TR., French, SW., Johansson, I., Schuppe-Koistinen, I., Sundberg, MI. (2009) The impact of CYP2E1 on the development of alcoholic liver disease as studied in the transgenic mouse model. J of Hepatology 50:572-583.

Carducci R, Armellino MF, Volpe C, Basile G, Caso N, Apicella A, Basile V (1996) [Silibinin and acute poisoning with Amanita phalloides]. Minerva Anestesiol 62(5):187-93.

Caro A, Cederbaum, AI. (2004) Oxidative stress, toxicology and pharmacology of CYP2E1. Annu Rev Pharmacol Toxicol 444:27-44.

Castañeda F, Kinne RKH (2000) Cytotoxicity of millimolar concentrations of ethanol on HepG2 human tumor cell line compared to normal rat hepatocytes in vitro. Journal of Cancer Research and Clinical Oncology 126(9):503-510.

Cederbaum A (2006) CYP2E1 - biochemical and toxicological aspects and role in alcohol-induced liver injury. Mt Sinai Journal of Medicine 73(4):657-672.

Chen G-F, Ronis, MJJ., Ingelman-Sundberg, M., Badger, TM. (1999) Hormonal regulation of microsomal cytochrome P4502E1 and P450 reductase in rat liver and kidney. Xenobiotica 29(5):437-451.

Chen P-N, Hsieh Y-S, Chiou H-L, Chu S-C (2005) Silibinin inhibits cell invasion through inactivation of both PI3K-Akt and MAPK signaling pathways. Chemico-Biological Interactions 156(2-3):141-150.

Cheung CW, Gibbons N, Johnson DW, Nicol DL (2010) Silibinin--a promising new treatment for cancer. Anticancer Agents Med Chem 10(3):186-95.

Chew V, Tow C, Teo M, Wong HL., Chan J, Gehring A, Loh M, Bolze. A., Quek R, Lee V, Lee K, Abastado J-P, Toh H, Nardin A (2010) Inflammatory tumour microenvironment is associated with superior survival in hepatocellular carcinoma patients. Journal of hepatology 52(3):370-379.

Chosay J, Essani, NA., Dunn, CJ., Jaeschke, H. (1997) Neutrophil margination and extravastation in sinusoids and venules of liver during endotoxin-induced injury. Am J Physiol 272:G 1195-1200.

Christof S, Thomas L, Claudia S, Peter B, Arianeb M, Grischa T, Jörg K, Volker E, Roland E, Peter L, Peter S, Bernhard R (2008) Etiology-dependent molecular mechanisms in human hepatocarcinogenesis. Hepatology 47(2):511-520.

Christopherson WM, Mays ET, Barrows GH (1975) Liver tumors in women on contraceptive steroids. Obstet Gynecol 46(2):221-3.

Corinti S, Albanesi C, la Sala A, Pastore S, Girolomoni G (2001) Regulatory activity of autocrine IL-10 on dendritic cell functions. J Immunol 166(7):4312-8.

Cornelli M, Mengs, U., Schneider, C., Prosdocimi, M. (2007) Toward the definition of hte mechanism of action of silymarin: Activities related to cellular protection from toxic damage induced chemotherapy. Integr Cancer Ther 6:120-129.

Crabb DW (1995) Ethanol oxidizing enzymes: roles in alcohol metabolism and alcoholic liver disease. Prog Liver Dis 13:151-72.

Crabb DW, Liangpunsakul S (2007) Acetaldehyde generating enzyme systems: roles of alcohol dehydrogenase, CYP2E1 and catalase, and speculations on the role of other enzymes and processes. Novartis Found Symp 285:4-16; discussion 16-22, 198-9.

Cunningham C, Bailey S (2001) Ethanol Consumption and Liver Mitochondria Function. Neurosignals 10(3-4):271-282.

Cunningham C, Van Horn, CG. (2003) Energy availability and alcohol-related liver pathology. Alochol Research & Health 27(4):281-299.

Czekaj P (2004) Molecular and Cellular Mechanisms of Chemically Induced Hepatocarcinogenesis. Polish Journal of Environmental Studies 13(5):477-486.

Davis G, Dempster, J., Meler, JD., Orr, DW., Walberg, MW., Brown, B., Berger, BD., O'Connor, JK., Goldstein, RM. (2008) Hepatoellular carcinoma: management of an increasingly common problem. Proc (Bayl Univ Med Cent) 21(3):266-280.

Day C (2006) From fat to inflammation. Gastroenterology 130:207-10.

Devadas S, Zaritskaya L, Rhee SG, Oberley L, Williams MS (2002) Discrete Generation of Superoxide and Hydrogen Peroxide by T Cell Receptor Stimulation. The Journal of Experimental Medicine 195(1):59-70.

Dhanalakshmi S, Mallikarjuna GU, Singh RP, Agarwal R (2004) Silibinin inhibits ultraviolet B-caused skin damage via up-regulation of p53 and p21/cip1 in SKH-1 hairless mice. AACR Meeting Abstracts 2004(1):932-c-933.

Dhiman RK, Chawla YK (2005) Herbal medicines for liver diseases. Dig Dis Sci 50(10):1807-12.

Domínguez-Malagón H, Gaytan-Graham, S. (2001) Hepatocellular Carcinoma: An Update. Ultrastructural Pathology 25:497-516.

Donato F, Tagger A, Gelatti U, Parrinello G, Boffetta P, Albertini A, Decarli A, Trevisi P, Ribero ML, Martelli C, Porru S, Nardi G (2002) Alcohol and hepatocellular carcinoma: the effect of lifetime intake and hepatitis virus infections in men and women. Am J Epidemiol 155(4):323-31.

Dragan YP, Pitot HC (1992) The role of the stages of initiation and promotion in phenotypic diversity during hepatocarcinogenesis in the rat. Carcinogenesis 13(5):739-750.

Duffy JP, Hiatt JR, Busuttil RW (2008) Surgical Resection of Hepatocellular Carcinoma. The Cancer Journal 14(2):100-110 10.1097/PPO.0b013e31816a5c1f.

Eagon P, Elm MS., Epley MJ., Shinozuka H., Rao KN. (1996) Sex steroid metabolism and receptor status in hepatic hyperplasia and cancer in rats. Gastroenterology 110:1199-1207.

Eagon P, Elm MS., Tadic SD., Nanji AA. (2001) Downregulation of nuclear sex steroid receptor activity correlates with severity of alcoholic liver injury. Am J Physiol Gastrointest Liver Physiol 281:G342-349.

Eagon P, Francavilla A., DiLeo A., Elm MS., Gennari L., Mazaferro V., Colella G., et al. (1991) Quantitation of estrogen and androgen receptors in hepatocellular carcinoma and adjacent normal liver. Dig Dis Sci 36:1303-1308.

Edenberg H (2007) The genetics of alcohol metabolism: role of alcohol dehydrogenase and aldehyde dehydrogenase variants. Alcohol Res Health 30:5-13.

Ekstrom G, Ingelman-Sundberg M (1989) Rat liver microsomal NADPH-supported oxidase activity and lipid peroxidation dependent on ethanol-inducible cytochrome P-450 (P-450IIE1). Biochem Pharmacol 38(8):1313-9.

El-Serag H (2002) Hepatocellular carcinoma and Hepatitis C in the United States. Hepatology 36(5, supplement 1):S75-S82.

El-Serag H, Marrero J, Rudolph L, Reddy K (2008) Diagnosis and Treatment of Hepatocellular Carcinoma. Gastroenterology 134(6):1752-1763.

El-Serag H, Rudolph, KL. (2007) Hepatocellular carcinoma: Epidemiology and molecular carcinogenesis. Gastroenterology 132:2557-2576.

Enomoto N, Ikejima K, Bradford B, Rivera C, Kono H, Brennerâ DA, Thurman RG (1998) Alcohol causes both tolerance and sensitization of rat Kupffer cells via mechanisms dependent on endotoxin. Gastroenterology 115(2):443-451.

Enomoto N, Schemmer P, Ikejima K, Takei Y, Sato N, Brenner DA, Thurman RG (2001) Long-term alcohol exposure changes sensitivity of rat Kupffer cells to lipopolysaccharide. Alcohol Clin Exp Res 25(9):1360-7.

Essers J, Theil, AF., Baldeyron, C., van Cappellen, WA., Houtsmuller, AB., Kanaar, R., Vermeulen, W. (2005) Nuclear dynamics of PCNA in DNA replication and repair. Molec and Cell Biology 25(21):9350-9359.

Farazi P, Glickman J, Jiang S, Yu A, Rudolph K, DePinho R (2003) Differential Impact of Telomere Dysfunction on Initiation and Progression of Hepatocellular Carcinoma. Cancer Research 63(16):5021-5027.

Farazi PA, DePinho RA (2006) Hepatocellular carcinoma pathogenesis: from genes to environment. Nat Rev Cancer 6(9):674-87.

Fausto N (2000) Liver regeneration. J of Hepatology 32 ((supplement 1)):19-31.

Fausto N, Campbell JS (2010) Mouse models of hepatocellular carcinoma. Semin Liver Dis 30(01):87-98.

Feher J, Lang, I., Nekam, K., Muzes, G., Deak, G. (1988) Effect of free radical scavengers on superoxide dismutase (SOD) enzyme in patients ith alcoholic cirrhosis. Acta Med Hung 45(3-4):265-276.

Ferenci P, Dragosics B, Dittrich H, Frank H, Benda L, Lochs H, Meryn S, Base W, Schneider B (1989) Randomized controlled trial of silymarin treatment in patients with cirrhosis of the liver. J Hepatol 9(1):105-13.

Ferenci P, Fried M, Labrecque D, Bruix J, Sherman M, Omata M, Heathcote J, Piratsivuth T, Kew M, Otegbayo JA, Zheng SS, Sarin S, Hamid SS, Modawi SB, Fleig W, Fedail S, Thomson A, Khan A, Malfertheiner P, Lau G, Carillo FJ, Krabshuis J, Le Mair A Hepatocellular carcinoma (HCC): a global perspective. J Clin Gastroenterol 44(4):239-45.

Ferlay J, Shin HR., Bray, F., Forman, D., Mathers, C., Parkin DM. GLOBOCAN 2008 v1.2, Cancer Incidence and Mortality Worldwide [Website Name]. 2008. Available at: http://globocan.iarc.fr. Accessed Date Accessed, 2008 Accessed.

Fernandez-Checa J, Kaplowitz, N., Garcia-Ruiz, C., Colell, A., Morales, A., Mari, M., Miranda, M., Ardite, E., Morales, A. (1997) GSH transport in mitochondria: defense against TNF-induced oxidative stress and alcohol-induced defect.

American Journal of Physiology - Gastrointestinal and Liver Physiology 273(1):G7-G17.

Forner A, Reig ME, de Lope CR, Bruix J (2009) Current strategy for staging and treatment: the BCLC update and future prospects. Semin Liver Dis 30(1):61-74.

Freeman TL, Tuma DJ, Thiele GM, Klassen LW, Worrall S, Niemela O, Parkkila S, Emery PW, Preedy VR (2005) Recent advances in alcohol-induced adduct formation. Alcohol Clin Exp Res 29(7):1310-6.

French S, Wong K, Jui L, Albano E, Hagbjork A, Ingelman-Sundberg M (1993) Effect of Ethanol on Cytochrome P450 2E1 (CYP2E1), Lipid Peroxidation, and Serum Protein Adduct Formation in Relation to Liver Pathology Pathogenesis. Experimental and Molecular Pathology 58(1):61-75.

Frezza M, di Padova C, Pozzato G, Terpin M, Baraona E, Lieber CS (1990) High blood alcohol levels in women. The role of decreased gastric alcohol dehydrogenase activity and first-pass metabolism. N Engl J Med 322(2):95-9.

Garcia-Ruiz C, Fernandez-Checa JC (2006) Mitochondrial glutathione: hepatocellular survival-death switch. J Gastroenterol Hepatol 21 Suppl 3:S3-6.

Gazak R, Walterova, D., and Kren, V. (2007) Silybin and silymarin--new and emerging applications in medicine. Curr Med Chem 14(3):315-338.

Gharagozloo M, Velardi E, Bruscoli S, Agostini M, Di Sante M, Donato V, Amirghofran Z, Riccardi C (2010) Silymarin suppress CD4+ T cell activation and proliferation: effects on NF-kappaB activity and IL-2 production. Pharmacol Res 61(5):405-9.

Goldberg SN, Gazelle GS, Compton CC, Mueller PR, Tanabe KK (2000) Treatment of intrahepatic malignancy with radiofrequency ablation. Cancer 88(11):2452-2463.

Goldfarb S, Pugh TD, Koen H, He YZ (1983) Preneoplastic and neoplastic progression during hepatocarcinogenesis in mice injected with diethylnitrosamine in infancy. Environ Health Perspect 50:149-61.

Goldsworthy T, Fransson-Steen, R. (2002) Quantification of the cancer process in C57BL/6J, B6C3F1and C3H/HeJ mice. Toxicol Pathol 30:97-105.

Gomaa A, Khan, SA., Toledano, MB., Waked, I., Taylor-Robinson, SD. (2008) Hepatocellular carcinoma: Epidemiology, risk factors and pathogenesis. World J Gastro 21(14):4300-4308.

Gonda TA, Tu S, Wang TC (2009) Chronic inflammation, the tumor microenvironment and carcinogenesis. Cell Cycle 8(13):2005-13.

Gramenzi A, Caputo F, Biselli M, Kuria F, Loggi E, Andreone P, Bernardi M (2006) Review article: alcoholic liver disease--pathophysiological aspects and risk factors. Aliment Pharmacol Ther 24(8):1151-61.

Guy JT, Auslander MO (1973) Androgenic steroids and hepatocellular carcinoma. Lancet 1(7795):148.

Hanahan D, Weinberg RA (2000) The hallmarks of cancer. Cell 100(1):57-70.

Harada S, Tachiyashiki K, Imaizumi K (1998) Effect of sex hormones on rat liver cytosolic alcohol dehydrogenase activity. J Nutr Sci Vitaminol (Tokyo) 44(5):625-39.

Haukeland J, Damas J, Konopski Z, Loberg E, Haaland T, Goverud I, Torjesen P, Birkeland K, Bjoro K, Aukrust P (2006) Systemic inflammation in nonalcoholic fatty liver disease is characterized by elevated levels of CCL2. Journal of hepatology 44(6):1167-1174.

He G, Yu G-Y, Temkin V, Ogata H, Kuntzen C, Sakurai T, Sieghart W, Peck-Radosavljevic M, Leffert H, Karin M (2008) Hepatocyte IKKβ/NF-kB Inhibits Tumor Promotion and Progression by Preventing Oxidative Stress-Driven STAT3 Activation. Cancer cell 17(3):286-297.

Henderson JT, Richmond J, Sumerling MD (1973) Androgenic-anabolic steroid therapy and hepatocellular carcinoma. Lancet 1(7809):934.

Hill D, Devalaraja R, Joshi-Barve S, Barve S, McClain C (1999) Antioxidants attenuate nuclear factor-kappa B activation and tumor necrosis factor-alpha production in alcoholic hepatitis patient monocytes and rat Kupffer cells, in vitro. Clinical Biochemistry 32(7):563-570.

Hines IN, Wheeler MD (2004) Recent Advances in Alcoholic Liver Disease III. Role of the innate immune response in alcoholic hepatitis. American Journal of Physiology - Gastrointestinal and Liver Physiology 287(2):G310-G314.

Hoek J, Pastorino, JG (2002) Ethanol oxidative stress and cytokine induced liver injury. Alcohol 27:63-68.

Homann N (2001) Alcohol and upper gastrointestinal tract cancer: the role of local acetaldehyde production. Addit Biol 6:309-23.

Ikejima K, Enomoto N, Iimuro Y, Ikejima A, Fang D, Xu J, Forman DT, Brenner DA, Thurman RG (1998) Estrogen increases sensitivity of hepatic Kupffer cells to endotoxin. Am J Physiol 274(4 Pt 1):G669-76.

Imoto S, Sugiyama K, Sekine Y, Matsuda T (2005) Roles for lysine residues of the MH2 domain of Smad3 in transforming growth factor-beta signaling. FEBS Lett 579(13):2853-62.

Ishihara Y, Takeuchi K, Ito F, Shimamoto N (2010) Dual regulation of hepatocyte apoptosis by reactive oxygen species: Increases in transcriptional expression and decreases in proteasomal degradation of BimEL. Journal of Cellular Physiology 226(4):1007-1016.

Israel Y, Orrego H, Niemela O (1988) Immune Responses to Alcohol Metabolites: Pathogenic and Diagnostic Implications. Semin Liver Dis 8(01):81,90.

Jacobs B, Dennehy C, Ramirez G, Sapp J, Lawrence V (2002) Milk thistle for the treatment of liver disease: A systematic review and meta-analysis. The American journal of medicine 113(6):506-515.

James S, Pogribny I, Pogribna M, Miller B, Jernigan S, Melnyk S (2003) Mechanisms of DNA Damage, DNA Hypomethylation, and Tumor Progression in the Folate/Methyl-Deficient Rat Model of Hepatocarcinogenesis. The Journal of Nutrition 133(11):3740S-3747S.

Jarvelainen H, Fang, C., Ingelman-Sundberg, M., Lindros, KO. (1999) Effect of chronic coadministration fo endotoxin and ethanol on rat liver pathology and proinflammatory and anti-inflammatory cytokines. Hepatology 29:1503-10.

Jelski W, Szmitkowksi, M. (2008a) Alcohol dehydrogenase (ADH) and aldehyde dehydrogenase (ALDH) in the cancer diseases. Clinica Chimica Acta 395:1-5.

Jelski W, Zalewski, B., Szmitkowksi, M. (2008b) The activity of Class I, II, III, and IV alcohol dehydrogenase (ADH) isoenzymes and aldehyde dehydrogenase (ALDH) in liver cancer. Dig Dis Sci 53:2550-2555.

Jeong DH, Lee GP, Jeong WI, Do SH, Yang HJ, Yuan DW, Park HY, Kim KJ, Jeong KS (2005) Alterations of mast cells and TGF-beta1 on the silymarin treatment for CCl(4)-induced hepatic fibrosis. World J Gastroenterol 11(8):1141-8.

Jinushi M, Takehara T, Tatsumi T, Hiramatsu N, Sakamori R, Yamaguchi S, Hayashi N (2005) Impairment of natural killer cell and dendritic cell functions by the soluble form of MHC class I-related chain A in advanced human hepatocellular carcinomas. Journal of Hepatology 43(6):1013-1020.

Jirillo E, Caccavo D, Magrone T, Piccigallo E, Amati L, Lembo A, Kalis C, Gumenscheimer M (2002) The role of the liver in the response to LPS: experimental and clinical findings. J Endotoxin Res 8(5):319-327.

Julkunen R, Tannenbaum., I., Baraona, E., Liber, CS. (1985) First pass metabolism of ethanol: an important determinant of blood levels after alcohol consumption. Alcohol 2:437-41.

Kakumu S, Ito S, Ishikawa T, Mita Y, Tagaya T, Fukuzawa Y, Yoshioka K (2000) Decreased function of peripheral blood dendritic cells in patients with hepatocellular carcinoma with hepatitis B and C virus infection. J Gastroenterol Hepatol 15(4):431-6.

Kang J, Wanibuchi, H., Morimura, K., Gonzalez, FJ., Fusushima, S. (2007) Role of CYP2E1 in diethylnitrosamine-induced hepatocarcinogenesis *in vivo*. Cancer Research 67:11141-11146.

Karaa A, Thompson KJ, McKillop IH, Clemens MG, Schrum LW (2008) S-adenosyl-L-methionine attenuates oxidative stress and hepatic stellate cell activation in an ethanol-LPS-induced fibrotic rat model. Shock 30(2):197-205.

Karin M (2009) NF-κB as a Critical Link Between Inflammation and Cancer. Cold Spring Harbor Perspectives in Biology 1(5).

Karin M, Greten F (2005) NF-kB: linking inflammation and immunity to cancer development and progression. Nature Reviews Immunology 5(10):749-759.

Kidd P, Head K (2005) A review of the bioavailability and clinical efficacy of milk thistle phytosome: a silybin-phosphatidylcholine complex (Siliphos). Altern Med Rev 10(3):193-203.

Knect K, Thurman, RG., Mason, RP. (1993) Role of superoxide and trance transition metals in teh production of α–hydroxylethyl radical from ethaonl by microsomes from alcohol dehydrogenase deficient deer mice. Arch Biochem Biophys 303:339-348.

Kono H, Wheeler M, Rusyn I, Lin M, Seabra V, Rivera C, Bradford B, Forman D, Thurman R (2000) Gender differences in early alcohol-induced liver injury: role of CD14, NF-κB, and TNFα. American Journal of Physiology - Gastrointestinal and Liver Physiology 278(4):G652-G661.

Koop D (1986) Hydroxylation of p-nitrophenol by rabbit ethanol-inducible cytochrome P-450 isozyme 3a. Molecular Pharmacology 29(4):399-404.

Koop D (1992) Oxidative and reductive metabolism by cytochrome P450 2E1. FASEB J 6(2):724-730.

Kovach SJ, Sitzmann JV, McKillop IH (2001) Inhibition of alcohol dehydrogenase blocks enhanced Gi-protein expression following ethanol treatment in

experimental hepatocellular carcinoma in vitro. Eur J Gastroenterol Hepatol 13(10):1209-16.

Kovacs E, Messingham KA. (2002) Influence of gender on immune response. Alcohol Res Health 26:257-263.

Lah JJ, Cui W, Hu KQ (2007) Effects and mechanisms of silibinin on human hepatoma cell lines. World J Gastroenterol 13(40):5299-305.

Lasagna N, FantappiÃ¨ O, Solazzo M, Morbidelli L, Marchetti S, Cipriani G, Ziche M, Mazzanti R (2006) Hepatocyte Growth Factor and Inducible Nitric Oxide Synthase Are Involved in Multidrug Resistance-Induced Angiogenesis in Hepatocellular Carcinoma Cell Lines. Cancer Research 66(5):2673-2682.

Lee D, Liu, Y. (2003) Molecular structure and stereochemistry of Silybin A, Silybin B, Isosilybin A and Isosilybin B, isolated for Silybum marianum (Milk Thistle). J Nat Prod 66:1171-1173.

Lee S-O, Jeong Y-J, Im HG, Kim C-H, Chang Y-C, Lee I-S (2007) Silibinin suppresses PMA-induced MMP-9 expression by blocking the AP-1 activation via MAPK signaling pathways in MCF-7 human breast carcinoma cells. Biochemical and Biophysical Research Communications 354(1):165-171.

Lencioni RA, Allgaier H-P, Cioni D, Olschewski M, Deibert P, Crocetti L, Frings H, Laubenberger J, Zuber I, Blum HE, Bartolozzi C (2003) Small Hepatocellular Carcinoma in Cirrhosis: Randomized Comparison of Radio-frequency Thermal Ablation versus Percutaneous Ethanol Injection1. Radiology 228(1):235-240.

Levings MK, Bacchetta R, Schulz U, Roncarolo MG (2002) The Role of IL-10 and TGF-β in the Differentiation and Effector Function of T Regulatory Cells. International Archives of Allergy and Immunology 129(4):263-276.

Lieber C (1997a) Cytochrome P-4502E1: its physiological and pathological role. Physiol Rev 77:517-544.

Lieber C (1997b) Ethanol metabolism, cirrhosis and alcoholism. Clin Chim Acta 257(1):59-84.

Lieber C (2000) Alcohol: Its metabolites and interaction with nutrients. Annu Rev Nutr 20:395-430.

Lieber C (2001) Alcoholic liver injury: pathogenesis and therapy in 2001. Pathol Biol 49:738-752.

Lieber C, Decarli L (1989) Liquid diet techinique of ethanol administration. Alcohol and Alcoholism 24(3):197-211.

Lin W-W, Karin M (2007) A cytokine-mediated link between innate immunity, inflammation, and cancer. The Journal of Clinical Investigation 117(5):1175-1183.

Liu Z-J, Yan L-N, Li X-H, Xu F-L, Chen X-F, You H-B, Gong J-P (2008) Up-Regulation of IRAK-M is Essential for Endotoxin Tolerance Induced by a Low Dose of Lipopolysaccharide in Kupffer Cells. Journal of Surgical Research 150(1):34-39.

Livak K, Schmittgen, TD. (2001) Analysis of relative gene expression data using Real-time quantitative PCR and the $2^{-\Delta\Delta CT}$ method. Methods 25:402-408.

Llovet JM, Ricci S, Mazzaferro V, Hilgard P, Gane E, Blanc JF, de Oliveira AC, Santoro A, Raoul JL, Forner A, Schwartz M, Porta C, Zeuzem S, Bolondi L, Greten TF, Galle PR, Seitz JF, Borbath I, Haussinger D, Giannaris T, Shan M, Moscovici M, Voliotis D, Bruix J (2008) Sorafenib in advanced hepatocellular carcinoma. N Engl J Med 359(4):378-90.

Lu S (1998) Regulation of hepatic glutathione synthesis. Semin Liver Dis 18:331-343.

Lu SC, Mato JM (2008) S-Adenosylmethionine in cell growth, apoptosis and liver cancer. J Gastroenterol Hepatol 23 Suppl 1:S73-7.

Lu Y, Cederbaum, AI. (2008) CYP2E1 and oxidative liver injury by alcohol. Free Radical Biol and Med 44:723-738.

Lui W, Lin H, Chau G, Liu T, Chi C (2000) Male predominance in hepatocellular carcinoma: new insight and a possible therapeutic alternative. Medical Hypotheses 55(4):348-350.

Lundquist F, Tygstrup, N., Winkler, K., Mellemgaard, K., Munck-Petersen, S. (1962) Ethanol metabolims and production of free acetate in the human liver. J of Clinic Invest 41(5):955-961

Maeda S, Kamata H, Luo JL, Leffert H, Karin M (2005) IKKbeta couples hepatocyte death to cytokine-driven compensatory proliferation that promotes chemical hepatocarcinogenesis. Cell 121(7):977-90.

Mandl J, Banhegyi, G., Garzo, T., Lapis, K., Antoni, F., Schaff, Z. (1989) Ethanol treatment inhibits the devlopment of diethylnitrosamine-induced tumors in rats. J Exp Pathol 4:227-235.

Mandrekar P, Bala S, Catalano D, Kodys K, Szabo G (2009) The Opposite Effects of Acute and Chronic Alcohol on Lipopolysaccharide-Induced Inflammation Are Linked to IRAK-M in Human Monocytes. The Journal of Immunology 183(2):1320-1327.

Mandrekar P, Catalano D, Dolganiuc A, Kodys K, Szabo G (2004) Inhibition of Myeloid Dendritic Cell Accessory Cell Function and Induction of T Cell Anergy by Alcohol Correlates with Decreased IL-12 Production. The Journal of Immunology 173(5):3398-3407.

Mandrekar P, Szabo G (2009) Signalling pathways in alcohol-induced liver inflammation. J Hepatol 50(6):1258-66.

Manna S, Gad, YP., Mukhopadhaya, A., Aggarwal, B. (1999) Lipopolysaccharide inhibits TNF-induced apoptosis: role of nuclear factor kB activatoina and reacitve oxygen intermediates. J Immunol 162(352):59-70.

Mantel P-Y, Kuipers H, Boyman O, Rhyner C, Ouaked N, RÃ¼ckert B, Karagiannidis C, Lambrecht BN, Hendriks RW, Crameri R, Akdis CA, Blaser K, Schmidt-Weber CB (2007) GATA3-Driven Th2 Responses Inhibit TGF β1 Induced FOXP3 Expression and the Formation of Regulatory T Cells. PLoS Biol 5(12):e329.

Mantovani A, Allavena, P., Sica, A., Balkwill, F. (2008) Cancer-related inflammation. Nature 454:436-444.

Mantovani A, Sozzani S, Locati M, Allavena P, Sica A (2002) Macrophage polarization: tumor-associated macrophages as a paradigm for polarized M2 mononuclear phagocytes. Trends Immunol 23(11):549-55.

Mathurin P, Deng QG, Keshavarzian A, Choudhary S, Holmes EW, Tsukamoto H (2000) Exacerbation of alcoholic liver injury by enteral endotoxin in rats. Hepatology 32(5):1008-17.

Mato J, Lu S (2007) Role of S-adenosyl-L-methionine in liver health and injury. Hepatology 45(5):1306-1312.

Matsuda T, Yamamoto T, Muraguchi A, Saatcioglu F (2001) Cross-talk between transforming growth factor-beta and estrogen receptor signaling through Smad3. J Biol Chem 276(46):42908-14.

McKillop I, Moran DM., Jin X., Koniaris LG. (2006) Molecular pathogenesis of hepatocellular carcinoma. J of Surgical Research

McKillop I, Shrum LW. (2005) Alcohol and liver cancer. Alcohol 35:195-203.

McKillop I, Vyas N., Schmidt CM., Cahill PA., Sitzmann JV. (1999) Enhanced Gi-protein-mediated mitogenesis following chronic ethanol exposure in a rat model of experimental hepatocellular carcinoma. Hepatology 29:412-420.

McKillop IH, Schmidt CM, Cahill PA, Sitzmann JV (1997) Altered expression of mitogen-activated protein kinases in a rat model of experimental hepatocellular carcinoma. Hepatology 26(6):1484-91.

McKillop IH, Schrum LW (2009) Role of alcohol in liver carcinogenesis. Semin Liver Dis 29(2):222-32.

Medina J, Moreno-Otero R (2005) Pathophysiological basis for antioxidant therapy in chronic liver disease. Drugs 65(17):2445-61.

Meeran SM, Katiyar SK (2008) Cell cycle control as a basis for cancer chemoprevention through dietary agents. Front Biosci 13:2191-202.

Miguez MP, Anundi I, Sainz-Pardo LA, Lindros KO (1994) Hepatoprotective mechanism of silymarin: no evidence for involvement of cytochrome P450 2E1. Chem Biol Interact 91(1):51-63.

Mira L, Silva M, Manso C (1994) Scavenging of reactive oxygen species by silibinin dihemisuccinate. Biochemical Pharmacology 48(4):753-759.

Momeny M, Khorramizadeh MR, Ghaffari SH, Yousefi M, Yekaninejad MS, Esmaeili R, Jahanshiri Z, Nooridaloii MR (2008) Effects of silibinin on cell growth and invasive properties of a human hepatocellular carcinoma cell line, HepG-2, through inhibition of extracellular signal-regulated kinase 1/2 phosphorylation. European Journal of Pharmacology 591(1-3):13-20.

Monzoni A, Msutti, F., Saccoccio, G., Bellentani, S., Tiribelli, C., Giacca, M. (2001) Genetic determinants of ethanol induced liver damage. Mol Med 7(4):255-262.

Moran D, Koniaris, L.G., Jablonsi, E.M., Cahill, P. A., Halberstadt, C.R., and McKillop, I.H. (2006) Microencapsulation of engineered cells to deliver sustained high circulating levels of interlukin-6 to study hepatocellular carcinoma progression. Cell Transplant 15:785-798.

Morgan K, French S, Morgan T (2002) Production of a cytochrome P450 2E1 transgenic mouse and initial evaluation of alcoholic liver damage. Hepatology 36(1):122-134.

Morgan T, Mandayam, S., and Jamal, MM. (2004) Alcohol and hepatocellular carcinoma. Gastroenterology 127:S87-96.

Mueller S, Simon, S., Chae, K., Metzler, M., Korach, KS. (2004) Phytoestrogens and their human metabolites show distinct agonistic and antagoinsitic properties on estorgen receptor ERa and ER. Toxicol Sci 80:14-25.

Muller A, Sies H (1987) Alcohol, aldehydes and lipid peroxidation: current notions. Alcohol Alcohol Suppl 1:67-74.

Muller C (2006) Liver, alcohol and gender. Wien Med Wochenschr 156(19-20):523-6.

Mumenthaler M, Taylor, JL., O'Hara, R., Yesavage, JA. (1999) Gender differences in moderate drinking effects. Alcohol Research & Health 23:55-59.

Nagy L (2004) Molecular aspects of alcohol metabolism: Transcription factors involved in early ethanol-induced liver injury. Annu Rev Nutr 24:55-78.

Nakagama H, Gunji T, Ohnishi S, Kaneko T, Ishikawa T, Makino R, Hayashi K, et al. (1991) Expression of androgen receptor mRNA in human hepatocellular carcinomas and hepatoma cell lines. Hepatology 14:99-102.

Nanji AA, French SW (2003) Animal models of alcoholic liver disease--focus on the intragastric feeding model. Alcohol Res Health 27(4):325-30.

Naugler W, Sakurai, T., Kim, S., Maeda, S., Kim, K., Elsharkawy, AM., Karin, M. (2007) Gender disparity in liver cancer due to sex differences in MyD88-dependent IL-6 production. Science 317.

Navasumrit P, Ward, TH., Dodd, NJF., O'Connor, PJ. (2000) Ethanol-induced free radicals and hepatic DNA strand breaks are prevented *in vivo* by antioxidants: effects of acute and chronic ethanol exposure. Carcinogenesis 21(1):93-99.

Nicolini A, Martinetti L, Crespi S, Maggioni M, Sangiovanni A (2010) Transarterial Chemoembolization with Epirubicin-eluting Beads versus Transarterial Embolization before Liver Transplantation for Hepatocellular Carcinoma. Journal of Vascular and Interventional Radiology 21(3):327-332.

Nieto N (2006) Oxidative-stress and IL-6 mediate the fibrogenic effects of rodent Kupffer cells on stellate cells. Hepatology 44:1487-1501.

Ogawa K (2009) Molecular pathology of early stage chemically induced hepatocarcinogenesis. Pathol Int 59(9):605-22.

Okuda K (2000) Hepatocellular carcinoma. J Hepatol 32:225-237.

Okuda K (2002) Natural history of hepatocellular carcinoma including fibrolamellar and hepato-cholangiocarcinoma variants. J Gastroenterol Hepatol 17(4):401-5.

Osna N, Duryee, MJ, Klassen, LW, Thiele, GM (2007) Immunological response in alcoholic liver disease. World J Gastroenterol 13(37):4938-4946.

Porta C, Rimoldi M, Raes G, Brys L, Ghezzi P, Di Liberto D, Dieli F, Ghisletti S, Natoli G, De Baetselier P, Mantovani A, Sica A (2009) Tolerance and M2 (alternative) macrophage polarization are related processes orchestrated by p50 nuclear factor kappaB. Proc Natl Acad Sci U S A 106(35):14978-83.

Poschl G, Seitz H (2004) Alcohol and Cancer. Alcohol 39(3):155-165.

Pradeep K, Mohan CV, Gobianand K, Karthikeyan S (2007) Silymarin modulates the oxidant-antioxidant imbalance during diethylnitrosamine induced oxidative stress in rats. Eur J Pharmacol 560(2-3):110-6.

Qulali M, Crabb D (1992) Estradiol regulates class I alcohol dehydrogenase gene expression in renal medulla of male rats by a post-transcriptional mechanism. Archives of Biochemistry and Biophysics 297(2):277-284.

Ramakrishnan G, Lo Muzio L, Elinos-Baez CM, Jagan S, Augustine TA, Kamaraj S, Anandakumar P, Devaki T (2009) Silymarin inhibited proliferation and induced apoptosis in hepatic cancer cells. Cell Prolif 42(2):229-40.

Ramasamy K, Agarwal R (2008) Multitargeted therapy of cancer by silymarin. Cancer Letters 269(2):352-362.

Rambaldi A, Jacobs BP, Gluud C (2007) Milk thistle for alcoholic and/or hepatitis B or C virus liver diseases. Cochrane Database Syst Rev (4):CD003620.

Ramhaldi AaC, C. (2001) S-adenacyl-L-methionine for alchololic liver diseases. Cochrane Database Suyst Rev CD002235.

ImageJ. Bethesda, MD USA: US National Institues of Health 1997-2011.

Reuter S, Gupta SC, Chaturvedi MM, Aggarwal BB (2010) Oxidative stress, inflammation, and cancer: how are they linked? Free Radic Biol Med 49(11):1603-16.

Roberts PJ, Der CJ (2007) Targeting the Raf-MEK-ERK mitogen-activated protein kinase cascade for the treatment of cancer. Oncogene 26(22):3291-310.

Rogers AB, Theve EJ, Feng Y, Fry RC, Taghizadeh K, Clapp KM, Boussahmain C, Cormier KS, Fox JG (2007) Hepatocellular carcinoma associated with liver-gender disruption in male mice. Cancer Res 67(24):11536-46.

Rogers CQ, Ajmo JM, You M (2008) Adiponectin and alcoholic fatty liver disease. IUBMB Life 60(12):790-797.

Ronis M, Lindros, KO, Ingelman-Sundberg. M. ed (1996) *The CYP2E family.* CRC Press, Boca Raton, FL.

Ronis MJ, Wands JR, Badger TM, de la Monte SM, Lang CH, Calissendorff J (2007) Alcohol-induced disruption of endocrine signaling. Alcohol Clin Exp Res 31(8):1269-85.

Rubbo H, Radi, R., Anselmi, D., Kirk, M., Barnes, S. ,Butler, J., Eiserich, JP., Freeman, BA. (2000) Nitric oxide reaction with lipid peroxyl radicals spares alpha-tocopererol during lipid peroxidation. Greater oxidant protection from the pair nitric oxide/α-tocopererol/ascorbate. J Biol Chem 275:10812-10818.

Sakurai T, Maeda S, Chang L, Karin M (2006) Loss of hepatic NF-kappa B activity enhances chemical hepatocarcinogenesis through sustained c-Jun N-terminal kinase 1 activation. Proc Natl Acad Sci U S A 103(28):10544-51.

Saliou C, Valacchi, G., Rimbach, G. (2001) Assessing bioflavinoids as regulators of NFkB activity and gene expression in mammalian cells. Methods in Enzy 335(34):380-387.

Saller R, Meier, R., Brignoli, R. (2001) The use of Silymarin in the treatment of liver diseases. Drugs 61(14):2035-2063.

Saller R, Melzer, J., Reichling, J., Brignoli, R., Meier, R. (2007) An updated systematic review of the pharmacology of silymarin. Forsch Komplementmed 14(2):70-80.

Sasaki Y (2006) Does oxidative stress participate in the development of hepatocellular carcinoma? Journal of Gastroenterology 41(12):1135-1148.

Scaffidi P, Misteli T, Bianchi ME (2002) Release of chromatin protein HMGB1 by necrotic cells triggers inflammation. Nature 418(6894):191-5.

Schumann J, Prockl J, K. Kiemer A, M. Vollmar A, Bang R, Tiegs G (2003) Silibinin protects mice from T cell-dependent liver injury Journal of Hepatology 39(3):333-340.

Schwarz M, Buchmann A, Wiesbeck G, Kunz W (1983) Effect of ethanol on early stages in nitrosamine carcinogenesis in rat liver. Cancer Lett 20(3):305-12.

Scoccia B, Kovar P, Benveniste R (1991) Gonadal and adrenal effects on hepatic epidermal growth factor receptor expression in a murine model. Endocrinology 129(6):3240-6.

Seidlova-Wuttke D, Becker T, Christoffel V, Jarry H, Wuttke W (2003) Silymarin is a selective estrogen receptor beta (ERbeta) agonist and has estrogenic effects in the

metaphysis of the femur but no or antiestrogenic effects in the uterus of ovariectomized (ovx) rats. J Steroid Biochem Mol Biol 86(2):179-88.

Seitz H, Pöschl G, Simanowski U (1998) Alcohol and Cancer, in Recent Developments in Alcoholism, vol 14, Recent Developments in Alcoholism ed^eds), pp 67-95. Springer US.

Seitz H, Stickel, F (2006) Risk factors and mechanisms of hepatocarcinogenesis with special emphasis on alcohol and oxidative stress. Biol Chem 387:349-360.

Seitz HK, Becker P (2007) Alcohol metabolism and cancer risk. Alcohol Res Health 30(1):38-41, 44-7.

Shaulian E, Karin M (2001) AP-1 in cell proliferation and survival. Oncogene 20(19):2390-400.

Shen Z, Liang X, Rogers CQ, Rideout D, You M (2010) Involvement of adiponectin-SIRT1-AMPK signaling in the protective action of rosiglitazone against alcoholic fatty liver in mice. Am J Physiol Gastrointest Liver Physiol 298(3):G364-74.

Shimizu I, Inoue H, Yano M, Shinomiya H, Wada S, Tsuji Y, Tsutsui A, Okamura S, Shibata H, Ito S (2001) Estrogen receptor levels and lipid peroxidation in hepatocellular carcinoma with hepatitis C virus infection. Liver 21(5):342-349.

Simon F, Fortune, J., Iwahashi, M., Sutherland, E. (2002) Sexual dimorphic expression fo ADH in rat liver: importance of the hypohtalamic-pituitary-liver axis. AM J Physiol Gastrointest Liver Physiol 283:646-655.

Singh R, Agarwal R (2004) A cancer chemopreventive agent silibinin, targets mitogenic and survival signaling in prostate cancer. Mutation Research/Fundamental and Molecular Mechanisms of Mutagenesis 555(1-2):21-32.

Singh R, Agarwal, R. (2004a) Prostate cancer prevention by silibinin. Current Cancer Drug Targets 4:1-11.

Singh R, Dhanalakshmi, S., Agarwal, C., Agarwal, R. (2004b) Silibinin strongly inhibits growth and survival of human endothelial cells via cell cycle arrest and downregulation of survivin, Akt and NF-[kappa]B: implications for angioprevention and antiangiogenic therapy. Oncogene 24(7):1188-1202.

Singh RP, Gu M, Agarwal R (2008) Silibinin inhibits colorectal cancer growth by inhibiting tumor cell proliferation and angiogenesis. Cancer Res 68(6):2043-50.

Sridar C, Goosen TC, Kent UM, Williams JA, Hollenberg PF (2004) Silybin inactivates cytochrome P450 3A4 and 2C9 and inhibits major hepatic glucuronosyltransferases Drug Metabolism and Disposition 32(6):587-594.

Stewart S, Vidali M, Day C, Albano E, Jones D (2004) Oxidative stress as a trigger for cellular immune responses in patients with alcoholic liver disease. Hepatology 39(1):197-203.

Stickel F, Schuppan D (2007) Herbal medicine in the treatment of liver diseases. Digestive and Liver Disease 39(4):293-304.

Storz P (2005) Reactive oxygen species in tumor progression. Front Biosci 10:1881-96.

Tabakoff B, Hoffman PL (2000) Animal models in alcohol research. Alcohol Res Health 24(2):77-84.

Tacke F, Luedde T, Trautwein C (2009) Inflammatory pathways in liver homeostasis and liver injury. Clin Rev Allergy Immunol 36(1):4-12.

Takada A, Nei, J., Takase, S., Matsuda, Y. (1986) Effects of ethanol on experimental hepatocarcinogenesis. Hepatology 6(1):65-72.

Thomas MB, Zhu AX (2005) Hepatocellular carcinoma: the need for progress. J Clin Oncol 23(13):2892-9.

Thorgeirsson S, Grisham, JW. (2002) Molecular pathogenesis of human carcinoma. Nature Genetics 31:339-346.

Thurman R (1998) II. Alcoholic liver injury involves activation of Kupffer cells by endotoxin. American Journal of Physiology - Gastrointestinal and Liver Physiology 275(4):G605-G611.

Tilg H, Moschen A (2006) Adipocytokines: mediators linking adipose tissue, inflammation and immunity. Nat Rev Immunol 6(10):772-783.

Torimura T, Sata M, Ueno T, Kin M, Tsuji R, Suzaku K, Hashimoto O, Sugawara H, Tanikawa K (1998) Increased expression of vascular endothelial growth factor is associated with tumor progression in hepatocellular carcinoma. Hum Pathol 29(9):986-91.

Trappoliere M, Caligiuri A, Schmid M, Bertolani C, Failli P, Vizzutti F, Novo E, di Manzano C, Marra F, Loguercio C, Pinzani M (2009) Silybin, a component of silymarin, exerts anti-inflammatory and anti-fibrogenic effects on human hepatic stellate cells. J Hepatol 50(6):1102-11.

Tsukamoto H, French S, Rektelberger R, Largman C (1985) Cyclical Pattern of Blood Alcohol Levels during Continuous Intragastric Ethanol Infusion in Rats. Alcoholism: Clinical and Experimental Research 9(1):31-37.

Tuma D, Thiele, GM., Xu, D., Klassen, LW., Sorrell, MF. (1996) Acetaldehyde and malondialdehyde react together to generate distinct protein adducts in the liver during long-term ethanol administration. Hepatology 23:872-880.

Tuma DJ, Casey CA (2003) Dangerous Byproducts of Alcohol Breakdown--Focus on Adducts. Alcohol Research & Health 27(4):285-290.

Tyagi A, Agarwal, C., Harrison, G., Glode, LM., Agarwal, R. (2004) Silibinin causes cell cycle arrest and apoptosis in human bladder transitional cell carcinoma cells by regulating CDKI–CDK–cyclin cascade, and caspase 3 and PARP cleavages. Carcinogenesis 25(9):1711-1720.

Tyagi A, Singh R, Ramasamy K, Raina K, Redente E, Dwyer-Nield L, Radcliffe R, Malkinson A, Agarwal R (2009) Growth Inhibition and Regression of Lung Tumors by Silibinin: Modulation of Angiogenesis by Macrophage-Associated Cytokines and Nuclear Factor-ÎºB and Signal Transducers and Activators of Transcription 3. Cancer Prevention Research 2(1):74-83.

Varghese L, Agarwai, C. Tyagi, A., Singh, RP., and Agarwal, R. (2005) Silibinn efficacy against heman hepatocellualr carcinoma. Clin Cancer Res 11:8441-8448.

Vasiliou V, Bairoch, A., Tipton, KF., Nebert, DW. (1999) Eukaryotic aldhehyde dehydrogeanse (ALDH gens: human polymorphisms and recommended nomenclature based on divergent evolution and chromosomal mapping. Parmacogenetics 9:421-34.

Vesselinovitch SD, Mihailovich N (1983) Kinetics of diethylnitrosamine hepatocarcinogenesis in the infant mouse. Cancer Res 43(9):4253-9.

Vidali M, Steware, SF., Albano, E. (2007) Interplay between oxidative stress adn immunity in the progression of alochol-mediated liver injury. Trends in Molec Med 14(2):63-71.

Wang J, Hu Y, Nekvindova J, Ingelman-Sundberg M, Neve EPA (2010) IL-4-mediated transcriptional regulation of human CYP2E1 by two independent signaling pathways. Biochemical Pharmacology 80(10):1592-1600.

Wen Z, Dumas TE, Schrieber SJ, Hawke RL, Fried MW, Smith PC (2008) Pharmacokinetics and Metabolic Profile of Free, Conjugated, and Total Silymarin Flavonolignans in Human Plasma after Oral Administration of Milk Thistle Extract. Drug Metabolism and Disposition 36(1):65-72.

Wheeler M, Thurman, RG. (2003) Up-regulation of CD14 in liver caused by acute ethanol involves oxidant-dependent AP-1 pathway. J Biol Chem 278:8435-8441.

Wu D, Cederbaum A (2003) Alcohol, Oxidative Stress, and Free Radical Damage. Alcohol Research & Health 27(4):277-284.

Wu JW, Lin LC, Hung SC, Chi CW, Tsai TH (2007) Analysis of silibinin in rat plasma and bile for hepatobiliary excretion and oral bioavailability application. J Pharm Biomed Anal 45(4):635-41.

Yamashina S, Takei Y, Ikejima K, Enomoto N, Kitamura T, Sato N (2005) Ethanol-induced sensitization to endotoxin in Kupffer cells is dependent upon oxidative stress. Alcohol Clin Exp Res 29(12 Suppl):246S-50S.

Yan L, Stanley SL, Jr. (2001) Blockade of caspases inhibits amebic liver abscess formation in a mouse model of disease. Infect Immun 69(12):7911-4.

Yang JD, Nakamura I, Roberts LR (2011) The tumor microenvironment in hepatocellular carcinoma: current status and therapeutic targets. Semin Cancer Biol 21(1):35-43.

Yang JD, Roberts LR (2010) Hepatocellular carcinoma: A global view. Nat Rev Gastroenterol Hepatol 7(8):448-58.

Yin S, Liao, CS., Uw, CW., Li, TT., Chen, LL, Lai, CL., Tsao, TY. (1997) Human stomach alcohol and aldhehyde dehydrogenase. Gastroenterology 112(3):766-775.

Yoshimura A (2006) Signal transduction of inflammatory cytokines and tumor development. Cancer Sci 97(6):439-47.

You M, Rogers CQ (2009) Adiponectin: a key adipokine in alcoholic fatty liver. Exp Biol Med (Maywood) 234(8):850-9.

Yu J, Wei M, Becknell B, Trotta R, Liu S, Boyd Z, Jaung MS, Blaser BW, Sun J, Benson Jr DM, Mao H, Yokohama A, Bhatt D, Shen L, Davuluri R, Weinstein M, Marcucci G, Caligiuri MA (2006) Pro- and Antiinflammatory Cytokine Signaling: Reciprocal Antagonism Regulates Interferon-gamma Production by Human Natural Killer Cells. Immunity 24(5):575-590.

Yu M-W, Chen C-J (1993) Elevated Serum Testosterone Levels and Risk of Hepatocellular Carcinoma. Cancer Research 53(4):790-794.

Z. Abdel-Razzak PL, A. Fautrel, J.C. Gautier, L. Corcos, B. Turlin et al. (1993) Cytokines down-regulate expression of major cytochrome P-450 enzymes in adult human hepatocytes in primary culture. Mol Pharmacol 44:707-715.

Zaman SN, Melia WM, Johnson RD, Portmann BC, Johnson PJ, Williams R (1985) Risk factors in development of hepatocellular carcinoma in cirrhosis: prospective study of 613 patients. Lancet 1(8442):1357-60.

Zhang BH, Yang BH, Tang ZY (2004) Randomized controlled trial of screening for hepatocellular carcinoma. J Cancer Res Clin Oncol 130(7):417-22.

Zhao J, Agarwal R (1999) Tissue distribution of silibinin, the major active constituent of silymarin, in mice and its association with enhancement of phase II enzymes: implications in cancer chemoprevention. Carcinogenesis 20(11):2101-8.

Zhu AX (2008) Development of sorafenib and other molecularly targeted agents in hepatocellular carcinoma. Cancer 112(2):250-259.

Zi X, Zhang, J., Agarwal, R., Pollak, M. (2008) Silibinin up-regulates insulin-like growth factor binding protein 3 expression and inhibits profileration of androgen-independent prostate cancer cells. Cancer Research 60:5617-.

APPENDIX A: SUPPLEMENTARY DATA

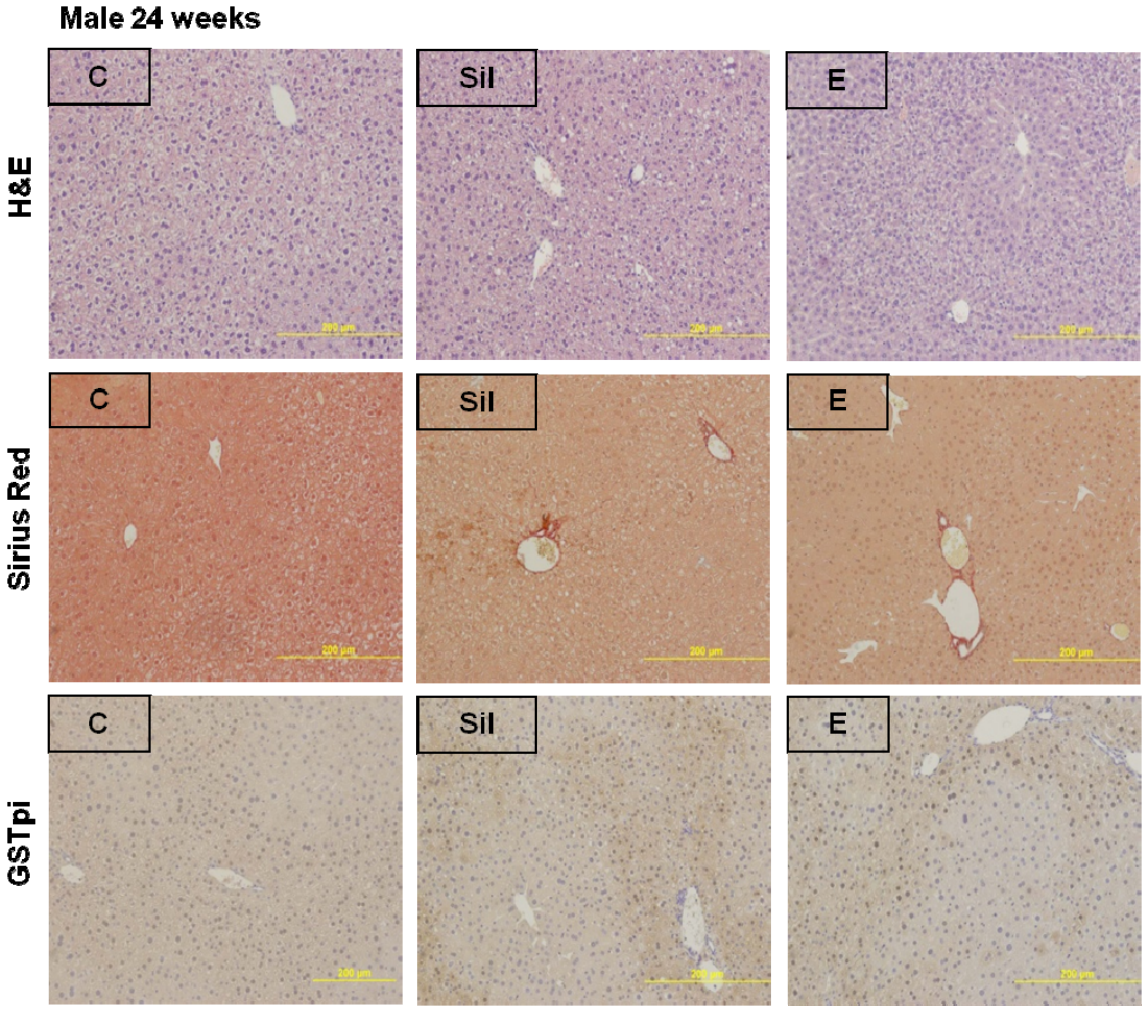

Appendix A Figure A.1: Representative micrographs (100X) of H&E, Sirius red and GSPpi stained liver sections from 24 week male mice in control (C), silibinin diet diet (0.5% (*w/w*) daily for 9 weeks) (Sil), and ethanol drinking water regime (10/20% (*v/v*) alternating daily for 8 weeks) (E) groups.

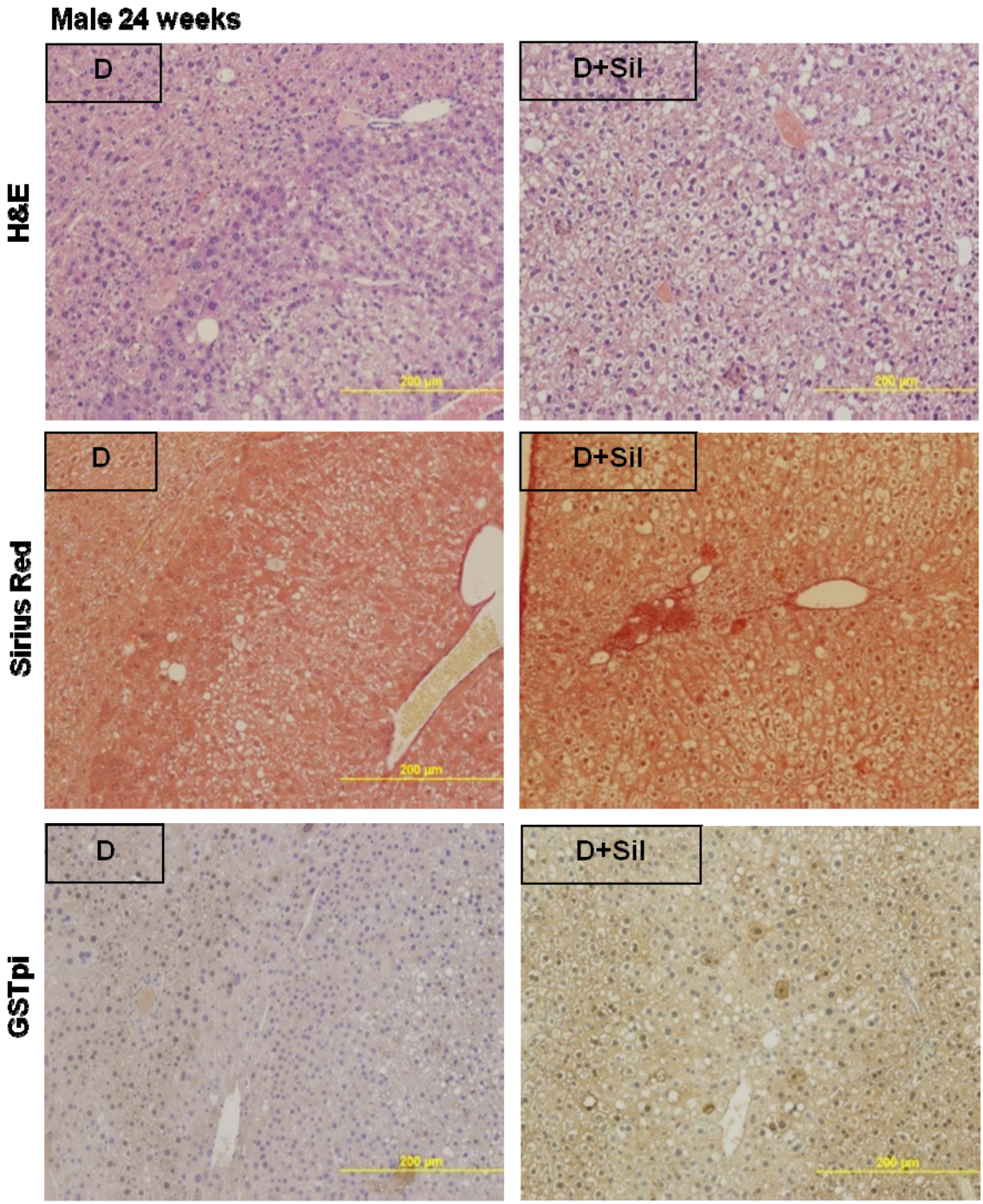

Appendix A Figure A.2: Representative micrographs (100X) of H&E, Sirius red and GSPpi stained liver sections from 24 week male DEN-initiated (D), and DEN-intitiated mice maintained on silibinin diet diet (0.5% (*w/w*) daily for 9 weeks) (D+Sil).

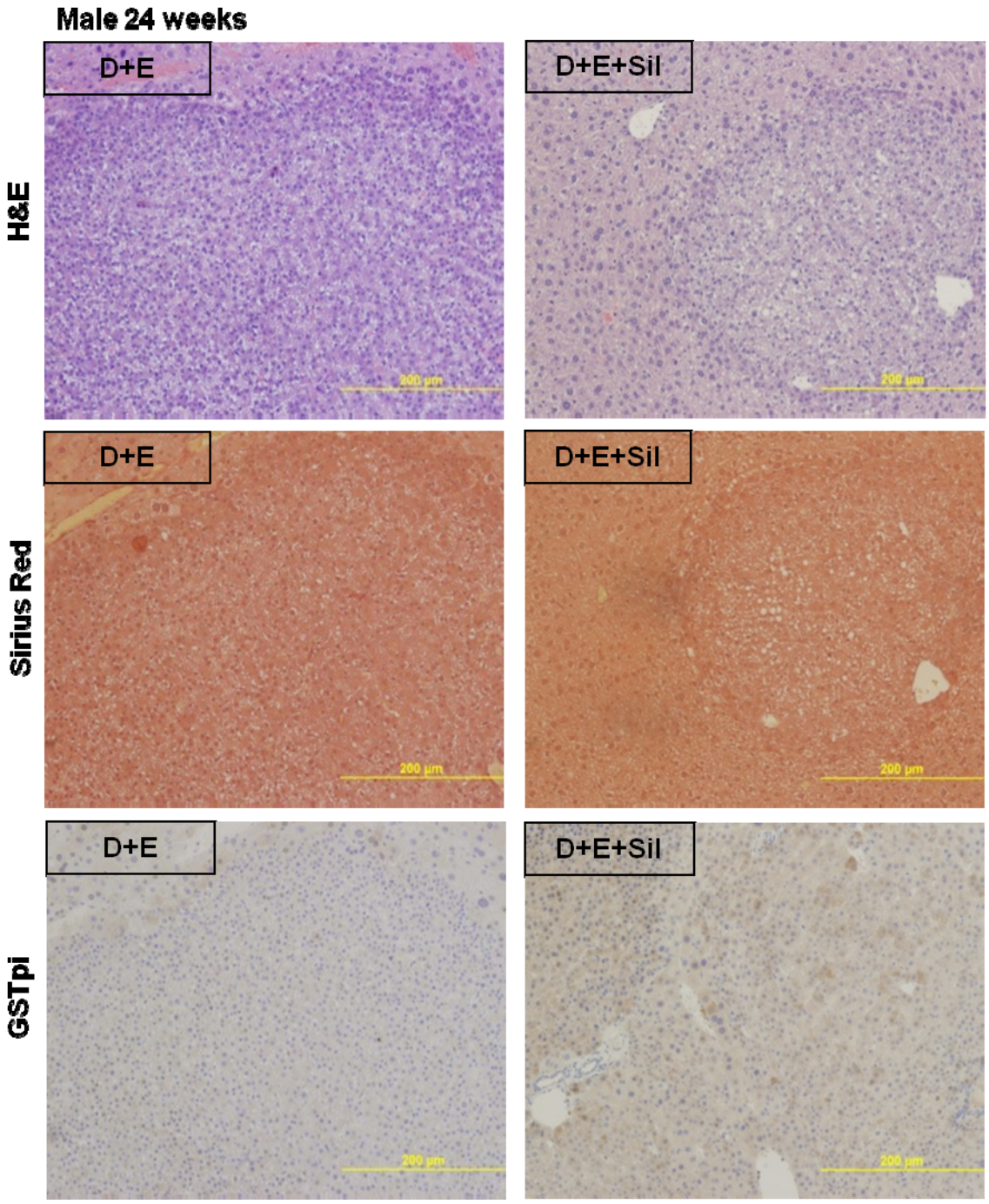

Appendix A Figure A.3: Representative micrographs (100X) of H&E, Sirius red and GSPpi stained liver sections from 24 week male DEN-initiated mice maintained on ethanol drinking-water regime (10/20% (*v/v*) alternating daily for 8 weeks) (D+E), and DEN-initiated female mice maintained on Silibinin diet (0.5% (*w/w*) daily for 9 weeks) with ethanol drinking-water (8 weeks) (D+E+Sil).

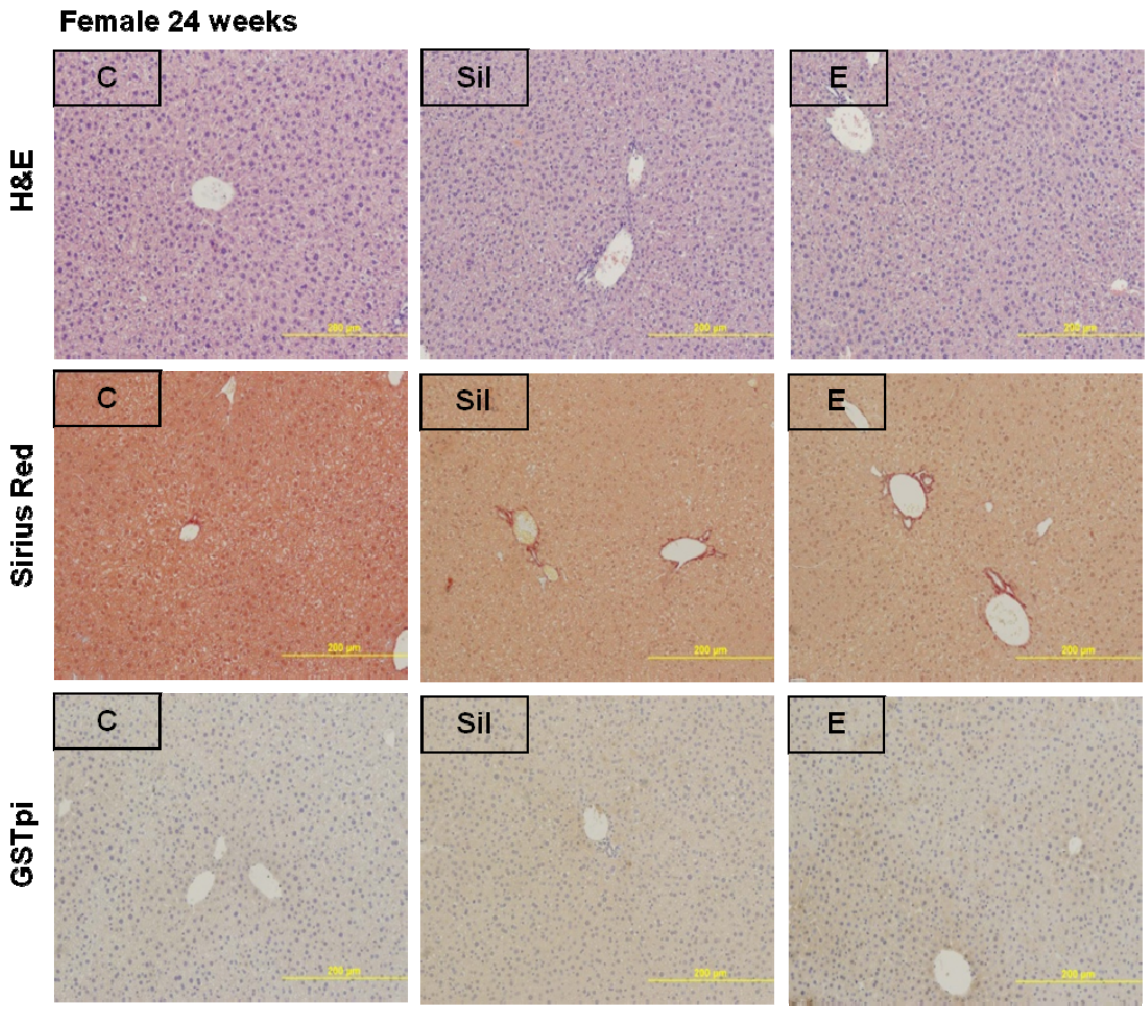

Appendix A Figure A.4: Representative micrographs (100X) of H&E, Sirius red and GSPpi stained liver sections from 24 week female mice in control (C), silibinin diet diet (0.5% (*w/w*) daily for 9 weeks) (Sil), and ethanol drinking water regime (10/20% (*v/v*) alternating daily for 8 weeks) (E) groups.

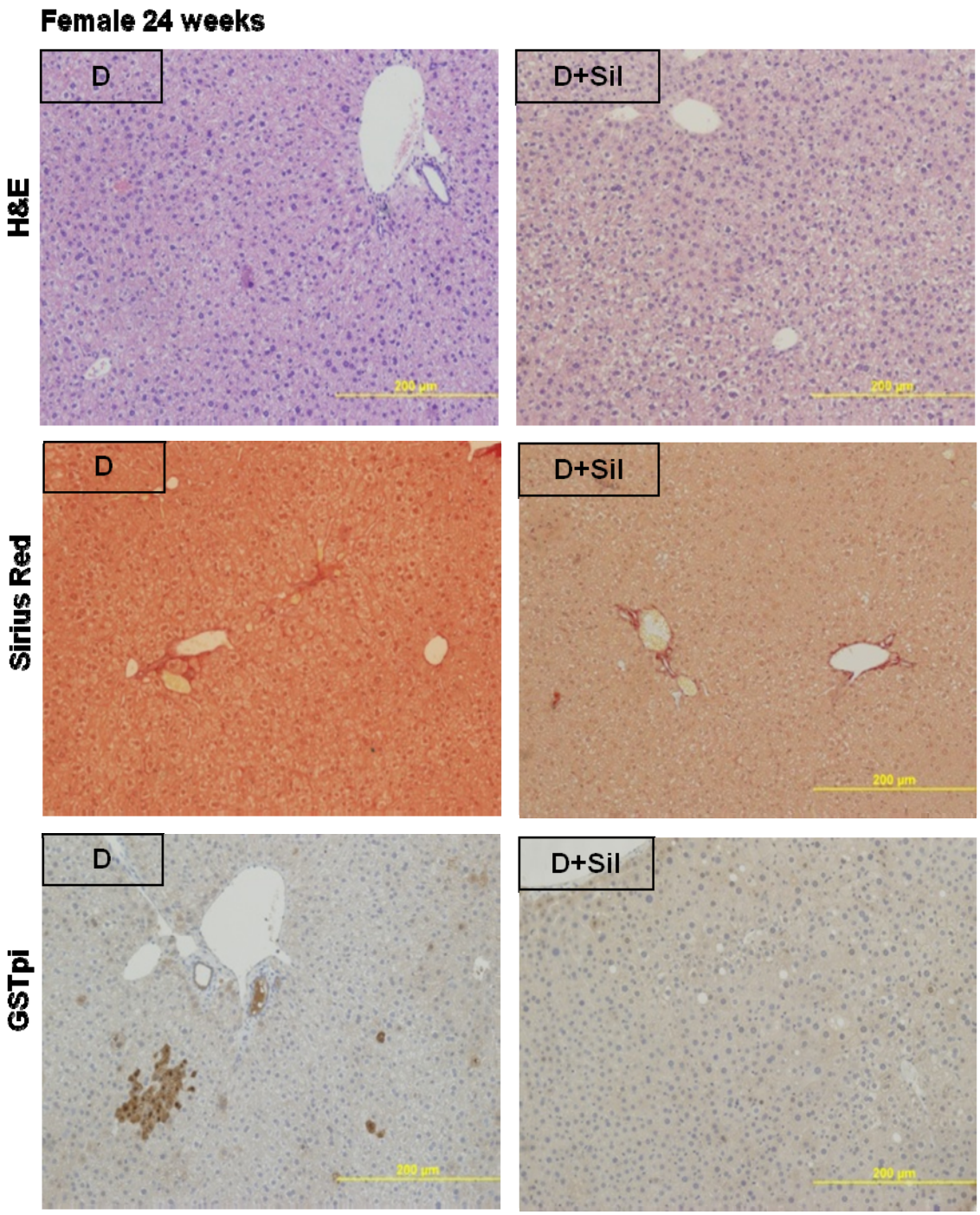

Appendix A Figure A.5: Representative micrographs (100X) of H&E, Sirius red and GSPpi stained liver sections from 24 week female DEN-initiated (D), and DEN-intitiated mice maintained on silibinin diet diet (0.5% (*w/w*) daily for 9 weeks) (D+Sil).

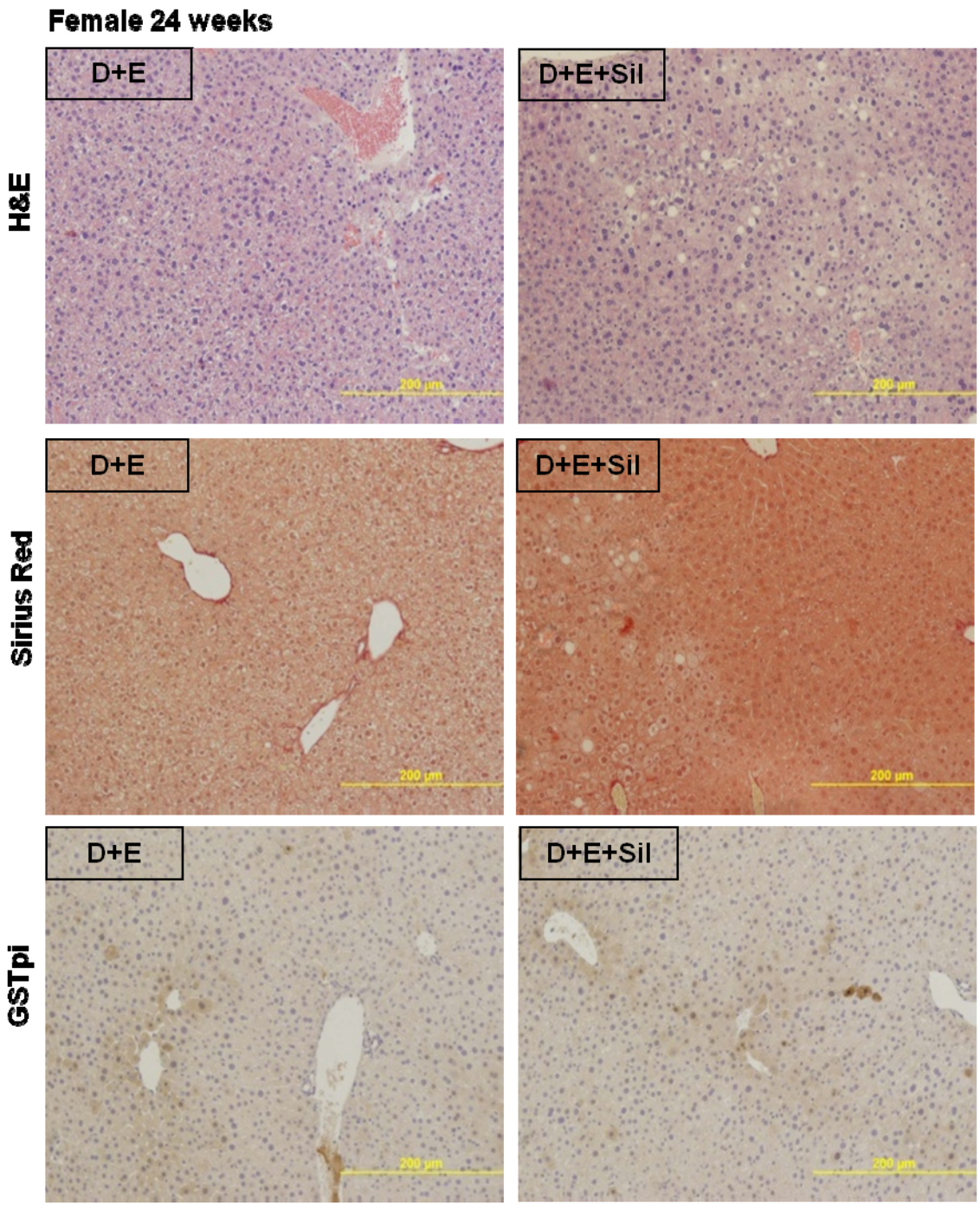

Appendix A Figure A.6: Representative micrographs (100X) of H&E, Sirius red and GSPpi stained liver sections from 24 week female DEN-initiated mice maintained on ethanol drinking-water regime (10/20% (*v/v*) alternating daily for 8 weeks) (D+E), and DEN-initiated female mice maintained on Silibinin diet (0.5% (*w/w*) daily for 9 weeks) with ethanol drinking-water (8 weeks) (D+E+Sil).

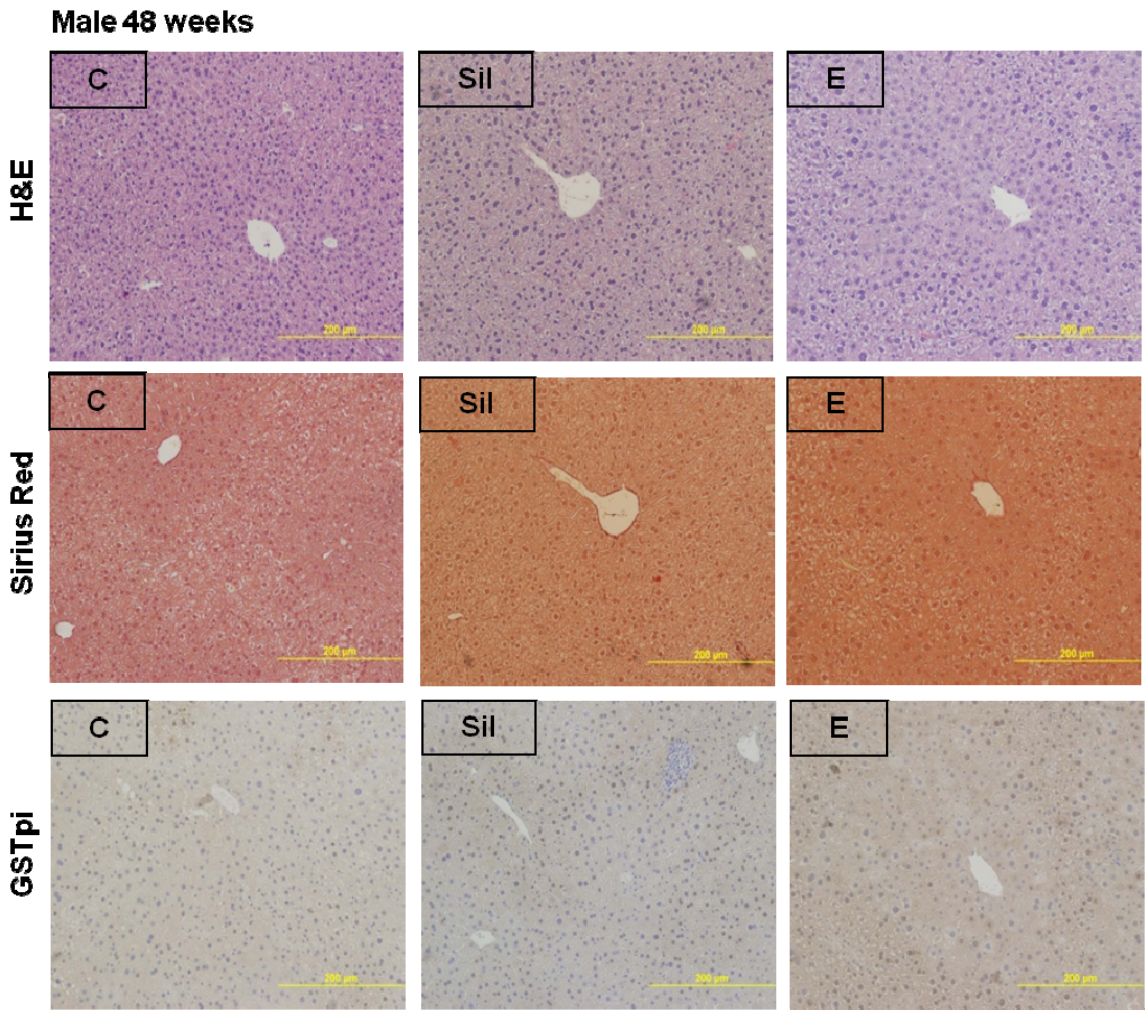

Appendix A Figure A.7: Representative micrographs (100X) of H&E, Sirius red and GSPpi stained liver sections from 48 week male mice in control (C), silibinin diet diet (0.5% (*w/w*) daily for 9 weeks) (Sil), and ethanol drinking water regime (10/20% (*v/v*) alternating daily for 8 weeks) (E) groups.

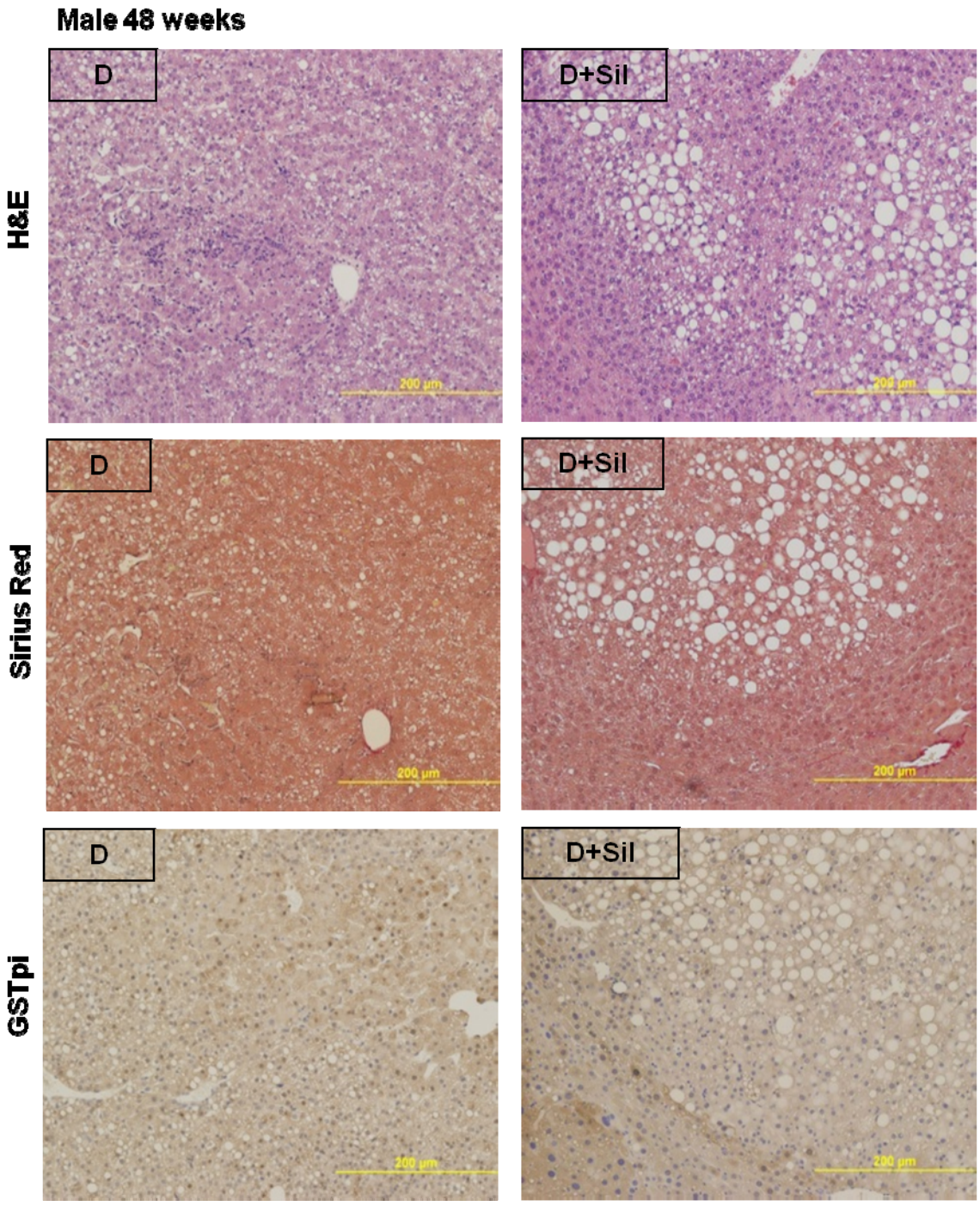

3

Appendix A Figure A.8: Representative micrographs (100X) of H&E, Sirius red and GSPpi stained liver sections from 48 week male DEN-initiated (D), and DEN-intitiated mice maintained on silibinin diet diet (0.5% (*w/w*) daily for 9 weeks) (D+Sil).

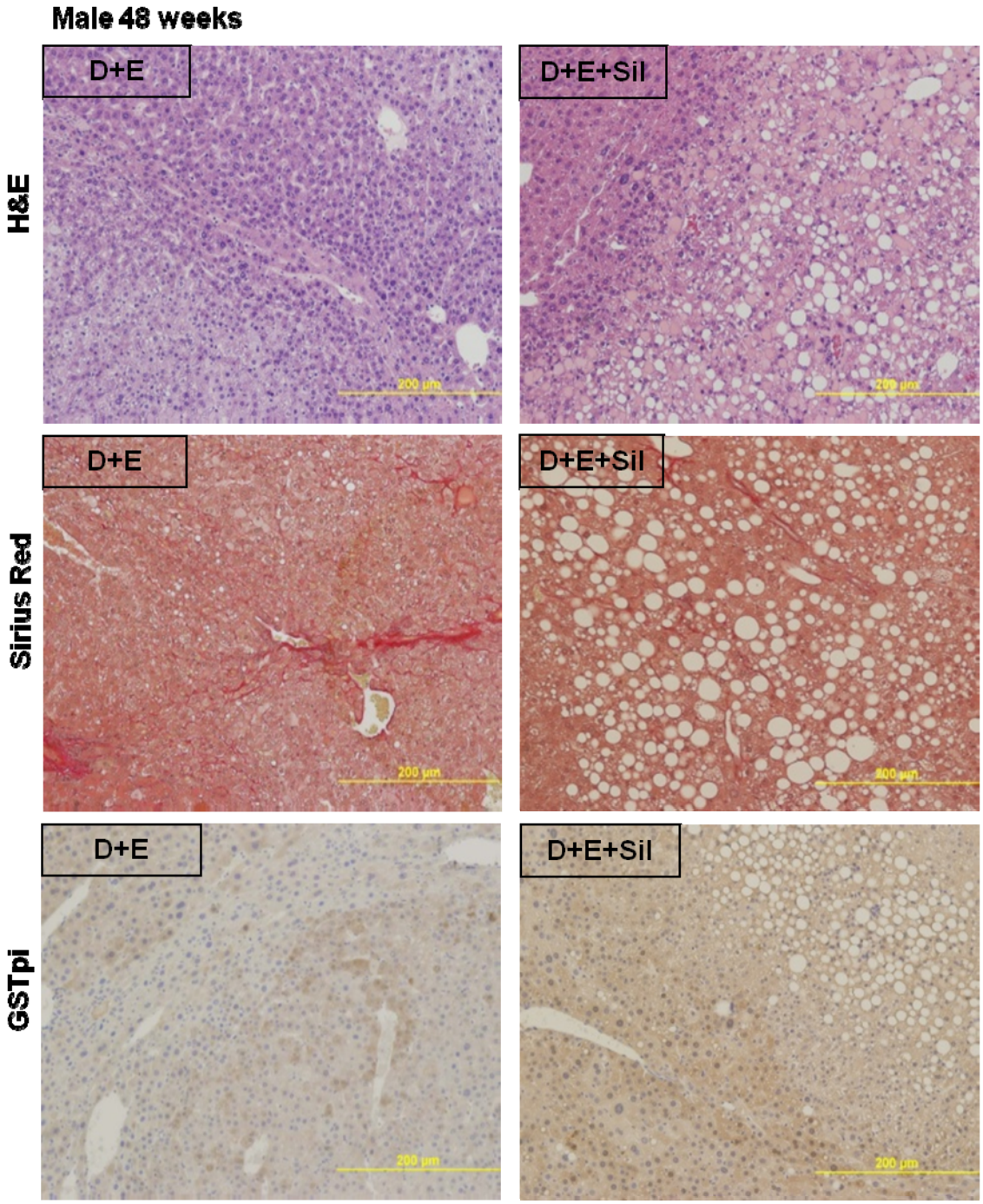

Appendix A Figure A.9: Representative micrographs (100X) of H&E, Sirius red and GSPpi stained liver sections from 48 week male DEN-initiated mice maintained on ethanol drinking-water regime (10/20% (*v/v*) alternating daily for 8 weeks) (D+E), and DEN-initiated female mice maintained on Silibinin diet (0.5% (*w/w*) daily for 9 weeks) with ethanol drinking-water (8 weeks) (D+E+Sil).

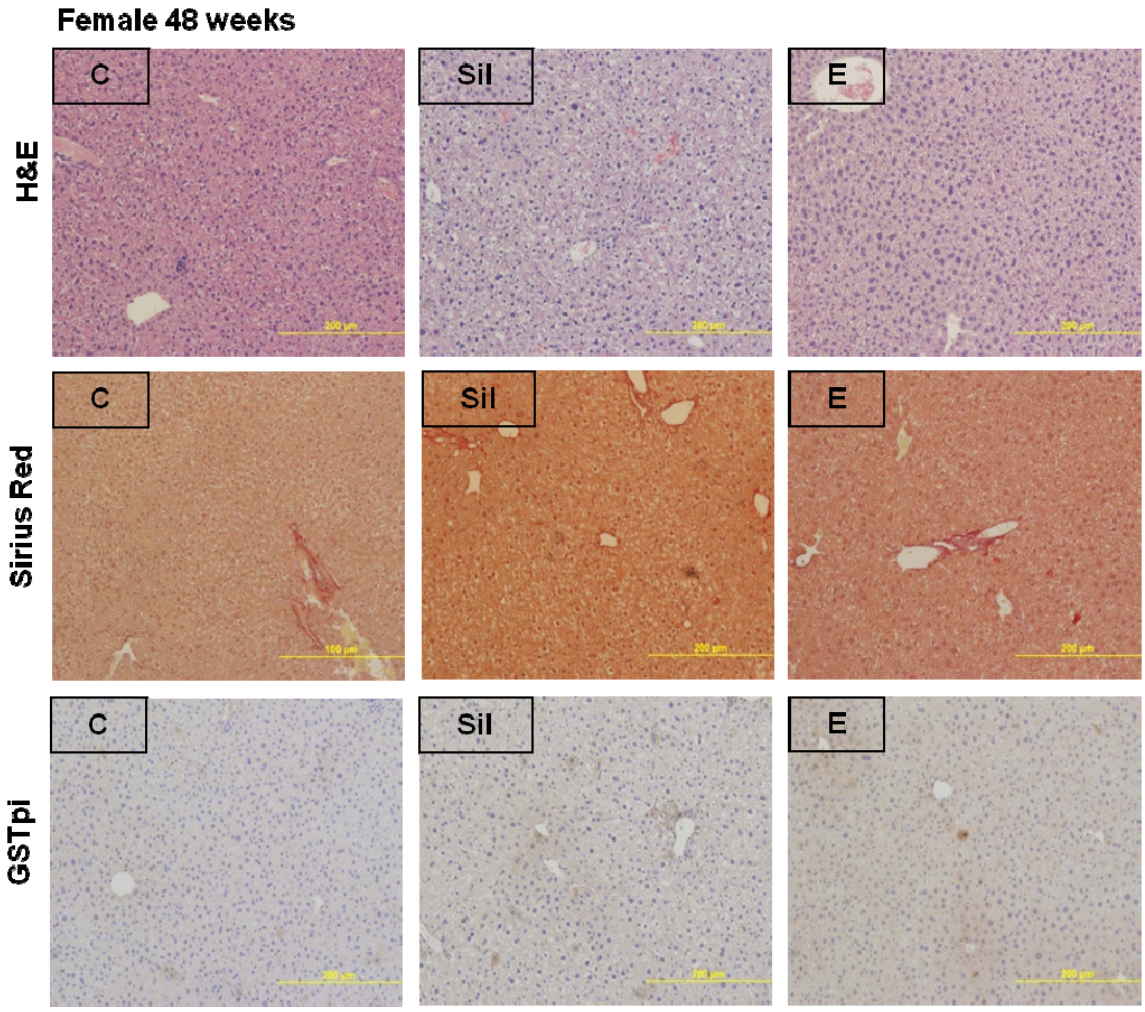

Appendix A Figure A.10: Representative micrographs (100X) of H&E, Sirius red and GSPpi stained liver sections from 48 week female mice in control (C), silibinin diet diet (0.5% (*w/w*) daily for 9 weeks) (Sil), and ethanol drinking water regime (10/20% (*v/v*) alternating daily for 8 weeks) (E) groups.

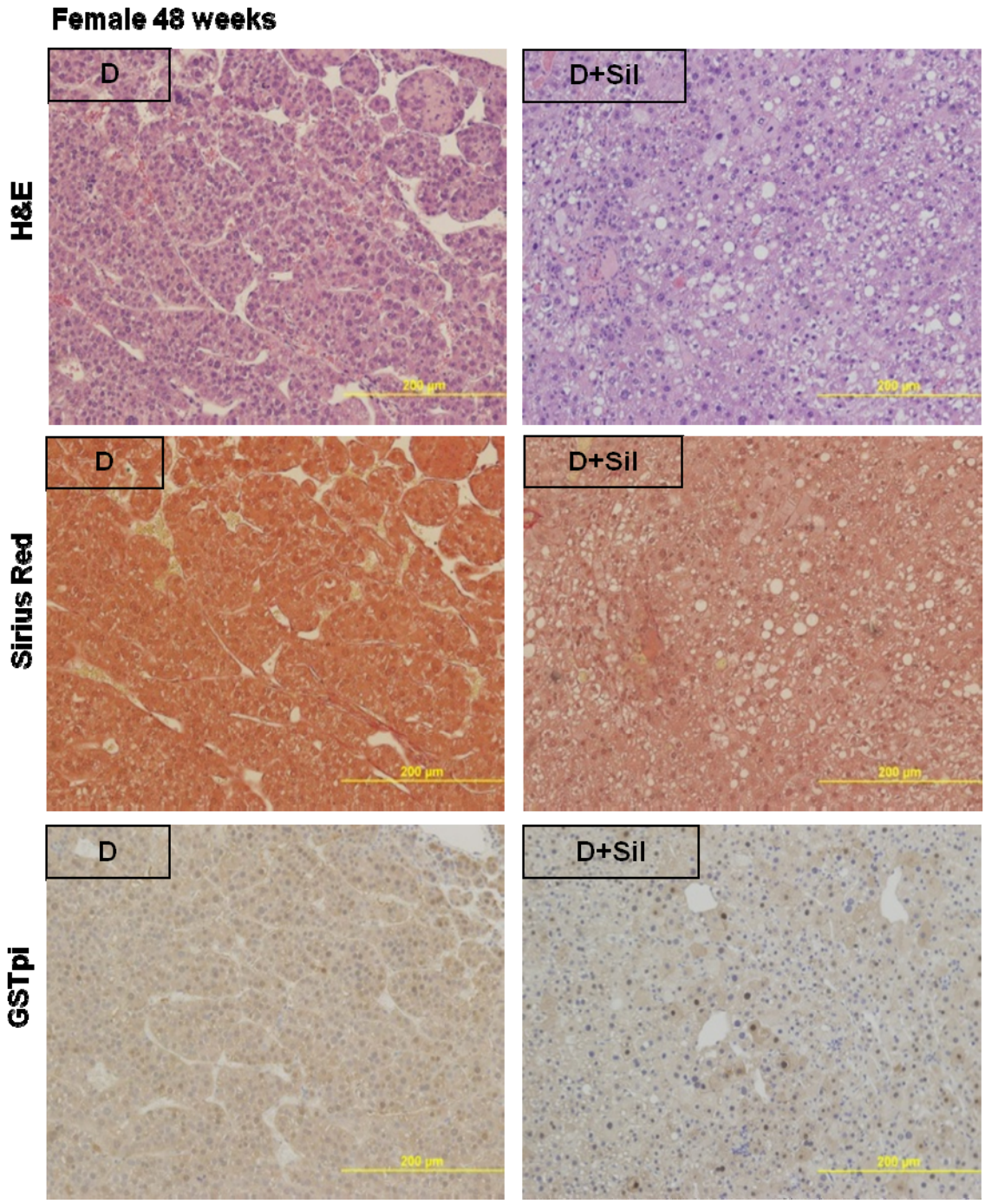

Appendix A Figure A.11: Representative micrographs (100X) of H&E, Sirius red and GSPpi stained liver sections from 48 week female DEN-initiated (D), and DEN-intitiated mice maintained on silibinin diet diet (0.5% (*w/w*) daily for 9 weeks) (D+Sil).

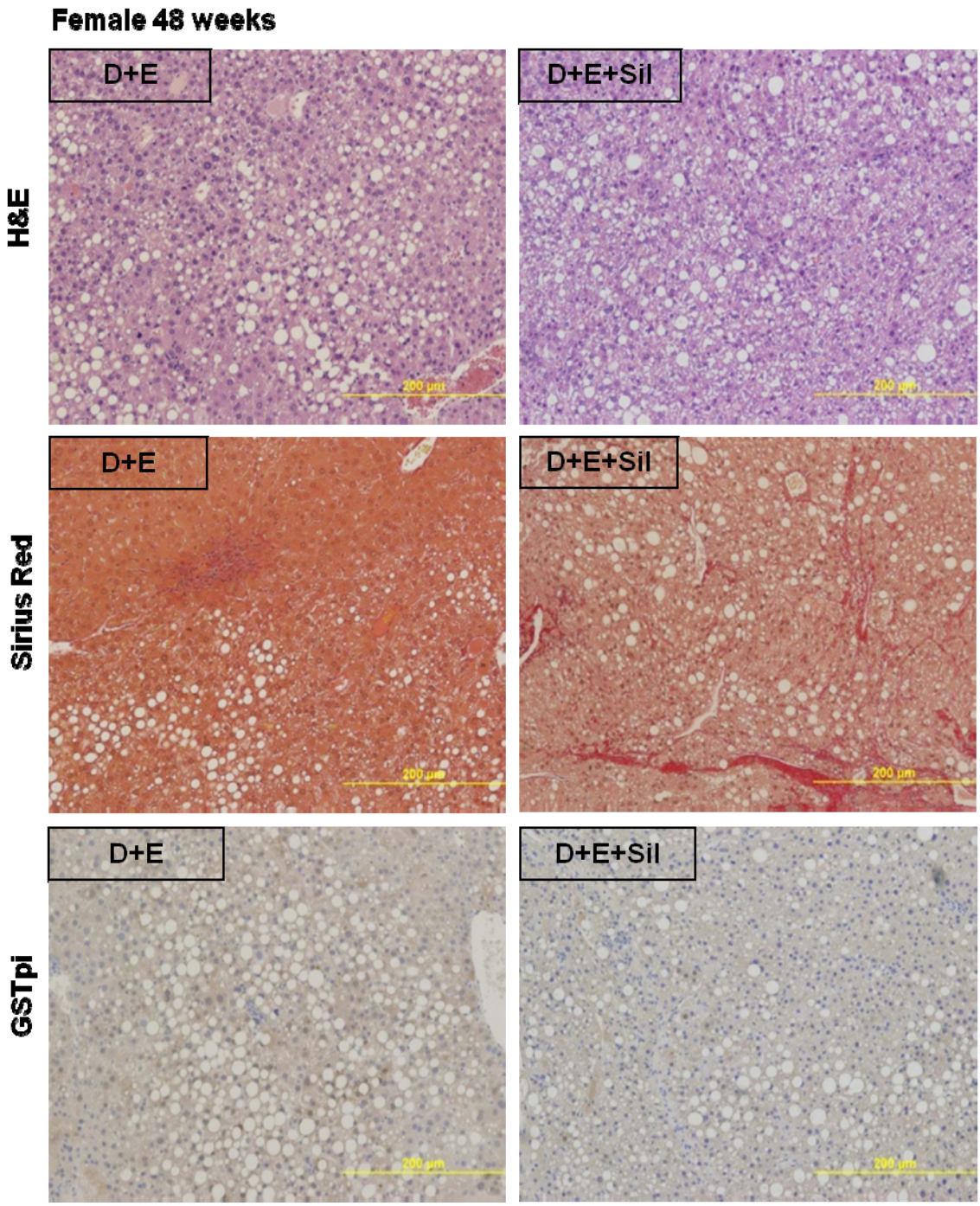

Appendix A Figure A.12: Representative micrographs (100X) of H&E, Sirius red and GSPpi stained liver sections from 48 week female DEN-initiated mice maintained on ethanol drinking-water regime (10/20% (*v/v*) alternating daily for 8 weeks) (D+E), and DEN-initiated female mice maintained on Silibinin diet (0.5% (*w/w*) daily for 9 weeks) with ethanol drinking-water (8 weeks) D+E+Sil

***Appendix A, Table A.1*:** Mean pathological scores following blind scoring for steatosis, necrosis , inflammation, and fibrosis (% sirius red stain for collagen) in Sil (S), DEN-initiated (D), DEN+Silibinin diet (D+Sil), DEN+EtOH-DW (D+E), and DEN+EtOH-DW+Silibinin diet (D+E+Sil). Data were collected at 24 and 48 weeks and totaled to generate a total liver injury score (TLIS).

Pathological parameter	**Male (24 weeks) Group (n)**					**Female (24 weeks) Group (n)**				
	Sil (9)	D (9)	D+Sil (8)	D+E (14)	D+E+Sil (14)	Sil (9)	D (9)	D+Sil (9)	D+E (14)	D+E+Sil (14)
Steatosis	0.61±0.08	1.84±0.26	2.00±0.10	1.93±0.13	2.07±0.05	0.33±0.10	1.37±0.08	1.66±0.17	1.35±0.14	1.68±0.16
Necrosis	0.15±0.05	0.97±0.12	1.30±0.07	1.14±0.12	0.56±0.07	0.14±0.03	1.01±0.10	0.57±0.09	0.93±0.05	0.86±0.17
Inflammation	0.13±0.03	0.80±0.18	1.06±0.06	1.01±0.13	0.53±0.08	0.27±0.03	0.96±0.12	1.14±0.13	0.73±0.08	1.21±0.11
Collagen (% sirius red)	0.37±0.05	0.57±0.15	0.78±0.05	0.68±0.13	1.03±0.05	0.44±0.05	0.78±0.07	0.78±0.06	0.68±0.07	0.80±0.11
TLIS	1.25±0.14	4.18±0.51	5.11±0.19	4.75±0.32	4.20±0.12	1.59±0.06	3.61±0.18	4.50±0.31	3.21±0.23	4.41±0.39
	Male (48 weeks) Group (n)					**Female (48 weeks) Group (n)**				
	Sil (9)	D (8)	D+Sil (9)	D+E (14)	D+E+Sil (14)	Sil (9)	D (9)	D+Sil (8)	D+E (14)	D+E+Sil (14)
Steatosis	0.82±0.17	1.76±0.27	3.02±0.19	3.00±0.13	3.63±0.18	0.57±0.11	1.10±0.21	1.98±0.30	1.24±0.30	2.10±0.34
Necrosis	0.34±0.05	0.93±0.06	1.53±0.27	2.19±0.16	2.14±0.29	0.33±0.05	0.90±0.08	0.75±0.20	0.84±0.10	1.29±0.13
Inflammation	0.27±0.07	0.64±0.13	0.82±0.27	1.61±0.31	1.59±0.22	0.45±0.06	0.89±0.10	1.08±0.10	1.63±0.31	1.13±0.15
Collagen (% sirius red)	0.27±0.07	1.83±0.08	1.37±0.13	2.31±0.11	2.18±0.16	0.27±0.03	1.37±0.07	1.23±0.15	1.51±0.13	1.80±0.16
TLIS	**1.72±0.22**	**5.16±0.29**	**6.73±0.52**	**9.11±0.54**	**9.26±0.67**	**1.70±0.22**	**3.96±0.44**	**4.45±0.47**	**5.13±0.53**	**6.31±0.53**

APPENDIX B: PUBLICATIONS, ABSTRACTS, AND AWARDS

Publications:

Elizabeth Brandon-Warner, Laura W. Schrum,Iain H. McKillop. Chronic ethanol feeding accelerates hepatocellular carcinoma progression in a mouse model of hepatocarcinogenesis. Alcohol Clinical & Experimental Research. In press.

Michele T. Yip-Schneider, Courtney Doyle, Iain H. McKillop, Sabrina C. Wentz, Elizabeth Brandon-Warner, Jesus M. Matos, Kumar Sandrasegaran, Romil Saxena, Matthew E. Hennig, Huangbing Wu, Patrick J. Klein, Janice C. Froehlich & C. Max Schmidt. Alcohol Induces Liver Neoplasia in a Novel Alcohol-Preferring Rat Model. Alcohol Clinical & Experimental Research. July 2011.

E. Brandon-Warner, J. A. Sugg, L. W. Schrum, I. H. McKillop. Silibinin inhibits ethanol metabolism and ethanol –dependent cell proliferation in an *in vitro* rat model of hepatocellular carcinoma. Cancer Letters. 2010 May. 291(1) 120-129.

C. Baker-Austin, J. V. McArthur, A. H. Lindell, M. S. Wright, R. C. Tuckfield, J. Gooch, E.B. Warner , J. D. Oliver, and R. Stepanauskas. Multi-site analysis reveals widespread antibiotic resistance in the marine pathogen *Vibrio vulnificus*. Microb. Ecol. 2009 January. 57(1) 151-159.

M. K. Jones, E.B. Warner, and J. D. Oliver. *csrA* inhibits the formation of biofilms by *Vibrio vulnificus*. Appl. Environ. Microbiol. 2008 November. 74(22) 7064-7066.

E. B. Warner, J. D. Oliver. Multiplex PCR assay for simultaneous identification and detection of *Vibrio vulnificus* biotype 1. Foodborne Pathogens and Disease. 2008 October, 5(5) 691-693.

M.K. Jones, E. B. Warner and J. D. Oliver. Survival and In Situ Gene Expression of *Vibrio vulnificus* at varying salinities in estuarine environments. Appl. Environ. Microbiol. 2008 January. 74(1) 182-187.

E. B. Warner, J. D. Oliver. Population dynamics of two distinct genotypes of *Vibrio vulnificus* in oysters (*Crassostrea virginica*) and sea water. App. Environ. Microbiol. 2008 January. 74(1):80-85

E. B. Warner, J. D. Oliver. Refined medium for direct isolation of *Vibrio vulnificus* from oyster tissue and sea water. Appl. Environ. Microbiol. 2007 September. 73(9)3098-100.

Abstracts:

Elizabeth Brandon-Warner, Hillary Gruce, Laura W. Schrum, Iain H. McKillop. Silibinin enhances ethanol-dependent tumor progression in a DEN model of hepatocarcinogenesis. June 2011 Research Society on Alcoholism, Atlanta, GA

Elizabeth Brandon-Warner, Laura W. Schrum, Iain H. McKillop. Ethanol promotes diethylnitrosamine-initiated hepatocarcinogenesis in male but not female mice. June 2011 Research Society on Alcoholism, Atlanta, GA**. NIH-NIAAA Student Merit Scholarship winner**

Elizabeth Brandon-Warner, Laura W. Schrum, Iain H. McKillop. Silibinin alters ethanol-dependent changes in hepatic pathophysiology and early hepatocarcinogenesis differently in male and female mouse models of hepatocellular carcinoma (HCC). June 2010 Research Society on Alcoholism, San Antonio, TX. **NIH-NIAAA Student Merit Scholarship winner**

Elizabeth Brandon-Warner, Laura W. Schrum, Iain H. McKillop. Ethanol promotes foci formation in a mouse model of hepatocarcinogenesis and is gender dependent. May 2010, Internation Liver Cancer Association (ILCA), Montreal, Quebec, Canada.

Elizabeth Brandon-Warner, J. Andrew Sugg, Laura W. Schrum, Iain H. McKillop. Silibinin inhibits CYP2E1-mediated ethanol metabolism and its associated oxidative stress in rat and human hepatocellular HCC cells. June 2009 Research Society on Alcoholism. San Diego, CA.

Elizabeth Brandon-Warner, J. Andrew Sugg, Laura W. Schrum, Iain H. McKillop. Silibinin inhibits CYP2E1-dependent ethanol metabolism, oxidative stress and cell proliferation in a rat model of hepatocellular carcinoma (HCC). May 2009 FASEB, New Orleans.

Elizabeth Brandon-Warner, J Andrew Sugg, Laura W. Schrum, Iain H. McKillop. Center for Biomedical Engineering Systems – Graduate student poster competition. Silibinin inhibits CYP2E1-mediated ethanol metabolism and its associated oxidative stress in rat and human hepatocellular HCC cells. **First Prize CBES April 2009.**